Ecotoxicity of Engineered Nanomaterials and the Pathway of Toxic Effects in an Environmental Model, *Caenorhabditis elegans*

Pawitrabhorn Samutrtai

Submitted to the degree of Doctor of Philosophy

Heriot-Watt University

School of Life Sciences

April 2016

Abstract

This thesis examined the adverse effects of engineered nanomaterials (NMs) and their potential mechanisms of toxicity. The research focussed on the toxicity of NMs and their dissolved ions, as well as bulk particles (larger size), if applicable, in the nematode, *Caenorhabditis elegans*. The physicochemical properties of chosen NMs were characterised using various techniques. The toxicity of NMs regarding their ability to kill nematodes was concentration-dependent. The dissolved ions of each type of NM were be the most toxic form. On the other hand, the mortality of nematodes was not observed when they were exposed to CuO NMs and bulk particles, which led to the decision to discontinue their study. The toxicity of AgNMs regarding the inhibition of reproduction was also in a concentration-dependent manner. Moreover, the concentrations inducing a decrease in the number of progeny were lower than those used in the mortality test, which suggested reproduction to be a more sensitive endpoint. The induction of oxidative stress, which was investigated by determination of reactive oxygen species (ROS) and related enzymes, was studied when nematodes were exposed to all silver substances. Nevertheless, there were differences observed across the different strains of nematodes. The initiation of apoptosis was examined by visualisation and determination of apoptotic proteins. However, induction of apoptosis was not observed in the testing conditions used in this thesis. The studies of transcriptome and proteome of nematodes treated with spherical AgNM, JRCNM03002a (previously NM300K) revealed that genes and proteins involved in ribosome and protein synthesis were mostly affected by the exposure to JRCNM03002a. However, time of exposure had an impact on the pathways of toxicity. The expression of genes and proteins in the pathways of oxidative stress were altered significantly within 30 minutes of exposure, while these pathways were not involved in 24 hours of exposure. In conclusion, engineered NMs, especially AgNMs, can trigger adverse effects in *C. elegans*. Although it was proven that the pathway of oxidative stress was related to the observed toxicity, the initiation of apoptosis was not established in the conditions used in this study.

Acknowledgement

First of all, I would like to thank my supervisors, Prof. Teresa Fernandes and Dr. Elizabeth Dyrynda for the opportunity to conduct this research and for the guidance when I struggled in my research.

I would also like to thank my colleagues in the lab and friends who always helped, supported and listened to me when I faced any problems in my studies.

Importantly, I would like to thank my funding provider who granted me the scholarship to carry out these postgraduate studies, and offered me the ability to continue working in this area.

Last, but not least, I would like to thank my Dad (Bowon), Mum (Saipin), brother (Chinnapat), sister (Waratsuda) and my best friends (Liou Bian) who have always been supportive in all situations. Although they are far away from me, their encouragement helped me fight against all the difficulties and inconveniences I confronted during my period in Scotland. I would have never been able to complete this thesis without them.

ACADEMIC REGISTRY
Research Thesis Submission

Name*:*	PAWITRABHORN SAMUTRTAI		
School/PGI:	School of Life Sciences		
Version: *(i.e. First, Resubmission, Final)*	Final	Degree Sought (Award **and** Subject area)	PhD

Declaration

In accordance with the appropriate regulations I hereby submit my thesis and I declare that:

1) the thesis embodies the results of my own work and has been composed by myself
2) where appropriate, I have made acknowledgement of the work of others and have made reference to work carried out in collaboration with other persons
3) the thesis is the correct version of the thesis for submission and is the same version as any electronic versions submitted*.
4) my thesis for the award referred to, deposited in the Heriot-Watt University Library, should be made available for loan or photocopying and be available via the Institutional Repository, subject to such conditions as the Librarian may require
5) I understand that as a student of the University I am required to abide by the Regulations of the University and to conform to its discipline.

* *Please note that it is the responsibility of the candidate to ensure that the correct version of the thesis is submitted.*

Signature of Candidate*:*		Date:	

Submission

Submitted By *(name in capitals):*	
Signature of Individual Submitting:	
Date Submitted:	

For Completion in the Student Service Centre (SSC)

Received in the SSC by *(name in capitals):*			
Method of Submission *(Handed in to SSC; posted through internal/external mail):*			
*E-thesis Submitted (**mandatory for final theses)***			
Signature:		Date:	

Please note this form should bound into the submitted thesis.

Updated February 2008, November 2008, February 2009, January 2011

Table of Contents

List of tables

Table 7.8: The list of annotated proteins found altered in their regulation in the comparison group of treatment relative to control at time-point of 24 hours. The negative values of fold change represent the down-regulation, the positive value the up-regulation.

Table 8.1: Summary of the findings in this thesis.

List of figures

Glossary

Analysis of variances (ANOVA)

Antioxidant response element (ARE)

Apoptosis inducing factor (AIF)

Bag of worms (BOW)

Bovine serum albumin (BSA)

c-Jun N-terminal kinase (JRK)

Catalase (CAT)

Circular ribonucleic acid (cRNA)

Copper oxide nanomaterial (CuO NM)

Cytotoxic T lymphocyte (CTL)

Death-inducing signalling complex (DISC)

Deoxyribonucleic acid (DNA)

Dichlorodihydrofluorescin diacetate (DCFH-DA)

Dynamic light scattering (DLS)

Effective median concentration; concentration of a chemical which effects a response at 50% compared to the control over a specificed amount of time (EC_{50})

Energy dispersive X-ray analysis (EDX)

Extracellular signal-regulated kinase (ERK)

Field flow fractionation (FFF)

Gene ontology (GO)

Glutaredoxins (GLRXs)

Glutathione (GSH)

Glutathione peroxidase (GPx)

Glutathione reductase (GR)

Glutathione-S-transferase (GST)

Heat shock protein (Hsp)

Hermaphrodite-specific neuron (HSN)

Humic acid (HA)

Hydrogen peroxide (H_2O_2)

Inductively coupled plasma mass spectrometry (ICP-MS)

Inductively coupled plasma optical emission spectrometry (ICP-OES)

Inhibitor of apoptotic proteins (IAP)

Inhibitor of caspase-activated deoxyribonuclease (ICAD)

Kelch-like ECH-associating protein 1 (Keap1)

Kyoto encyclopaedia of genes and genomes (KEGG)

Laser-induced breakdown spectroscopy (LIBS)

Median lethal concentration; oncentration at which 50% of the exposed population is killed over a specified amount of time (LC_{50})

Lipid peroxidation (LPO)

Malondialdehyde (MDA)

Messenger ribonucleic acid (mRNA)

Micro ribonucleic acid (miRNA)

Minimum inhibitory concentration (MIC)

Mitochondrial deoxyribonucleic acid (MtDNA)

Mitogen-activated protein kinases (MAPK)

Moderately hard reconstituted water (MHRW)

N-acetylcysteine (NAC)

Nanomaterial (NM)

Nanoparticle tracking analysis (NTA)

Natural organic matter (NOM)

Nematode growth medium (NGM)

Neuro-secretory motorneuron (NSM)

Noncoding ribonucleic acid (ncRNA)

Organisation for Economic Co-operation and Development (OECD)

Peroxiredoxins (PRDXs)

Phosphatidylserine (PS)

Programmed cell death (PCD)

Protein kinase C (PKC)

Reactive oxygen species (ROS)

Reduced Nicotinamide Adenine Dinucleotide (NADH)

Reproduction inhibitory concentration at which 50% of the progeny of *C. elegans* reduced in 72 hours (RC_{50})

Rho-associated coil-coil forming kinase I (ROCKI)

Ribonucleic acid (RNA)

Ribonucleic acid integrity number (RIN)

Ribosomal ribonucleic acid (rRNA)

Scanning electron microscopy (SEM)

Selected area electron diffractometry (SAED)

Silver nanomaterial (AgNM)

Simulated soil pore water (SSPW)

Simulated soil pore water without humic acid (SSPW-HA)

Small nuclear ribonucleic acid (snRNA)

Small nucleolar ribonucleic acid (snoRNA)

Superoxide dismutase (SOD)

Total organic carbon (TOC)

Transfer ribonucleic acid (tRNA)

Transmission electron microscopy (TEM)

Tumour necrosis factor (TNF)

United States Environmental Protection Agency (USEPA)

X-ray diffractometry (XRD)

Chapter 1: Introduction

1.1 Nanotechnology, nanomaterials, and definitions

The growth of nanotechnology has brought improvements in the product quality of many applications such as pharmaceuticals, electronics, catalysis, energy production, sensor development, and environmental remediation (Ma *et al.*, 2009). Nanotechnology has been applied to a wide range of sectors and has been predicted to continue to increase at a steady pace and to be applied to a diverse array of consumer products, medicine, and industries. However, the application of nanotechnology has raised concerns regarding toxicity from nanomaterials (NMs) which is likely to involve their high surface reactivity when compared with their conventional larger (bulk) forms. According to the European Commission (2011), NM has been defined as materials consisting of unbound, aggregated or agglomerated particles with more than 50% of these particles in the size range of 1-100 nm in the size distribution in one or more external dimensions (SCENIHR, 2011).

1.2 Environmental nanomaterials and their toxicity

Major sources of NMs in the environment can be placed into three categories: natural, intentional, and incidental NMs (Handy *et al.*, 2008). Natural NMs such as particles produced from soil erosion, volcanic eruption, or colloids in water have existed before the emergence of nanotechnology (Handy *et al.*, 2008). One example of intentional NMs is zerovalent iron NMs which have been used to remediate polluted water. Moreover, NMs which are derived from combustion or decomposition of some materials are described as incidental NMs (Lead, 2010). In the field of environmental nanotoxicology, the work is focused on the study of the hazard of engineered NMs which are accidentally released into the environment. Emitted NMs from industries may occur during some processes in their production facilities, landfills, wastewater treatment, or even during transportation (Nowack and Bucheli, 2007). Along with the growth of nanotechnology, the nanotechnology-applying industries are increasing, thus the impact of NMs on the environment is becoming more important (Ju-Nam and Lead, 2008). To assess the risk of NMs, the potential of exposure and toxicity, are two major aspects to be considered. Therefore, fate and adverse effects from NMs in the environment are used to determine the risk of NMs.

1.3 Fate and behaviour of NMs in the environment

According to Nowack and Bucheli (2007), soil or sediments are considered to be the main environmental compartments in which NMs will tend to accumulate. These particles are likely to originate from sewage treatment plants, waste handling, run-off or aerial deposition, which are transported and may tend to settle and deposit in certain areas. NMs in water tend to aggregate and form larger particles which can be deposited in the sediments and re-dispersed by sediment-dwelling animals. NMs in the environment can be taken up by humans through air, water, soil, or from plants or animals (Nowack and Bucheli, 2007).

After entering the environment, NMs can be transformed, in which the processes are controlled by the surrounding environment. The transformation of NMs in the environment can occur following a redox reaction, dissolution, sulphidation, aggregation, and adsorption to complexing ions in the environment. These transformations affect the properties of NMs in terms of their toxicity, which might lead to an enhanced or inhibitory effect. For example, the breakdown of Cd-Se quantum dots can increase the toxicity of this particular NM (Mahendra et al, 2008), while the adsorption of silver nanomaterials (AgNMs) to natural organic matter (NOM) may lead to reduce bactericidal activity (Fabrega et al, 2009).

One type of transformation, redox reactions, are the electron-transferring processes which comprise reduction and oxidation. These coupled reactions usually occur in metal NMs, such as silver (Ag) and iron (Fe) (Lowry et al, 2012). The oxidation of AgNMs is important for their dissolution and ionic silver (Ag^+) release, and Ag^+ consequently possesses the ability to kill bacteria (Lok et al, 2007). In the oxidised environment such as in natural waters and oxygenated soils, the bactericidal effect of NMs is increased due to Ag^+ availability, whereas low dissolved oxygen in groundwaters or in carbon-rich soils, results in less oxidation, which decreases Ag toxicity (Lowry et al, 2012).

Other transformation processes such as dissolution and sulphidation also alter the surface properties of NMs, toxicity, and their persistence in the environment. Metal cation NMs, e.g. Ag, zinc (Zn), and copper (Cu) can be oxidised to metal oxides, which are partially soluble. These metal cations also have a high affinity to sulphide molecules (Lowry et al, 2012). Moreover sulphidation can lead to the generation of an outer metal-sulphide shell, which affects surface charge and causes aggregates of NMs

(Levard et al, 2011). The aggregation of NMs decreases their surface area, and thus alters their reactivity. Since the reactivity of NMs decreases by aggregation, toxicity is likely to decrease as well if those NMs express their toxicity through surface area. However, this might not be the case when aggregation between NMs and soft biogenic particles (heteroaggregation) takes place, which may lead to increases in the bioavailability of NMs to certain species. In addition, the results from aggregation may lead to an enhancement of NM persistence, caused by a reduction in dissolution and degradation of NMs (Lowry et al, 2012).

1.4 Using *Caenorhabditis elegans* as an ecotoxicological model

Caenorhabditis elegans is a globally distributed nematode which lives in both sediments and soil. It has important roles in decomposition and nutrient cycling (Meyer *et al.*, 2010; Kim, Nam and An, 2012). This roundworm has a transparent body approximately 1 mm in length. Although it has a small cell number of approximately 1000 cells, this worm consists of complex tissues such as intestine, muscle, gonad, and nervous system (Pluskota, Horzowski and von Mikecz, 2009). The life span of the adult worm is 2-3 weeks which is antedated by approximately 3 days of embryogenesis and postembryonic development under normal growth condition. *C. elegans* has been well studied and its genome described. The genome of *C. elegans* has been fully sequenced and it has homologs of 60-80% of human genes with 12 out of 17 known signal transduction pathways which are conserved in both human and *C. elegans* (Kaletta and Hengartner, 2006; Leung *et al.*, 2008). This makes the results from *C. elegans* studies predictive in a human context.

In addition, *C. elegans* has been proven to be a sensitive indicator for pollutant-induced stress and ecological disturbances (Sohlenius, 1980; Neher, 2001). It is also a model species used to assess toxicity from metals in eukaryotes. Since its habitats are soil and sediment, *C. elegans* is a useful model to investigate ecotoxicity in both terrestrial and aquatic environments. Because of the knowledge of its genome, short life span, large progeny production and ease of maintenance in the laboratory, *C. elegans* has become a popular model for environmental investigation of many toxicants, including long term risk assessment, given its short life cycle (Ellegaard-Jensen, Jensen and Johansen, 2012). The transparent body of *C. elegans* is also useful for *in vivo* imaging and to assess the fate of toxicants (Leung *et al.*, 2008). Furthermore, the small

size of the worm allows the study to be conducted in a microplate format. Another advantage of using *C. elegans* over cell models is that it can be more biologically relevant (Zhang *et al.*, 2011).

As previously stated, an accumulation of aggregated NMs is likely to be found in soil or water sediments, which are habitats of *C. elegans*; furthermore the re-dispersion of NMs can take place by soil/sediment-living organism. Therefore, the presence of NMs in the environment can affect and be affected by this test organism.

1.5 Toxicity of NMs in *C. elegans* model

As described in section 1.1, nanotechnology has been used widely in many applications ranging from household to medicinal products. However, the toxicity of NMs, which might be released from these products is still under investigated. Some studies have assessed the environmental risk of these particles using *C. elegans*. In this section, the published toxicity of different types of NMs in *C. elegans* is discussed.

1.5.1 Zinc oxide nanomaterials (ZnO NMs)

A study focused on lethality, growth, behaviour and reproduction of *C. elegans* has reported that exposures to ZnO NM (1.5 nm) resulted in a significantly lower number of offspring compared to the control group (Ma *et al.*, 2009). However, the significance of the toxicity regarding lethality, growth, behaviour and reproduction from ZnO NM compared to $ZnCl_2$, could not be established. It was suggested that both ZnO NM and $ZnCl_2$ shared similar bioavailability since the induction of *mtl-2*::GFP expression by ZnO NM was concentration-dependent as was observed in $ZnCl_2$. The same study also found that the reproductive system of *C. elegans* was a more sensitive endpoint in the presence of NM than survival or behaviour (Ma *et al.*, 2009). Another study used ultrapure water to assess the toxicity of ZnO NMs and it showed that pure water caused osmotic stress which might have led to the reduction in tolerance to toxicants when in the presence of ZnO NM (20 nm) (Wang, Wick and Xing, 2009). The number of offspring was also found to be smaller in exposures to ZnO NM compared with exposures to bulk ZnO (532 nm). It was also found that ZnO NM inhibited the reproductive system of *C. elegans* more significantly than that of the supernatant of ZnO NM in the same concentration. This indicated that the toxicity from dissolved Zn^{2+}

was partially due to the toxicity of ZnO NM, therefore the toxicity of the nanoparticulate form of ZnO was deduced (Wang, Wick and Xing, 2009). Another study focussing on growth, behaviour and reproduction of *C. elegans* exposed to different sized ZnO NMs (35, 50, 100 nm) showed that the toxicity from ZnO NMs was size-dependent. The smallest ZnO NM exerted the highest toxicity. This size-dependent pattern was also observed in the molecular response where genes in the pathways of insulin/IGF-like signalling and stress response were altered by different degrees according to the size. The same study also found a change in the expression of apoptotic genes where the exposure to ZnO NMs induced up-regulation of pro-apoptotic genes, and down-regulation of anti-apoptotic genes (Khare *et al.*, 2015).

1.5.2 AgNMs

Different studies have investigated the effects of various coated AgNMs since these NMs are widely used in many applications. The research investigated the internalization of citrate and polyvinylpyrrolidone (PVP) coated NMs and found that smaller size PVP (21 ± 17 nm) and citrated coated (7 ± 11 nm) AgNMs could be taken up by *C. elegans* in greater amounts than larger size PVP coated AgNM (75 ± 21 nm) (Meyer *et al.*, 2010). Furthermore, Cytoviva/hyperspectral imaging indicated that the citrate coated AgNM was translocated to the fertilized eggs. This has led to the assumption that AgNM can be passed to another generation (Meyer *et al.*, 2010). Another study focused on the effect of citrated coated AgNM (50.6 nm) on the skin of *C. elegans* using scanning electron microscopy (SEM) found that AgNM caused epidermal fissuring at the concentration of 10 mg/L, and induced an epidermal burst effect at a higher concentration of 100 mg/L, which might lead to secondary infection of the worms (Kim, Nam and An, 2012). It has to be considered that the concentrations used in this study might be unrealistic compared with that observed in the environment. The growth suppression observed by Meyer *et al.* (2010), and the mortality of *C. elegans* exposed to AgNMs in the study by Ellegaard-Jensen and colleagues (2012), concluded that dissolved silver ions (Ag^{+}) were not the only explanation of Ag toxicity. Since the supernatant fraction did not induce significant adverse effects in the nematodes, these studies suggested the possible nanoparticulate effect of AgNMs to the toxicity in *C. elegans* (Meyer *et al.*, 2010; Ellegaard-Jensen, Jensen and Johansen, 2012). It should be taken into account that the medium used in these studies was K-medium, which contains chloride ions. The dissolved silver might be chelated out of

the system, and thus the toxicity may be underestimated. Other studies have focused on ecotoxicogenomics of AgNM (20 nm) in *C. elegans* by using microarray and quantitative RT-PCR. Up- and down-regulation of various genes, were investigated and up-regulation of the genes *sod-3*, *mtl-2* were suggested to be involved in oxidative stress, therefore implication a role for AgNMs was relevant to oxidative stress (Roh *et al.*, 2009). A transcriptomic study of *C. elegans* exposed to pristine AgNM (79.6 ± 0.5 nm), $AgNO_3$, and the sulphidised AgNM (sAgNM) (88.5 ± 0.5 nm) highlighted different pathways of toxicity according to the types of silver substances. The authors found that all types of Ag substances induced a change of expression of various genes with only 11% in common. The main pathway of the metabolic process was triggered by AgNM, while the sulphidation of AgNM induced the alteration of genes in the pathway involved with moulting and the cuticle, and $AgNO_3$ affected the stress-related pathway. From this finding, the authors concluded that the toxicity of AgNM was partially related to Ag^+ release (Starnes *et al.*, 2016). A study focused on the uptake of AgNM (25 ± 9 nm) by endocytosis was conducted in *C. elegans*. Using chlorpromazine, the endocytosis inhibitor, the authors found a reduction in the mortality of nematodes exposed to AgNM, but the lethality of nematodes exposed to $AgNO_3$ was unaffected. Therefore the authors suggested the importance of endocytosis in the toxicity of AgNM (Maurer *et al.*, 2015).

1.5.3 Titanium dioxide nanoparticle (TiO_2 NM)

A study which investigated lethality, growth, and reproduction of *C. elegans* exposed to TiO_2 NM (50 nm) showed a significant difference in LC_{50} at 24 hours in TiO_2 NM and bulk TiO_2 (285 nm) exposed groups (Wang, Wick and Xing, 2009). The LC_{50} of the TiO_2 NM exposed group was lower than the group exposed to bulk TiO_2 with LC_{50} of 79.9 and 135.5 mg/L, respectively. Moreover, the body length, the number of eggs inside the body, and the number of offspring per worm were statistically lower in the 47.9 mg/L TiO_2 NM exposed group than obtained in the control group; there was also a significant difference obtained for exposures to bulk TiO_2 at the concentration of 95.9 mg/L compared to the control group. Since the dissolution of TiO_2 NM was low (0.020 mgTi/L at 96 h), the authors suggested the toxicity of TiO_2 NM was from the attachment of positively charged NM to the surface of *C. elegans*. (Wang, Wick and Xing, 2009). A genomic study of *C. elegans* exposed to TiO_2 NM and bulk TiO_2 found a significant alteration of genes encoding glutathione-S-

transferase, cytochrome P450, stress resistance regulator, oxidoreductase, and embryonic development. However, the difference in the pathway affected by bulk and nano-TiO_2 were not clearly distinguished (Rocheleau *et al.*, 2015).

1.5.4 Aluminium oxide nanoparticle (Al_2O_3 NM)

The toxicity of Al_2O_3 NM has been assessed in regards to lethality, growth, and reproductive suppression. The comparison of toxicity of Al_2O_3 NM (60 nm), bulk Al_2O_3 (429 nm), and dissolved ionic aluminium (Al^{3+}) in the form of $AlCl_3$ was made. LC_{50} values obtained for Al_2O_3 NM, bulk Al_2O_3, and $AlCl_3$ were 81.6, 152.9 and 2.5 mg/L, respectively. Significant differences were found between Al_2O_3 NM and bulk, but not between Al_2O_3 NM and $AlCl_3$, which led to the suggestion that toxicity might be induced by the dissolved aluminium ions. A significant reduction in body length, the number of eggs inside the body, and the number of offspring per worm was found after exposure to 51.0 mg/L Al_2O_3 NM compared to bulk Al_2O_3, while the supernatant of Al_2O_3 NM at the same concentration did not result in a statistically significant reduction in these endpoints. Thus the dissolved Al^{3+} alone was not the only reason for aluminium toxicity (Wang, Wick and Xing, 2009). Although the authors concluded that the adverse effect of Al_2O_3 NM might be from a nanospecific mechanism as the toxicity from the supernatant fraction was not significant, it has to be considered that the dissolution of Al_2O_3 NM was limited (0.096% at 96 h), therefore the amount of Al^{3+} in the supernatant might be too low to induce the toxicity observed in this study.

1.5.5 Silica NM

The translocation of fluorescent-labelled silica NM in *C. elegans* has been studied and it was found that silica NM accumulated in the pharynx and intestine (Pluskota, Horzowski and von Mikecz, 2009). This led to the deduction that silica NMs were taken up during food intake. However, the life span of worms treated with silica NM and untreated worms were nearly identical. Although the survival rate was not affected, progeny production of *C. elegans* was significantly decreased with the increasing in bag of worms (BOW; Riddle *et al.*, 1997) phenotype, that is, the eggs hatched inside the body. Pluskota, Horzowski and von Mikecz (2009) concluded that silica NM affected progeny production without translocating directly into the

reproductive system. Given that the decrease in progeny production and BOW phenotype are usually found in aged nematodes, the authors suggested that the degeneration of the reproductive system of *C. elegans* was induced by silica NM via an aging process (Pluskota, Horzowski and von Mikecz, 2009).

1.5.6 Fullerene NM

A study assessing the toxicity of fullerene NM showed that reduction in the life span of *C. elegans* exposed to this NM was concentration-dependent. The authors claimed that the decrease in bacterial food source as the result from fullerol NMs were not enough to lead to starvation of *C. elegans* (data not provided). The number of eggs inside the body was reduced in the presence of fullerol NMs. However, the majority of eggs (98%) from worms exposed to NM were completely hatched, suggesting that fullerol NM did not interfere with embryonic development (Cha, Lee and Choi, 2012). The same study also investigated the effect of fullerol NM via apoptosis using apoptotic gene regulator knockout strains (*ced-3* and *ced-4* deletion strains). The wild type *C. elegans* exposed to fullerol NM exhibited apoptotic cell corpses, whereas the pro-apoptotic gene knockout strains showed the increase in survival as well as the decrease in apoptotic cell corpses detected by differential interference contrast (DIC) equipped microscopy. This implied the possible connection between apoptosis and fullerol NM. Moreover, since these pro-apoptotic deletion strains were not prone to apoptosis in the normal condition, the detection of cell death in these strains after exposure to fullerol NM indicated that fullerol NM could trigger the initiation of apoptosis. Therefore, apoptotic cell death was proposed to be one of the pathways of the toxicity from fullerol NM (Cha, Lee and Choi, 2012).

1.6 NMs used in this study

This project focuses on two types of NMs, Ag and CuO. The reason behind this selection is the broad variety of applications of these particular NMs. AgNMs production is estimated to be approximately 55 tons annually (Piccinno *et al.*, 2012). Although the annual production of CuO NMs could not be estimated, the expanding uses of CuO NMs draws the attention to the importance of studying their effects in the environment.

1.6.1 AgNMs

Ag^{+} was shown to be efficient in fighting infections since ancient Greek and Egyptian times. During World War I, it was used to prevent and treat infections before the discovery of antibiotics (Bondarenko *et al.*, 2013). The nanoparticulate form of Ag has been widely used in consumer products as antimicrobials, such as in cosmetics, clothing, shoes, detergent, surface coatings in water filters, phones, laptops, including household water purification systems (Bystrzejewska-Piotrowska, Golimowski and Urban, 2009; Marambio-Jones and Hoek, 2010; Cerkez *et al.*, 2012). The ability to accelerate wound healing from AgNMs has also been established (Nair and Laurencin, 2007). Aside from the disinfection properties, AgNMs show unique plasmon-resonant scattering, therefore, the application of nanoparticulate Ag has expanded into the field of optics such as sensing, biomarkers, and *in vivo* imaging agents (Lesniak *et al.*, 2005). The efficiency of AgNMs as a disinfectant is not limited to only bacteria, these nanomaterials have also the ability to inhibit fungi, and viruses (Marambio-Jones and Hoek, 2010).

1.6.2 CuO NMs

CuO NMs have been utilized to a great extent in the field of electronics and technology due to their remarkable thermophysical properties. Examples of CuO NMs applications have been found in semiconductors, electronic chips, and heat transfer nanofluids (Ebrahimnia-Bajestan *et al.*, 2011). Other utilizations of CuO NMs include gas sensors (Li *et al.*, 2007), catalysis (Carnes and Klabunde, 2003), solar cells and lithium batteries (Guo *et al.*, 2009; Sau *et al.*, 2010). In addition, CuO NMs inhibit growth of microorganisms and have antiviral properties (Borkow and Gabbay, 2004; Gabbay *et al.*, 2006), which leads to their use in face masks, wound dressings, and socks (Borkow, Zatcoff and Gabbay, 2009; Borkow *et al.*, 2010a; Borkow *et al.*, 2010b).

1.7 Established Toxicity of AgNMs and CuO NMs

1.7.1 AgNMs

The toxicity of AgNMs has been widely studied in many models. In the bacterial model, it was found that the growth of many bacteria such as *Escherichia coli*, *Staphylococcus aureus*, *Leuconostoc mesenteroides*, some clinical-isolated strains, as well as the aerobic and anaerobic bacteria obtained from wastewater treatment plants, was suppressed by exposure to AgNMs (Kim, 2007; Choi and Hu, 2008; Kvitek *et al.*, 2008; Raffi *et al.*, 2008; Vertelov *et al.*, 2008). In addition, it was found that not only concentration, shape, and size of AgNMs, but also the release of Ag^+, were important factors in causing cell damage. Ag^+ has also been considered as a key factor of antibacterial properties and toxicity to algae of AgNMs (Fent, 2010). However, the antimicrobial activity of AgNMs is partially involved in the release of Ag^+. There was additional activity against microorganisms that was found in only the nanoparticulate form of Ag, not in the bulk or ionic forms (Chen and Schluesener, 2008). The minimum inhibitory concentration (MIC) of AgNMs to bacteria was found to be in the range of 0.1-20 mg/L, and 10-100 mg/L in eukaryotic cells (Chernousova and Epple, 2013). The growth of fungi, *Aspergillus niger* and *Saccharomyces cerevisiae*, was inhibited by the commercial antiseptic Myramistin® which contains 10 nM AgNM with MIC of 5 mg/L (Vertelov *et al.*, 2008). As well as in viruses, the replication of Hepatitis B virus was inhibited by 10 nm AgNM, while the attachment to host cells of HIV-1 was interrupted by 16 nm AgNM (Elechiguerra *et al.*, 2005; Lu *et al.*, 2008).

Toxicological studies of AgNMs in other organism cell lines such as zebrafish, fruit fly, clams, rats, and humans also indicated adverse effects from exposures to AgNMs (Braydich-Stolle *et al.*, 2005; Hussain *et al.*, 2005; Arora *et al.*, 2008; Asharani *et al.*, 2008; Hsin *et al.*, 2008; Kim *et al.*, 2008a; Kim *et al.*, 2008b; Sung *et al.*, 2008; Yeo and Kang, 2008; Arora *et al.*, 2009; Yeo and Yoon, 2009; Ahamed *et al.*, 2010a). A study in zebrafish observed the diffusion of AgNMs (5-46 nm) to embryos through chorion pore canals, and the critical concentration to induce deformities and abnormalities to embryos was 0.19 nM (Hydutsky *et al.*, 2007). A biodistribution study of AgNMs in rodents found that liver, lung, and olfactory bulb were the sites where AgNMs can accumulate, and in some instances, cause damage (Braydich-Stolle *et al.*, 2005; Hussain *et al.*, 2005; Arora *et al.*, 2009). In addition, AgNMs were also found to pass through the blood-brain barrier (Sung *et al.*, 2008). A study in normal human lung

fibroblast cells, and human glioblastoma cells observed genotoxicity from AgNM (Asharani *et al.*, 2009). Other studies found that the toxicity in neuroendocrine cells, liver cells, lung cells and germline stem cells was mediated via oxidative stress by 5-100 mg/L AgNM, and the toxicity to these cell lines was in a concentration- and size-dependent manner (Braydich-Stolle *et al.*, 2005; Hussain *et al.*, 2005; Hussain *et al.*, 2006; Carlson *et al.*, 2008; Schrand *et al.*, 2008). The potential of AgNMs to produce reactive oxygen species (ROS) and oxidative stress has raised concern in their use in imaging neural tissues and cells since they might contribute to neurodegenerative diseases (Kedar, 2003; Jendelová *et al.*, 2004).

The hazard categories of NMs according to EU Directive 93/67/EEC (CEC, 1996) are depicted in Table 1.1. The toxicological review of three different metal NMs, Ag, CuO, and ZnO has categorised AgNMs as very toxic to aquatic organisms with median L(E)C_{50} of 0.01 mg/L (Bondarenko *et al.*, 2013). Since AgNMs are widely applied as antimicrobials and algicides (Nowack, Krug and Height, 2011), therefore AgNMs are considered to be the most toxic NM towards non-target aquatic organisms when compared to CuO and ZnO NMs with the median L(E)C_{50} of 2-3 and 0.08-3 mg/L, respectively (Bondarenko *et al.*, 2013).

Table 1.1: Classification of chemical substances acording to their hazard categories following the EU-Directive 93/67/EEC. The classification is based on the lowest median L(E)C_{50} of the key environmental organisms (CEC, 1996)).

Median L(E)C_{50} (mg/L)	Hazard categories
< 1	Very toxic
1-10	Toxic
10-100	Harmful
> 100	Not classified

1.7.2 CuO NMs

From the review of three NMs toxicity, Ag, CuO, and ZnO, CuO NMs were not as toxic as AgNMs to bacteria with the MIC of more than 250 mg/L (Bondarenko *et al.*, 2013). However, in crustaceans and algae, CuO NMs were the most toxic with a median L(E)C_{50} of 2-3 mg CuO/L. According to EU Directive 93/67/EEC (CEC, 1996), the authors suggested CuO NMs to be classified as toxic to aquatic organisms. The apparently contradictory findings of toxicity from CuO NMs to bacteria, crustaceans

and algae might be explained by the differences in test media and toxicological endpoints. The organic media used in bacteriological tests usually have high potential to complex with Cu ions, while the mineral media normally used in crustacean and algae studies often have not. From this fact, the life cycle of antibacterial products containing CuO NMs should be considered in terms of their ecological safety (Bondarenko *et al.*, 2013).

Cu ions were found to be more toxic than CuO NMs to all models except yeast and mammalian cells (Bondarenko *et al.*, 2013). In addition, CuO NMs might exert particle-specific toxicity in mammalian cell models. The authors suggested that endocytosis and solubility of CuO NM inside the cells (a 'Trojan horse' model) may lead to availability of Cu ions that cannot be regulated by standard homeostatic mechanisms (Bondarenko *et al.*, 2013). However, the toxicological tests reported were usually carried out in serum which might have coated or dispersed the NMs, therefore the increase in bioavailability by preventing the aggregation of NMs might be another explanation to this finding (Zook *et al.*, 2012). In the yeast model, *S. cerevisiae*, protein-rich medium and deionised water were chosen to conduct the experiment. It was found that CuO NMs were coated by peptides and proteins in the medium, and the sorption to the yeast surface became greater than that found in the deionised water. The viability of yeast was higher in the protein-rich medium. The authors suggested the dissolution of CuO NMs in the proximity of yeast cells might lead to stress caused by Cu ions (Kasemets *et al.*, 2013).

The studies on toxicity of CuO NMs in other aquatic organisms, including freshwater shredders (crustaceans), carp, protozoa, and mussels have also resulted in adverse effects mediated by CuO NMs (Mortimer, Kasemets and Kahru, 2010; Zhao *et al.*, 2011; Gomes *et al.*, 2012; Pradhan *et al.*, 2012). Studies in human respiratory and hepatocarcinoma cells also found that CuO NMs exerted adverse effects in terms of cell viability in a concentration-dependent manner (Sun *et al.*, 2012; Siddiqui *et al.*, 2013).

1.8 Possible Mechanisms of toxicity from AgNMs and CuO NMs

1.8.1 AgNMs

Although AgNMs are widely used as antimicrobials, the exact mechanisms of AgNMs to inhibit the growth of bacteria are not fully understood. Three common hypotheses proposed to explain the antibacterial properties are: (1) release of Ag^+ from AgNMs, which consequently leads to the interruption of ATP production and DNA replication (Hwang *et al.*, 2008; Smetana *et al.*, 2008), (2) generation of ROS mediated by Ag^+ and AgNMs (Kim, 2007; Hwang *et al.*, 2008), and (3) AgNMs directly damaging the cell membrane (Sondi and Salopek-Sondi, 2004; Choi and Hu, 2008; Raffi *et al.*, 2008; Smetana *et al.*, 2008). However, some studies have reported the inconsistency in these findings (Marambio-Jones and Hoek, 2010). To take into account of Ag^+, the full mechanisms of Ag^+ toxicity may not yet have been established, but it might be explained by the interaction with enzymes in the respiratory chain reaction such as NADH dehydrogenases, binding to the transport proteins, and disruption of phosphate uptake (Schreurs and Rosenberg, 1982; Dibrov *et al.*, 2002; Holt and Bard, 2005; Lok *et al.*, 2006). It is likely that dissolved Ag^+ from AgNMs should be at least a contribution to the toxicity of AgNMs (Marambio-Jones and Hoek, 2010). Asharani *et al.* (2009) have suggested that mechanisms of toxicity from AgNM to human cells might include the disruption of the respiratory chain, induction of ROS production, and interruption of ATP synthesis, resulting in DNA damage (Asharani *et al.*, 2009). Yang *et al.* (2009) have found the increase in frequencies of DNA mutation by AgNM in polymerase chain reaction (Yang *et al.*, 2009).

To explain the toxicity of AgNMs, the connection between Ag^+ and AgNMs must be considered. Smetana *et al.* (2008) found greater toxicity to bacterial cells from high surface area AgNMs compared to the coated Ag powder which has limited potential for the release of Ag^+. However, these authors suggested that coating Ag NMs might prevent their attachment to the surface of bacteria (Smetana *et al.*, 2008). In addition, Hwang *et al*. (2008) suggested that the toxicity of AgNM arises from the release of Ag^+ that distribute into cells and lead to ROS production. They observed a slightly lower effect from Ag^+ compared to AgNM in bacteria sensitive to superoxides, while the effect in bacteria prone to membrane damage was the same in Ag^+ and AgNM exposures indicating the specific nanoparticulate effect in generating oxidative stress (Hwang *et al.*, 2008). In human fibrosarcoma, and human skin/carcinoma cells, the

decrease in cellular glutathione levels was observed in the presence of AgNM, which indicates oxidative stress leading to cell damage and lipid peroxidation. In the same study, it was also found that the concentration causing apoptosis was much lower (0.79-1.56 µg/mL) than the concentration causing necrosis (12.5 µg/mL) (Arora *et al.*, 2008).

Another study in mouse fibroblast, and human colon cancer cells found that 50 µg/mL AgNM led to apoptosis in 43.4% of fibroblast cells, while 100 µg/mL AgNM induced necrosis in 40.2% of cancer cells (Hsin *et al.*, 2008). Le Pape *et al*. (2004) found the effects of Ag^{+}, superoxides, and hydrogen peroxide to inhibit the growth of *E. coli* on activated carbon fibres (Le Pape *et al.*, 2004). Similarly, Kim *et al.* (2007) indicated that the antimicrobial effect of AgNMs to *S. aureus* and *E. coli* was from free radical generation. Choi *et al*. (2008) observed the induction of ROS by Ag^{+}, AgCl, and AgNM. When comparing the growth inhibition of nitrifying bacteria through ROS production, AgNM showed the highest toxicity. This indicated that ROS was not the only factor in toxicity (Choi and Hu, 2008). In the presence of dissolved oxygen, metals such as Ag catalyse the generation of ROS (Stohs and Bagchi, 1995). Therefore, AgNMs may catalyse the production of free radicals, as well as inhibiting antioxidant defence mechanisms by interacting with glutathione (GSH) or binding to antioxidant enzymes (Carlson *et al.*, 2008).

1.8.2 CuO NMs

In the same way as AgNMs, toxicity from CuO NMs is suggested to be involved in the induction of ROS (Karlsson *et al.*, 2008; Fahmy and Cormier, 2009; Wang *et al.*, 2012). CuO NMs have been considered to interact with cellular oxidative components such as mitochondria, and redox active proteins (Wang *et al.*, 2012). As well as the released Cu^{2+} ions from CuO NMs, these NMs might produce free radicals, which sunsequently damage DNA strands and affect gene expression (Karlsson *et al.*, 2008). Moreover, Cu^{2+} ions are reactive chelators that might bind to other biomolecules or replace the metal ions in some metalloproteins, which might cause protein dysfunction. The dissolved Cu^{2+} ions from CuO NMs can also increase the local concentration of Cu^{2+} which might interfere with cellular ion homeostasis (Chang *et al.*, 2012). However, the study from Siddiqui *et al.* (2013) showed that toxicity from CuO NM in human liver carcinoma cells was not related to Cu^{2+} release since the amount of Cu^{2+} in

the medium was low and the study of Cu^{2+} on cell viability showed no apparent effect (Siddiqui *et al.*, 2013).

Adverse effects from CuO NMs in cell lines such as human lung epithelial, human cardiac microvascular endothelial, human kidney, human neuronal, human liver carcinoma cells, and catfish primary hepatocytes were found to involve oxidative stress (Fahmy and Cormier, 2009; Ahamed *et al.*, 2010b; Sun *et al.*, 2011; Wang *et al.*, 2011; Perreault *et al.*, 2012; Xu *et al.*, 2012). Piret *et al.* (2012) found cytotoxicity and proinflammatory response in human liver carcinoma cells exposed to CuO NMs, and suggested the mechanism of toxicity was from ROS production. Although evidence of apoptosis found in the transcriptomic study was found, the underlying mechanism to type I programmed cell death was still unclear (Piret *et al.*, 2012).

In contrast to Piret and colleagues' work, Siddiqui *et al.* (2013) confirmed oxidative stress and apoptosis was induced by CuO NM exposure (Siddiqui *et al.*, 2013). The level of end product of membrane lipid peroxidation, malondialdehyde (MDA), was significantly increased along with the decrease in intracellular glutathione (GSH) in a concentration-dependent manner. In addition, the rescue effect from N-acetyl cysteine (NAC) was observed in all concentrations of CuO NM (Siddiqui *et al.*, 2013). Furthermore, mitochondrial membrane potential (MMP) was significantly decreased after exposure to CuO NMs, which indicated the occurrence of apoptosis via the intrinsic pathway. In the same study, the regulation of apoptotic genes was also examined by quantitative RT-PCR. The significantly up-regulated genes included tumour suppressor gene (*p53*), and pro-apoptotic genes (*bax* and *caspase-3*), while the anti-apoptotic gene (*bcl-2*) was significantly down-regulated. The similar finding from the protein expression study confirmed the pattern of apoptotic gene regulation (Siddiqui *et al.*, 2013). A study on CuO NM exposure to airway respiratory cells also observed the reduction of catalase (CAT) and glutathione reductase (GR) enzymes along with the increase in glutathione peroxidase (GPx) activity, which indicated oxidative stress. From the ratio of oxidised to glutathione and the decreased in the activities of CAT and GR, the authors also concluded that the oxidative damage from CuO NM was caused by both the increase in production of ROS and the inhibition of antioxidant defence (Fahmy and Cormier, 2009).

1.9 Toxicological mechanisms investigated in this project

Although recent studies have proposed many possible mechanisms of toxic effects from Ag and CuO NMs, this project investigated two key possible mechanisms, oxidative stress and apoptosis.

1.9.1 Oxidative stress

ROS have functions, which are either potentially advantageous or noxious. The appropriate amount of ROS supports the signal transmission pathways (Suzuki, Forman and Sevanian, 1997), and ROS also have an important role in immunological defence mechanisms. The production of ROS inside cells is mainly from oxidative phosphorylation, which occurs in aerobic respiration. Some enzymes, such as xanthine oxidase and metal-catalysed oxidation are also involved in the release of ROS inside cells (Hancock, Desikan and Neill, 2001). Moreover, ROS are released by activated neutrophils and phagocytes to destroy invading bacteria (Babier, 1978). However, an excess amount of ROS leads to oxidative damage to cells, so called oxidative stress. Many biological macromolecules such as lipids, proteins, nucleic acids, and carbohydrates are subject to oxidative chain reaction by ROS, and one important biological outcome of oxidative stress is lipid peroxidation (Kannan and Jain, 2000).

The connection between oxidative stress and apoptosis has been suggested. ROS has been proposed to play a role in the initiation and execution phase of apoptosis (Ott *et al.*, 2007). The mitochondrial genome has been found to be prone to oxidative damage, and it has been suggested that the mitochondrial arrest induced by oxidative stress is one of the factors causing programmed cell death (Kannan and Jain, 2000). Many reports focusing on toxicity from NMs have pointed out oxidative stress induced by NMs (Fahmy and Cormier, 2009; Xu *et al.*, 2012; Manke, Wang and Rojanasakul, 2013). A proposed model has suggested that the antioxidant enzyme system is the cellular response to oxidative damage. In mild oxidative stress, phase II antioxidant enzymes are up-regulated through the induction of nuclear factor (erythroid derived 2)-like 2 (Nrf2). At a higher oxidative stress level, a proinflammatory response is induced by mitogen activated protein kinase (MAPK) and nuclear factor kappa-light-chain-enhancer of activated B-cells (NF-κB). In the utmost degree of oxidative stress, cell death occurs by mitochondrial membrane damage and electron chain dysfunction, as shown in Figure 1.1 (Manke, Wang and Rojanasakul, 2013). A suggestion to explain

toxicity from NMs indicates that small particle size leads to the change in structure and electronic properties on the surface of particles, thus the surface of NMs become more reactive (Donaldson and Tran, 2002; Oberdörster *et al.*, 2005). In addition, the dissolution of metal NMs releases ions that are able to increase the production of ROS (Knaapen *et al.*, 2004).

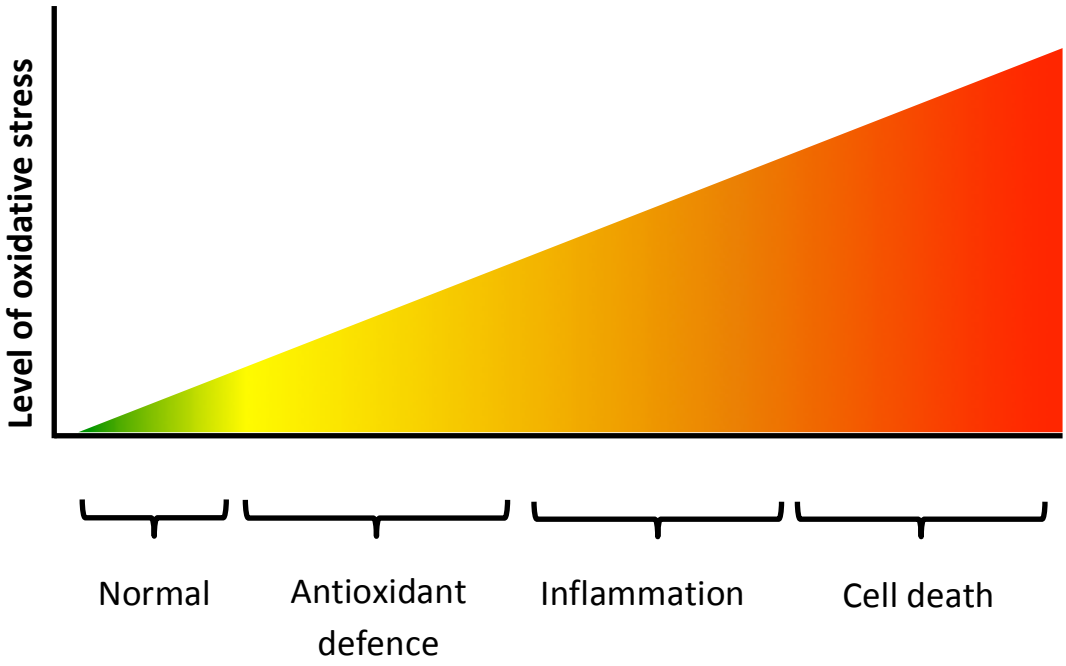

Figure 1.1: A model representing the consequences of oxidative stress. The lowest amount of oxidative stress results in normal cell response, however, at a particular threshold, oxidative stress induces the production of antioxidants. At a higher amount of oxidative stress, the inflammatory response is the major outcome. At the highest level, a cytotoxic response is induced via apoptosis (adapted from Nel, Xia and Li (2006)).

Based on Figure 1.1, the author investigated the effect of NMs by exploring the response in the alteration of antioxidant defence, and the induction of cell death.

1.9.2 Programmed cell death (PCD)

PCD is a mechanism to remove unwanted cells. This death mechanism is used with many biological processes, such as in development and homeostasis to balance the number of cells, as a defensive response to destroy infected or injured cells, and in aging (Vaux and Strasser, 1996). PCD is also found in unicellular organisms which is thought to be an altruistic process, for example, to prevent the spreading of infection to the entire colony of bacteria (Shub, 1994). This mechanism can be triggered by the dying cell itself (intrinsic) or from the neighbouring cells (extrinsic). There is also another pathway involved in cytotoxic T lymphocytes that rely on the activity of perforin and granzyme to destroy the dying cells. These three pathways are connected at the activation of execution caspase, caspase-3, and they influence one another (Igney and Krammer, 2002; Martinvalet, Zhu and Lieberman, 2005).

Necrosis is different from PCD in that it responds to the acute injury or physical damage in an unordered manner, and it involves inflammation. The stages of necrosis are also different from programmed cell death type I (Apoptosis). Necrosis is a response which occurs in a large number of injured cells, leading to cell swelling, rupture of organelles and plasma membrane, consequently leakage of cell contents. While the elimination of cells in apoptosis is cleaner, starting from the separation of the dying cell, cell shrinkage, condensation of cytoplasm and chromatin, and fragmentation of cell contents producing apoptotic bodies, which are ingested by phagocytes and degraded. However, response to stimuli can lead to either apoptosis or necrosis, depending on the type and/or degree of those stimuli (Elmore, 2007). The activation of apoptosis is also results from an extremely high level of oxidative stress, as shown in Figure 1.1.

Defects in apoptosis can lead to various types of diseases, for example, some neurodegenerative diseases such as Parkinson's disease are caused by the increase in apoptosis of neurons, whereas reduced apoptosis induces cancers or autoimmune diseases (Lawen, 2003). Apoptosis has been shown to be a consequence of oxidative stress induced by NMs (Hsin *et al.*, 2008), in which the mitochondrial pathway is the main pathway to cell death from metal oxide NMs (Xia *et al.*, 2006).

1.10 The potential contribution of this thesis to the current literature

The purpose of the research work described in this thesis was to understand the toxicity of widely used NMs, Ag and CuO, in the whole organism, *Caenorhabditis elegans* to provide information on how the toxicity, if any, is induced in the nematode. Since numerous toxicological studies were conducted in particular cell lines, using the whole organism like the nematode would provide better understanding on how the toxicity occurs. Moreover, *C. elegans* is a soil/sediment dwelling organism. It has been well established that NMs usually end up in this part of the environment. Therefore the study of this species is essential to understand the toxicity of NMs.

Although a number of studies on *C. elegans* are available in the literature, those were conducted in laboratory media, which might not be suitable to understand the behaviour of NMs in environmental systems. The research described in this thesis was carried out in simulated soil pore water (SSPW), which is more appropriate to conduct toxicological studies with *C. elegans*. Furthermore, the pathways of toxicity induced by NMs have not been fully explained. Since the *C. elegans* genome has been fully sequenced, and this nematode shares highly conserved genes with other higher eukaryotes, this was an area of focus in this study. The pathways of toxicity studied in this project and the results obtained will inform the potential pathways of toxicity of the NMs studied and will also potentially be applicable to other species.

1.11 Aim and objectives of this study

1.11.1 Aim of the study

The aim of this study is to examine the toxicity of engineered NMs in *C. elegans,* and identify the potential mechanisms of any adverse effects observed.

1.11.2 Objectives

1. To optimise the conditions required to maintain and test *C. elegans* in the laboratory.
2. To obtain a set of NMs, e.g. AgNMs (OECD JRCNM03002a, previously NM300K), Ag rods (OECD NM302) and CuO NMs (Sigma-Aldrich), and characterise their physicochemical properties in terms of size, shape, zeta-potential, and dissolved fraction, to study the relation between NMs properties and their possible toxicity.
3. To assess the toxicity of these NMs compared to their ion counterpart to different strains of *C. elegans* with various knockout genes to study the likely differences in sensitivity of each strain to help elucidate the possible mechanistic pathways of toxicity arising from NM exposure.
4. To assess the effects of NMs exposure using transcriptomics and proteomics to provide further insight into the mechanisms of toxicity of the selected NMs. Genes and proteins of particular interest include those related to to oxidative stress and apoptosis.

1.11.3 Aims by chapter

Chapter 2 – To optimise the conditions required to maintain and test *C. elegans* in the laboratory including the investigation of medium and the presence of bacterial food source.

Chapter 3 – To determine the physicochemical properties and behaviour of NMs in the test medium, and compare their characteristics in the test medium to SSPW without humic acid (SSPW-HA) and milli-Q water.

Chapter 4 – To investigate any adverse effects regarding mortality and inhibition of reproduction, induced by NMs. To compare any toxic effects of NMs with ionic form and bulk particles, if available.

Chapter 5 – To establish the induction of oxidative stress from NMs and compare any toxic effects with the ionic form or bulk particles, if available. The toxic effects in terms of the generation of reactive oxygen species and the alteration of oxidative stress-related enzymes are investigated.

Chapter 6 – To investigate the induction of apoptosis by NMs. The experiment is conducted by using a visualisation technique and apoptotic proteins determination.

Chapter 7 – To gather detailed information on how transcriptomes and proteomes of wild type *C. elegans* have altered when exposed to JRCNM03002a. Knowledge on molecular endpoints such as genes and proteins would provide an explanatory understanding on the pathways of toxicity.

Chapter 2: Optimising the conditions of *C. elegans* culture

2.1 Introduction

The *C. elegans* model had not been used at Heriot-Watt University when these studies started and so the first step was to set up a successful animal culture. It was necessary to determine which conditions were optimal and practical for maintaining the *C. elegans* culture, such as selection of growth medium (solid or liquid medium), frequency of transferring *C. elegans* to fresh medium to avoid starvation and desiccation, the method used for transferring *C. elegans*, and synchronising the nematodes for the experiments.

2.2 Aims of this chapter

Apart from establishing the *C. elegans* facility, at the beginning of this project it was important to generate a protocol to avoid contamination of the *C. elegans* culture. The medium used, nematode growth medium (NGM), is also a good potential environment for other bacteria and mould to grow. Contamination was observed even when *C. elegans* cultures were freshly delivered from the supplier. In addition, the laboratory where these studies were performed, is not an aseptic room, where it is not possible to control the in full level of airborne particulates. Therefore, contamination can often be found in *C. elegans* cultures if they are not well managed.

The medium used in the toxicity tests was another important variable to consider. When studying metal NMs, it is important to consider that, at least partially, they may dissolve in the medium. These released metal ions may form complexes with other ions in the medium, which results in lower toxicity, if the toxicity of NMs is primarily caused by the released ions. Furthermore, the medium should be ecologically relevant, so that the results from this project should be able to predict the consequences of NMs in the real environment. Therefore, medium selection was another goal at the beginning of this project.

Another important factor was the determination whether the food source, *E. coli* strain OP50, should be present during the tests. There is no consistent approach with regards to whether *C. elegans* should be fed when conducting nanotoxicology studies. The presence of a bacterial food source might complicate the investigation of NMs' toxicity due to potential interactions or artefacts. This is particularly relevant, if metal

NMs are studied, which may have anti-bacterial function (e.g. Ag and Cu NMs). Absence of food may lead to starvation of *C. elegans* which may complicate the interpretation of results. Conducting experiments without feeding may lead to an extra stress to the worms. Comparative studies were therefore required to determine the impact of food availability on the toxicity of the chemicals studied.

2.3 Materials and Methods

2.3.1 Test organisms

Different strains of *C. elegans* were used in the experiments. *C. elegans* was cultured on nematode growth medium (NGM) plates (Stiernagle, 2006) seeded with *E. coli* strain OP50, and stored in the incubator to control the temperature to 20 ± 1 ˚C. Worms were transferred to the new seeded NGM plates every week to prevent the starvation and desiccation.

Chosen strains of *C. elegans* included wild type (N2), *mtl-2* deletion (VC128), *sod-3* deletion (VC433), and *ced-3* deletion (MT1522). The detailed description of each strain is provided below.

- *mtl-2* gene encodes metallothioneins which are a part of a defence mechanism. Metallothioneins prevent oxidative stress by chelating with the metal ions that induce the production of ROS via Fenton chemistry. Some studies also proposed that metallothioneins counteract with ROS directly, as seen in Figure 2.1. However, it needs to be considered that the scavenging with ROS might be non-specific and occur to any proteins not limited to metallothioneins. The *mtl-2* knockout *C. elegans* (VC128) should be less tolerant to oxidative stress than the wild type (Zeitoun-Ghandour *et al.*, 2011; Ruttkey-Nedecky *et al.* 2013).
- *sod-3* gene encodes superoxide dismutases which are the enzymes used to get rid of superoxide, one of the ROS, as shown in Figure 2.1. *C. elegans* with *sod-3* deletion (VC433) should be prone to oxidative damage (Honda and Honda, 2002)
- *ced-3* gene has pro-apoptotic function in *C. elegans*, as described in Figure 6.2. The lack of *ced-3* gene results in less apoptosis. This strain of *C.*

elegans (MT1522) should have tolerance than wild type in the presence of apoptotic-stimulating agents (Lettre and Hengartner, 2006).

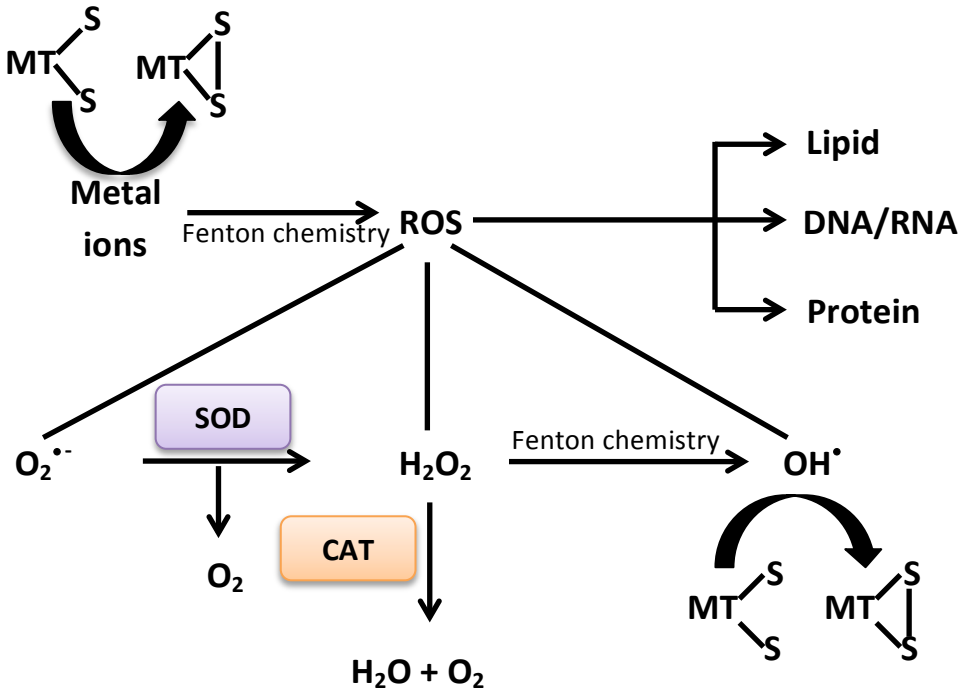

Figure 2.1: The mechanism of ROS in the induction of antioxidants. ROS leads to the damage of DNA, proteins, and lipids in cells. The detoxification processes such as superoxide dismutase (SOD), catalase (CAT), and metallothionein (MT) act together to remove or prevent the damage of molecules inside the cells. SOD catalyses the conversion of superoxide ($O_2^{\bullet-}$) to hydrogen peroxide (H_2O_2) and oxygen (O_2). CAT removes H_2O_2 to produce water (H_2O) and O_2. MT chelates with metal ions and prevents the Fenton chemistry and redox cycling that induce ROS generation. It is also proposed that MT scavenges the hydroxyl radical ($OH^{\bullet}$) (Adapted from Ruttkey-Nedecky *et al.,* 2013).

2.3.2 Maintaining the culture of food source E. coli strain OP50 (solid culture)

Nutrient agar (NA) plates were prepared by autoclaving the mixture of 2.3% w/v of NA and distilled water at 121 ˚C for 15 minutes, and pouring onto the 90 mm petri dishes. The NA plates were left on the bench with the lids on to let the condensed water evaporate for 1-2 weeks before use. To maintain the culture of *E. coli* strain OP50, a single colony of OP50 from the previous culture was picked and streaked onto the new

plate using an aseptic technique. Then, the seeded plate was incubated at 37 ˚C overnight to grow the OP50 culture. The *E- coli* culture was renewed into the new NA plates once a month.

2.3.3 Preparing the food source E. coli strain OP50 (liquid culture)

Nutrient broth (NB) was prepared by autoclaving the solution of 1.3 g of NB in 100 mL distilled water at 121 ˚C for 15 minutes. The broth was allowed to cool down before seeding with the OP50. To seed the broth with *E. coli*, a single colony of OP50 from the culture was picked and added into the broth using the aseptic technique. The seeded broth was incubated at 37 °C overnight, and then stored in the fridge (4°C) in the static condition. This liquid medium was renewed every week to avoid contamination.

2.3.4 Preparation of NGM plates and transferring the worms to NGM plates

Based on the maintenance guide of WormBook.org, a brief procedure of nematode growth medium (NGM) plate preparation for culturing *C. elegans* is described below.

To prepare a half-litre of NGM, 488 mL of distilled water was used to dissolve 1.5 g of NaCl, 8.5 g of agar, and 1.25 g of peptone. This was autoclaved at 121 ˚C for 30 minutes, and cooled in 55 ˚C water bath. After that, 0.5 mL of 1 M $CaCl_2$, 0.5 mL of 5 mg/mL cholesterol in ethanol, and 12.5 mL of 1 M KPO_4 buffer were added into the mixture using sterile technique. Then, the mixture was poured into the plates with a sterile technique to obtain approximately one-third of the volume of the plates. *E. coli* OP50 liquid culture was seeded onto the NGM plates by pipetting and streaking to distribute it all over the plate. The plates were left overnight at 37 ˚C to allow *E. coli* to grow.

C. elegans was transferred onto NGM plates by cutting a chunk of agar from a stock plate using sterile scalpel, and then putting it onto the new plates.

2.3.5 Procedure to avoid the contamination and cleaning of mould-contaminated C. elegans cultures

To avoid contamination, the bench was wiped down with 70% ethyl alcohol, and a laminar flow hood used for a preparation of NGM plates and transferring procedure of *C. elegans* culture maintenance.

The procedure to clean mould-contaminated cultures was adapted from the WormBook.org, and described in Figure 2.2. Briefly, a nematode in the contaminated plate is transferred into the new plate. The nematode is left to crawl past the bacterial (food) lawn to let the sticky bacteria trap and clean the mould out of the nematode's body. Once the nematode crawled to another side of the plate (away from the contaminated agar chunk), the nematode was transferred again to a new plate. This procedure was carried out twice to ensure the mould was removed completely from the nematode.

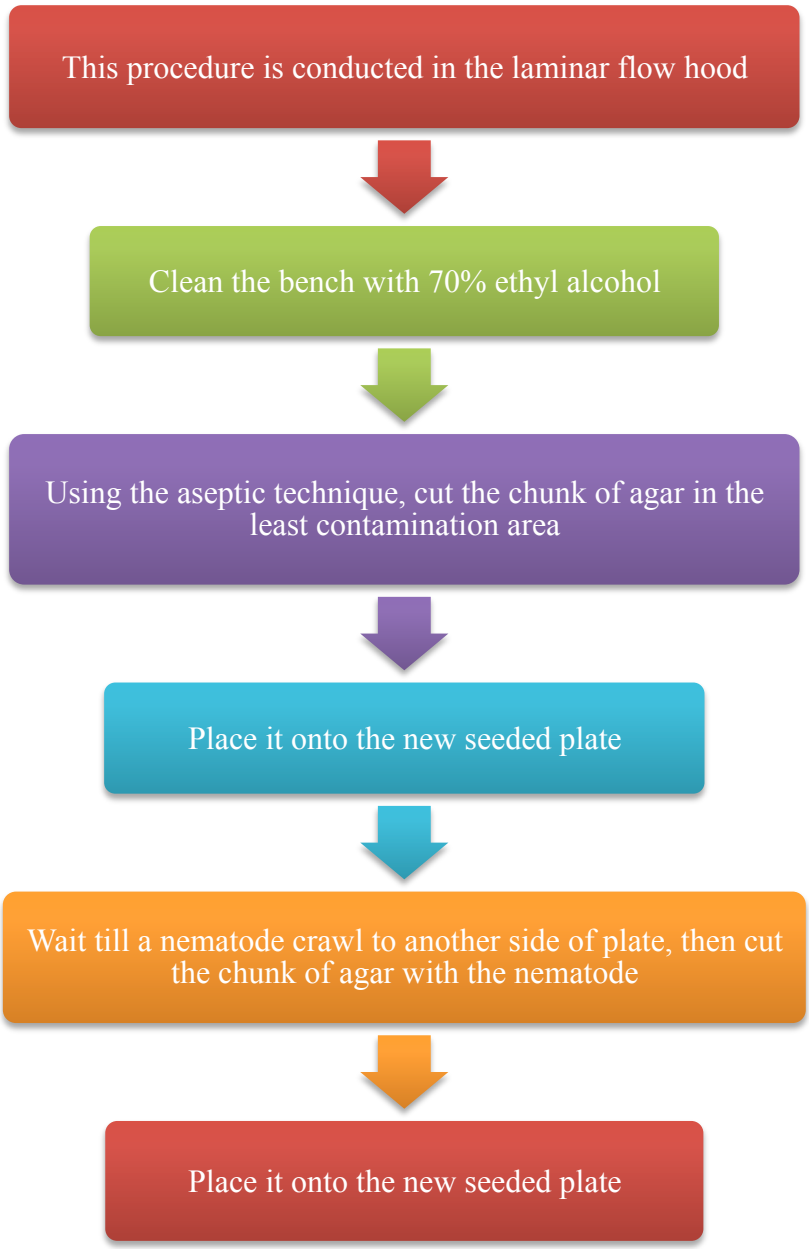

Figure 2.2: A schematic describing the process of cleaning mould-contaminated nematode cultures.

2.3.6 Synchronisation of C. elegans and cleaning the bacterial-contaminated cultures

Adapted from the maintenance guide Wormbook.org, synchronization of *C. elegans* was carried out as described in Figure 2.3. Briefly, the alkali bleach solution selectively dissolves the body of adult nematodes, but does not harm the eggs when they are exposed for a short amount of time (less than 12 minutes).

The eggshell of *C. elegans* consists of three outer layers; vitelline layer, chitin layer and proteoglycan layer. The outermost, vitelline layer can be removed by the alkali bleach solution, while the chitin layer is tolerant, and can be removed by chitinase. The shape of eggs is retained by the chitin layer. The proteoglycan layer is thought to be filled with fluid and proteins. The inner layers of eggshell are separated from the outer layers by the extra-embryonic matrix. This inner lipid-rich layers are composed of the thin permeability barrier layer and the peri-embryonic layer, which covers the embryo (Stein and Golden, 2015).

Figure 2.3: A schematic describing the process of *C. elegans* synchronisation.

2.3.7 Preparation of test media

The suitability of three commonly used test media, K-medium, U.S. EPA moderately hard reconstituted water (MHRW) and SSPW, was tested in this chapter. The compositions and ionic strength of all 3 media are presented in Table 2.1. (Meyer *et al.*, 2010; Ellegaard-Jensen, Jensen and Johansen, 2012; Tyne *et al.*, 2013).

Table 2.1: Compositions and ionic strength of K-medium, U.S. EPA moderately hard reconstituted water (MHRW), and simulated soil pore water (SSPW)

		K-medium	MHRW	SSPW
Compositions	KCl	32 mM	0.05 mM	
	NaCl	51 mM		
	Cholesterol	13 µM		
	$CaCl_2$	3 mM		
	$MgSO_4$	3 mM	0.50 mM	0.5 mM
	$NaHCO_3$		1.14 mM	4 mM
	$CaSO_4.2H_2O$		0.35 mM	
	KNO_3			1 mM
	$Ca(NO_3)_2$			1.25 mM
	Na_2HPO_4			1 µM
	HNO_3			1 mM
	Iron			1 mM
	Aluminium			1 mM
	Humic acid			1 mM
Ionic strength		254 mM	4.74 mM	10.3 mM

2.3.8 Preparation of $AgNO_3$ stock concentration

In this chapter, $AgNO_3$ was used to determine the applicability of each test medium, as well as the influence of bacterial food source, OP50. A stock concentration of $AgNO_3$ was prepared by diluting the correct amount of 0.1 N $AgNO_3$ (Sigma-Aldrich) with test media, and adjusting to 5 mL in a volumetric flask.

2.3.9 Preparation of bacterial food source in the test media

E. coli strain OP50 was pipetted out of the broth culture (NB) and spun at 8000 xg for 15 minutes. The supernatant was discarded and the bacteria were re-suspended in the media. The absorbance of bacterial in the media was measure at 600 nm and adjusted to 0.70 using media to ensure the sufficient amount of bacteria as food source for the nematodes during a 24 hour experiment (Budd, 2008).

2.3.10 Preparation of worm suspension

The suspension of nematodes was prepared by washing them out of the cultures using the media. Nematodes were let to settle for 10 minutes and the supernatant was removed. Worms were collected as a pellet, redistributed in the media and the concentration adjusted to be suitable for the tests. The concentration of the worm suspension was adjusted by adding media and pipetting the volume of worm suspension onto a slide. The number of worms per volume of suspension was counted and adjusted accordingly.

2.3.11 Preparation of exposures

The test was conducted in a 24-microwell plate with the total volume of 400 µL in each well. Worm suspensions were prepared to contain ~10 worms/10 µL. The correct volume of worm suspension was added into each well to obtain 10±5 of worms per well, as shown below in Table 2.2. The mixture containing $AgNO_3$ was prepared as shown in Table 2.2 for the study groups with food (OP50). To study the survival of nematodes in the absence of OP50, 40 µL of media was added to each well instead of the OP50 suspension to obtain the final volume of 400 µL. In the 72-hour exposure, half of the test solutions in each well were removed and the new test solution (including or excluding food source, depending on the condition of nematodes' group) was added accordingly. This procedure was carried out to maintain the food source and the required concentrations of $AgNO_3$ in the test exposures.

Table 2.2: Volume of $AgNO_3$ added into each well to make up the required concentrations (in the presence of OP50).

Concentration (µg/L)	OP50 (µL)	Media (µL)	1000 µg/L $AgNO_3$ stock solution (µL)	Worm suspension (µL)
500	40	150	200	10
400	40	190	160	10
300	40	230	120	10
200	40	270	80	10
100	40	310	40	10
50	40	330	20	10
0	40	350	0	10

2.3.12 Statistical analyses

The lethality models comparing the influence of OP50 were built using logistic regression in R (version 3.2.4). The significance of any differences in lethality across the treatments was compared using likelihood ratio test. The lethality plots were created in MS Excel (version 15.0.4805.1001).

2.4 Results

2.4.1 Media test

Both K-medium and EPA medium induced Ag precipitation when $AgNO_3$ was added into the media. Precipitation was observed with the naked eye even in the lowest concentration of $AgNO_3$ in the preliminary test (concentrations in the low µg/L). In addition, the reproduction of nematodes was lower than usual in EPA medium (data not shown). Therefore, both K-medium and EPA medium were excluded.

2.4.2 The presence of food source, OP50

C. elegans is capable to feed on dead bacteria (Meyer *et al.*, 2010). Therefore, the antibacterial effects of NMs should not affect the lethality of nematodes. From the initial test (preliminary test) results it was clear that the bacterial food source was key to

the viability of the longer test (over a 72 h time period), as shown in Figure 2.4. Therefore, the bacterial food source (*E. coli* strain OP50) should be added in the experiments with more than one-day exposure. In reality, food was included in all experiments except the ROS production assay (2-hour experiment) to maintain consistency across experiments.

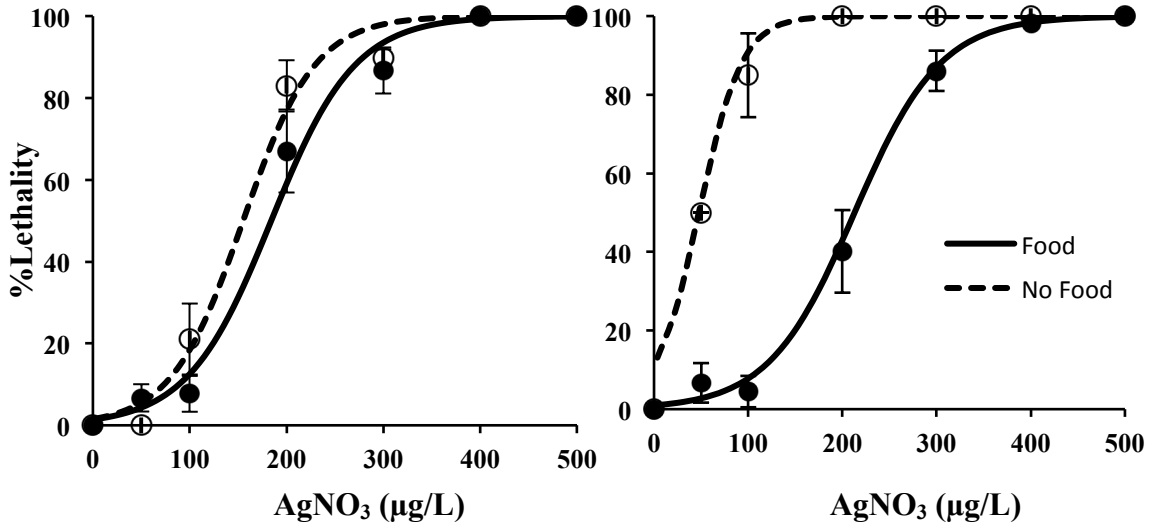

Figure 2.4: Lethality of wild-type *C. elegans* exposed to silver nitrate in the presence (solid line) and absence (dash line) of bacterial food source in 24 hours (left), and 72 hours exposures (right). In the group of 72-h exposure, the test concentrations were renewed everyday by removing half of the old test concentrations and refilling with the new test concentrations (with or without food) to maintain the food source, as described in section 2.3.11. Significant differences in lethality between food and non-food conditions were established only at 72 hours of exposure ($p < 0.01$).

2.5 Discussion

The experiments in this chapter were carried out to determine appropriate conditions for the toxicity tests. The purpose was to determine the most relevant conditions for *C. elegans* to grow in the test controls, and to avoid the effects from medium characteristics, such as ionic strength, salt concentration, water hardness, etc. to the NMs.

According to Donkin and Williams (1995), the testing medium was the most important factor in the study of *C. elegans* exposed to a range of chemicals. They stated that media with K^+ and Na^+ had a significant reduction in the observed adverse effects caused by various test chemicals i.e. cadmium (Cd), lead (Pb), Cu, and mercury (Hg) (Donkin and Williams, 1995). Khanna and colleagues (1997) also studied survival of *C. elegans* under different conditions in two media, K-medium and MHRW. They reported that *C. elegans* was able to live in K-medium and MHRW for 24 and 96 hours in the pH range of 3.1-11.9. They pointed out that *C. elegans* was more adaptable to a wide range of test conditions compared to other organisms used in aquatic toxicity tests (Khanna *et al.*, 1997). The pH of the medium in these tests was controlled to be in the narrow range of 6.5-7.0 to exclude the change in behaviour of NMs in the most acidic or basic conditions. However, the health condition of *C. elegans* might not be the only aspect to discuss in the toxicity tests since some chemicals in the media may form complexes with the test chemicals, leading to a possible reduction in toxicity. Although the mechanisms of toxicity from AgNMs are yet to be fully understood, it is thought that dissolution leading to the release of ionic silver (Ag^+) is likely to be involved at least to some extent, in the adverse effects from AgNMs (Hwang *et al.*, 2008; Smetana *et al.*, 2008). The dissolution of Ag is highly dependent on the conditions of the surrounding environment, such as pH, ionic strength and composition, NOM, therefore, bioavailability and toxicity of AgNMs caused by Ag^+ are varied in different media (Fabrega *et al.*, 2011). It is widely known that Ag(0) is not thermodynamically stable in the presence of oxygen, and is susceptible to oxidation with other ligands, such as sulphide, chloride, and organic matter (Levard *et al.*, 2012). Therefore, in the widely used aquatic media containing a range of relevant compounds, such as chloride, this could induce the precipitation of released Ag^+, and alter its bioavailability and toxicity.

As it was observed in the tests conducted and described here, precipitation was found in both K-medium and MHRW. However, Khanna and colleagues (1997) who focused on the lethality of *C. elegans* in the different media conditions, did not observe

a change in reproduction, which was found in this project, where nematodes were found to have a lower reproduction rate in MHRW than that found in SSPW. Therefore, and based on the above results, SSPW was chosen for the toxicity tests. This finding on the change of behaviour was in accordance to the studies from Yang *et al*. (2012) and Tyne *et al*. (2013). In terms of bacterial food source, OP50, was found to be important to nematodes' health where studies were carried out for longer than 24 hours, which corroborated the study by Donkin and Williams (1995), who found that the presence of bacterial food source, OP50, did not affect the health condition of nematodes in the test duration of 24 hours, whereas in the longer period of 96 hours, the absence of OP50 negatively influenced the growth and viability of the nematodes (Donkin and Williams, 1995).

Although the indirect effect of AgNMs to nematodes due to their bactericidal properties on bacterial food source was not studied in this project, there is evidence from Meyer *et al*. (2010) who showed that growth inhibition of AgNMs in nematodes fed by UvrA bacteria, which was prone to DNA damage by UVC, was not different in the UVC-treated, and non-treated group. Therefore, the authors concluded that growth inhibition was a direct effect from AgNMs (Meyer *et al.*, 2010).

2.6 Summary of this chapter

It was necessary to set up initially the best conditions for culturing of, and testing with, nematodes *C. elegans*, before starting the toxicological experiments. The results from these tests were essential to optimise the test conditions, and minimise interference from other factors. In this chapter, it was found that the most suitable medium to study the effects of metal NMs on *C. elegans* should consist of a low ionic strength medium. High ionic strength would likely lead to the complexation of any dissolved metal ions from NMs to the counterpart ion/chemical in the medium. Moreover, the selected medium should not interfere with the viability or reproduction of nematodes themselves, therefore, SSPW was considered to be the most suitable medium to use in this project. In terms of bacterial food source, *E. coli* strain OP50, it was demonstrated that nematodes were able to tolerate Ag^{+} in the presence of OP50 better than in the absence of a food source. This finding was significantly established in the longer test period (72 h). Although the food source was proven to be important in the longer period of exposure, the OP50 was added in all experiments, except the ROS production assay since it was conducted in the shorter period (2 h). The addition of OP50 to most experiments was to maintain the consistency of results between the studies which might be complicated by the presence of *E. coli*.

Chapter 3: Characterisation of AgNMs

3.1 Introduction

The risk assessment of NMs in the environment requires the evaluation on both effects and exposure (SCENIHR, 2005; Maynard *et al.*, 2006; Crane and Handy, 2007; EPA, 2007), and the possibility of exposure to NMs depends on their concentration in the environment. The prediction of the concentration of released NMs into the environment should be considered in relation to predicted releases of NMs which may cause toxicity, and this can be described by studying the fate and behaviour of NMs (Hassellöv *et al.*, 2008). As described in Chapter 1, NMs possess specific properties, such as size, shape, surface charge, composition, etc., which are different from conventional chemicals, therefore, solely forecasting NMs concentration in the environment is not sufficient to determine the risk of these particles in the ecosystem (Hassellöv *et al.*, 2008). In this chapter, the behaviour of NMs in the test conditions is investigated.

Characterisation of NMs is able to provide information on NMs evolution in the test system and also to provide information on the relationship between NM properties and any observed effects in *C. elegans*. Moreover, since the use of NMs is increasing in various types of end products and applications, the toxicological effects of NMs can potentially be compared (and extrapolations made) based on their characteristics, which again relate to their fate and behaviour in the environment (Hassellöv *et al.*, 2008). As well as the medium used in this project, which includes natural organic matter (NOM), Suwannee river humic acid, the characterisation of NMs in the presence and absence of organic matter is important to predict their fate in different environments.

Natural NMs such as colloidal clays, divalent metal oxides, and suspended organic matters (fulvic and humic acids) can be found in both aquatic and terrestrial environments (Wilkinson and Lead, 2007). These humic substances are a dominant part of these environments, and play an important role on the mobility and bioavailability of trace metals (Ghabbour *et al.*, 2001). It has been observed that these organic substances affect the stability and ion release of NMs. Liu and Hurt (2010) found that both humic and fulvic acids prevented the dissolution of AgNM in a concentration-dependent manner, where the increase in the concentration of organic matter inhibited the dissolution of AgNM (Liu and Hurt, 2010). The decrease in dissolution was suggested to be due to the adsorption of NOM to NMs (Dubas and Pimpan, 2008) and/or the

inhibition of oxidation by NOM as these organic matters act as reductant and induce the reversible formation of Ag^0 from Ag^+ (Sal'nikov *et al.*, 2009). The adsorption of NOM to NM enhances the repulsive energy between NMs by transferring the negative charge to the surface of NMs, thus the aggregation between NMs is inhibited (Zhang *et al.*, 2009). Gao and colleagues (2012) have also confirmed that the surface chemistry of AgNM in the aqueous phase was a major factor to NOM adsorption. However, they found the stability of AgNM was enhanced only in the low concentrations of NOM (< 10 mg/L of total organic carbon), while AgNM tended to aggregate and settle when higher levels of NOM (> 10 mg/L total organic carbon) were present (Gao *et al.*, 2012). The destabilisation of AgNM in the presence of high concentrations of NOM was proposed to be due to a bridging effect which was commonly found in industrial systems and water treatment systems where dispersants were used (Salehisadeh and Shojaosadati, 2001).

The dose-metric based on mass concentration is commonly used in ecotoxicological studies. It might be more informative to consider other dose-metrics such as surface area, particle number, particle mass, etc. in an addition to the mass concentration when studying the toxicity of NMs (Kennedy et al, 2015), although it is not always possible to record them in aqueous exposures. It was widely shown that nano-scale particles exhibit greater adverse effects than conventional bulk (larger) particles, which may arise from the larger surface area of those NMs. Therefore, it has been suggested that surface area of NMs is a relevant dose-metric for nanotoxicological study (Simko et al, 2014). Surface area also relates to the surface characteristics such as chemistry, charge, coating, porosity and reactivity, therefore it was proposed to be the best parameter to explain the toxicity from ultrafine particles (Oberdorster, 2005). While Oberdörster (2005) suggested the use of surface area in exposure studies, Wittmaack (2006)proposed that particle number should be a better metric to study the toxicity from the NMs- (Wittmaack, 2006). However, it should be taken into account that the toxicological mechanisms of NMs are varied. Particles which exert their toxicity through surface (dissolution, oxidation, photoreactivity, etc.) might be best described by the surface area, while particle number might be suitable for the toxicological study of the insoluble particles (Kennedy et al, 2015).

To date, there is no specific single method to analyse NMs. The techniques used for NM characterisation have been chosen by their appropriateness to evaluate their physicochemical properties of NMs as seen in Table 3.1. The main physicochemical

parameters to assess and thought to affect NMs toxicity are their structure, size, chemical composition, and dissolution (López-Serrano et al., 2014). The dissolution was widely proven to relate to the toxicity from NMs, especially for AgNMs (Li and Lenhart, 2012). Considering the impact of dissolution on toxicity, other characteristics of NMs that affect the dissolution, such as size, shape, and aggregation/agglomeration should also relate to the toxicity from NMs (Liu and Hurt, 2010). Particle size directly affects the surface area and reactivity of particles. Small particles have a larger surface area compared to larger particles. This large surface area drives the particles to be reactive, and have the tendency to interact with other molecules in the medium (Midander et al., 2009). The different degree of toxicity from different shaped NMs can also be explained by their surface area and reactivity. Surface coating and the tendency to aggregate also affect NMs toxicity by altering their surface reactivity. The aggregation/agglomeration commonly hinders the surface of particle, and causes the particles to have less interaction with the molecules around them (Li and Lenhart, 2012). Although these properties can be measured by various methods as described in Table 3.1, the techniques used in this thesis were based on their suitability and widespread use. Therefore, shape and size of NMs were visualised by transmission electron microscopy (TEM), the hydrodynamic diameter and aggregation state were determined by dynamic light scattering (DLS), and chemical composition and dissolution of NMs were measured by inductively coupled plasma-mass Spectroscopy (ICP-MS).

Table 3.1: Physicochemical properties of NMs and the methods that are used to determine these properties (Handy *et al.*, 2008; Hassellöv *et al.*, 2008; López-Serrano *et al.*, 2014)

	Methods	Benefits	Limitations
Physical properties			
Size/Size distribution/Shape/ Morphology	DLS	Non-invasive, sensitive, fast	Interference from larger particles, not suitable for polydispersed particles, not accurate for non-spherical particles
	FFF	High resolution, can be equipped with the detection techniques	Require large volume of samples
	TEM/SEM/AFM	Can visualise single particle	Time-consuming for statistical analysis, high sample perturbation
	NTA	Non-invasive, sensitive, fast	Limited to particles with high refractive index
Surface charge	Zeta-potential/ Electrophoretic mobility	High surface specific	No information on charge-heterogeneity
Crystal structure	XRD	Well established in geology	Require large amount of samples, has low sensitivity and spatial resolution compared to TEM/SEM
	TEM-XRD (SAED)	Very high resolution	Require specialised skill to perform
Chemical properties			
Composition	TEM-EDX	Can be used for elemental composition and quantitative analysis	Work best for heavy element with high concentration (>0.1%)

Table 3.1 (Cont.): Physicochemical properties of NMs and the methods that are used to determine these properties (Handy *et al.*, 2008; Hassellöv *et al.*, 2008; López-Serrano *et al.*, 2014)

	Methods	Benefits	Limitations
Other properties			
Bulk particle concentration	ICP-MS	High sensitivity, can be used in biological samples	Cannot distinguish between NM and ionic form
	ICP-OES	Simultaneous analysis of different particles	Low detection limit compared to LIBS
	LIBS	Most sensitive, need small sample volume	Reproducibility is limited to variation of laser spark and resultant plasma
	UV-Vis spectrometry	Non-invasive	Interference can be generated from turbidity of particles

FFF: field flow fractionation, SEM: scanning electron microscopy, AFM: atomic force microscopy, NTA: nanoparticle tracking analysis, XRD: X-ray diffractometry, SAED: selected area electron diffraction, EDX: energy dispersive X-ray analysis, ICP-OES: inductively coupled plasma-optical emission spectrometry, LIBS: laser-induced breakdown spectroscopy

3.1.1 Description of characterisation techniques conducted in this study

Dynamic light scattering (DLS)

DLS is a method to identify particle size in regards to its hydrodynamic diameter. Particles measured by this technique have to be suspended in a liquid. Size detection is examined using the radiation by a polarised laser beam. Excited particles consequently scatter the signal in all directions. The movement of particles, so called Brownian motion, affects the variation of scattered intensity at a given angle. The primary result obtained from the DLS equipment is the time Auto-correlation Function (ACF) of the scattered light intensity, which is further analysed to acquire the Particle Size Distribution (PSD) (Koniakhin *et al.*, 2015; Naiim *et al.*, 2015). The technique is non-invasive, quick, and has low running costs (Bootz *et al.*, 2004; Naiim *et al.*, 2015). It is capable of measuring particles in a wide size range of 3 to > 1000 nm. It also has

low sample perturbation (Ledin *et al.*, 1994). However, the drawbacks of this technique include the potential difficulty in the interpretation of the results. Furthermore, small particles are not be properly detected in the presence of large particles or aggregates/agglomerates. Therefore, it is problematic to measure the size of polydispersed particles as well as reading of highly aggregated or agglomerated samples (Hassellöv *et al.*, 2008). Another disadvantage of DLS is that this technique is based on the assumption of spherical particles, and so it is not in general suitable for the measurement of other shapes of particles (Malvern, 2010).

There are some parameters to be considered when using DLS. Firstly, the polydispersity index (PdI) of the sample. As stated above, polydispersed particles will potentially lead to an incorrect interpretation of the results, as larger particles hinder the scattered light intensity from the smaller particles. The PdI provided by Malvern Zetasizer is set to be between 0 and 1. This index is an estimate of the width of the particle size distribution, with a PdI below 0.5 normally considered as acceptable (Malvern, 2010). Another parameter to be considered is the intercept value. This value derives from the intercept of the correlation function of scattered light intensity. It determines signal-noise ratio and indicates data quality. Malvern Zetasizer is also programmed to be between 0 and 1 with an acceptable value of 0.85-0.95 (Malvern, 2010). The last parameter to be considered is the count rate, which determines the number of photons detected during the measurement. This value indicates the stability of the light intensity over time, thus the sample quality is monitored. A sufficient amount of photon signal during a particular reading should be at least 10 kilo-counts per second (kcps) above the dispersant count to allow accurate interpretation of the results (Malvern, 2010).

Zeta potential

With contact to aqueous solution, charges between particle surface and the solution are induced. Consequently free ions in the solution adjacent to the surface of particle are rearranged and a non-zero net charge layer is formed near this interface, where it is called the compact or stern layer. The non-zero net charge in the compact layer therefore attracts the counterions in the solution to balance the charges, and assembles another layer called slipping/shear plane or diffuse layer, where stationary and mobile phases are dissociated according to the movement of the particle in the liquid. The counterions in the compact layer are static because of the strong electrostatic attraction, while the ions in the diffuse layer are mobile (Sze *et al.*, 2003). These two layers together formed an electrical double layer (EDL) as seen in Figure 3.1. The electrostatic potential of both compact and diffuse layers is called electrokinetic potential or zeta potential, ζ (Xu, 2008). Studying the zeta potential is very important to predict the stability of NMs in the colloidal system in terms of their capability to agglomerate (Leroy, Tournassat and Bizi, 2011). Particles with a low absolute zeta potential are considered to have insufficient force to repulse other particles, therefore they tend to agglomerate, while large positive or negative zeta potentials ($> |\pm 30|$ mV) will have higher tendency to repel each other and therefore considered to form a stable suspension. However, the stability of NMs in aqueous suspensions is not only defined by zeta potential alone, other factors include the difference in density between particles and medium, pH, conductivity and the concentration of other components in the liquid (Malvern, 2010).

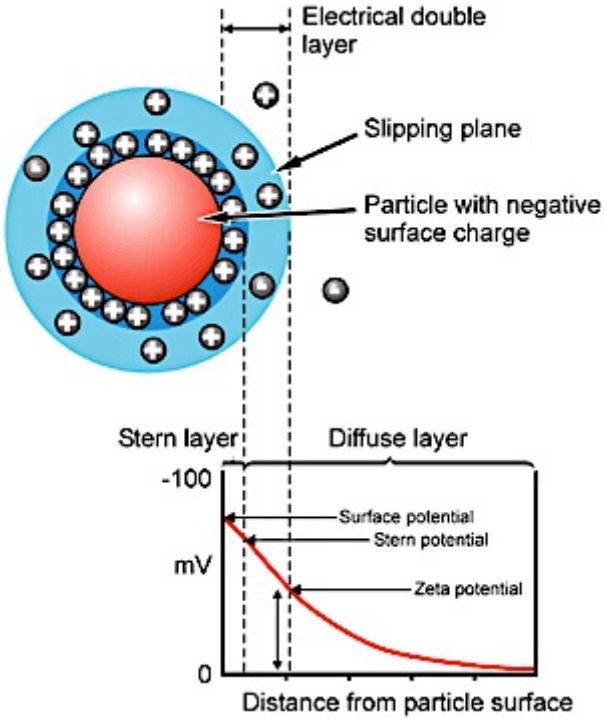

Figure 3.1: The electrical double layer at the surface of a NM in the aqueous solution (Taken from Nanocomposix, 2015)

Transmission Electron Microscope (TEM)

The general operation of electron microscopy is that an electron beam is used to visualise the sample instead of using a light beam as in light microscopy. Using the short wavelength electron beam gives the better optimal resolution than using light as the power source (Leadley, 2010). In electron microscopy, the beam of electrons collides with the sample surface, leading to the generation of secondary electrons, back scattered electrons, and transmitted electrons. These electrons are detected by different approaches. Secondary and back-scattered electrons are detected by Scanning Electron Microscopy (SEM), while transmitted electrons are detected by Transmitted Electron Microscopy (TEM). Types of electron generated from the bombardment reveal the different details of sample. Back scattered electrons exhibit only surface shape or surface arrangement of the sample, while transmitted electrons provide both three-dimensional structure and composition of the sample (Tikekar, 2015).

Inductively Coupled Plasma-Mass Spectroscopy (ICP-MS)

Inductively coupled plasma (ICP), tandem with mass spectroscopy (MS), is a sensitive and robust technique to determine the elemental composition of a sample. It provides an analysis of a sample with a wide range of concentrations from sub part-per-trillion (ppt) to part-per-million (ppm). In addition, it is useful to determine multi-element compositions as well as to distinguish only specific single elements within complex matrices with high speed analysis. Therefore, this technique is suitable to assess the concentration of NM in an organic sample (Scheffer *et al.*, 2008; Thomas, 2013). The brief principle of this technique is that the ICP source provides the ionised sample, which is detected and quantified by the MS. The major components of ICP-MS are illustrated in Figure 3.2. A liquid sample is injected into the spray chamber and converted into a fine aerosol by the nebuliser, then the aerosol is transported into the plasma torch to generate ions which are later extracted in the interface region, and transported into the vacuum chamber as an ion beam. This ion beam contains all ions in the sample, which are separated in the MS component by their mass-to-charge ratio and is refined to detect only ions of interest. The chosen ions are then converted into an electrical signal by the detector, and transformed into computational data, which gives the concentration of the analyte by calibrating with the relevant standards (Thomas, 2013).

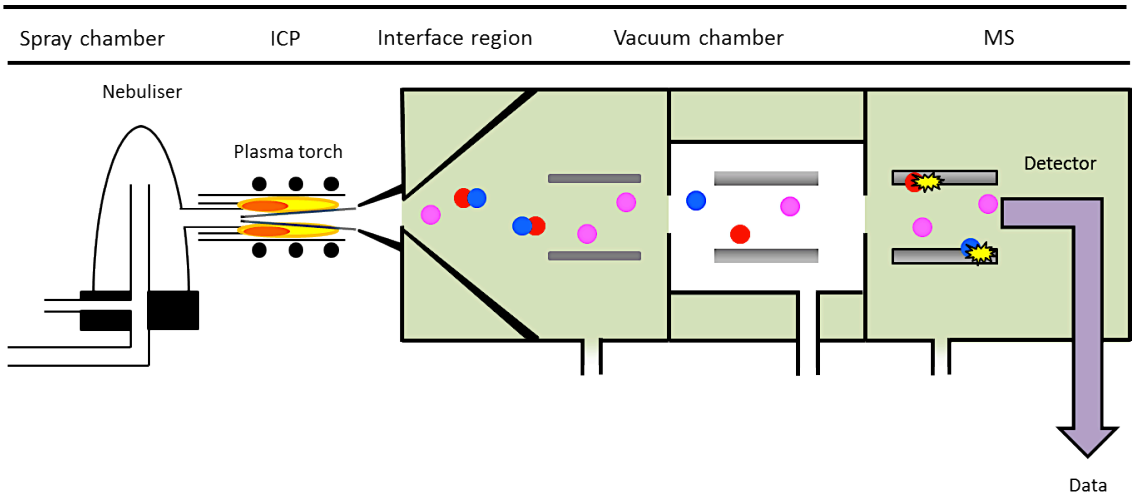

Figure 3.2: Major components of ICP-MS equipment (Adapted from Lung *et al.*, 2012)

3.2 Aim of this chapter

The main aim of this chapter was to determine the physicochemical properties and behaviour regarding aggregation/agglomeration of AgNMs in the test medium, simulated soil pore water (SSPW), compared to their characteristics in the test medium (SSPW) without humic acid (SSPW-HA) and milli-Q water. The results of this work will provide information necessary for the interpretation of the hazard data. This characterisation work concentrated on Ag NMs (instead of also CuO NMs) since they were the focus of the hazard research studies undertaken in this thesis.

3.2.1 Aims of DLS and zeta potential study

This study was conducted to examine the level of aggregation/agglomeration of AgNMs in the test medium, simulated soil pore water (SSPW) over the time period of 0-72 hours. Since the test medium contains NOM, Suwannee river humic acid, the experiment was conducted to compare the behaviour of AgNMs in the test medium without organic matter, as well as in milli-Q water in order to establish the influence of the salt components and organic matter on the behaviour of AgNMs in the test medium. The null hypothesis was that the level of agglomeration/aggregation of AgNMs was not influenced by the presence of the salt components, organic matter nor time period.

3.2.2 Aim of TEM study

The aim of the TEM study was to visualise AgNMs and examine the level of aggregation/agglomeration in the test medium, SSPW, compared to the medium without humic acid and to milli-Q water. The null hypothesis was that the level of agglomeration/aggregation of AgNMs was not influenced by the presence of the salt components nor by organic matter during the time period of 24 hours.

3.2.3 Aims of ICP-MS study

The aim of ICP-MS study was to quantify the amount of released Ag^{+} from AgNMs in SSPW during 24 hours.

3.3 Materials and Methods

3.3.1 Media preparation

SSPW and SSPW-HA were prepared by compiling the salts presented in Table 3.2. Each salt was purchased from Fisher Scientific, Longborough, UK, at the analytical reagent grade. Iron and aluminium standards were supplied from VWR international limited, UK. Suwannee river humic acid was sourced from International humic substances society. The stock solution of each salt was prepared by weighing and dissolving in milli-Q water to obtain 0.1 M with the weight provided in Table 3.3. Preparation of media was done by pipetting the correct volume of salt constituents as shown in Table 3.4 into a sufficient volume of milli-Q water to prevent the precipitation of some of the salts. After the addition of all components, the amount of milli-Q water was topped up to obtain 1 litre of media. Then the media were bubbled overnight to stabilise pH to be 8.2, which was later adjusted to 6.0-7.0 by using nitric acid 0.1 M before adding AgNMs.

Table 3.2: Composition of simulated soil pore water (SSPW) and SSPW without humic acid (SSPW-HA)

Composition	SSPW	SSPW-HA
$MgSO_4$	0.5 mM	0.5 mM
$NaHCO_3$	4 mM	4 mM
KNO_3	1 mM	1 mM
$Ca(NO_3)_2$	1.25 mM	1.25 mM
Na_2HPO_4	1 μM	1 μM
HNO_3	1 mM	1 mM
Iron standard	1 mM	1 mM
Aluminium standard	1 mM	1 mM
Humic acid	1 mM	

Table 3.3: Preparation of stock solution for each salt component

Composition	Stock	Weight per litre
$MgSO_4$	0.1 M	24.63 g of $MgSO_4.7H_2O$
$NaHCO_3$	0.1 M	8.4 g
KNO_3	0.1 M	10.1 g
$Ca(NO_3)_2$	0.1 M	16.41 g
Na_2HPO_4	0.1 M	35.8 g of $Na_2HPO_4.12H_2O$

Table 3.4: The amount of stock solution (0.1 M) added into the litre of media

Composition	SSPW	SSPW-HA
$MgSO_4$	5 mL	5 mL
$NaHCO_3$	40 mL	40 mL
KNO_3	10 mL	10 mL
$Ca(NO_3)_2$	12.5 mL	12.5 mL
Na_2HPO_4	10 µL	10 µL
HNO_3	10 mL	10 mL
Iron standard	0.559 mL	0.559 mL
Aluminium standard	0.270 mL	0.270 mL
Humic acid	50 mg	

3.3.2 DLS and Zeta potential

To compare size and zeta-potential of NMs in the absence and presence of organic matter, NMs were added into milli-Q water, SSPW-HA, and SSPW. Size and zeta-potential of NMs in different media were measured in the Malvern Zetasizer Nanoseries – Nano-ZS in the time-points of 0, 24, and 72 hours with the concentrations of 1, 5, and 10 mg/L for both AgNMs. Each concentration was prepared in three replicates. The equipment, Malvern Zetasizer Nanoseries, Nano – ZS was switched on at least 30 minutes before the measurements took place to allow thermal equilibration. Approximately 1 mL of sample was taken in the middle of the tube after a gentle shake, then carefully injected into the cuvette to prevent air bubbles which interfere with the reading. Hydrodynamic diameter and zeta potential were measured once per sample. The machine operated a number of measurement times (determined based on the

sample) to obtain the average hydrodynamic diameter. After the hydrodynamic diameter of the sample was attained, the same settings were adjusted to determine zeta potential.

3.3.3 TEM

To visualise the shape of the NMs, as well as to examine the agglomeration of AgNMs in the medium, NMs were spiked into milli-Q water, SSPW-HA, and SSPW 24 hours prior to the TEM analysis. The samples were prepared at Heriot-Watt University, and the TEM visualisation was performed in the University of Edinburgh. The suspension was gently shaken before sampling for TEM determination. A droplet taken from each sample was put on a Formvar/Carbon coated 200 mesh copper grid and left to dry for 15 minutes, then visualised in a Phillips CM120 transmission electron microscope (TEM, FEI UK Ltd, Cambridge, England) and the images were derived from a Gatan Orius CCD camera (Gatan UK, Oxon, England). The concentration of JRCNM03002a was prepared in the range of 1-5 mg/L as this was the concentration range tested in the hazard studies, while the concentration of NM302 was visualised in the wider range of 5-500 mg/L to study its agglomeration.

3.3.4 ICP-MS

Samples were prepared at Heriot-Watt University by the author. To determine the amount of dissolved silver from AgNMs in SSPW, the suspensions of AgNMs were prepared in the range of 1-5 mg/L for JRCNM03002a and 100-500 mg/L for NM302, as these ranges of concentration were used in the hazard studies. AgNMs suspensions were left standing for 24 hours in a static condition. They were then centrifuged at 25000 xg for an hour (Beckman Coulter Avanti J-26 XP centrifuge with JA-25.15 rotor). The supernatant, where dissolved silver equilibrated in, was collected for ICP-MS determination. The sample preparation was carried out by digesting the supernatant with 1% HNO_3. The pellet where AgNMs accumulated was collected and digested with 50% HNO_3. The pellet samples were used to determine the recovery of total silver. The ICP-MS analysis was performed by Dr. Lorna Eades at the University of Edinburgh using Agilent 7500ce operating by an octopole reaction system with an Rf forward power of 1540 W and backward power of 1 W. Argon gas in the carrier and makeup flows were at the rate of 0.81 L/min and 0.19 L/min, respectively. Sample solutions

were drawn into the Micro mist nebuliser at a rate of 1.0 mL/min. The analysis was performed with three replicate runs per sample. Rhodium isotope 103 (^{103}Rh) was used as an internal standard and added at a concentration of 200 µg/L. A series of standards were prepared using single element 1000 mg/L Ag (Perkin Elmer Pure) diluted with 2% v/v HNO_3 to give a range from 0.05-500 µg/L.

3.4 Results

3.4.1 DLS and zeta potential study

The hydrodynamic diameter of spherical AgNM was derived from DLS by taking into account the key parameters PdI, intercept, and count rate. It was found that all samples obtained the acceptable values for intercept and count rate, however, PdI values were higher than 0.5 in SSPW-HA and SSPW samples, which indicated the polydispersity of these samples. As seen in Figure 3.3, spherical AgNM in aqueous suspension exhibited a hydrodynamic diameter in the range of 60-80 nm in all samples. This range was also observed in SSPW-HA and SSPW. Nevertheless, the lowest tested concentration, 1 mg/L, showed a larger Z-average of 120-180 nm. However, considering these samples to be polydispersed, it might be the case that there was a higher level of aggregation/agglomeration of this material in the low concentration than in the higher concentrations of 5 or 10 mg/L. The zeta potential of the spherical AgNM suspension in milli-Q water indicated its stability in this medium. Over time, the zeta potential decreased (absolute value increase) from approximately -10 to -15 mV (0 hour) to -20 to -25 mV (24, 72 hours) whereas the zeta potential of spherical AgNM suspended in SSPW-HA and SSPW indicated that this material was unstable in these media, with values of -3 to -15 and -10 mV, respectively.

As illustrated in Figure 3.4, silver nanorod suspensions exhibited a Z-average value in the range of 500-1500 nm in aqueous medium and SSPW. Its hydrodynamic diameter was larger in SSPW-HA where it was found to be in the range of 1500-3000 nm. The zeta potential of 5 and 10 mg/L silver nanorod in milli-Q water ranged from -25 to -45 mV, which indicated good stability. However, the lower concentration of 1 mg/L displayed a zeta potential of +3 to -15 mV at the time points of 0 and 72 hours, which suggested that this suspension was unstable at those time points. Silver nanorod suspensions were also unstable in SSPW-HA and SSPW media with zeta potentials in

the range of -3 to -15 mV. However, most of the data obtained from these nanorod suspensions failed the acceptable values of PdI and intercept, which indicated that this AgNM was polydispersed and gained poor quality during the analysis. It was acknowledged that the principle of the DLS technique is derived from the Stokes-Einstein relation, which is applicable to spherical particles, therefore the application of DLS to rod-shaped NMs might not be suitable in the first place. Nevertheless, data from DLS might be informative to obtain an idea of these NM's behaviour in the chosen media. Visualisation via TEM provides more detail on size and agglomeration/aggregation state of this material, which will be discussed in section 3.4.2.

It has to be considered that the data provided in Figures 3.3 and 3.4 were derived from the Z-average of particle population with the highest intensity. As shown in Figures 3.6 and 3.7, there were different size distributions of AgNMs in SSPW. The data derived from the SSPW alone without AgNMs (figure 3.5) suggested that the size distribution of humic acid was in the range of 100-1000 d.nm. The samples of spherical AgNM, JRCNM03002a in SSPW clearly showed the size distribution of both AgNM (10-100 d.nm) and humic acid (100-1000 d.nm). The change in the intensities of size distribution was also observed within 72-hour experiments, as shown in Figure 3.6. As for the silver nanorod, this finding was observed in all samples, which could be explained by the tendency to aggregate/agglomerate as will be discussed in section 3.4.2, and from the principle that this technique is accurate for the spherical particle. Therefore this finding might not provide the correct results for silver nanorod samples. On the other hand, DLS was useful to explain the behaviour of spherical AgNM. It was indicated that there was aggregation/agglomeration of spherical AgNM in SSPW, and led to the high PdI of these samples. Moreover, it should also be considered that one of the size distributions retrieved from SSPW samples should also represent the particulate fraction of humic acid.

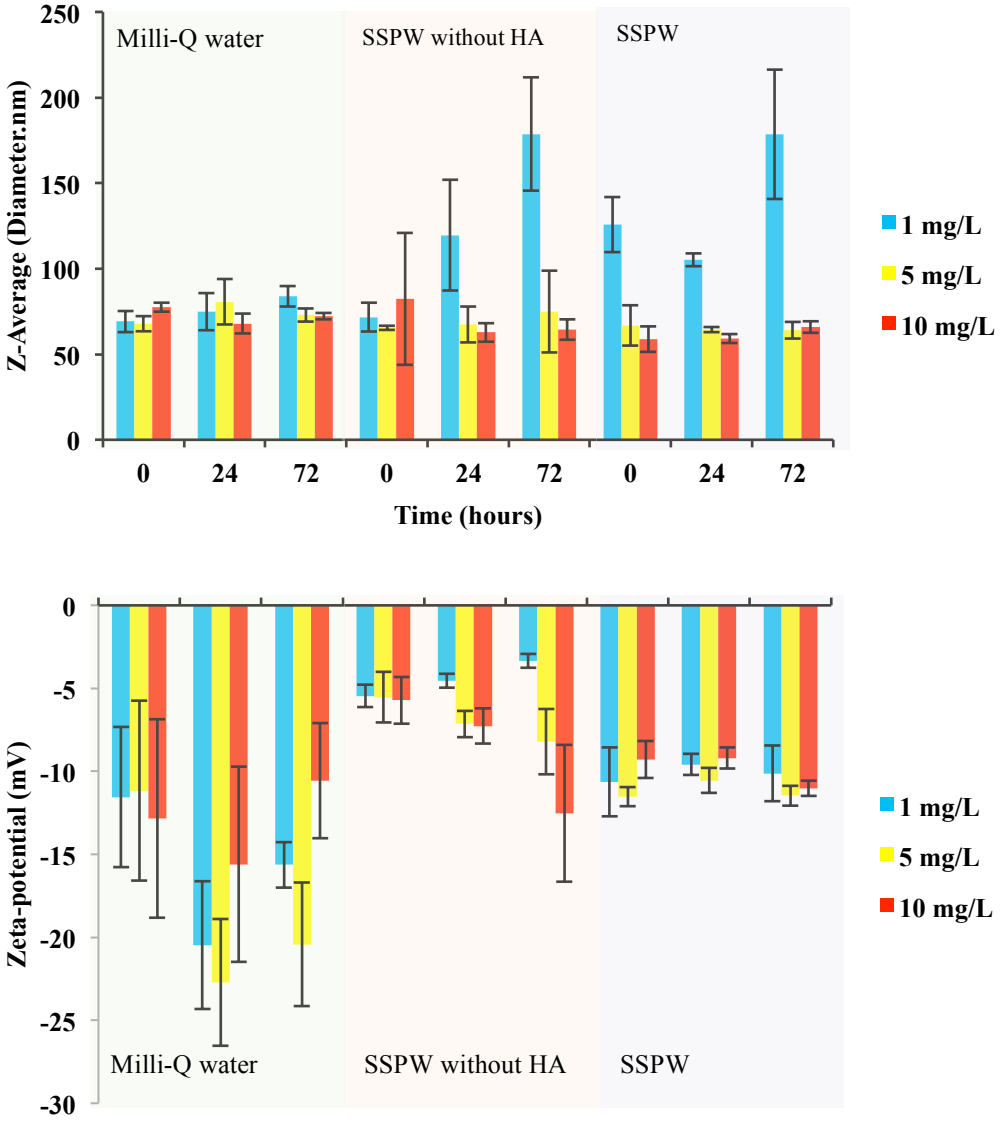

Figure 3.3: Hydrodynamic diameter (Z-Average) and absolute zeta-potential of 1-10 mg/L JRCNM03002a (spherical AgNM) in milli-Q water, SSPW-HA and SSPW in the time period of 0-72 hours. (Data shown as Mean ± standard error (SE) with 3 replicates)

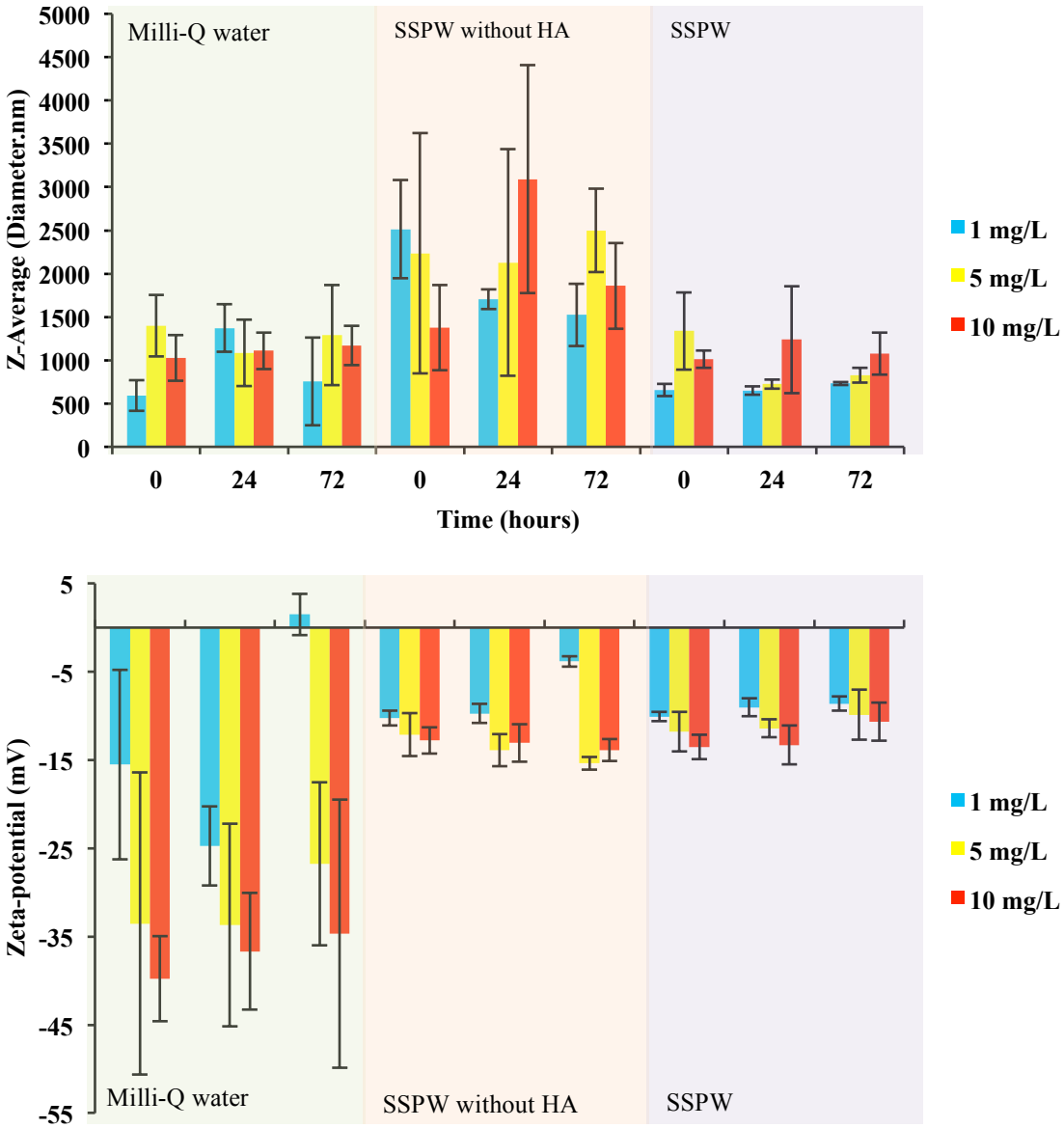

Figure 3.4: Hydrodynamic diameter (Z-Average) and absolute zeta-potential of 1-10 mg/L NM302 (rod-shaped AgNM) in milli-Q water, SSPW-HA and SSPW in the time period of 0-72 hours. (Data shown as Mean ± SE with 3 replicates)

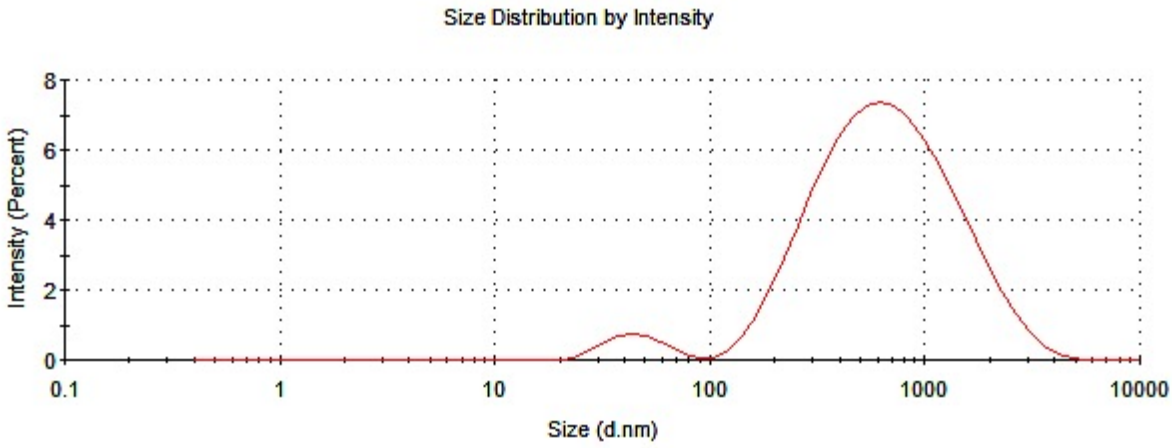

Figure 3.5: Size distribution by intensity of humic acid (50mg/L) in SSPW. The Z-average of humic acid was 456.2 d.nm. The data obtained with a PdI of 0.375.

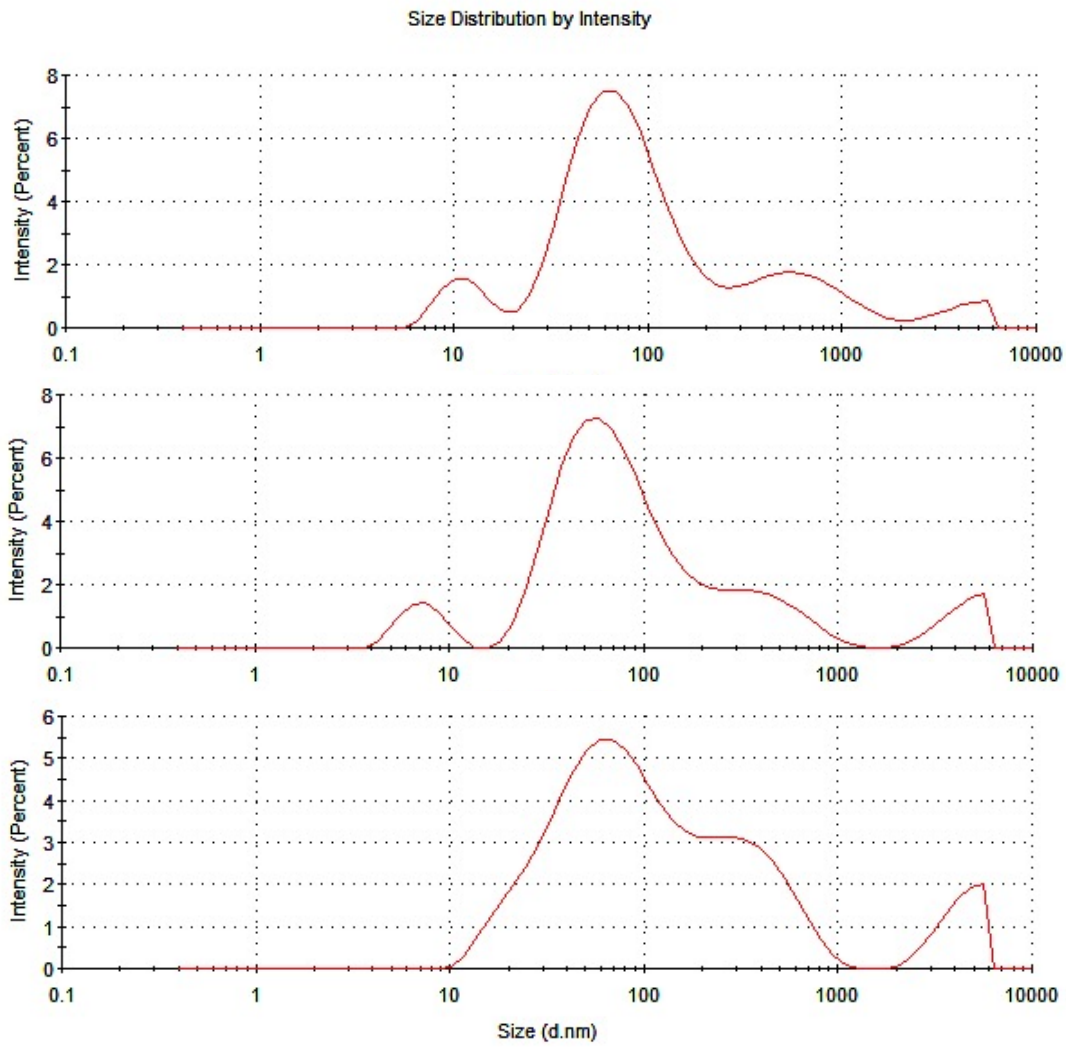

Figure 3.6: Size distribution by intensity of 10 mg/L JRCNM03002a in SSPW at A: 0 hours, B: 24 hours, and C: 72 hours. The PdI of these samples were between 0.623-0.819, which indicated the polydispersity of samples.

The highest signal from JRCNM03002a was found in the range of 10-100 d.nm. The small peak between 100-1000 d.nm was suggested to be humic acid particles, as seen in Figure 3.5. It was observed that the intensities of JRCNM03002a and humic acid changed during the experimental period. The intensity of JRCNM03002a tended to decrease, while the intensity from humic acid particles tended to increase. From this finding, it was suggested that JRCNM03002a formed aggregates/agglomerates with humic acid, therefore, its intensity was shifted to the higher size distribution. Although, the shift in intensity of JRCNM03002a was observed, it was still higher than the intensity in the range of 100-1000 d.nm, therefore, the Z-average remained stable, as shown in Figure 3.3.

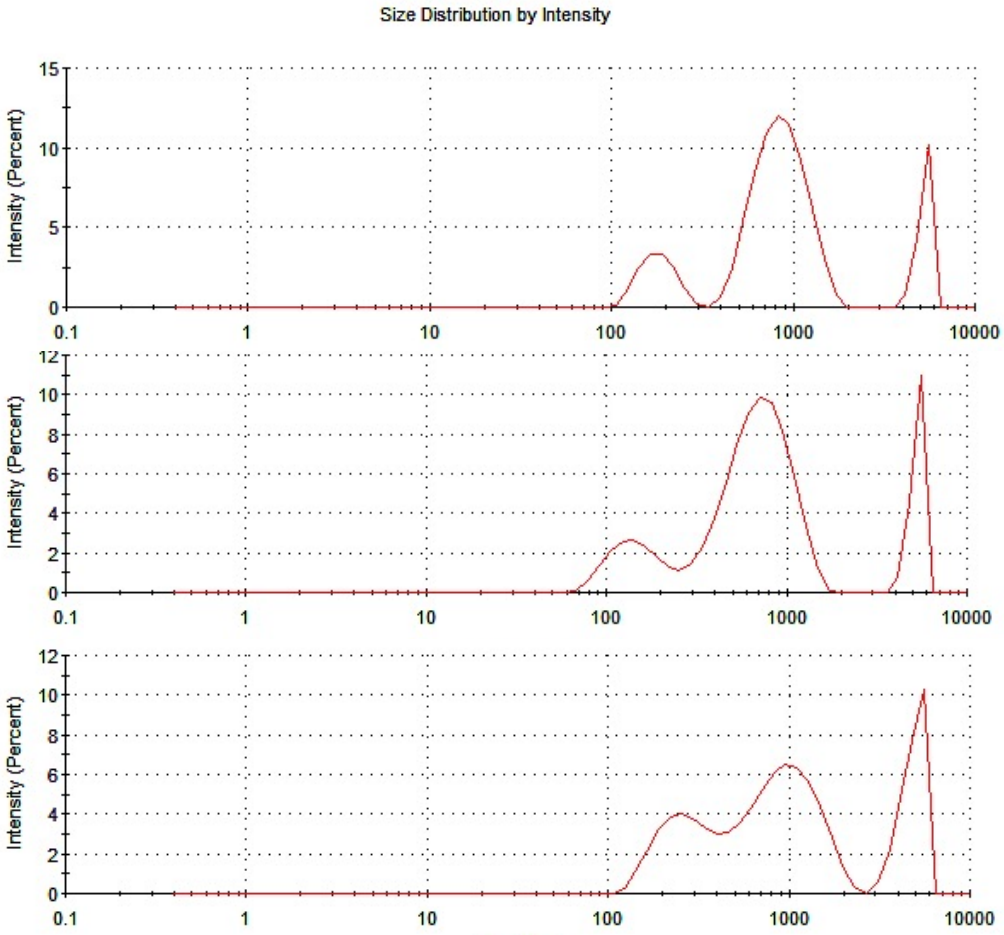

Figure 3.7: Size distribution by intensity of 10 mg/L NM302 in SSPW at A: 0 hours, B: 24 hours, and C: 72 hours. The PdI of these samples were in between 0.675-0.854, which indicated the polydispersity of samples.

Although, there were different size distributions in each sample, the highest signal was found in the range of 100-1000 d.nm, which was in the same range as the humic acid. The intensities of size distribution did not change as clearly as observed in the JRCNM03002a samples. However, it was obvious that this AgNM formed aggregate/agglomerate in SSPW.

3.4.2 TEM

The visualisation of AgNMs in milli-Q water, as illustrated in Figure 3.8, shows the appearance of NMs without other influential factors such as other salt components or organic matter in the medium. JRCNM03002a was observed as a spherical AgNM of about 20 nm in diameter, as described by the supplier. It existed as a single particle without any aggregation/agglomeration at any concentration (1-5 mg/L). The size of Ag nanorod, NM302, as given by the supplier, should be 50 nm in diameter, however the length was unstated. It was found in this study that the diameter of NM302 was 50 nm and the length was approximately 4-6 µm. Unlike JRCNM03002a, NM302 appeared as a homo-agglomerate in milli-Q water. The agglomeration of NM302 was found even in the lowest concentration of 5 mg/L as shown in Figure 3.8.

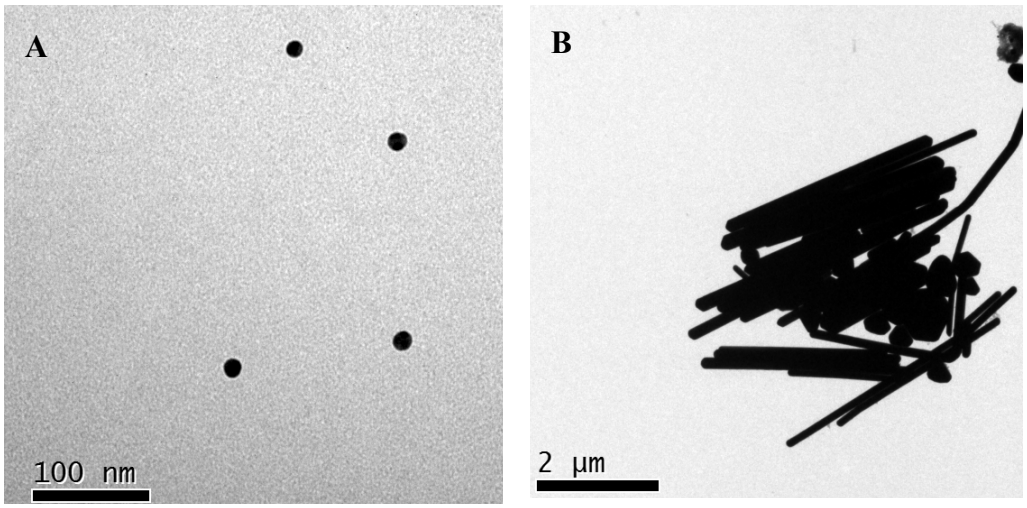

Figure 3.8: TEM micrograph of AgNMs in milli-Q water. A: 2 mg/L of JRCNM03002a, B: 5 mg/L of NM302, variable in length, some non-rod like material are the cross-section of the particles presented as the circles in the bunch of rods as they were organised randomly.

The imaging of AgNMs in the other two media, SSPW-HA and SSPW, was obtained to investigate the influence of other salt components and organic matter on the level of aggregation/agglomeration of AgNMs. The aggregation/agglomeration of spherical AgNM was observed in only SSPW, while it still appeared as a single particle in SSPW-HA (figure. 3.9). These aggregates/agglomerates of spherical AgNM were found more frequently in SSPW as higher concentrations as depicted in Figure 3.9. This finding indicated the impact of humic acid on the aggregation/agglomeration of spherical AgNM. This aggregation/agglomeration of spherical AgNM in SSPW might impair the suitability of using DLS to determine their size as they appeared as various sized particles, which explained the high value of PdI. Moreover, JRCNM03002a aggregates/agglomerates in SSPW were dense and the DLS signal from these larger particles might not be accurate. The agglomeration/aggregation of Ag nanorod was also observed in SSPW-HA and SSPW, as seen in Figure 3.10, however, it was difficult to state the influence of humic acid on the behaviour of nanorod since they tended to bind to each other in all media including milli-Q water.

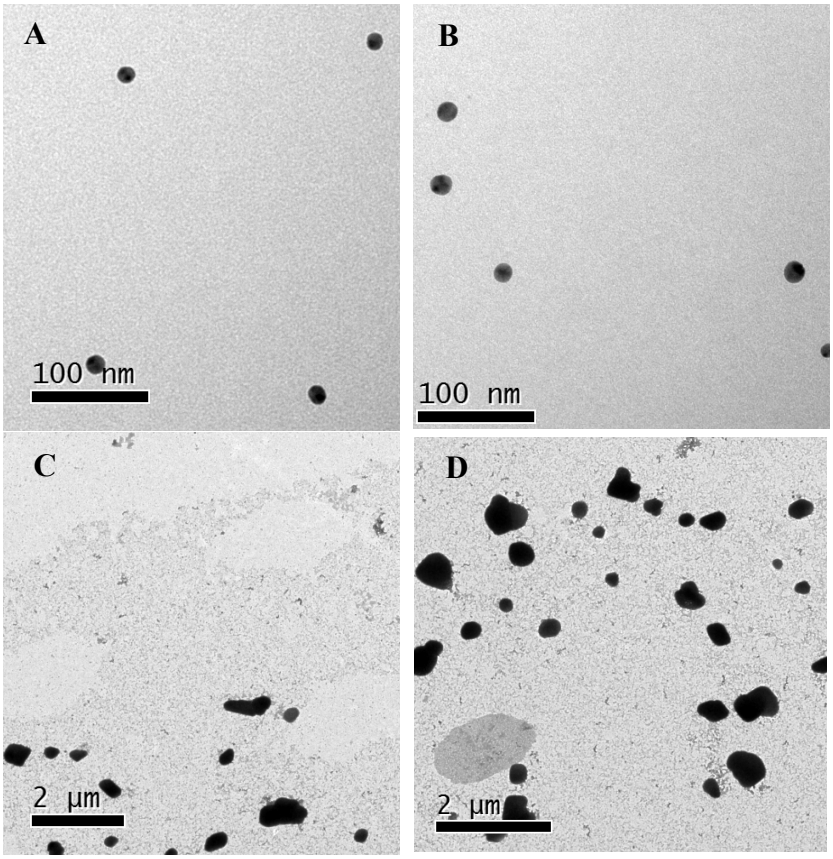

Figure 3.9: TEM micrograph of JRCNM03002a in the different media. The upper images (A-B) illustrated in SSPW-HA and the lower images (C-D) in SSPW. Images on the left were 1 mg/L AgNM and 5 mg/L in the right.

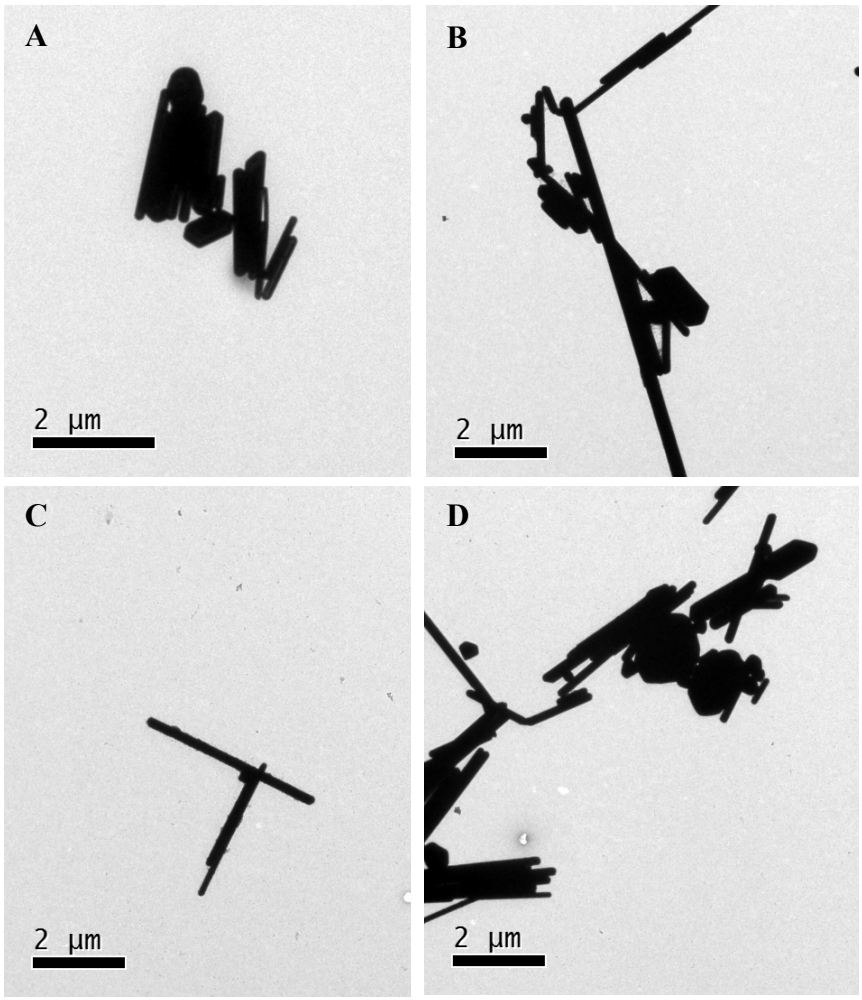

Figure 3.10: TEM micrograph of NM302 in the different media. The upper images (A-B) illustrated in SSPW-HA and the lower (C-D) in SSPW. Images on the left were 10 mg/L AgNM and 250 mg/L in the right.

3.4.3 ICP-MS

It was found that spherical AgNM suspensions resulted in higher silver dissolution than the silver nanorod. As shown in Figure 3.11, the amount of Ag^{+} released from JRCNM03002a (1-5 mg/L) was ~0.5-2.8 mg/L, and that from NM302 (100-500 mg/L) was ~0.1-0.6 mg/L. It was clear that the lower concentration of spherical AgNM produced a higher amount of dissolved silver than that generated from Ag nanorod suspensions.

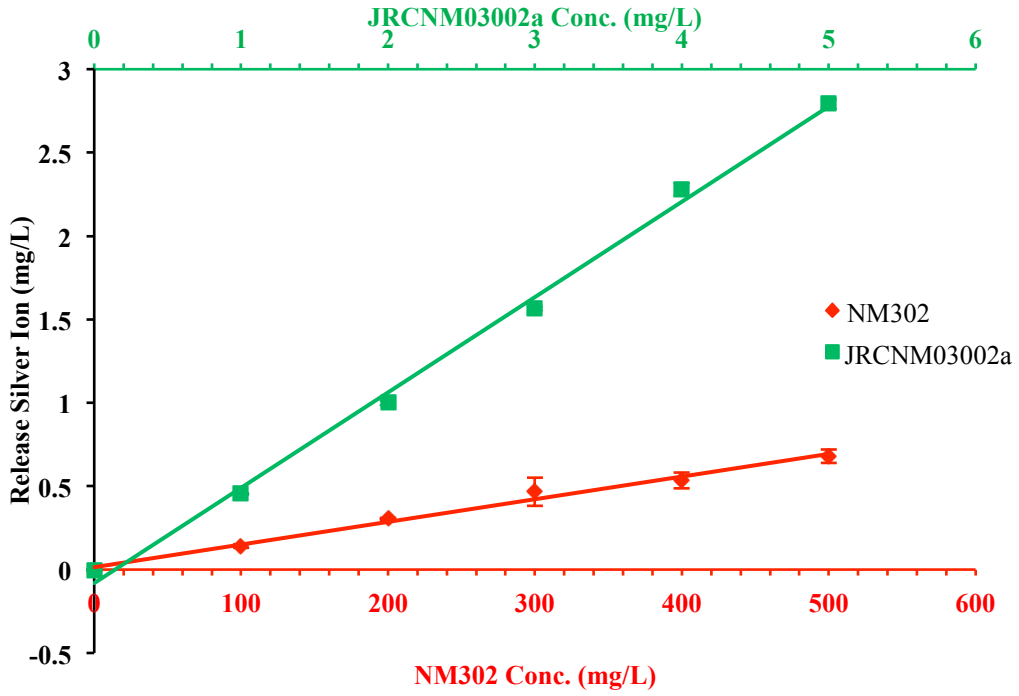

Figure 3.11: Amount of released Ag^{+} from spherical AgNM (green) and Ag nanorod (red) in SSPW over the time period of 24 hours (mean ± standard error (SE)). The dissolution of AgNMs was measured only in SSPW because it was used as the medium in the hazard assessment.

3.5 Discussion

As mentioned in section 3.1, the importance of NM characterisation was not limited to NMs risk evaluation, but also to assess the fate of NMs in media during assays, as well as to link the properties of NMs to their potential toxic effects (Brown and Gilham, 2010; López-Serrano *et al.*, 2014). Characterisation has now become an essential aspect in the studies of toxicity from NMs. Therefore, the work in this chapter was performed to gather information of AgNMs properties in the test conditions, which is important in the assessment of NMs risks.

3.5.1 DLS and Zeta-potential

To investigate the behaviour of AgNMs in regards to their aggregation/agglomeration in SSPW, as well as the impact of salt components and NOM (humic acid), samples of AgNMs in milli-Q water, SSPW-HA and SSPW were collected over the time period of 0, 24 and 72 hours. In milli-Q water, JRCNM03002a

was considerably stable with a relatively constant hydrodynamic diameter of 60-80 nm over 72 hours in all concentrations and the PdI showed no broad size distribution. It was also confirmed by its zeta potential that this spherical AgNM was moderately stable in aqueous dispersion. At 24 and 72 hours, with the zeta potential values were in the range of -20 to -25 mV.

Even though the mean hydrodynamic diameter of JRCNM03002a was approximately 55-80 nm in most samples, the low concentration of 1 mg/L in SSPW-HA and SSPW exhibited the average hydrodynamic diameter to be in the range of 120-180 nm. Moreover, the PdI derived from these samples indicated a broad size distribution with zeta potential values around -3 to -15 mV, which suggested that particles were not stable in these media. Therefore, it was suggested that there was an aggregation/agglomeration of spherical AgNM in SSPW-HA and SSPW. It might be the case that other salt components and organic matter had an influence on NM behaviour, while other factors such as time and concentration might not have a strong role in the aggregation/agglomeration, as seen in aqueous medium that these particles were dispersed as single particles.

It has been reported by the JRC that the hydrodynamic diameter of JRCNM03002a is dependent on the medium, although it is typically around 50-70 nm (Klein *et al.*, 2011). Therefore, a comparison of the results obtained from DLS measurement to other publications focused on JRCNM03002a in aqueous medium since there is a variety of media used in the literature. Connolly and colleagues found that a concentration of 93.5 mg/L of JRCNM03002a was stable in aqueous suspension with a hydrodynamic diameter of 54±6 nm (Connolly *et al.*, 2015). This finding was quite similar to the results reported in this thesis. However, it has to be considered that there are some limitations when comparing the DLS results to other studies since the methods and instrumentation used in the different laboratories are varied and can result in different values of size and size distribution (Klein *et al.*, 2011).

The stability of JRCNM03002a determined by zeta potential has shown that humic acid did not stabilise spherical AgNM in any concentration, which was contrary to some of the findings from the literature which indicate that stability of NMs increases in the presence of humic acid (Zhang *et al.*, 2009). However, the findings from this study were in agreement with the results from Gao and colleagues (2012), who proposed that a high amount of 10 mg/L organic matter could result in the instability of AgNM in aqueous suspension via bridging effect (Gao *et al.*, 2012).

The use of DLS to obtain the zeta potential and the agglomerate/aggregate size of rod-shaped NM, NM302, is unlikely to be a suitable approach since the principle of this equipment was generalised for spherical particles. However, it was decided to conduct the DLS measurements of Ag nanorod in order to obtain an overview of how these materials may behave in the media. The results showed that the hydrodynamic diameter of NM302 was in a range of 500-1500 nm in both milli-Q water and SSPW, and 1500-3000 nm in SSPW-HA. However, this NM gave PdI values of more than 0.5 in all samples, which meant that the size distribution was wide. Zeta potential values of NM302 ranged from +3 to -45 mV in aqueous suspension and -3 to -15 mV in SSPW-HA and SSPW, which suggested that they were not stable in any media.

Unlike JRCNM03002a, NM302 has not been widely studied. Therefore, it was challenging to compare the results obtained in this study with the available literature. Although, as stated above, the DLS technique is not suitable to determine size in regards to diameter and length of rod-shaped NMs, there are some studies focused on fitting mathematical models to estimate those metrics so that the dimensions of rod-shaped materials can be determined by the light scattering technique (Bolak and Danumah, 2014; Khouri, Shams and Tam, 2014). However, this estimation is based on the dynamic parameters and dimensions of cellulose nanocrystal, while the information on Ag is still absent. Furthermore, the use of visualisation techniques such as electron microscopy, is still required to confirm the estimates from these mathematical models. Therefore, it was decided to work on visualisation techniques to determine the dimensions of rod-shaped materials in this work.

3.5.2 TEM

To visualise and support the determination of size/dimensions of AgNMs from the provider, as well as to examine the presence of NMs aggregates/agglomerates, samples of AgNMs in milli-Q water were analysed to determine their natural state without including other potential factors such as salts or organic matter. The AgNMs dispersed in SSPW-HA and SSPW were also performed to examine the impact of salts and humic acid on AgNMs behaviour. All samples were prepared 24 hours prior to TEM analysis. It was observed that spherical JRCNM03002a was stable and dispersed in milli-Q water as single particles, whereas rod-shaped NM302 tended to attach to each other as agglomerates/aggregates. JRCNM03002a was confirmed to have the diameter

of approximate 20 nm as stated by the supplier, while NM302 had the diameter of ~50 nm with the length range of 4-6 μm.

It was found that the salt components in SSPW-HA did not affect the aggregation/agglomeration of any AgNMs. As JRCNM03002a was measured as single particles, this was contrary to the finding from DLS that the particles were polydispersed. The disagreement between these analyses might be described by the precipitation of some salts in the medium, leading to the detection as polydispersed particles in samples detected by DLS, while it was not observed in TEM. As for silver nanorods, the visualisation of aggregate/agglomerate of particles supported the presence of polydispersed particles in samples. Considering the presence of humic acid, JRCNM03002a were observed as clear aggregates/agglomerates. The aggregates/agglomerates of spherical AgNM in SSPW might complicate the determination of JRCNM03002a by using DLS since these aggregates/agglomerates were dense, which supported the wide size distribution of JRCNM03002a in SSPW. Although it was obvious that the humic acid had a clear role in spherical AgNM aggregation/agglomeration, it has to be taken into account that the clusters of rod-shaped NM302 in SSPW might not be fully comparable to the aggregates/agglomerates in milli-Q water or SSPW-HA. Therefore, the influence of humic acid on the behaviour of NM302 is still inconclusive.

Although Ag is not thermodynamically stable and should be fully dissolved, it was found that AgNMs did not dissolve completely in most cases (Peretyazhko, Zhang and Colvin, 2014) (Liu *et al.*, 2010a). The incomplete dissolution of AgNMs was suggested to be due to the adsorption of Ag^+ to the surface of AgNMs, which blocks the oxygen molecules to react with metallic silver, or else this could have been due to AgNMs aggregation (Liu *et al.*, 2010a). This might be one of the explanations also in this study, where lower amounts of Ag^+ released from silver nanorod were observed when compared to that from spherical AgNM. As visualised by TEM, rod-shaped NM302 tended to homo-agglomerate/aggregate, therefore this agglomeration/aggregation might have obstructed the reaction sites of AgNM and inhibit dissolution. The second reason might be that smaller size spherical JRCNM03002a might provide the higher surface area for reactions with the molecule of oxygen than the bigger nanorod, NM302.

3.5.3 ICP-MS

To study the toxicity of AgNMs, it was important to understand their dissolution profiles to assess the effect of Ag^+ might have on the potential toxicity of AgNMs (Fent, 2010). The quantification of the released Ag^+ from AgNMs in SSPW during the time period of 24 hours showed that smaller spherical NM, JRCNM03002a dissolved and yielded a higher amount of Ag^+ than bigger nanorod, NM302. According to Peretyazhko and colleagues (2014), the size of AgNMs has an essential impact on dissolution. The dissolution rate constant (pseudo-first-order) of Ag^+ released from AgNMs sized 6, 9 and 13 nm in water was found to be 1.24, 0.43 and 0.15, respectively. The rate of AgNMs size 70 nm dissolution could not be determined (could not be fitted) since it was not well dissolved and only yielded ~ 0.2 μM of Ag^+ throughout the 80-day experiments. In addition, Ag^+ released from 6 and 9 nm AgNMs reached a plateau after 2 days, while it took 3 days for AgNM sized 13 nm to reach that state. Furthermore, the same authors found the growth of AgNMs during the experiment and proposed the relevance of oxidation during dissolution of AgNMs. According to their explanation, metallic silver on the surface of AgNM reacts with dissolved oxygen in water and forms a shell of silver (I) oxide (Ag_2O), which explains the increase in AgNMs diameter. This Ag_2O layer later dissolves and yields Ag^+ (Peretyazhko, Zhang and Colvin, 2014).

Although Ag is not thermodynamically stable and should be fully dissolved, it was found that AgNMs did not dissolve completely in most cases (Peretyazhko, Zhang and Colvin, 2014) (Liu *et al.*, 2010a). The incomplete dissolution of AgNMs was suggested to be due to the adsorption of Ag^+ to the surface of AgNMs, which blocks the oxygen molecules to react with metallic silver, or else this could have been due to AgNMs aggregation (Liu *et al.*, 2010a). This might be one of the explanations also in this study, in which lower amounts of Ag^+ released from silver nanorod was lower than that from spherical AgNM. As visualised by TEM, rod-shaped NM302 tended to agglomerate/aggregate to each other, therefore this agglomeration/aggregation might have obstructed the reaction sites of AgNM and inhibit dissolution. The second reason might be that smaller size spherical JRCNM03002a might provide the higher surface area for reactions with the molecule of oxygen than the bigger nanorod, NM302.

3.6 Summary of this chapter

The null hypothesis of the DLS study proposed that the level of agglomeration/aggregation of AgNMs was not influenced by the presence of the salt components, organic matter nor time period. To accept or reject the null hypothesis, consideration should be made in a case-by-case basis. As for the silver nanorod, this study was unable to support the hypothesis as the principle of this technique is not suitable to analyse the non-spherical shaped material. Therefore, it was not practical to establish the change in level of aggregation/agglomeration of NM302 by using DLS. However, the null hypothesis that salts and humic acid would not influence the aggregation/agglomeration of JRCNM03002a was rejected. Rejection of the hypothesis was based on the observation that the samples of AgNMs of 1 mg/mL containing salts and NOM had a higher PdI, suggesting a greater size distribution and therefore more agglomeration/aggregation. However, the null hypothesis was accepted when considering time period as the hydrodynamic diameter of spherical AgNM remained steady during the 72-h experiment in milli-Q water.

In the TEM analysis, the hypothesis was proposed as the conjunction to the DLS determination to assess if agglomeration/aggregation of AgNMs was influenced by the presence of the salt components or organic matter. The TEM studies were not quantitative and so no null hypothesis could be tested as such. Nevertheless, this study was unable to determine NM fate changes in relation to media in the case of rod-shaped AgNM as this material binds as aggregates/agglomerates in their natural state. However, focusing on spherical AgNM, it is clear that there are changes across media., which was in contrast to the conclusion from DLS study. The explanation might be that the salt precipitates (salt crystals) might complicate the hydrodynamic size determination, resulting in the high polydispersity of samples. However, the assessment with regards to the presence of NOM resulted in aggregates/agglomerates clearly observed when JRCNM03002a was suspended in SSPW.

The summary of AgNMs properties obtained from this study and from the supplier is displayed in Table 3.5.

Table 3.5: Summary of characterization metrics obtained from the supplier and from this work

Properties	JRCNM03002a	NM302
Composition[a]	10.16 %w/w Ag	8.3 %w/w Ag
Stabilisers[a]	4 % of Polyethylene glycerol trioleate 4 % of Polyoxyethylene 20 4 % of Tween 20	No Data
Size	~20 nm (TEM)[a, b]	~50 nm diameter[a, b], 2-4 µm in length[b]
Shape[a, b]	Sphere	Elongated rod
Form[a]	Suspension	Suspension
Hydrodynamic diameter (nm)[b,c]	69.18 ± 6.25 nm	591.97 ± 176.15 nm
Zeta potential (mV)[b,c]	-11.55 ± 4.24 mV	-15.51 ± 10.74 mV
State[b]	Stable with no aggregation/agglomeration	Tend to agglomerate to each other
Dissolution[b]	~50%	~0.1%

a = data obtained from the supplier (Joint research centre, European commission), b = data obtained from this study, c = from samples containing 1 mg/L AgNMs in milli-Q water

Chapter 4: Standard methods of hazard assessment

4.1 Introduction

It was mentioned in section 1.4 that *C. elegans* provides a number of advantages in their use in toxicological studies. The introduction of this chapter will focus on the life cycle and sexual forms of *C. elegans*. This nematode has a life cycle of three days, from egg until its development into egg-laying adults. This life cycle can be observed when the nematode is maintained at 25˚C. However, the life cycle can be shorter or longer depending on the temperature of the culture (Lewis and Fleming, 1995). Starting from embryogenesis, which takes approximately 18 hours at 20˚C, the embryo is capable to develop independently inside its mother, an egg is laid when the embryo is evolved into 30-cell stage. After that, the embryo is hatched when it has 558 nuclei and then the first larval stage (L1) begins. *C. elegans* has four larval stage developments, L1-L4. At the end of each larval stage, the nematode enters a sleeping period called lethargus, when it starts to produce the new cuticle. The nematode is active again by moulting its old cuticle, in which the next larval stage begins. *C. elegans* usually occurs as a hermaphrodite, which is reproductive for 2-3 days, and lives for 2-3 weeks before dying (Corsi, Wightman and Chalfie, 2015), as can be seen in Figure 4.1.

When the culture is too crowded or the food source is depleted, an alternative life cycle can be activated in the L2 animal. Instead of moulting into a normal L3 stage, the nematode is develops into a dauer larva (Hu, 2007), whose cuticle covers its mouth preventing it from eating, consequently stopping its development. The cuticle of the dauer nematode provides the protection against chemicals, caustic agents, and environmental stresses which allows the animal to survive for months. When the dauer larva is introduced into the food source, it is able to develop into a slightly different L4 larva (Corsi, Wightman and Chalfie, 2015) , as seen in Figure 4.1.

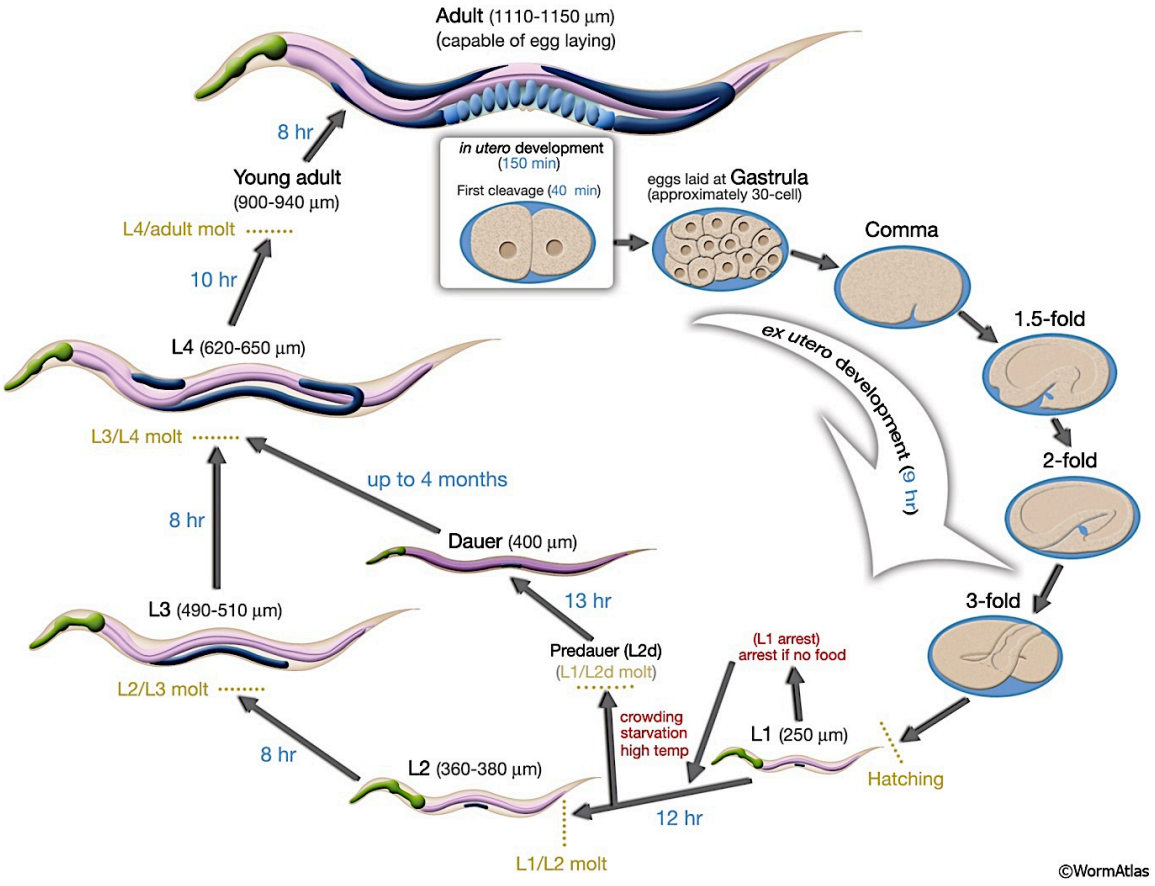

Figure 4.1: *C. elegans* life cycle at 22˚C (Taken from Altun and Hall, 2009)

The sexual forms of the wild type *C. elegans* are hermaphrodites and males. However, the frequency of male nematodes is less than 0.2%, therefore, the reproductive system of hermaphrodite will be the focus in this section. The hermaphrodite nematode contains two arms of a U-shaped gonad, which contains ovotestis that generates sperm. During the L4 stage, sperm is stored in the spermathecal, as illustrated in Figure 4.2. When the nematodes enter adulthood, germ cells shift their function to produce the oocytes. The hermaphrodite can then become self-fertilised and produce up to 300 offspring. When mating with a male nematode, the hermaphrodite can reproduce approximately 1000 progeny (Corsi, Wightman and Chalfie, 2015).

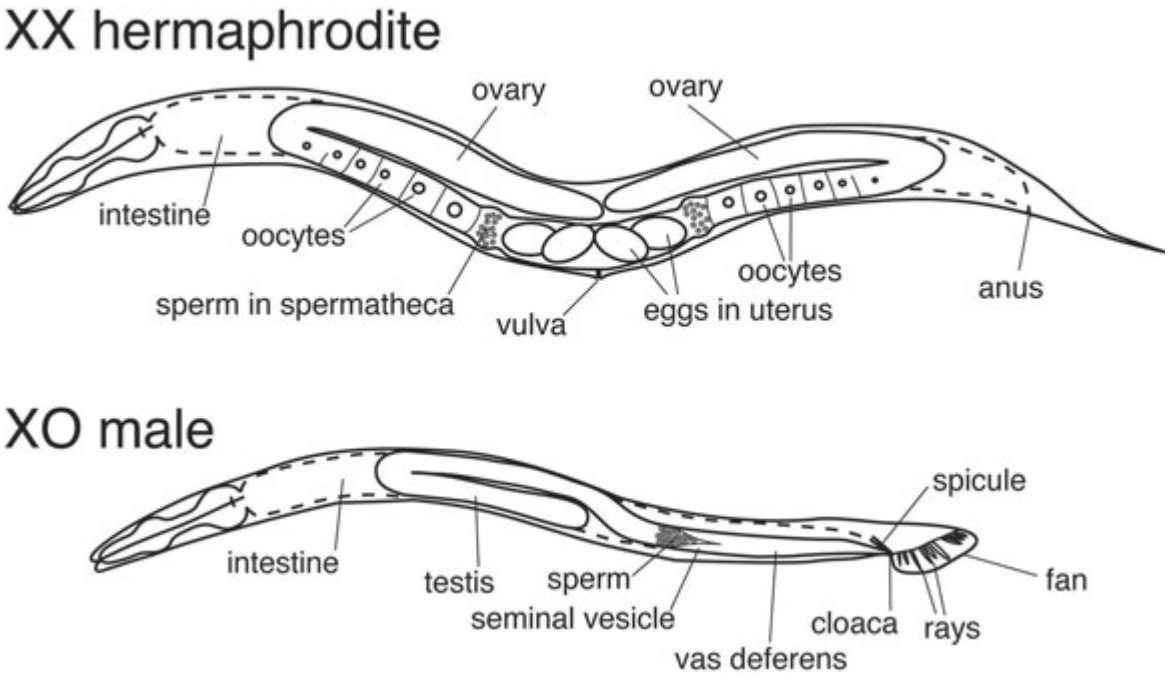

Figure 4.2: Sexual forms of *C. elegans* (Taken from Zarkower, 2006)

Focusing on the endpoints to be studied, although *C. elegans* has been investigated widely, standard toxicological assessments performed on this organism are not established. There are endpoints such as lethality (Williams and Dusenbery, 1990) and reproduction (Middendorf and Dusenbery, 1993) which have been suggested to be the guideline to investigate the environmental toxicants since they are commonly used in other organisms (Dhawan, Dusenbery and Williams, 1999). Furthermore, many *C. elegans* studies conducted in both aquatic and soil media have also focused on other

endpoints such as movement, growth, and feeding behaviour (Mutwakil *et al.*, 1997; Dhawan, Dusenbery and Williams, 1999; Jones and Candido, 1999). To study NM toxicity in *C. elegans*, lethality (Ma *et al.*, 2009; Roh *et al.*, 2009; Kim, Nam and An, 2012) and reproduction (Ma *et al.*, 2009; Roh *et al.*, 2009; Zhang *et al.*, 2011; Kim, Nam and An, 2012; Tyne *et al.*, 2013) are also the commonly used endpoints, while lifespan (Zhang *et al.*, 2011), locomotion behaviour (Ma *et al.*, 2009), growth (Roh *et al.*, 2009), and feeding behaviour (Zhang *et al.*, 2011) have barely been investigated. Since lethality and reproduction are to the standard endpoints to study *C. elegans*, these were initially chosen.

4.2 Aims of this chapter

This study was carried out to investigate the adverse effects induced by NMs compared to the ionic form and bulk particles, if available. The experiment focused on the effects of toxicants in terms of mortality and reproduction effects. In addition, this work was conducted to identify the possible pathways of toxicity from NMs by comparing the susceptibility of nematodes' different strains to toxicants, as well as comparing the effects of NMs' characteristics. The null hypotheses tested in this chapter were:

1. Ionic metal, bulk particles, and corresponding NMs, have no effect on mortality and reproduction of nematodes during the time of exposure and at the tested concentrations
2. Different strains of nematodes lacking of particular genes in oxidative stress or apoptosis would have the same response as the wild type when exposed to toxicants
3. Different types of AgNMs would induce the same response in the nematodes.

4.3 Materials and Methods

4.3.1 Pilot studies

A wide range of concentrations of each material was used to study the mortality of nematodes. The range of concentrations was shifted to higher or lower concentrations to find the appropriate range for the following hazard studies. The pilot studies were conducted in order to obtain the narrow range of concentrations where it provided the sigmoidal-curve response, and the median lethal concentration could be established.

4.3.2 Preparation of toxicant stock solutions

Stock solutions/suspensions of each test substance were prepared by either pipetting or weighing, depending on how materials were provided by the suppliers. $AgNO_3$ stock solution was prepared by pipetting the correct amount of 0.1 N $AgNO_3$ and adjusting to final volume in a volumetric flask. Other test substances were prepared by weighing the powder or suspension of materials and adjusting to final volume with SSPW in a volumetric flask. To ensure that NMs were well dispersed in the stock solutions, the final stock solutions/suspensions were bath sonicated for 8 minutes (Kerry ultrasonic water bath, 38 ± 10 KHz). All stock solutions/suspensions were prepared freshly prior to use to prevent the aggregation of NMs over time. The information of the amount of test substances used in the preparation is provided in Appendix A1.

4.3.3 Preparation of toxicant test concentrations

Test concentrations were prepared by adding the correct amount of stock solutions/suspensions to the medium and inverted and mixed. To prepare test concentrations containing NMs, samples were sonicated for 8 minutes after adding NM stock suspensions into test medium. The pH of medium was measured and adjusted to the range of 6.50-7.00 by using 0.1 M nitric acid.

4.3.4 Lethality test

Adult worms (15±5) were added into each well of a 24-well plate to determine their survival rate in the different concentrations of nanoparticulate Ag and CuO, as well as their bulk particles (if applicable), and a dissolved ionic counterpart. Lethality was assessed after 24 hours of exposure by counting the number of live and dead worms which can be judged by any movement after a gentle poke with an eyebrow hair on a stick. The experiment was carried out in six replicates. Information on the volume of $AgNO_3$ in the test solutions is shown in section 2.3.11, while for other test substances are presented in Appendix A1.

4.3.5 Reproduction test

One adult worm in each well of a 24-well plate was exposed to different concentrations of nanoparticulate Ag and $AgNO_3$, as CuO materials were discontinued for the toxicity tests due to the low toxicity observed in lethality tests. Although Cu materials might induce adverse effects on sublethal endpoints, the aim of this project was to explore the pathways of toxicity and so it was decided that the focus should be on a particular type of NM rather than testing many materials.

During the test period, the test solutions/suspensions were renewed everyday by replacing half of the old solutions/suspension with the fresh test solutions/suspensions. The number of progeny produced in the test period of three days was counted and the concentration induced mean reproductive suppression (RC_{50}) was calculated compared to the control group with the absence of the test substances. The experiment was carried out using six replicates. Detailed information on the medium preparation is presented in Appendix A1.

4.3.6 Statistical analyses

The lethality models were built using logistic regression in R (version 3.2.4), and results were plotted in MS Excel (version 15.0.4805.1001). Median lethal concentrations and 95% confidence interval of each test substance were derived from these models. A significance in lethality models of mutant strains compared to the wild type regarding the test substances was calculated using the package “gmodels” in R.

Reproduction models were built using package "drc" in R (version 3.2.4), and also plotted in MS Excel (version 15.0.4805.1001). Median concentrations for reproduction test (RC_{50}) as well as their 95% confidence interval were calculated within the model from R. The difference in reproduction plots between mutant strains and the wild type comparing exposed to the same test substances was calculated using the package "gmodels" in R.

4.4 Results

4.4.1 Lethality test

To compare the toxicity between test substances by composition, the ionic form (Ag^+ and Cu^{2+}) exhibited the highest adverse effect in terms of lethality with the lowest LC_{50} at 24 h of exposure. Generally, the rank of toxicity regardless of composition of toxicant, was: Ag^+ > JRCNM03002a > Cu^{2+} > NM302 > CuO micro/nano, as shown in Figure 4.3. Different types of AgNMs induced different degree of responses in *C. elegans*. JRCNM03002a, a 20 nm spherical AgNM, was more toxic than Ag nanorod, NM302 (Ø = 50 nm). The difference in toxicity of CuO NM and microparticles could not be established since the death of nematodes was not observed even up to a high concentration of 750 mg/L, as seen in Table 4.1.

Comparisons between strains showed that *ced-3* (-ve) was the most tolerant to all test substances. Its LC_{50} value was generally the highest compared to all other strains, whereas *sod-3* (-ve) was the most sensitive strains with the lowest LC_{50} values across all toxicants, as shown in Table 4.1 and Figure 4.4. Although *ced-3* (-ve) and *sod-3* (-ve) strains had higher tolerance or susceptibility to all toxicants, the response of the other strains was varied. The trend of susceptibility was ranked as *sod-3* (-ve) > wild type > *mtl-2* (-ve) > *ced-3* (-ve) in exposure to Ag^+, Cu^{2+}, and NM302, while the rank of sensitivity was *mtl-2* (-ve) > *sod-3* (-ve) > wild type > *ced-3* (-ve) when tested with JRCNM03002a.

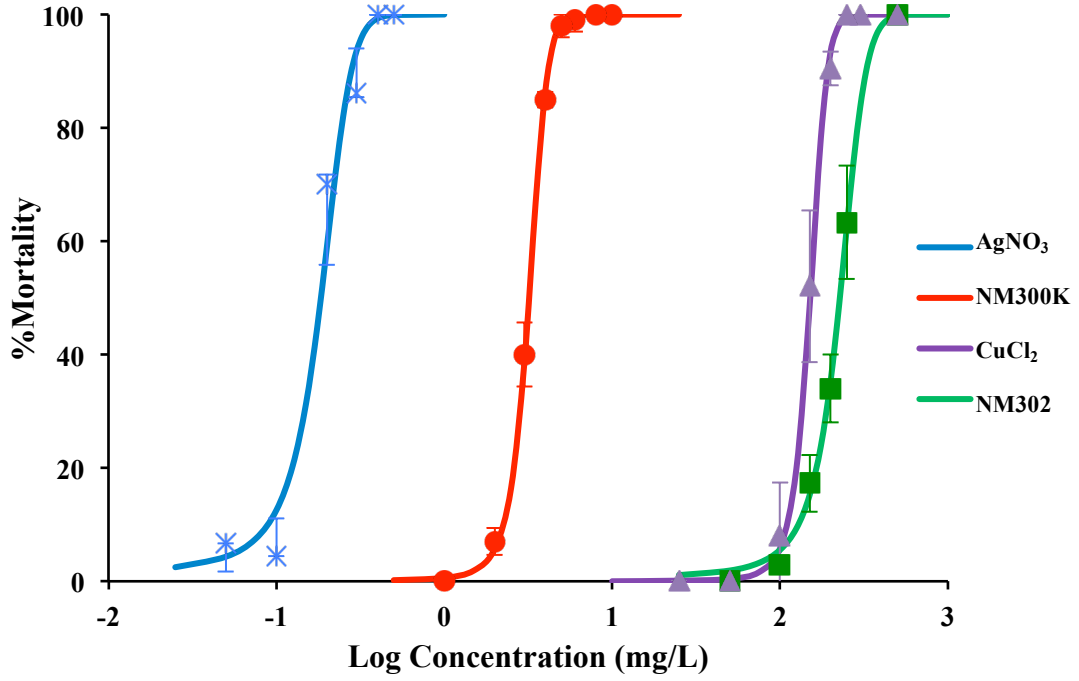

Figure 4.3: Mortality plots of wild type nematodes exposed to different test substances for 24 hours. The data are displayed as mean ± standard error (SE) for all test substances, except $AgNO_3$, which were shown as median ± interquartile range (IQR) because the data was not normally distributed. The experiment was conducted with 6 replicates with > 60 nematodes.

Table 4.1: Median lethal concentration (LC_{50} ± 95% confidence interval) of each test substances in different strains of *C. elegans*, tested in SSPW for 24 hours.

Strains	LC_{50} (mg/L)					
	$AgNO_3$	JRCNM03002a	NM302	$CuCl_2$	CuO micro	CuO nano
Wild type	0.17 (0.15-0.19)	3.13 (2.93-3.33)	202.21 (183.51-222.81)	177.96 (173.70-182.31)	>750	>750
ced-3 (-ve)	0.26 (0.24-0.27)	3.80 (3.66-3.94)	274.64 (248.89-303.06)	212.11 (205.51-218.93)	>750	>750
sod-3 (-ve)	0.16 (0.15-0.18)	3.01 (2.87-3.16)	199.90 (182.36-219.13)	160.56 (155.83-165.43)	>750	>750
mtl-2 (-ve)	0.24 (0.21-0.27)	2.92 (2.78-3.08)	267.57 (242.30-295.49)	193.69 (184.93-202.86)	>750	>750

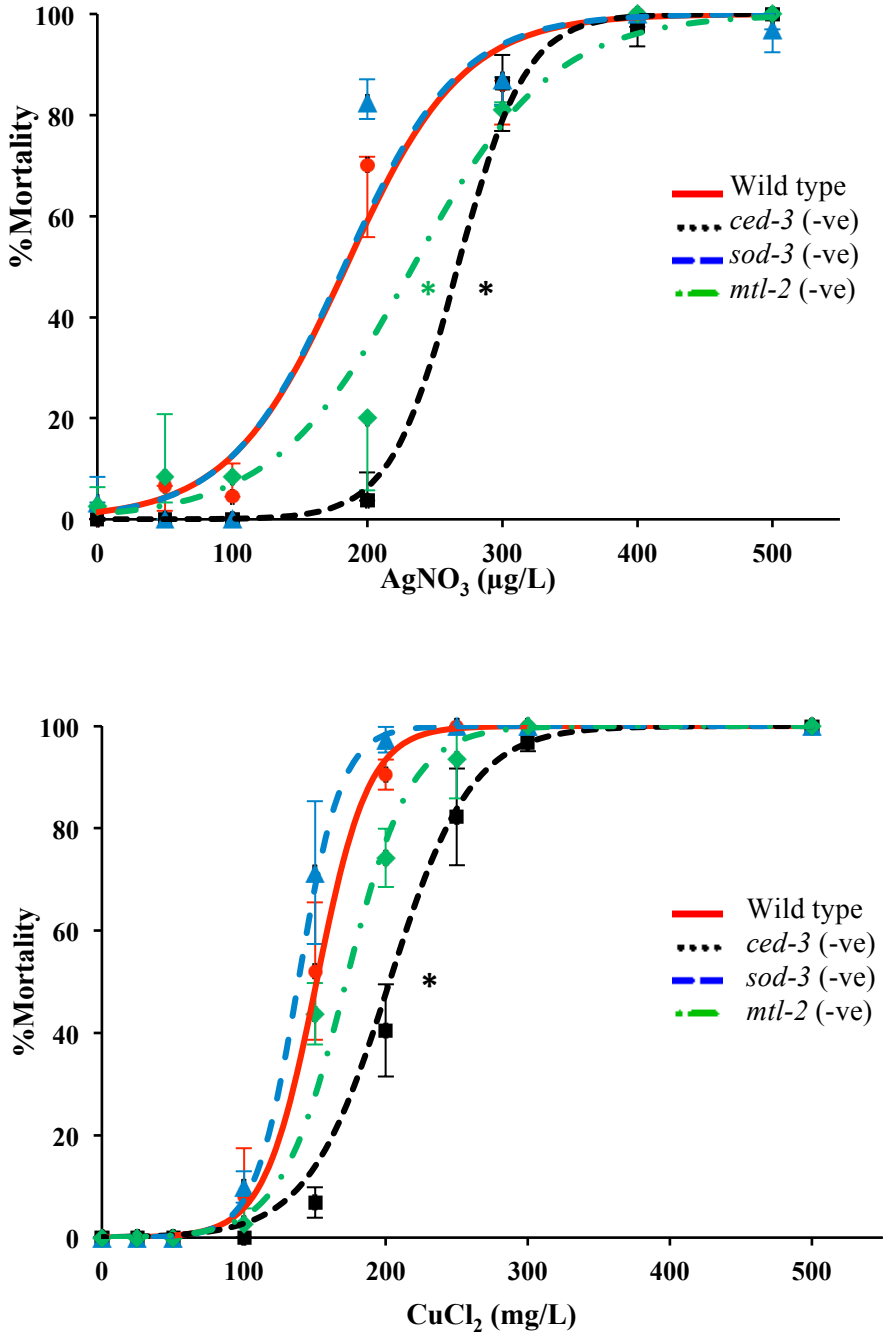

Figure 4.4: Effects of different test substances on mortality of *C. elegans* after 24 h exposure. A significance in mortality compared to wild type is symbolised as * when $p < 0.01$. (wild type, pro-apoptotic gene knockout, *ced-3* (-ve), superoxide dismutase knockout, *sod-3* (-ve), metallothionein knockout, *mtl-2* (-ve)). The data are displayed as mean ± standard error (SE) for all test substances, except $AgNO_3$ was shown as median ± interquartile range (IQR)

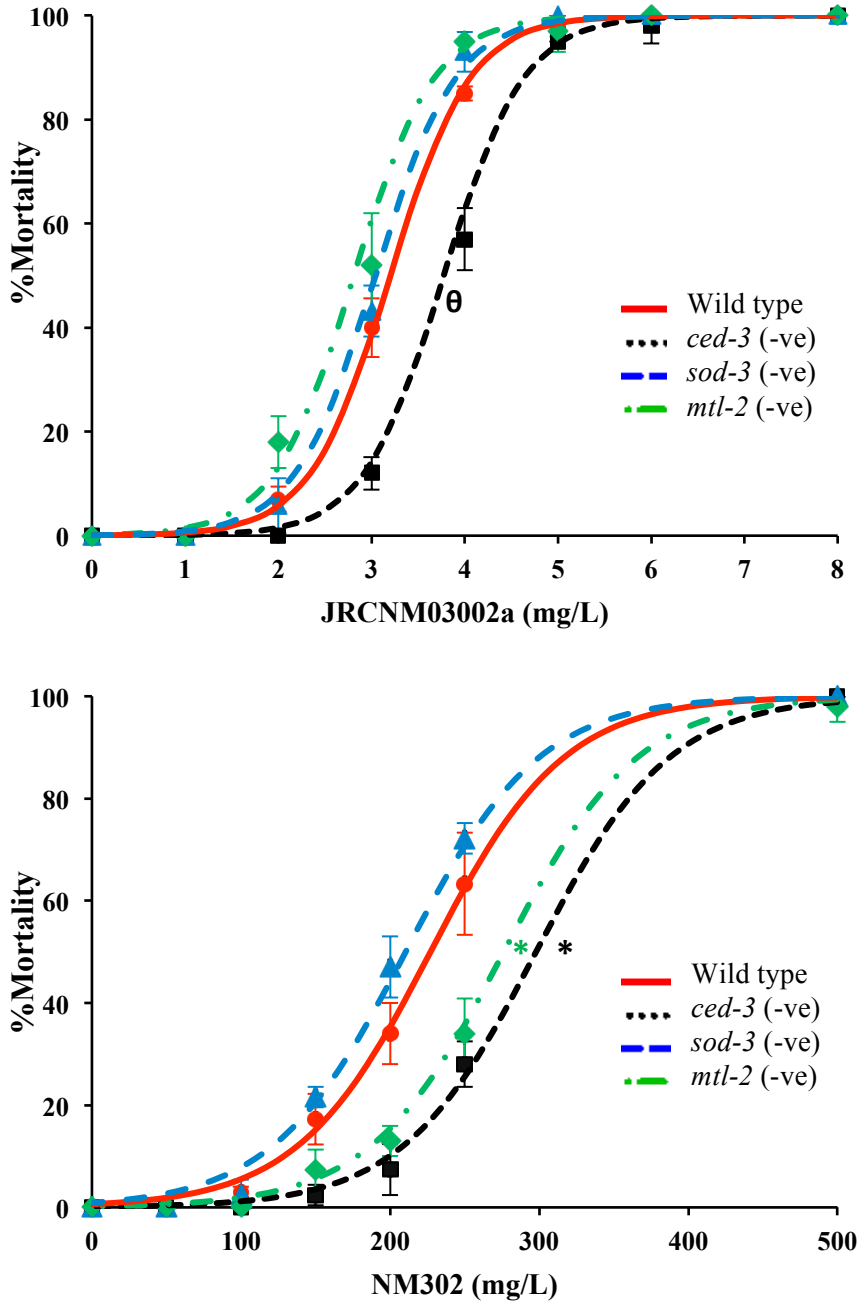

Figure 4.4 (Cont.): Effects of different test substances on mortality of *C. elegans* after 24 h exposure. A significance in mortality comparing to wild type was symbolised as * when $p < 0.01$, and θ when $p < 0.05$. (wild type, pro-apoptotic gene knockout, *ced-3* (-ve), superoxide dismutase knowckout, *sod-3* (-ve), metallothionein knockout, *mtl-2* (-ve)). The data are displayed as mean ± standard error (SE).

4.4.2 Reproduction test

Since no toxicity was observed for CuO materials in section 4.4.1, the use of Cu materials was discontinued. Further toxicity tests on the inhibition of reproduction were focussed on AgNMs. Results from the reproduction test showed that in the ionic form, Ag^+ exposures resulted in the lowest number of progeny. Comparing two types of AgNMs, the spherical 20-nm AgNM (JRNM03002a) induced greater toxicity than NM302, the rod-shaped AgNM with 50 nm in diameter. Generally, the rank of toxicity deduced from this test was Ag^+ > JRCNM03002a > NM302, which was in accordance with the findings from section 4.4.1, as seen in Figure 4.5.

The reproduction test revealed that not only *ced-3* (-ve) was the most tolerant strain, but also the wild type. The *ced-3* (-ve), which lacks pro-apoptotic genes, was able to produce significantly more progeny than the wild type when exposed to the spherical AgNM. Nonetheless, the significance of RC_{50} was not established between the wild type and *ced-3* (-ve) in neither Ag^+ nor silver nanorod. On the other hand, *sod-3* (-ve) and *mtl-2* (-ve) were found to be significantly more vulnerable than the wild type when exposed to all Ag substances. Comparing between *mtl-2* (-ve) and *sod-3* (-ve), the *mtl-2* (-ve) generally produced more offspring than *sod-3* (-ve) when exposed to Ag^+ and spherical AgNM, but the number of progeny generated by *mtl-2* (-ve) was as much as sod-3 (-ve) when exposed to silver nanorod. Overall, the tolerance of nematodes was ranked as *ced-3* (-ve) = wild type > *mtl-2* (-ve) > *sod-3* (-ve), as illustrated in Table 4.2 and Figure 4.6.

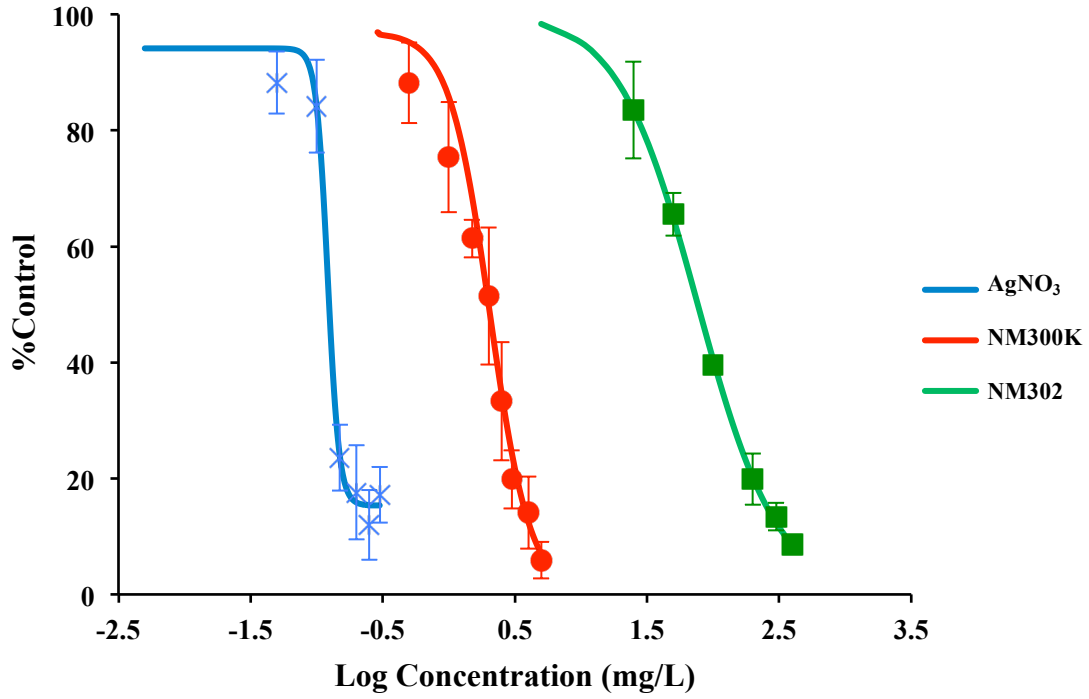

Figure 4.5: The percentage of the reproduction of the wild type nematodes compared to the un-treated group in the exposure to silver toxicants for 72 hours. The data are shown as mean ± SE. The experiment was conducted with 6 replicates with > 60 nematodes.

Table 4.2: Median concentration (RC_{50} ± 95% CI) of each test substances in four strains of *C. elegans*, tested in SSPW for 72 hours.

Strains	RC_{50} (mg/L)		
	$AgNO_3$	JRCNM03002a	NM302
Wild type	0.12 (0.10-0.14)	2.04 (1.83-2.25)	76.22 (72.00-80.45)
ced-3 (-ve)	0.13 (0.11-0.15)	2.61 (2.528-2.69)	57.55 (31.22-83.89)
sod-3 (-ve)	0.055 (0.049-0.061)	1.40 (1.094-1.71)	42.49 (33.61-51.36)
mtl-2 (-ve)	0.086 (0.037-0.14)	1.59 (1.311-1.86)	29.97 (16.15-43.78)

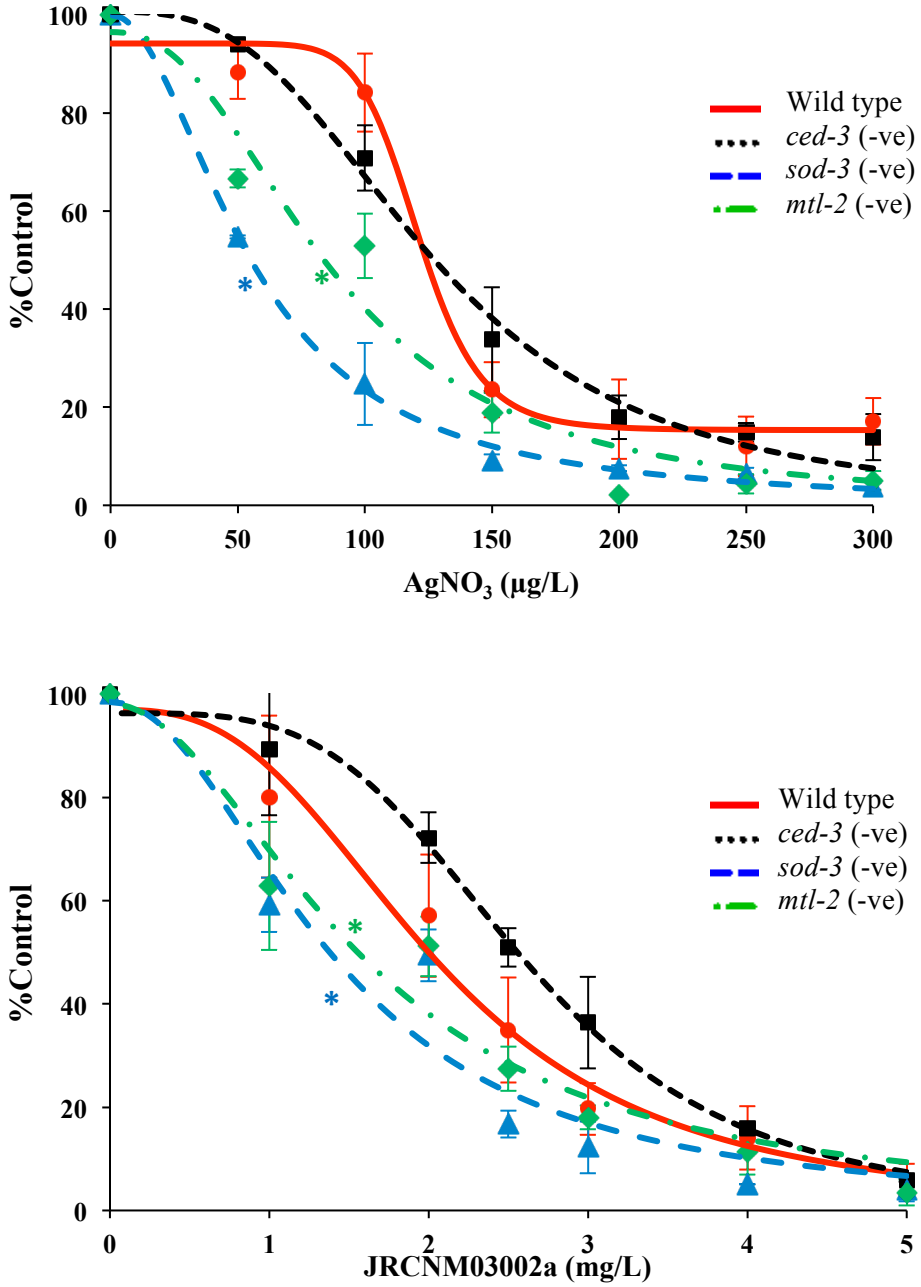

Figure 4.6: Effects of different test substances on the reproduction of *C. elegans* after 72 h exposure. Significant in the difference compared to the wild type is represented with * when $p < 0.01$. (wild type, pro-apoptotic gene knockout, *ced-3* (-ve), superoxide dismutase knowckout, *sod-3* (-ve), metallothionein knockout, *mtl-2* (-ve)). The data are shown as mean ± SE.

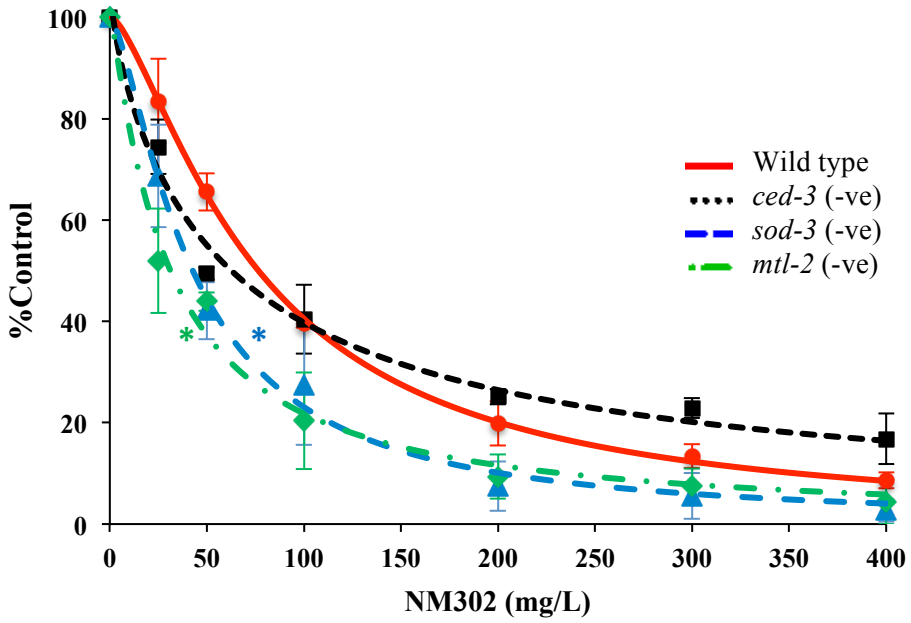

Figure 4.6 (Cont.): Effects of different test substances on the reproduction of *C. elegans* after 72 h exposure. Significant in the difference compared to the wild type is represented with * when $p < 0.01$. (wild type, pro-apoptotic gene knockout, *ced-3* (-ve), superoxide dismutase knowckout, *sod-3* (-ve), metallothionein knockout, *mtl-2* (-ve)). The data are shown as mean ± SE.

4.5 Discussion

4.5.1 Lethality test

The experiment was carried out to assess the viability of nematodes exposed to different NMs as well as their ionic form and bulk particles (where applicable) in the period of 24 hours. Comparison between two compositions of test substances showed that Ag^{+} was more toxic than Cu^{2+} with the LC_{50} in wild type of 0.17 (0.15-0.19), and 177.96 (173.70-182.31) mg/L, respectively. However, the mortality of wild type nematodes in this project was induced at lower concentrations of $AgNO_3$ as compared to results from other publications as the medium used in those studies were K-medium (Roh *et al.*, 2009; Kim, Nam and An, 2012; Yang *et al.*, 2012) or MHRW (Yang *et al.*, 2012; Ahn *et al.*, 2014a). It has been mentioned in section 2.5 that K-medium is not appropriate to study Ag toxicants as it contains a high chloride content, which forms precipitates with ionic silver and results in under estimation of silver toxicity. Nematodes did not produce the normal number of progeny in MHRW. Therefore, the results obtained from this endpoint are not comparable to other publications due to the difference in medium used. While the LC_{50} value of $CuSO_4$ stated by Calafato et al. (2008) was 253.80 mg/L (Calafato *et al.*, 2008), it was shown that different salt compartments of $CuCl_2$ from this study gave the derived value of LC_{50}. Therefore, the LC_{50} values obtained in this work are also not comparable to this study due to the difference in the substances used. Although it would be interesting to display the mortality of nematodes against other dose-metrics e.g. surface area, it was not possible to obtain any of these parameters for the particles studied, given that it is not possible to measure them for NMs suspended in medium. If there any information of the surface area or particle number of these materials becomes available in the future, the comparison between the toxicity to this metric would provide a better understanding on how AgNMs exhibit their toxicity.

Comparison of the same composition AgNMs, smaller spherical particles, JRCNM03002a induced higher lethality than larger nanorod, NM302. This finding might be explained by the smaller size and shape of JRCNM03002a by possibly increasing Ag bioavailability to *C. elegans*. Although Ellegaard-Jensen et al. (2012) found that larger PVP-coated AgNM induced higher mortality in *C. elegans* than the smaller non-coated AgNM, they suggested that the coating decreased the agglomeration of AgNM thus increasing its bioavailability. They also suggested that the larger

particles might enhance the ingestion by the nematodes by fitting into their mouth better than the smaller NMs (Ellegaard-Jensen, Jensen and Johansen, 2012). In contrast, Ahn et al (2014) studied the viability of nematodes exposed to pristine AgNM and two different sizes of PVP-coated AgNMs and found that LC_{50} values increased with the size of AgNMs (Ahn *et al.*, 2014a) while Yang and colleagues (2012) disagreed on this and proposed that neither size nor surface charge contributed to the toxicity from AgNMs. They suggested that only the dissolved silver and the coating mattered in this respect (Yang *et al.*, 2012). From the observations in this study and in other publications, it was deduced that the smaller JRCNM03002a was more bioavailable to nematodes, and might fit in their mouth better than the long rod-shaped NM302. Furthermore, the higher amount of Ag released from JRCNM03002a, as found in section 3.4.3, might be another explanation to the toxicity observed.

The comparison between CuO micro- and nano-materials was not able to establish differences between both particles since they were not be able to kill the nematodes. Therefore, the experiments with Cu test substances were stopped.

The susceptibility of strains lacking genes of interest compared to the wild type was examined in this study. It was found that *ced-3* (-ve) had the highest tolerance to all test substances. A pro-apoptotic gene, *ced-3* is very important in the induction of the apoptotic process in *C. elegans*. It encodes the cell death protease, CED-3, which activates the process of DNA fragmentation and cell degradation, as shown in Figure 6.2. The deletion of *ced-3* in this mutant results in less occurrence of apoptosis. Therefore, *ced-3* (-ve) was expected to endure the presence of apoptotic-stimulating substances. The observation that *ced-3* (-ve) was the most tolerant strain could lead to the suggestion that apoptosis might be relevant to the toxicity from these materials. In addition, a strain lacking the superoxide dismutase gene, (*sod-3* (-ve)), was the most susceptible strain. Since superoxide dismutase is one of the detoxification enzymes, which removes superoxide (one of the ROS) by converting it into hydrogen peroxide and oxygen, and hydrogen peroxide is further removed by catalase, as shown in Figure 2.1. The susceptibility of *sod-3* (-ve) mutant to the test substances proposed that oxidative stress might also be one of the toxicological mechanisms induced by the test substances .

Although it was obvious that *ced-3* (-ve) and *sod-3* (-ve) were the least and most sensitive strain, respectively, it was less clear if *mtl-2* (-ve) was more susceptible than the wild type. The *mtl-2* gene encodes metallothionein, which chelates metal ions and

prevents the production of ROS via Fenton chemistry (figure 2.1). It was expected that *mtl-2* (-ve) would be more vulnerable to test substances than the wild type. However, the results from the lethality tests showed that *mtl-2* (-ve), on the other hand, was more tolerant than the wild type when exposed to Ag^{+}, Cu^{2+}, and silver nanorod. This could suggest that there might be some adaptation of *mtl-2* (-ve) to stress and therefore they were able to survive better than wild type.

Dhawan and colleagues (1999) found that mortality was the least sensitive endpoint when compared to reproduction and behavioural change (Dhawan, Dusenbery and Williams, 1999). This endpoint is also not appropriate to establish the pathways of toxicity following chemical exposure. Therefore, other endpoints such as reproduction and biochemical analysis would help elucidate the pathway of an adverse outcome from test substances, particularly AgNMs. However, the findings from this test were informative in the design of experiments regarding the test concentrations of further studies. In addition, the suggested pathway of apoptosis led to a future study, apoptosis, which will be discussed in chapter 6.

4.5.2 Reproduction test

This study was conducted to compare the toxicity of Ag^{+} and AgNMs at sublethal levels, by focusing on reproduction. The range of toxicant concentrations in this study was lower than in the lethality test, which was planned to avoid killing nematodes during the longer exposure time (72 h) than in the lethality test (24 h). The toxicity of the test substances in terms of reproduction was ranked as Ag^{+} > spherical AgNM > silver nanorod, which was similar to the finding from the lethality test. Median concentration for the reduction in the number of progeny (RC_{50}) in wild type exposed to $AgNO_3$ in this study was 0.12 (0.10-0.14) mg/L, which was less than that found by Tyne and colleagues. They proposed the median concentration at 72 hours to be 0.25 (0.23-0.27) mg Ag/L (Tyne *et al.*, 2013). Although the toxicity was tested in the same medium, SSPW as in this project, the source of $AgNO_3$ was different. In this project, 0.1 N $AgNO_3$ solution (Sigma-Aldrich) was used for the toxicity test, whereas Tyne and colleagues had $AgNO_3$ supplied by BDH in a solid form. Therefore, the result from this work might not be comparable.

Comparing between AgNMs, the toxicity regarding the reproduction of nematodes exposed to spherical AgNM was higher than that exposed to silver nanorod.

The explanation may be that the bioavailability of spherical AgNM might be better than silver nanorod, and could lead to higher toxicity in nematodes as previously mentioned in section 4.5.1. It was obvious that the median concentration to induce the reduction of progeny (RC_{50}) was less than the median concentration to kill nematodes (LC_{50}); this finding was in the agreement to Dhawan and colleagues (1999), who suggested the lethality to be the least sensitive endpoint compared to reproduction and behaviour (Dhawan, Dusenbery and Williams, 1999).

One of the clear points observed in this study which was different from the mortality test, was the fact that the wild type nematode was as tolerant as *ced-3* (-ve) when exposed to most Ag toxicants. In addition, *mtl-2* (-ve) was more sensitive than the wild type in all toxicants. As stated in section 4.5.1, the viability of nematodes was not a distinguishable endpoint, therefore, the results from sublethal tests i.e. reproduction are informative to elucidate the pathway of toxicity from toxicants. Although the significance in RC_{50} values was not found between the wild type and *ced-3* (-ve), it was clear that both oxidative stress-sensitive mutants, *sod-3* (-ve) and *mtl-2* (-ve) were more susceptible than wild type. From this observation, it was able to prove that oxidative stress was also the pathway of toxicity from AgNMs in conjunction to apoptosis. The findings from this test have influenced the study of oxidative stress as will be described in chapter 5.

4.6 Summary of this chapter

This chapter to investigated any adverse effects induced by NMs in a comparison to their ionic form and bulk particles (when applicable). The negative effects focused on in this chapter were mortality and the reduction of progeny in nematodes. To summarise, the viability of nematode decreased in a concentration-dependent manner when exposed to most test substances for 24 hours except for the CuO micro- and NM. The 72-hour study of reproduction also showed a concentration-dependent toxicity from Ag toxicants. The toxicity from different types of AgNMs was also compared to determine the property-related adverse effects. It was observed that nematodes responded to smaller, spherical AgNM (JRCNM03002a) more than the bigger, rod shape (NM302) AgNM. From this finding, it can be deduced that the physicochemical characteristics of NMs played a role in the toxicity, which might be involved in the amelioration of NM availability to nematodes. Furthermore, the

pathway of toxicity was also examined by the degree of tolerance in mutant strains lacking particular genes of interest. Statistically, it was found that a strain lacking a pro-apoptotic gene, *ced-3* (-ve) survived in the presence of all test substances more than wild type, while a *sod-3* knockout strain was the most susceptible strain to all toxicants. The reproduction study also showed that the mutant lacking *mtl-2* had a higher degree of reduction in the number of progeny than wild type after exposure to all Ag toxicants. From these findings, it can be proposed that apoptosis and oxidative stress would be the important pathways of adverse outcomes from NMs.

The findings of this study can be summarised according to the null hypotheses , as stated below.

1. "Ionic metal, bulk particles, and their NMs, have no effect on the mortality and reproduction of nematodes during the time of exposure and at the tested concentration"

This null hypothesis was accepted for the CuO micro- and NM regarding the mortality, however, these materials were discontinued in the reproduction test, therefore the null hypothesis was not proven in the sublethal endpoint. The null hypothesis was rejected when considering the ionic metals and AgNMs.

2. "Different strains of nematodes lacking of particular genes in oxidative stress or apoptosis would have the same response as the wild type when exposed to toxicants"

This null hypothesis was rejected. Each strain had the different degree of tolerance varied across the test substances.

3. "Different types of AgNMs would induce the same response in the nematodes"

This null hypothesis was rejected. Both AgNMs induced the varied response in nematodes. This difference was found in both mortality and reproduction endpoints.

Chapter 5: Oxidative stress

5.1 Introduction

As stated in section 1.8.1, an excess amount of ROS might be relevant to the toxicity from AgNMs. Oxidative stress induced by NMs has been reported in the literature, and therefore a toxicological study focusing on the generation of ROS and the activity of enzymes related to oxidative stress would broaden the knowledge of NMs toxicity, and assess the toxicological effects of AgNMs via oxidative stress. In this chapter, the general response of cells to ROS and the assessment of oxidative damage from NMs will be reviewed.

5.1.1 The cellular response to oxidative stress

ROS exhibit both beneficial and harmful effects in organisms. They are produced during the metabolism of oxygen, as well as taken up from the extracellular environment (Martindale and Holbrook, 2002). Although ROS act as signalling transmitters and function in anti-bacterial defence, an excess ROS can lead to oxidative stress, which consequently damages DNA, proteins, and lipids (Kannan and Jain, 2000). Furthermore, oxidative stress has been correlated with some diseases such as atherosclerosis, diabetes, neurodegenerative disorders, and arthritis (Finkel and Holbrook, 2000). At the cellular level, oxidative stress can lead to a variety of outcomes. A mild dose of ROS promotes a cellular proliferative effect, an intermediate dose induces growth arrest, and a high dose leads to cell death, which can be either apoptotic or necrotic (Martindale and Holbrook, 2002). There are many signalling pathways involved in the response to ROS as shown in Figure 5.1. In this section, the major pathways involved in the response to oxidative stress will be discussed.

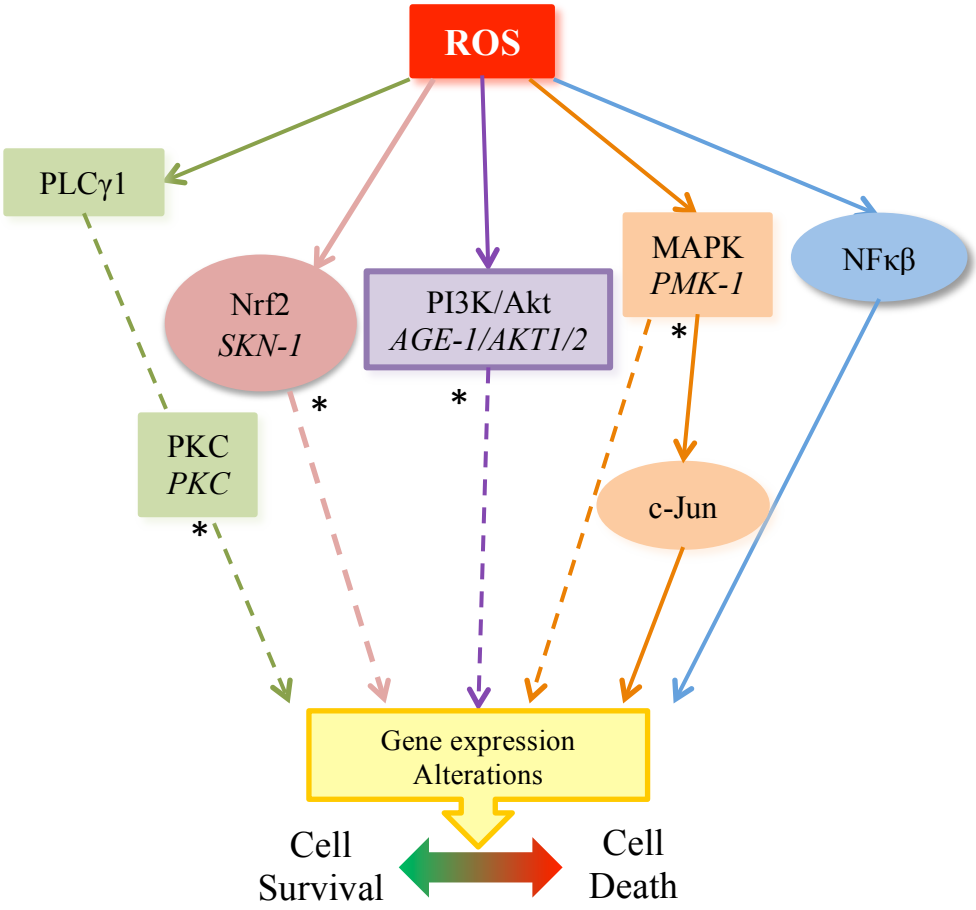

Figure 5.1: The pathways activated by ROS in eukaryotes (Adapted from Martindale and Holbrook, 2002). The pathways which are conserved in *C. elegans* are indicated as *, and the homologue proteins found in *C. elegans* are presented in italic. The main pathways of interest in this chapter are PI3K/Akt (eukaryotes) and specifically AGE-1/AKT1/2 (*C. elegans*), as these relate to the expression of superoxide dismutase and catalase.

One of the stress-response pathways, the mitogen-activated protein kinases (MAPK) signalling pathway is well known for the regulation of various cellular processes, including proliferation, differentiation, response to stress, and apoptosis. This pathway consists of many serine/threonine kinases. According to their structures, they are divided into three groups; the extracellular signal-regulated kinases (ERK), c-Jun N-terminal kinases (JNK), and the p38 kinases. The activation of these proteins is independent of each other; however they can overlap. ERK pathway activation is usually involved in cell proliferation, while the activation of JNK and p38 affect the

response to stress, and thus can lead to cell death. Stimuli such as cytokines, radiation, osmotic stress, physical injury, heat stress, and oxidative damage are among the inducers of the JNK and p38 signalling pathways (Martindale and Holbrook, 2002). Between two isoforms of JNK, only JNK-1 has been linked to oxidant-induced apoptosis (Garay *et al.*, 2000). The p38 pathway is also required for apoptosis, but only in the response of singlet oxygen (Zhuang, Demirs and Kochevar, 2000). It was found that with mild oxidative stress, the mitotic arrest is the outcome of the p38 signalling pathway instead of apoptosis (Kurata, 2000). The targets of the MAPK pathway include c-Jun and tumour suppressor protein, p53. While c-Jun is a target in JNK signalling, p53 can be activated by both JNK and p38. In the JNK cascade, JNK is upstream to c-Jun and the activation of c-Jun can result in both pro- and anti-apoptotic effects (Bossy-Wetzel, Bakiri and Yaniv, 1997; Luo *et al.*, 1998; Potapova *et al.*, 2001). The activation of p53 by oxidative stress results in pro-apoptotic signalling, however, in this case, c-Jun has an opposing effect, which results in the transcriptional inhibition of p53, and thus causes cell survival (Martindale and Holbrook, 2002).

Another pathway, which responds to the ROS, is protein kinase C (PKC). These proteins are also serine/threonine kinases that are dependent on Ca^{2+} (Martindale and Holbrook, 2002). The functions of these proteins include the regulation of cellular growth, death, and stress response (Gopalakrishna and Jaken, 2000). It was found that the activation of PKC by hydrogen peroxide (H_2O_2) is linked to apoptosis, while the down-regulation or inhibition of PKC resulted in necrosis (Li *et al.*, 1999). The functions of various PKC isoforms were found to be different. PKCδ might be correlated with apoptosis, while other isoforms have anti-apoptotic activity (Majumder *et al.*, 2001).

Pathways such as the PI3-kinase/Akt pathway and heat shock protein (Hsp) expression are among those pro-survival pathways that counteract apoptosis induced by ROS. Akt is the anti-apoptotic protein, which is activated by a phosphoinositide 3-kinase (PI3K) pathway. The signal transduction of this pathway is believed to be involved in the apoptotic factors such as Bad and caspase-9 (Datta, Brunet and Greenberg, 1991). Akt also phosphorylates and inhibits the important activator of JNK and p38, ASK1, results in the survival of cell exposed to H_2O_2 (Martindale and Holbrook, 2002). It was also shown that the excess amount of ROS also increased the regulation of detoxification enzymes such as SOD and CAT via FoxO3a transcription factors-regulated by the PI3K/Akt pathway (Rojo *et al.*, 2004; Lu *et al.*, 2013; Uranga,

Katz and Salvador, 2013; Glorieux *et al.*, 2015). Moving on to the heat shock proteins (Hsp), their functions are to promote the assembly, folding, and translocation of other proteins (Jolly and Morimoto, 2000). The activation of Hsp through the heat shock transcription factor 1 (HSF1) is induced by protein damage. It was found that various stimuli including oxidative damage are likely to activate the HSF1. Consequently, the misfolding and aggregation of proteins caused by oxidative injury are inhibited (Pirkkala, Nykanen and Sistonen, 2001).

Another pathway to enhance the pro-survival signal in cells during environmental stress is the nuclear factor E2-related factor (Nrf2). The transduction of this pathway starts when the excess amount of ROS induces the dissociation of Nrf2 protein and its inhibitor, Kelch-like ECH-associating protein 1 (Keap1). The free Nrf2 then translocates from the cytoplasm to the nucleus, and binds to the antioxidant response element (ARE) which is located within the promoter of stress genes. The activation of ARE results in the increase in the expression of the number of antioxidants and detoxification genes that transcribed into glutathione-synthesising enzymes, thioredoxins, and proteasomal subunits (Staab *et al.*, 2013).

5.1.2 Oxidative stress in C. elegans

In the response to oxidative stress, *C. elegans* possesses many antioxidant genes including superoxide dismutase (SOD), catalase (CTL), peroxiredoxins (PRDXs), glutaredoxins (GLRXs), and glutathione-S-transferase (GST). Unlike other eukaryotes, which contain two or three SOD genes, *C. elegans* has at least six SOD isoforms (Landis and Tower, 2005). There are two types of SOD in *C. elegans*; CuZnSODs and MnSODs. The CuZnSODs are the products of *sod-1*, *sod-4* and *sod-5* genes. The location of these CuZnSODs differs by their genes. Cytosolic CuZnSODs are encoded by *sod-1* and *sod-5* genes (Larsen, 1993; Jensen and Culotta, 2005), while *sod-4* produces two extracellular CuZnSODs by alternative splicing (Fujii *et al.*, 1998). The MnSODs are localised in the mitochondrial matrix and are encoded by *sod-2* and *sod-3* genes (Giglio *et al.*, 1994; Hunter, Bannister and Hunter, 1997). The major SOD activity under normal development is contributed to SOD-1 and SOD-2, while SOD-3 and SOD-5 dominates SOD activity in dauers and under oxidative stress (Doonan *et al.*, 2008). The effects of SOD knockout *C. elegans* on the ROS levels, oxidative damage, and lifespan under stress described in the literature are shown in Table 5.1.

As for catalase enzymes in *C. elegans*, the nematode possesses three isoforms of catalase; CTL-1, CTL-2 and CTL-3. The major activity of catalase enzyme belongs to CTL-2, which is highly localized in the peroxisome (Taub *et al.*, 1999). Moving on to glutathione-S-transferase (GST), *C. elegans* has 57 genes encode for GST. It was found the *gst-4* is highly up-regulated during oxidative stress (Leiers *et al.*, 2003), and GST-10 detoxifies the end-product of lipid peroxidation (Ayyadevara *et al.*, 2005).

Table 5.1: Overview of the effect of *sod* knockout of *C. elegans* superoxide dismutases on ROS levels, oxidative damage, and lifespan under stressed conditions, where ND: not determined; PQ: paraquat (superoxide-inducing agent); J: juglone (superoxide-inducing agent); DR: dietary restriction (Adapted from Back, Braeckman and Matthijssen, 2012).

	***sod* gene**	**ROS level**	**Oxidative damage**	**Effect on stress survival**
MnSOD	*sod-2*	Increased or no effect	Increased	Decreased (PQ-J) or no effect (Hyperoxia)
	sod-3	Increased	ND	Decreased (PQ-J) or no effect (PQ-hyperoxia) or increase
CuZnSOD	*sod-1*	Increased	Increased or no effect	Decreased (PQ-J-hyperoxia)
	sod-4	ND	ND	No effect (PQ) or increased (DR)
	sod-5	ND	ND	No effect (DR)

In this chapter, the activity of SOD and CAT is mainly considered. The expression of these enzymes is controlled by the homologues of PI3K/Akt, AGE-1 and AKT-1/2, as shown in Figure 5.1. The main target of this pathway during stress condition is DAF-16/FoxO. The up-regulation of DAF-16/FoxO induces the expression of many genes whose products are important to counteract with the stress. These proteins include SOD and CAT, as illustrated in Figure 5.2. The regulation of DAF-16/FoxO is negatively controlled by the phosphorylation of DAF-2, which results in the activation of AGE-1 (PI3K homologue), 3-phosphoinositide-dependent kinase-1 (PDK-1), AKT-1/2 (Akt homologue), and serum- and glucocorticoid-inducible kinase 1 (SGK-

1). DAF-16 is also regulated by heat-shock transcription factor 1 (HSF-1) and SKN-1 (Nrf2 homologue) (Murphy and Hu, 2013; Koch *et al.*, 2014).

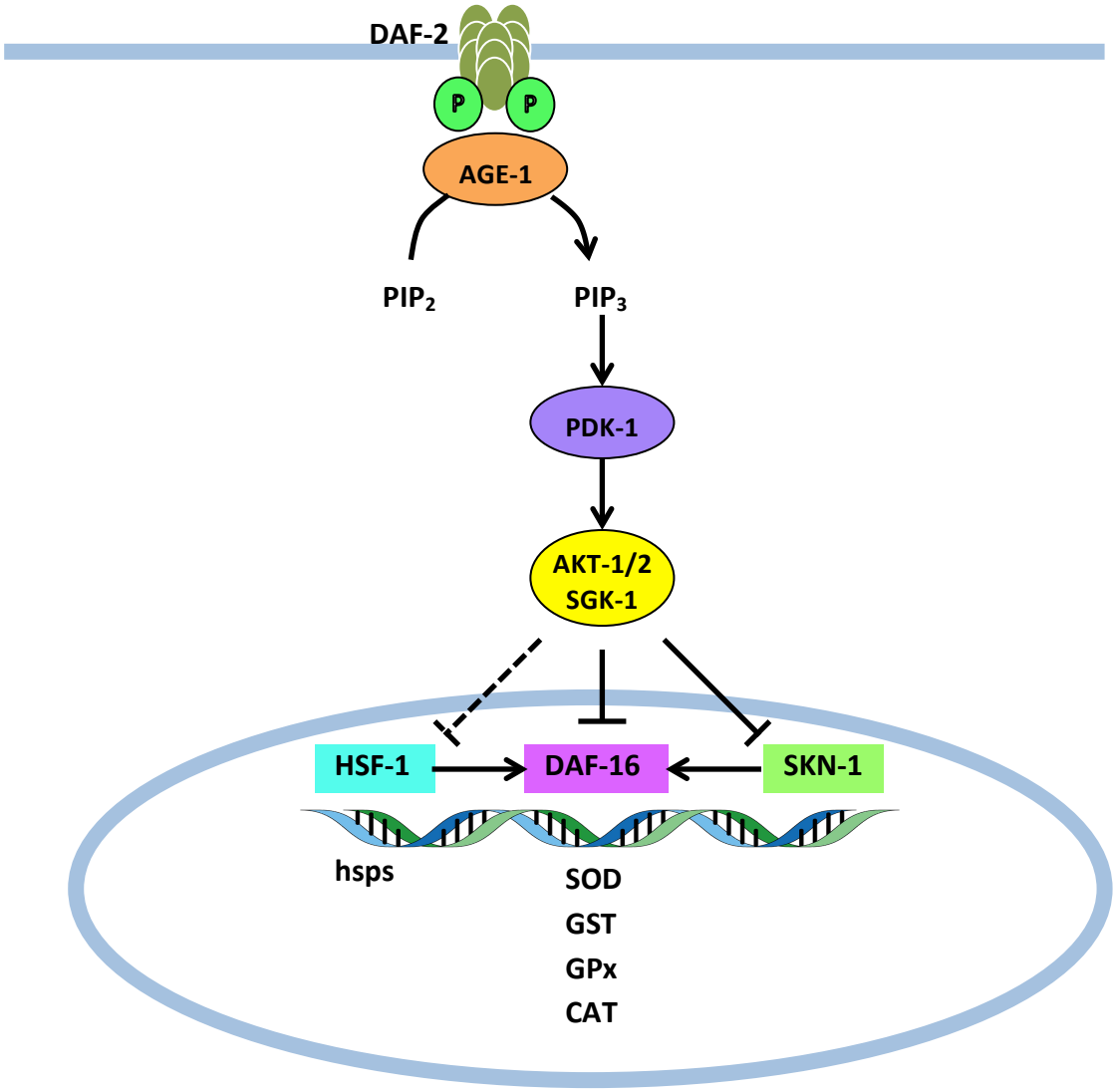

Figure 5.2: The DAF-16/FoxO signalling pathway in *C. elegans*. The activation of DAF-16 results in the production of genes translating into detoxification enzymes (Adapted from Koch *et al*., 2014).

5.1.3 Oxidative stress induced by NMs

It is evident that various NMs are involved in the induction of ROS, for example NMs ranging from carbon-based ones such as fullerenes and carbon nanotubes (CNTs), to metal- or metal oxide-based NMs, such as titanium dioxide (TiO_2), cerium oxide (CeO_2), ZnO, and Ag, which exhibit their toxicological responses via oxidative stress (Donaldson *et al.*, 2001; Oberdörster, 2004; Schvedova *et al.*, 2012; Manke, Wang and Rojanasakul, 2013). The induction of ROS was proposed to be due to: (1) the functional group on the surface of NMs that could induce oxidative stress, (2) the surface of transition metal NMs that could undergo redox reactions, and (3) the interaction between NMs and cells (Donaldson *et al.*, 2001; Oberdörster, 2004; Schvedova *et al.*, 2012; Manke, Wang and Rojanasakul, 2013). In this section, the oxidative damage induced by AgNMs will be assessed.

It has been widely observed that oxidative damage, including lipid peroxidation (LPO), is evident, along with alteration in activity of detoxification proteins (glutathione (GSH), glutathione peroxidase (GPx), SOD, and catalase (CAT)), after exposure to AgNMs in various test models. In addition, oxidative damage in many of these studies was shown to correlate with DNA damage, immune response, and proinflammatory response (Arora *et al.*, 2008; Asharani *et al.*, 2009; Eom and Choi, 2010; Suliman *et al.*, 2013; Ahn *et al.*, 2014b). A summary of the literature from the past five years linking oxidative stress to the toxicity of AgNMs, is provided in Table 5.2.

Table 5.2: The findings of oxidative stress, genotoxicity, inflammatory responses, and apoptosis induced by AgNMs in various cells and animal models (Adapted from (Kim and Ryu, 2013))

Cells/ species	Size (nm)	Coating	Conc.	Time of exposure	Toxicological outcomes		Ref.
					Oxidative stress	Genotoxicity/Inflammatory/Apoptosis	
Human jurkat T-cells	5-10		0.05-0.2 mg/L	Up to 24 h	↑ ROS generation	↑ DNA break, apoptosis, expression of ϒ-H2AX	Eom and Choi, 2010
Human hepatoma cells	5.9± 3.3; 23.8 ± 6.7; 47.5 ± 22.1		Up to 50 µg/mL	24 h	↑ ROS generation, ↓ GSH level and SOD activity	↑ apoptosis, cell cycle arrest in S phase	Liu, 2010
Human lung adenocarcinoma cells	30-50	PVP	Up to 15 µg/mL	24 h	↑ ROS generation	Formation of DNA adduct	Foldbjerg, 2011
Human macrophages	20, 40	Peptide/Citrate	Up to 100 µg/mL	Up to 24 h	↑ Protein carbonylation, expression of HO-1 (indicator for oxidative cellular stress), membrane level of ceramide		Hasse, 2011
Human liver cells	5-10		4 µg/mL	Up to 24 h	↑ ROS generation, ↓ GSH level, ↑ LPO and protein carbonylation	↑ apoptotic body formation, DNA breakage, cell cycle arrest in subG1 fraction, ↓ expression of Bcl-2 & ↑ expression of Bax, caspase-3, caspase-9. Mitochondrial membrane depolarisation	Piao, 2011
Human colon cancer cells	172.6 ± 27.1	Stabilised with Chitosan	Up to 48 µg/mL	Up to 24 h	↑ ROS generation	↑ Apoptosis, DNA fragmentation, expression of caspase-3. Mitochondrial membrane depolarisation	SaNMui, 2011
Human hepatocytes	37.8 ± 6.7		Up to 100 µg/mL	24 h	↑ MDA formation, ↓ GSH level and SOD activity	↑ DNA breakage	Liu, 2011

Table 5.2 (Cont.): The findings of oxidative stress, genotoxicity, inflammatory responses, and apoptosis induced by AgNMs in various cells and animal models (Adapted from (Kim and Ryu, 2013))

Cells/ species	Size (nm)	Coating	Conc.	Time of exposure	Toxicological outcomes		Ref.
					Oxidative stress	Genotoxicity/Inflammatory/Apoptosis	
Mixed primary neural cells	20, 40	Peptide	10, 20 μg/mL	Up to 24 h	↑ expression of HO-1, protein carbonylation, ROS production		Haase, 2012
Human liver carcinoma cells	10, 75	PVP/Citrate	Up to 30 μg/mL	24 h	↓ GSH level	Induced stress response reporters (ARE/NRF-2, NF-κB, AP-1)	Prasad, 2013
Human umbilical vein endothelial cells	65		Up to 2 mg/L	24 h	↑ ROS generation which can be suppressed by NAC	↑ early apoptotic rate, which can be rescued by NAC, ↑ MCP-1 (pro-inflammatory response), IL-6, IL-8, ↑ phosphorylation levels of IKKα/β, IκBα (key proteins of NF-κB)	Shi, 2014
Human lung epithelial cells	< 100		10, 25, 50, 100 μg/mL	Up to 24 h	↓ GSH level, ↑ LPO, SOD and CAT activity	↓ Mitochondrial activity, ↑ caspase-3, caspase-9 activity	Suliman, 2013
Mouse germline stem cells	10	Polysaccharide	10 μg/mL	48 h	↑ ROS generation	↑ cell membrane permeability	Braydich-Stolle, 2010
Rat pheochromocytoma cells	10, 50	Citrate/PVP	Up to 100 μM	24 h, 4 d	↑ LPO		Powers, 2011
Mouse peritoneal macrophages	15, 25,40, 45	Bare/Carbon	5 μg/mL	24 h	↑ ROS generation	Activation & nuclear translation of NF-κB	Nishanth, 2011
Mouse lymphoma cells	5		3, 6 μg/mL	4 h	Alteration of genes in oxidative stress and antioxidant genes	Chromosomal aberration	Mei, 2012
Mouse embryonic fibroblasts	26.2 ± 7.6		Up to 15 μg/mL	3, 6 h	↓ GSH level, ↑ expression of HO-1	↑Nuclear fragmentation, ↑ % of apoptotic cell, ↑ PARP, caspase-3	Lee, 2014

Table 5.2 (Cont.): The findings of oxidative stress, genotoxicity, inflammatory responses, and apoptosis induced by AgNMs in various cells and animal models (Adapted from (Kim and Ryu, 2013))

Cells/ species	Size (nm)	Coating	Conc.	Time of exposure	Toxicological outcomes		Ref.
					Oxidative stress	Genotoxicity/Inflammatory/Apoptosis	
Mouse peritoneal macrophages	68.9 ± 30.3		Up to 1.6 ppm	24 h	↓ GSH level	Cell cycle arrest in subG1 fraction	Park, 2010
Wistar rats,8-10 wk-old	15-40		4, 10, 20, 40 mg/kg (IV)	32 d (5 d interval)	↑ ROS generation in serum	↑ DNA damage in blood cells	Tiwari, 2011
Rainbow trout hepatocytes	1-10	Citrate	Up to 19 mg/L	2 h	Did not observe ROS production		Farkas, 2010
Rainbow trout gill cells	3-40	Citrate/PVP	Up to 10 mg/L	48 h	↑ GSH level		Farkas, 2011
Japanese medaka (*Oryzias latipes*) embryos	29.9 ± 5	PVP	62.5-1000 µg/L	Up to 9 d	↑ LDH, ROS, MDA levels and SOD activity, ↓ GSH		Wu and Zhou, 2012
Zebrafish (*Danio rerio*) adults	5-20		30, 60, 120 mgAg/L	24 h	↑ LPO, GSH and MT2 expression	↑ expression of apoptotic related genes (*Bax1, Noxa, p21*), ↑ DNA breakage, ↑ expression of ϒ-H2AX and *p53*	Choi, 2010
Eastern oyster (*Crassostrea virginica*) adults & embryos	15 ± 6		0.16 mg/L	48 h	↑ metallothionein gene expression		Ringwood, 2010
Fruit fly (*Drosophila melanogaster*) 3rd instar larvae	10	Polysaccharide	50, 100 µg/mL	24, 48 h	↓ GSH level, ↑ LPO, SOD expression	↑ Expression of *p53, p38*. ↑caspase-3, caspase-9 activity	Ahamed, 2010
Fruit fly (*D. melanogaster*)	60		30 µg/mL	24 h	↓ GSH, ↑ SOD activity		Posgai, 2011
Roundworm (*C. elegans*) 3 d-old	20-30		0.1, 0.5, 1 mg/L	24 h	↑ ROS generation which can be rescued by NAC, ↑ GST	↑ expression of genes in MAPK signalling (*pmk-1, hif-1, p38*)	Lim, 2012
Bloodworm (*Chironomus riparius*) 4th instar larvae	40-70		0.2, 0.5, 1 mg/L	Up to 72 h	Change in regulation of GST		Nair and Choi, 2011

Table 5.2 (Cont.): The findings of oxidative stress, genotoxicity, inflammatory responses, and apoptosis induced by AgNMs in various cells and animal models (Adapted from (Kim and Ryu, 2013))

Cells/ species	Size (nm)	Coating	Conc.	Time of exposure	Toxicological outcomes		Ref.
					Oxidative stress	Genotoxicity/Inflammatory/Apoptosis	
C. elegans, 3 d-old	< 100	Bare/PVP	Up to 3.262 mg/L	24 h	↑ ROS production which can be suppressed by NAC and Trolox	↓ Mitochondrial membrane potential, ↑ DNA damage	Ahn, 2014
Ragworm (*Nereis diversicolor*)	100		2.5, 5, 10 µg/g sediment	Up to 11 d	↓ SOD and CAT activity		Cozzari, 2015
E. coli	60		1, 10, 50 mg/L	Up to 2 h	Changes of oxidative stress related genes (*oxyR, sod, kat*, etc.)	Changes of DNA damage related genes (*recN, uvrA, y6fE*, etc.)	Gou, 2010

5.2 Aim of this chapter

The work described in this chapter was carried out to assess the induction of oxidative stress from AgNMs as results from previous chapters suggested that oxidative stress was involved in the negative effects of AgNMs. The main aim of this chapter is to investigate whether the chosen concentrations of toxicants and period of exposure would lead to the increase in the production of detoxification enzymes, since a low amount of oxidative stress tends to enhance defence mechanisms, as depicted in Figure 1.1. The null hypotheses tested were:

1. NMs would not induce the production of ROS in *C. elegans*,
2. NMs would not alter the activity of enzymes which are antioxidants,
3. There would be no difference in the response regarding oxidative stress endpoints between strains of nematodes exposed to the same toxicant,
4. There would be no difference in the response between various Ag toxicants tested in the same strain of nematode.

5.3 Materials and methods

5.3.1 Pilot studies for reactive oxygen species (ROS) production assay

The uptake of fluorescence probe into the nematodes was explored by exposing the nematodes to 10 μM H_2O_2 and 2 mM DCFH-DA for one hour prior to visualisation under the fluorescence microscope (Zeiss Axiophot) at a wavelength of 485/520 nm. To measure the fluorescence intensity, the time of reaction was explored by comparing the H_2O_2 treated- and untreated groups. The fluorescence intensity was measured every 15 minutes.

5.3.2 ROS production

The production of ROS was detected by using the fluorescence probe, dichlorodihydrofluorescin diacetate (DCFH-DA) obtained from Sigma-Aldrich. The principle of DCFH-DA is illustrated in Figure 5.3. Briefly, DCFH-DA itself is not fluorescent, but it can penetrate through the cell membrane and be converted inside an organism by cellular esterase to dichlorodihydrofluorescin (DCFH). In the presence of ROS, DCFH can be activated to its fluorescent form, dichlorofluorescein (DCF) (Hipler 2002).

Samples were prepared by exposing nematodes (~4,500 nematodes/replicate, 6 replicates) to the toxicants and 2 mM DCFH-DA for 2 hours as chosen by the pilot studies. The experiment was conducted in a fluorescence 96-well plate in the dark. The exact volume of reagents in each well is presented in Appendix A2. The concentrations of toxicants used in this experiment were LC_{10} and $2*LC_{10}$. The assay was conducted using 10 µM H_2O_2 as a positive control. Any interference from NMs to the probe was evaluated during pilot studies, and it was found to have no effect. Fluorescence intensity was measured using the plate reader (SpectroMax M5) at the excitation wavelength of 485 nm and emission wavelength of 530 nm. As the number of nematodes in each well was an approximation, the fluorescence intensity was standardised by the amount of protein from nematodes. Therefore nematodes were pipetted out of each well to be homogenised. Quantification of protein in each well was carried out using a protein assay, which is described in section 5.3.4. The standardised fluorescence intensity was calculated by dividing the obtained fluorescence intensity and the amount of protein in each well, respectively.

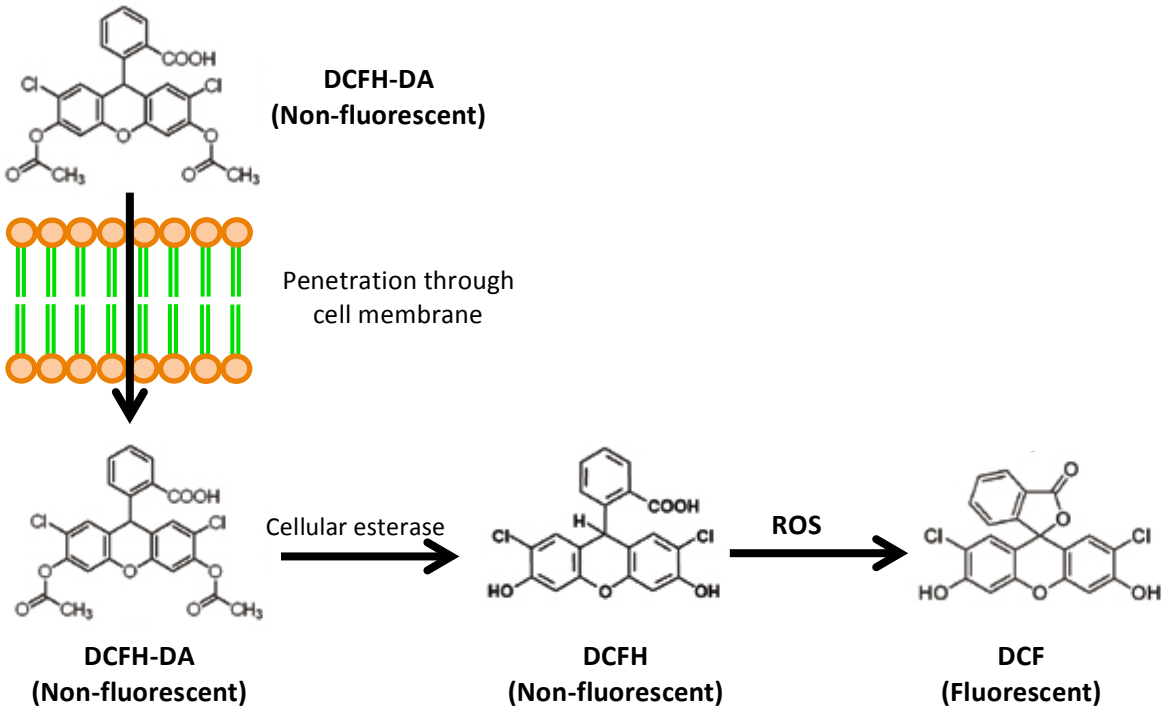

Figure 5.3: Principle of DCFH-DA fluorescence probe on the detection of reactive oxygen species (ROS).

5.3.3 Superoxide dismutase assay

The activity of SOD was analysed by a method based on Del Maestro and McDonald (1987). The method provides an indirect quantification of SOD activity by using UV spectrophotometry to detect the auto-oxidation product of pyrogallol as shown in Figure 5.4. In the presence of SOD, the production rate of the auto-oxidation product is slower than in the absence of SOD. Samples were prepared by exposing nematodes to the toxicants in petri dishes, then nematodes were collected by pipetting, and washed using phosphate buffer pH 7.0 three times. After that they were re-suspended in 250 µL phosphate buffer, and homogenised using a crusher to extract the tissues.

The pyrogallol stock solution (20 mM) was prepared by weighing 12.61 mg pyrogallol and dissolved in 10 mM HCl. The buffer used in this assay was 50 mM tris-HCl buffer mixed with 1 mM DTPA. The pH of tris buffer was adjusted to 8.2. All reagents were freshly prepared prior to use. The concentration of toxicants in this experiment was LC_{10} and $2*LC_{10}$ with the time of exposure of 24 hours. Another experiment was also conducted in a time-course fashion using the concentration of toxicant at $2*LC_{10}$ at time-points of 2, 6, or 24 hours. There were approximately 4,500 (three plates) of nematodes per replicate, six replicates were exposed to the test substances in the conditions described. An amount of 20 µL of the homogenised tissue was added into 96-microwell plate. The pyrogallol stock solution was diluted 1:100 with DTPA-tris buffer immediately before the assay. Then 180 µL of the mixture was pipetted into each well. The change in UV absorbance was determined using the fluorimeter during a 6 minutes period at 420 nm. According to Del Maestro and McDonald (1987), the amount of SOD was then calculated using the following:

$$ngSOD/_{mg\ Protein} = \frac{\%Inhibit}{50} \times 125 \times 0.2 \times \frac{1000}{Sv} \times \frac{1}{Prot} \qquad (1)$$

Where:

% Inhibit = magnitude of inhibition in samples in comparison to blank

125 = amount of bovine CuZn SOD to cause 50% inhibition (ng/ml)

0.2 = total well volume (mL)

Sv = sample volume (µL)

Prot = protein content of sample per ml

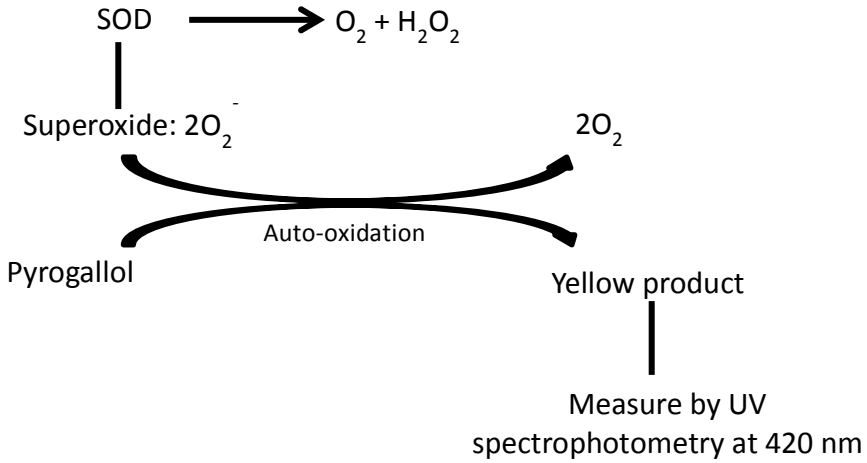

Figure 5.4: The principle of SOD activity determination

5.3.4 Catalase assay (CAT)

The activity of catalase was examined by the method of Claiborne (1985). The detection was the direct quantification of H_2O_2, a substrate of CAT as illustrated in Figure 5.5. UV spectrophotometry was used to quantify the turnover rate of H_2O_2. In the presence of CAT, the turnover rate of H_2O_2 is faster than in the absence of CAT. Samples were prepared as described in section 5.3.2. The positive control, 3% H_2O_2, was prepared by diluting 30% H_2O_2 with 50 mM potassium phosphate buffer pH 7.0. All reagents were prepared freshly before use. At the start of the experiment, 50 µL of homogenised tissue were added into each well, then 180 µL of phosphate buffer pH 7.0 was pipetted into the wells, and 20 µL of 3% H_2O_2 was added into each well. A UV reading was carried out immediately after adding H_2O_2 in the period of 8 minutes at 240 nm using the plate reader (Spectromax M5). According to Claiborne (1985), catalase activity was calculated using this equation:

$$Specific\ Activity\ \left(units/mg\right) = \frac{\Delta A \times 1000}{\frac{43.6 \times mg\ Protein}{mL\ reaction\ mixture}} \qquad (2)$$

Where:

ΔA = the difference of UV absorbance reading of the first 4 minutes

43.6 = the molar coefficient of H_2O_2 in the reaction at 240 nm

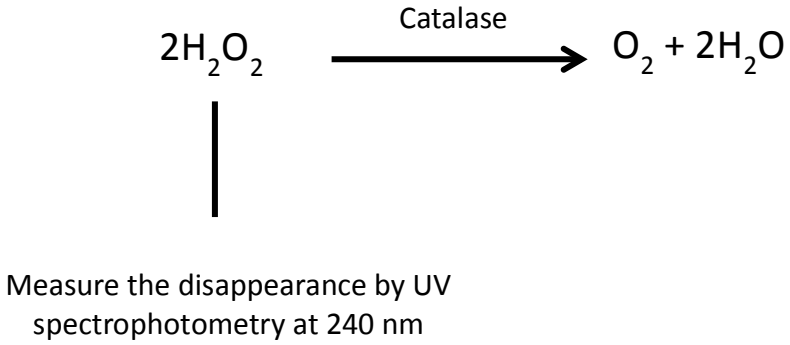

Figure 5.5: The principle of CAT activity determination

5.3.5 Protein assay

A protein assay was conducted to determine the amount of proteins in the homogenised tissue, which can be standardised to the protein/enzyme of interest. It was done by preparing the standard protein, bovine serum albumin (BSA) (1 mg/mL stock solution) at different concentrations, and using the Bio-Rad protein assay (based on Bradford reaction) solution to determine the amount of proteins in a sample comparing to the standard curve. The range of concentrations used to prepare the standard protein is described in Table 5.3.

Table 5.3: The concentrations of standard protein used in the protein assay

Standard (mg/ml)	Label	
1	A	1 mL BSA stock
0.5	B	500 µL A + 500 µL distilled water
0.25	C	500 µL B + 500 µL distilled water
0.125	D	500 µL C + 500 µL distilled water
0.0625	E	500 µL D + 500 µL distilled water
0.03125	F	500 µL E + 500 µL distilled water
0	G	1 mL distilled water

The protein assay was determined in a 96-well plate. A total of 10 µL of either standard protein or sample was pipetted into each well in triplicate, then 200 µL of Bio-

Rad protein assay solution was added into each well. The amount of protein in a sample was calculated from a standard curve using the Revelation software.

5.3.6 Statistical analyses

Statistical analyses were performed on the data using SPSS (version 22). Data normality was assessed using a Kolmogorov-Smirnov test followed by the Shapiro-Wilk test, as the default setting in the software. Two-way ANOVA (for ROS) or three-way ANOVA (for SOD and CAT) tests, with the homogeneity of variances test, were performed to assess the impact of main effects and interactions between factors at the significance level of $p < 0.05$. The two-way ANOVA test was performed for the ROS production results to establish the influence of two factors; strains and toxicants, on the amount of ROS, while 3-way ANOVA was performed in SOD and CAT assays to establish the effect of three factors; strains, toxicants, and time points, to the activities of antioxidant enzymes. The interaction, if any, indicates the different pattern of response, which might be complicated by any of these factors. To establish the difference between the control groups of strains, the comparison for each response between control groups was performed using one-way ANOVA with the homogeneity of variances test (the test assumes that the data in the sample set are equivalently distributed) followed by the post hoc Tukey test. The data that did not conform to the test of homogeneity were analysed using Welch ANOVA followed by the Games-Howell test. The normalisation of the treatment response using the mean control response was applied when there was a significant difference between controls of the different strains in order to establish any significance of response between the various strains.

5.4 Results

5.4.1 Pilot studies for ROS production assay

It was observed that the fluorescence dye was taken up successfully into the nematodes. However, some procedures needed to be adapted to explore the most suitable time for the assessment of uptake. The nematodes were initially cleaned from the excess dye to avoid the interference from the dye in the medium. This procedure was considered to induce stress in the nematodes since they needed to be centrifuged.

Therefore, the fluorescence intensity of the mixture containing nematodes, H_2O_2, and the fluorescence intensity was measured and compared to that from the mixture without the dye. It was shown that the fluorescence intensity of these two groups was similar. To investigate the interference of AgNMs with the fluorescence reading, the mixture of AgNMs, and dye in the medium was read and compared to suspensions without AgNMs. It was also found that these groups gave a similar fluorescence reading. Therefore, the pilot study to explore the time of reading was conducted without cleaning the nematodes. It was found that the fluorescence intensity peaked 2 hours after exposure. Therefore, the ROS production assay was conducted at 2 hours exposure.

5.4.2 ROS production

Boxplots of fluorescence intensity representing the production of ROS in nematodes exposed to various toxicants are presented in Figure 5.6. The influence of toxicants and strains on the production of ROS was determined by two-way ANOVA. The types of toxicant and strain that had a statistically significant impact on the production of ROS were assessed using the Tukey post hoc test. The results from the two-way ANOVA showed that both variables (strains and toxicants) had a significant impact on the production of ROS. Moreover, the interaction between these two factors (toxicants*strains) was not statistically significant, as shown in Table 5.4. The nonsignificant interaction indicated that the relation between factors (toxicants and strains) was not modified by each other. Therefore, it was deduced from the two-way ANOVA that both strains and toxicants had an impact on the production of ROS, and the effects of strains and toxicants on ROS production were not dependent on each other. Results indicated that the nematodes exposed to 200 µg/L $AgNO_3$, 2 mg/L JRCNM03002a, 200 mg/L NM302, and 10 µM H_2O_2, showed increased production of ROS, when compared to the non-treated groups. Moreover, results also indicated that *ced-3* (-ve) and *mtl-2* (-ve) strains produced lower levels of ROS than the wild type ($p < 0.05$).

Table 5.4: Statistical results obtained from the two-way ANOVA analysis

Factors	Type III Sum of Squares	df	Mean Square	F	Sig.
Toxicants	0.037	7	0.005	12.75	<0.001
Strains	0.044	3	0.015	35.20	<0.001
Toxicants*Strains	0.008	21	<0.001	0.90	0.597

Note: Type III sum of squares is a summation of the squares of the differences from the mean. This value represents how much deviation there is from the mean. The df (degrees of freedom) is the number of values in the final calculation of a statistic that are free to vary. The mean square is the value obtained by dividing the sum of squares by the number of degrees of freedom, which also represents the deviation from the mean. The F (F-value) is used to determine the distribution under the null hypothesis. Sig. (*p*-value) determines the significance in the results. If the *p*-value is less than the significance level (α), 0.05 in this test, the null hypothesis is rejected.

The two-way ANOVA test was performed using the compiled data from all groups to establish the overall effects from strains and toxicants on the production of ROS in nematodes. It is clearly shown in Figure 5.6 that each strain of nematodes had a different level of ROS in the non-treated groups. This difference was confirmed by using one-way ANOVA ($p < 0.05$). Therefore, the comparison of ROS production between treated and non-treated groups was done within strain rather than testing the overall influence of strains and toxicants by using two-way ANOVA tests. To determine the impact of toxicants on the production of ROS within strains, one-way ANOVA followed by post hoc analysis (Tukey test), was performed. It was found that 10 μM H_2O_2 significantly induced the production of ROS in the wild type, *sod-3* (-ve), and *mtl-2* (-ve), while for other Ag toxicants i.e. 200 μg/L $AgNO_3$ and 200 mg/L NM302, the significance was established only in *sod-3* (-ve), as depicted in Figure 5.6.

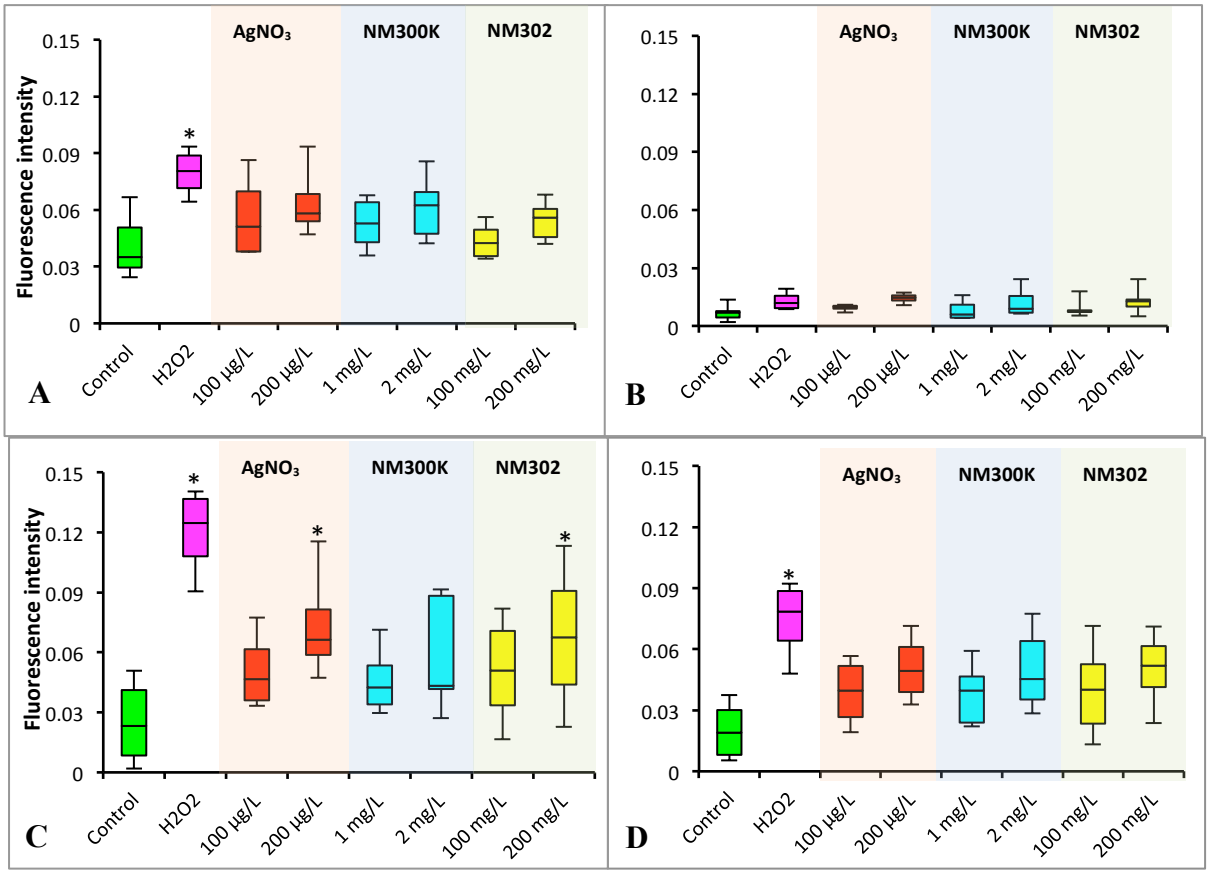

Figure 5.6: Standardised DCF fluorescence intensity in the response of exposure to different toxicants after 2 hours, **A**: Wild type, **B**: *ced-3* (-ve), **C**: *sod-3* (-ve), and **D**: *mtl-2* (-ve). The asterisk indicates statistical differences relative to the respective non-treated groups, comparing within strains ($p < 0.05$).

It has to be considered that including the H_2O_2-treated groups, which had a big impact on the production of ROS might mask the influence of the other toxicants when performing an ANOVA. As shown in Figure 5.6, other test substances induced the production of ROS when compared to the non-treated groups. Significance might have been demonstrated, but it might have been masked by the large difference from the H_2O_2-treated groups. Therefore, a one-way ANOVA with post hoc Tukey analysis was performed again excluding the H_2O_2-treated groups to focus on the impact of other

toxicants. By doing this, the influence of other silver toxicants was established in the groups exposed to 2*LC_{10} of most silver substances, as shown in Figure 5.7. It was also shown that the toxicity was likely to be concentration-dependent.

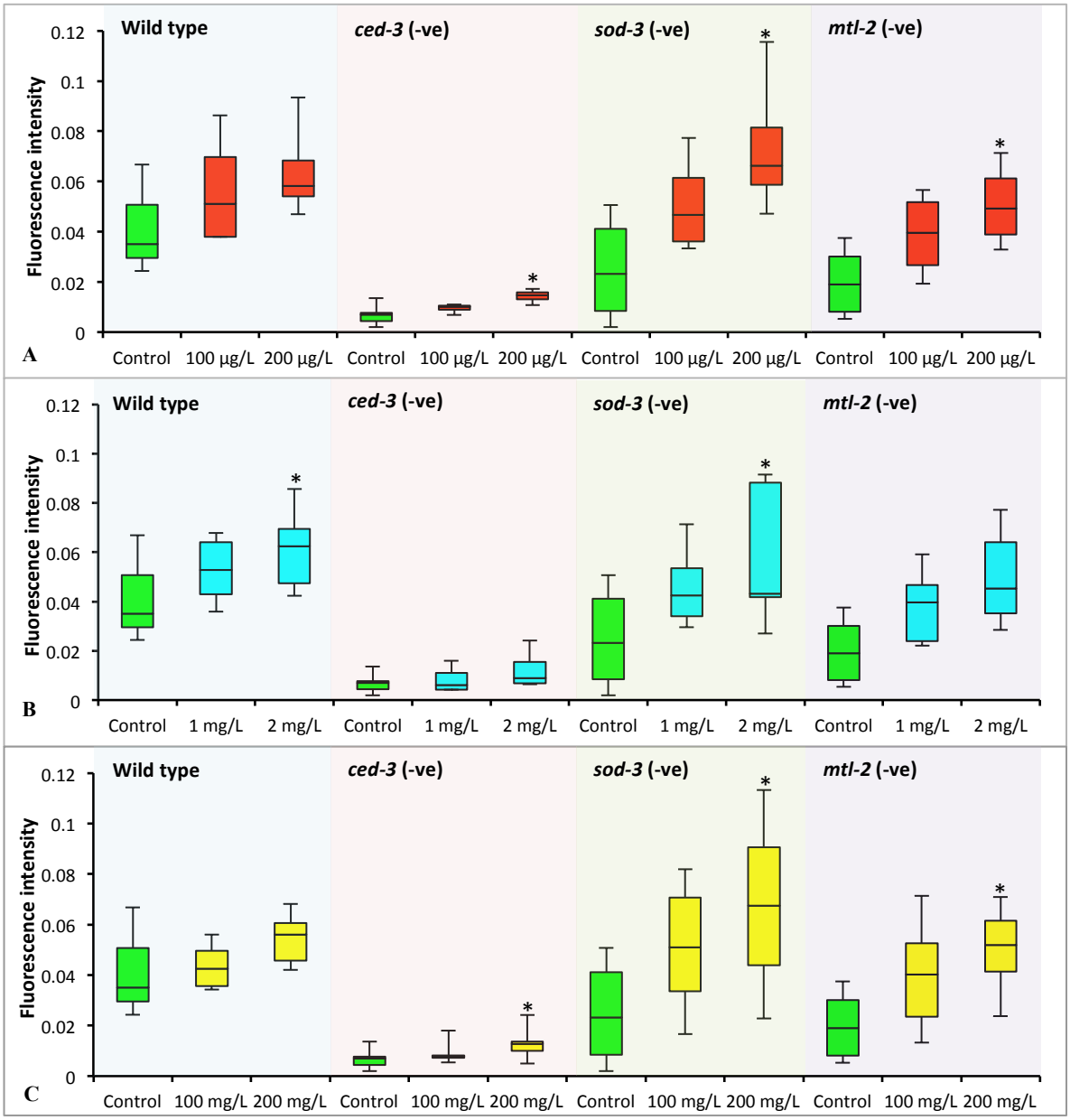

Figure 5.7: Reanalysis of Figure 5.6 excluding H_2O_2-treated group. The effect of different concentrations of Ag toxicants (A: $AgNO_3$; B: JRCNM03002a; C: NM302) on the DCF fluorescence intensity representing the ROS production of various strains of nematodes compared to the non-treated groups within strains (green box). Differences were assessed using one-way ANOVA followed by post hoc Tukey test at the level of $p < 0.05$, and significant differences are shown with asterisks.

As it was evident from the two-way ANOVA that the strain was another important factor in the production of ROS, it is important to understand which strains had different ROS production compared to the wild type. Since there was variation in ROS production between strains, even in the non-treated groups, the data were normalised using the mean values of the non-treated groups to emphasise the effects of the test substances. The adjusted response of nematodes is depicted in Figure 5.8. The difference in ROS production in the exposure to the particular toxicants comparing between the mutants and wild type was established using a one-way ANOVA followed by Tukey post hoc analysis. It was observed in all toxicants that both *sod-3* (-ve) and *mtl-2* (-ve) significantly produced ROS at a higher degree than the wild type. On the other hand, *ced-3* (-ve) did not exhibit any meaningful impact of toxicant exposures on ROS generation relative to wild type.

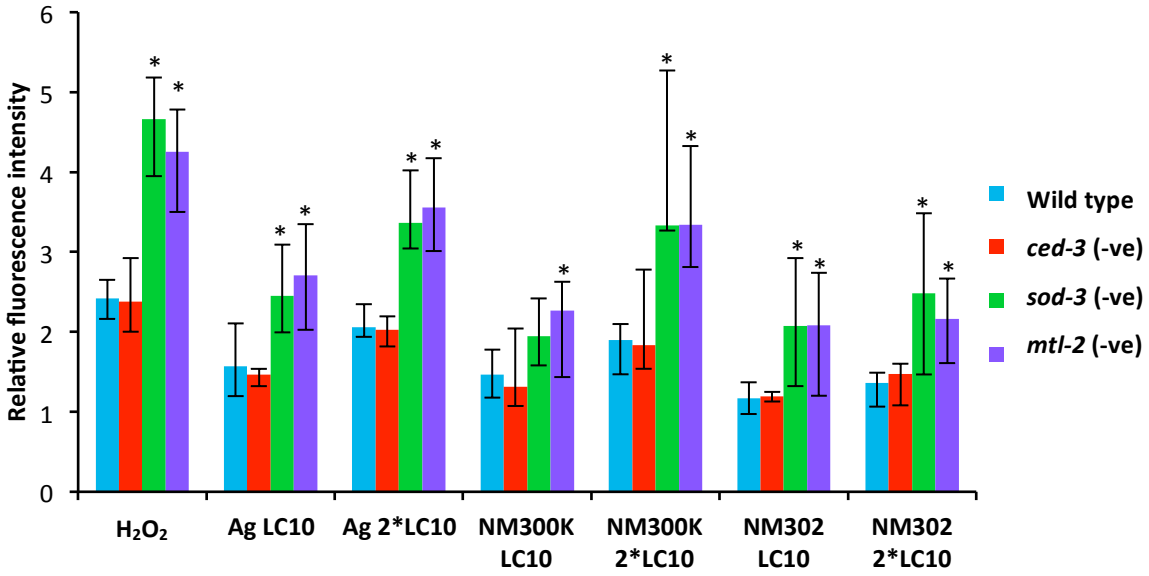

Figure 5.8: Reanalysis of Figure 5.6 by normalising the data to the non-treated respective strains. The reanalysis was performed to focus on the susceptibility of mutants compared to the wild type when exposed to different toxicants. The relative DCF fluorescence intensity to the control groups in the response to various toxicants is shown as median ± interquartile range (IQR). The comparison to the wild type was performed by one-way ANOVA and the significance is shown as * ($p < 0.05$).

5.4.3 Superoxide dismutase assay

In the time study, the effects of strain, time points, and toxicants on the activity of SOD were analysed using three-way ANOVA. The concentration of each toxicant used in this time study was 2*LC_{10}. The types of toxicant included control, 200 µg/L $AgNO_3$, 2 mg/L JRCNM03002a, and 200 mg/L NM302. Strains consisted of N2, MT1522, VC433, and VC128. Time points were 2, 6, and 24 hours exposure. By using three-way ANOVA, it was found that all factors were significant ($p < 0.05$). However, the three-way interaction (toxicants*time points*strains) was found to be significant, as shown in Table 5.5. The three-way interaction indicated that the relation between the three factors (toxicants, time points, strains) was modified by at least one factor. When the three-way interaction was found to be significant, it is not possible to deduce the impact of factors (toxicants, time points, strains) even if individually they were found to have a statistically significant influence on the SOD activity. It was required to investigate which factor(s) may influence others to ensure that the impact on SOD activity was analysed in an unbiased manner.

Table 5.5: Statistical results obtained from the three-way ANOVA analysis

Factors	Type III Sum of Squares	df	Mean Square	F	Sig.
Toxicants	260.14	3	86.71	29.43	<0.001
Time points	2240.11	2	1120.05	380.12	<0.001
Strains	1136.60	3	378.87	128.58	<0.001
Toxicants*Time points	424.88	6	70.81	24.03	<0.001
Toxicants*Strains	110.78	9	12.31	4.17	<0.001
Time points*Strains	179.44	6	29.91	10.15	<0.001
Toxicants*Time points*Strains	106.68	18	5.93	2.01	0.013

To investigate which factor(s) influenced other factors, thus leading into a three-way interaction, a two-way ANOVA was performed to analyse the effects of two factors (toxicants and strains) on the activity of SOD at the different levels (2, 6, and 24 hours) on the third factor (time points). An interaction between toxicants and strains was not established in the time point of 2 and 6 hours, and results indicated that effects were different across the different strains, but not across toxicants. However, the two-way interaction between toxicants and strains was significant at the time point of 24

hours. Profile plots of interaction revealed that the trend of SOD activity from *sod-3* (-ve) and *mtl-2* (-ve) was higher than that from wild type and *ced-3* (-ve) in all toxicants, as shown in Figure 5.9. However, there was a different pattern of SOD activity between strains, e.g. in the 2-hour experiment, the non-treated group of *mtl-2* (-ve) had a lower amount of SOD than the non-treated group of *sod-3* (-ve), but the amount of SOD in *mtl-2* (-ve) increased when exposed to other toxicants to levels that were higher than that from the *sod-3* (-ve) (figure 5.9, graph A). This pattern was different in the 6-hour experiment where the amount of SOD in the *mtl-2* (-ve) mutant was higher than that from the *sod-3* (-ve) in all exposures, including the non-treated group (figure 5.9, graph B). This difference in pattern of SOD activity supported the interaction between two factors (toxicants and strains), that was modified by the third factor (time points).

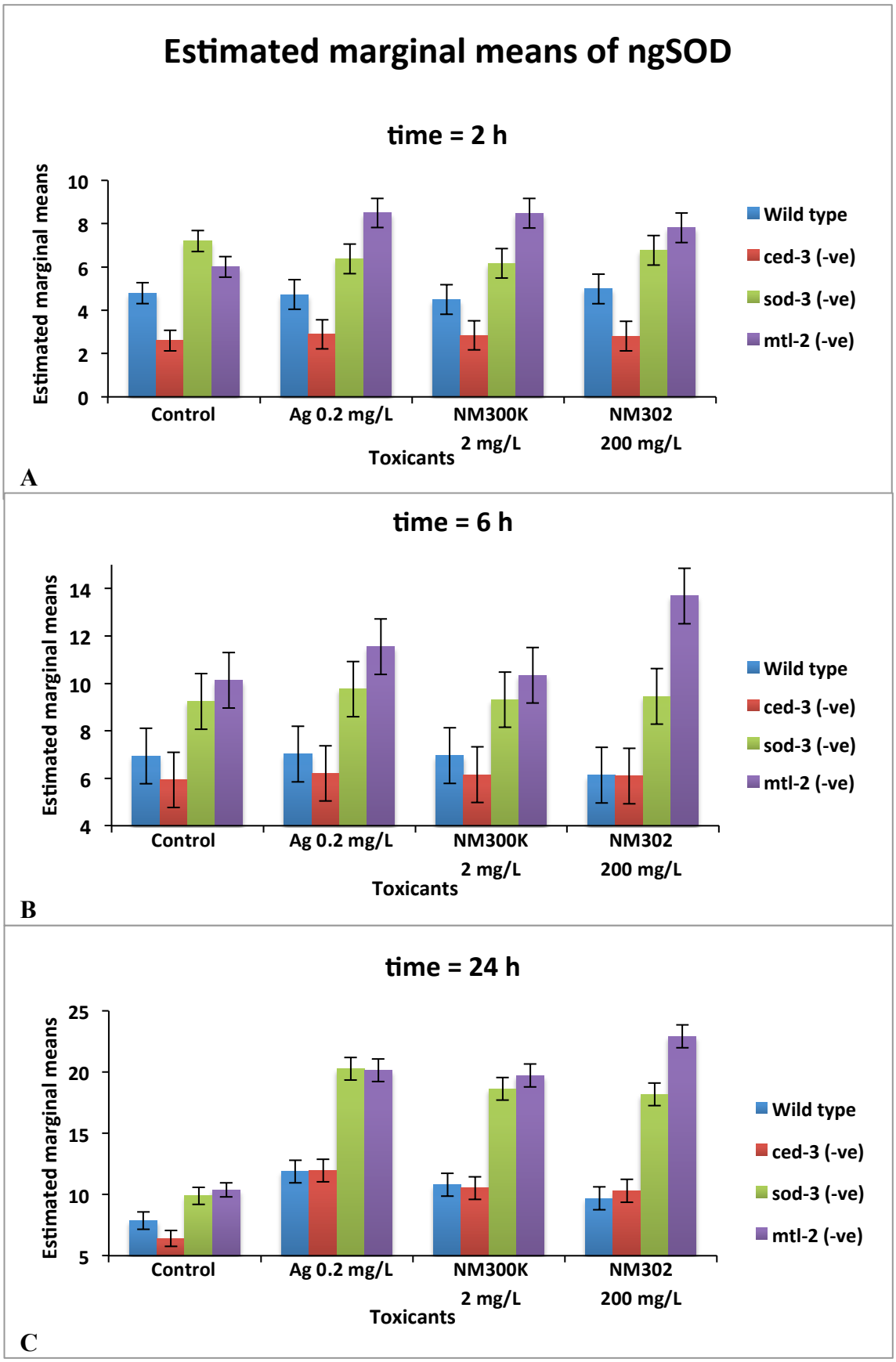

Figure 5.9: Interaction between toxicants and strains at the different time points (mean ± SE), A: 2 hours; B: 6 hours; C: 24 hours.

As there was an interaction between toxicants and strains in the 24-hour experiment, another post hoc analysis, Sidak pairwise comparison, was used to evaluate the effect of toxicants on the SOD activity within strains. Sidak pairwise comparison is another multiple comparison test that is more powerful, and based on more strict assumptions than the Tukey post hoc test. It was chosen in this case since the Tukey post hoc analysis was not able to establish any differences in SOD activity in the presence of the two-way interaction. The results from Sidak test showed that each strain wereinfluenced differently by the different toxicants, compared to the non-treated group. All mutants had significant different levels of SOD compared to the non-treated groups. However, significant differences were only found in the wild type exposed to $AgNO_3$ and JRCNM03002a, as shown in Table 5.6. From the results of this two-way ANOVA test, it was deduced that only the effect of strain was influential to the activity of SOD in the time points of 2 and 6 hours. The *mtl-2* (-ve) had the highest SOD activity, while in the 24-hour experiment, it was not possible to assess the impact of the two factors toxicants and strains because these factors were dependent on each other, resulting in a significant interaction between them (toxicants*strains).

Table 5.6: Sidak pairwise comparisons between toxicant and control in the different strains of nematodes at the time point of 24 hours. The significance was calculated at the level of 0.05 and shown as asterisks (*).

Strains	Comparison between		Mean differences	Std. Error	Sig.
N2	Control	$AgNO_3$*	-4.01	0.80	0.001
		NM300K*	-2.94	0.80	0.014
		NM302	-1.82	0.80	0.206
MT1522	Control	$AgNO_3$*	-5.54	0.92	0.000
		NM300K*	-4.11	0.92	0.002
		NM302*	-3.87	0.92	0.004
VC433	Control	$AgNO_3$*	-10.37	1.42	<0.001
		NM300K*	-8.73	1.42	<0.001
		NM302*	-8.29	1.42	<0.001
VC128	Control	$AgNO_3$*	-9.76	1.26	<0.001
		NM300K*	-9.33	1.26	<0.001
		NM302*	-12.53	1.26	<0.001

Since it was clearly shown in Figure 5.9 that SOD activity varied among the strains, as well as time points, it was important to compare the SOD activity in the response to toxicants within strains and time points. One-way ANOVA analysis, followed by the post hoc Tukey test, was performed to investigate which toxicants induced SOD activity. From this one-way analysis, a difference in SOD activity between the silver-treated and the non-treated groups was established at the time point of 24 hours. However, this was not demonstrated throughout, as shown in Figure 5.10. The wild type and *ced-3* (-ve) significantly increased their SOD activity following exposure to 200 μg/L $AgNO_3$ and 2 mg/L JRCNM03002a (figure 5.10, graph A and B), while this response was found when *sod-3* (-ve) and *mtl-2* (-ve) were exposed to all Ag toxicants (figure 5.10, graph C and D).

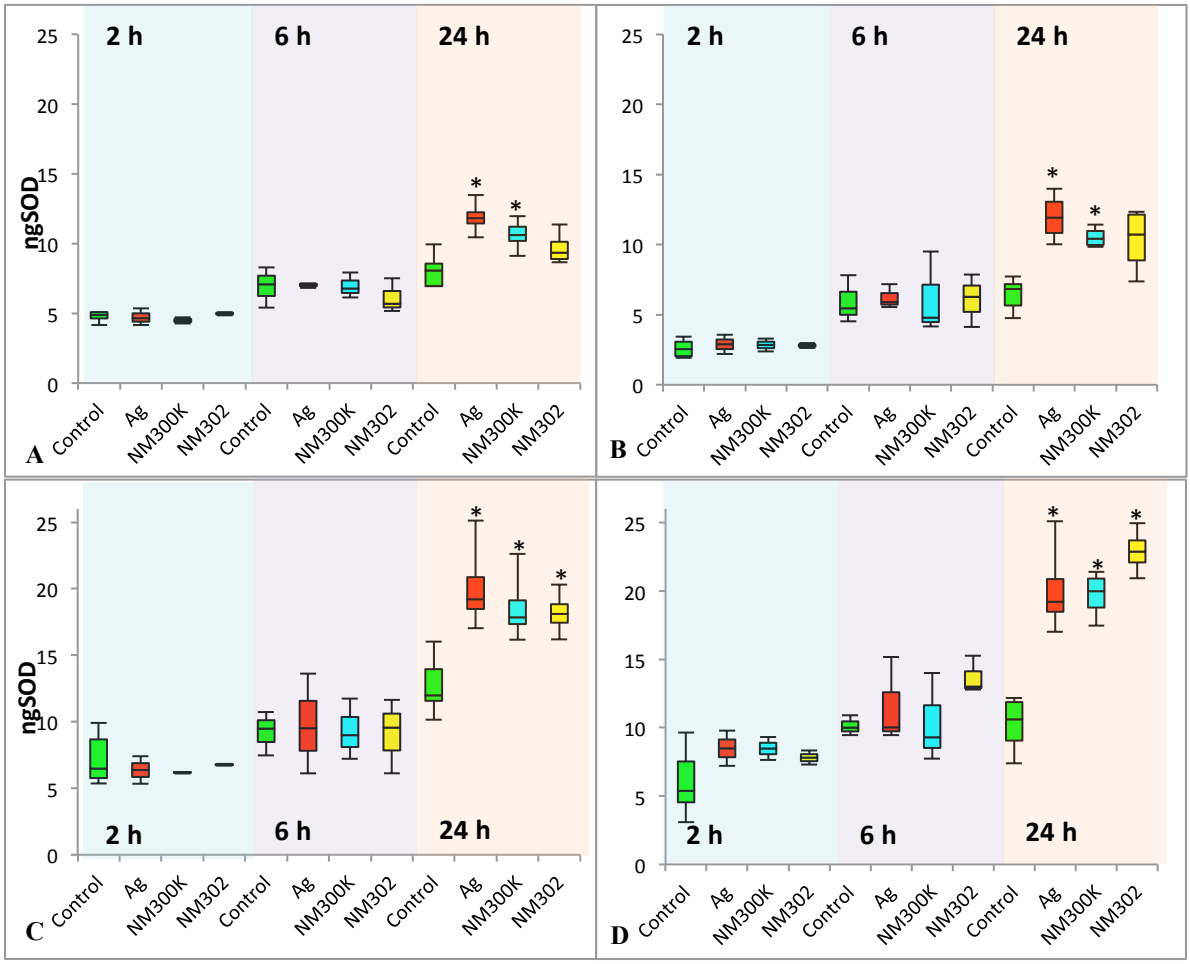

Figure 5.10: Amount of superoxide dismutase (ng) following exposure to different toxicants at the concentration of 2*LC_{10} at the different time points, **A**: Wild type *C. elegans*, **B**: *ced-3* (-ve), **C**: *sod-3* (-ve), and **D**: *mtl-2* (-ve). Significant differences within strains and time points are shown as *.

In the concentration study, the impact of concentrations (LC_{10} and 2*LC_{10}) of toxicants on SOD activity in the test period of 24 hours was investigated. One-way ANOVA, followed by the post hoc Tukey test, was used to establish the significance of SOD activity in the treated groups compared to the non-treated groups. The comparison was made within each strain. Figure 5.11 indicates that the pattern of toxicity is concentration-dependent. It was also found that the concentration of 2*LC_{10} of $AgNO_3$ and JRCNM03002a induced a significant response in every strain. In addition, SOD activity of the *sod-3* (-ve) exposed to 200 mg/L NM302 was statistically higher than the respective non-treated group. Moreover, the *mtl-2* (-ve) increased their levels of SOD

significantly after exposure to both concentrations of all toxicants, indicating that it was the most sensitive strain.

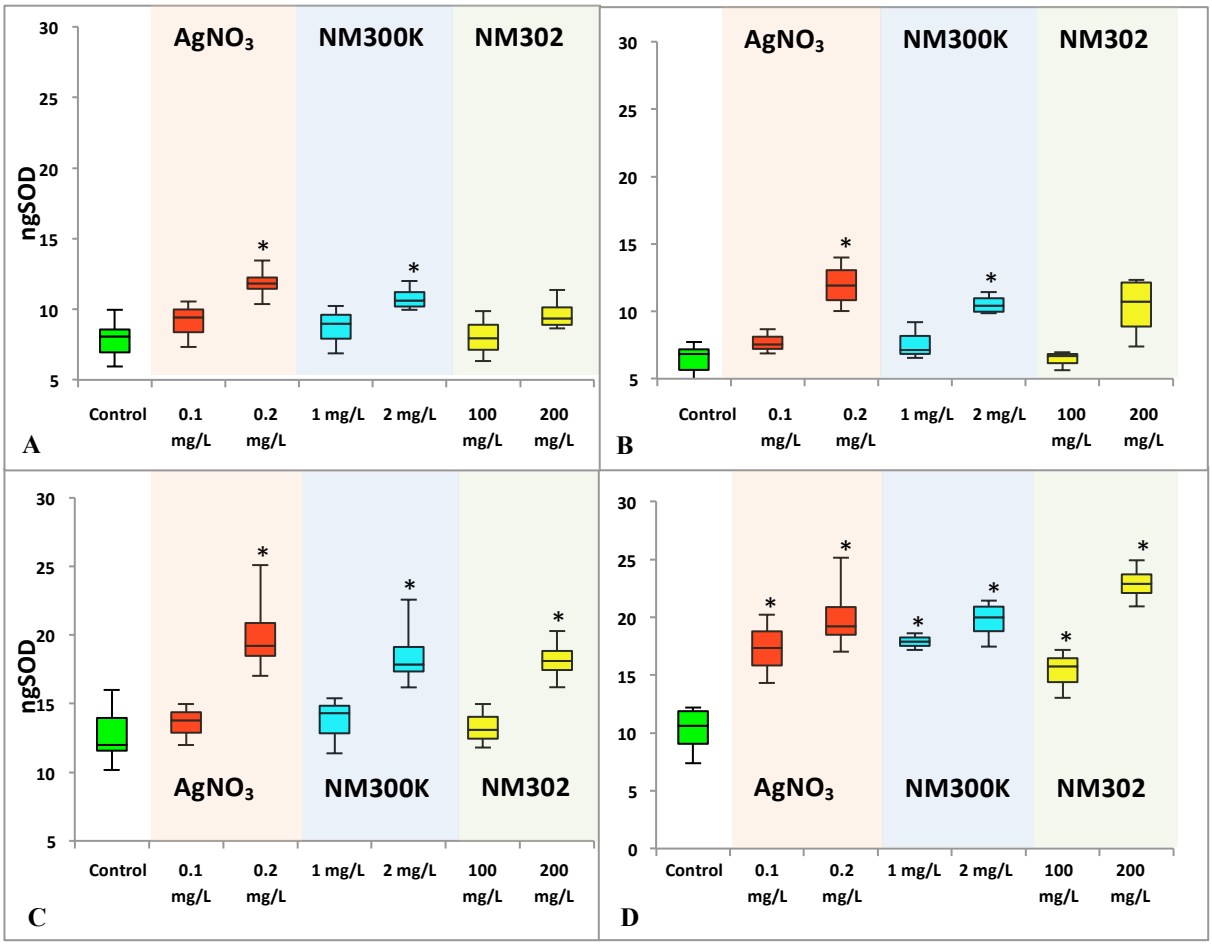

Figure 5.11: Amount of superoxide dismutase (ng) following exposure to each toxicant in 24 hours, **A**: Wild type *C. elegans*, **B**: *ced-3* (-ve), **C**: *sod-3* (-ve), and **D**: *mtl-2* (-ve). Significant differences comparing to the non-treated groups are shown as *.

To investigate the susceptibility of the mutants compared to the wild type, any differences in SOD activity after exposure to various test substances was analysed. Since there was a variation between the levels of SOD in the non-treated groups of the various strains (determined by one-way ANOVA, $p < 0.05$), comparison between strains was made by normalising the data to the mean values of the respective non-treated groups. Comparisons were made between the mutants and the wild type following exposures to the different concentrations (LC_{10} and $2*LC_{10}$) of Ag toxicants after 24 hours of exposure. The normalised levels of SOD activity in each strain are

shown in Figure 5.12. It was found that *mtl-2* (-ve) and *sod-3* (-ve) had significantly higher levels of SOD than the wild type. This observation was found when comparing *mtl-2* (-ve) to the wild type at the concentrations 200 µg/L $AgNO_3$, 1 mg/L JRCNM03002a, 100 mg/L NM302, and 200 mg/L NM302, and when comparing *sod-3* (-ve) to the wild type at the concentration 200 mg/L NM302.

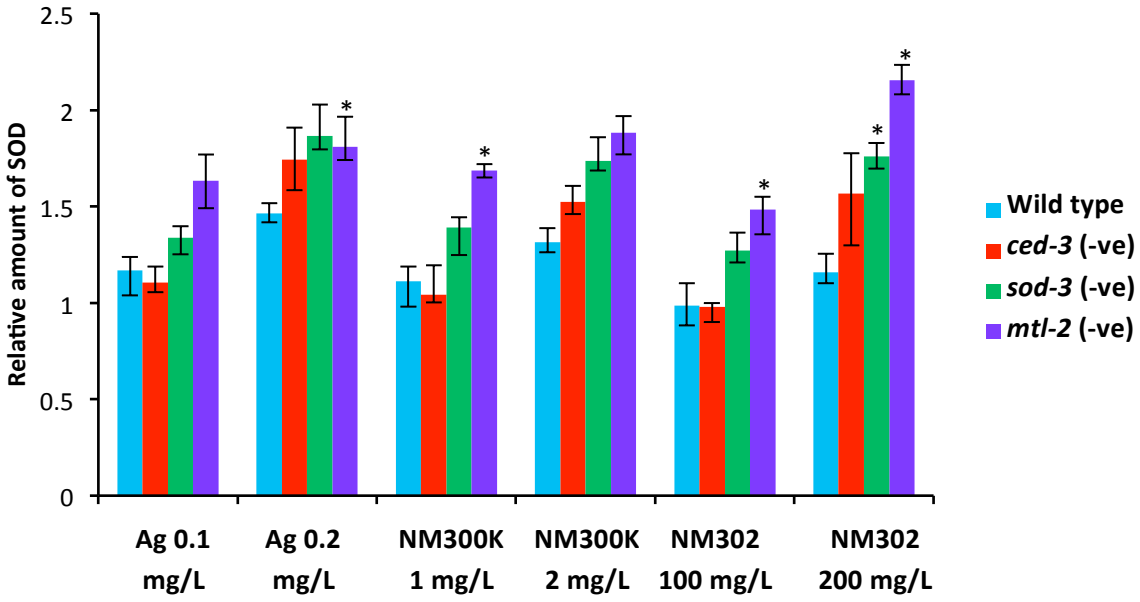

Figure 5.12: Reanalysis of Figure 5.11 by normalising the data with the mean values of the non-treated groups within strains to investigate the susceptibility of mutants compared to the wild type. Relative amounts of superoxide dismutase in relation to the control groups following exposure to various toxicants (median ± IQR). Comparison to the wild type was performed by one-way ANOVA and significant differences are shown as * ($p < 0.05$).

5.4.4 Catalase assay

In the time study, the statistical analysis of CAT assay was performed in the same way as in the SOD assay. Three-way ANOVA was used to analyse the effects of strain, time points, and toxicants on the activity of CAT. The levels of each main effect were described in section 5.4.3. All effects were statistically significant ($p < 0.05$) whereas the three-way interaction was not. However, the two-way interaction between strains and time points was statistically significant, as shown in Table 5.7. This

indicated that the toxicants did not affect the influence from the other factors (strains and time points), and the effect of toxicants on CAT activity was independent from strains and time points. It was deduced from the three-way analysis that toxicants constituted the factor that affected the activity of CAT, while it was unclear how strains and time points impacted CAT activity, given the significant interaction between these factors (strains*time points). Since it was shown that the toxicants had an effect on CAT activity, Tukey post hoc analysis of toxicants revealed that 200 µg/L $AgNO_3$ and 2 mg/L NM300K significantly increased CAT activity when compared to the non-treated group. The rank of toxicity was found to be: 200 µg/L $AgNO_3$ > 2 mg/L JRCNM03002a > 200 mg/L NM302, however, any differences between 200 µg/L $AgNO_3$ and 2 mg/L JRCNM03002a, and 2 mg/L JRCNM03002a and 200 mg/L NM302 were not statistically significant.

Table 5.7: Statistical results obtained from the three-way ANOVA analysis

Factors	Type III Sum of Squares	df	Mean Square	F	Sig.
Toxicants	2.42E-5	3	8.06E-6	6.27	<0.001
Time points	<0.001	2	<0.001	192.20	0.038
Strains	1.76E-5	3	5.88E-6	4.59	0.003
Toxicants*Time points	1.91E-5	6	3.18E-6	2.48	0.456
Toxicants*Strains	1.78E-5	9	1.97E-6	1.54	0.280
Time points*Strains	3.09E-5	6	5.15E-6	4.02	0.003
Toxicants*Time points*Strains	1.28E-5	18	7.1E-7	0.56	0.906

Since a significant interaction was found between strains and time points, it was important to assess how CAT activity responded to the different toxicants within similar strains and time points. One-way ANOVA analysis followed by post hoc Tukey was performed to investigate which toxicants significantly induced SOD activity. As illustrated in Figure 5.13, CAT activity was highest at the 6 h timepoint. However, an impact of toxicants on CAT activity was not consistent between strains i.e. *sod-3* (-ve) and *mtl-2* (-ve) tended to have higher CAT activity than wild type and *ced-3* (-ve). The CAT activity of *sod-3* (-ve) increased significantly after 6 hours exposure to 200 µg/L $AgNO_3$ and 2 mg/L JRCNM03002a, while the *mtl-2* (-ve) had more CAT activity when exposed to all toxicants for 2 hours. The CAT activity of the *mtl-2* (-ve) also increased

when exposed to 200 µg/L $AgNO_3$ for 6 hours. On the other hand, CAT activity decreased significantly in the wild type after 2 hours of exposure to 200 mg/L NM302.

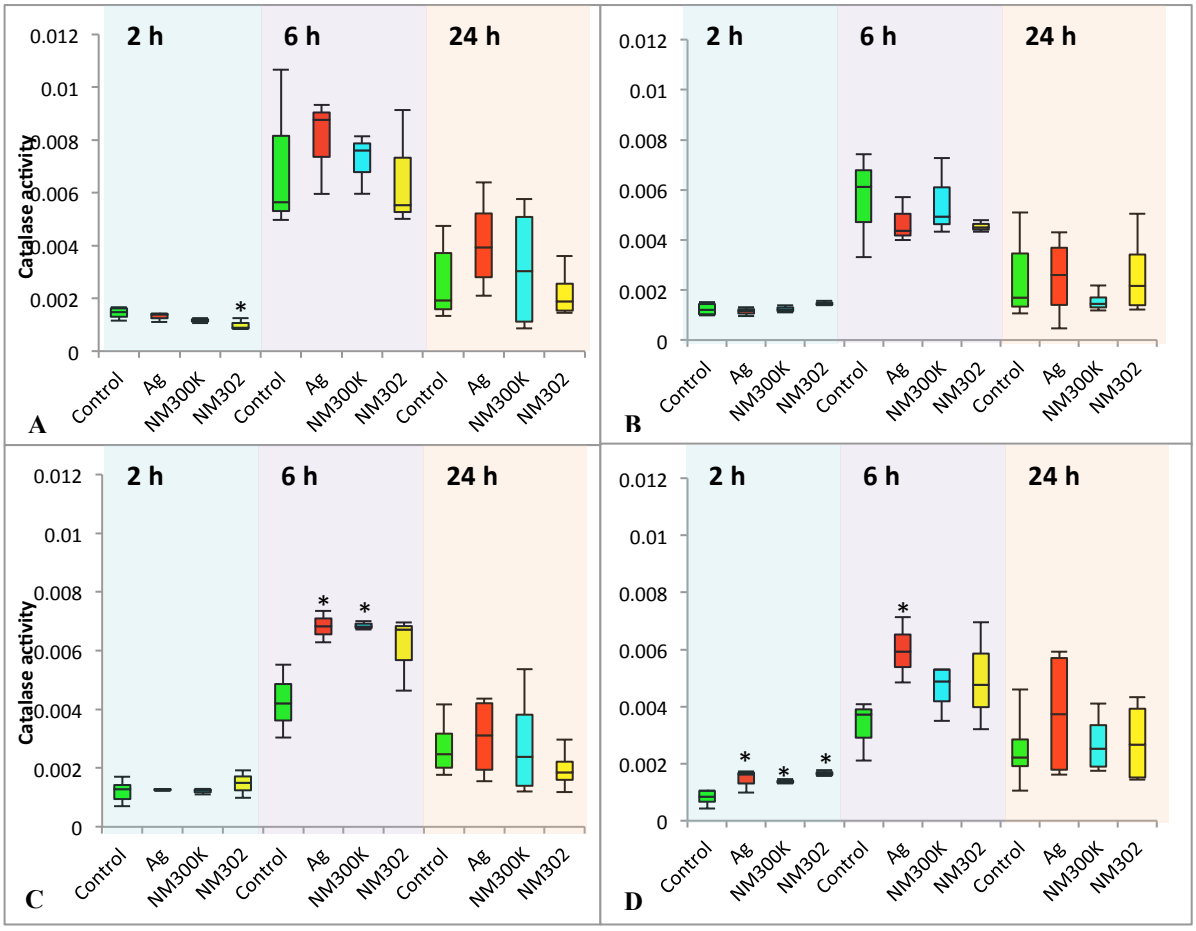

Figure 5.13: Activity of catalase following exposure to different toxicants (2*LC_{10}) at each time-point, **A**: Wild type *C. elegans*, **B**: *ced-3* (-ve), **C**: *sod-3* -(-ve), and **D**: *mtl-2* (-ve). Differences between CAT activity compared to the non-treated group were assessed within strains and time points using one-way ANOVA, any significant differences are represented with *.

In the concentration study, the effect of concentrations of each test toxicant was assessed at LC_{10} and 2*LC_{10} after 24 hours exposure. One-way ANOVA, followed by post hoc Tukey analysis, was used to assess any significant differences in CAT activity following exposure to Ag toxicants compared to the control groups within each strain. Unlike the SOD activity, the pattern of CAT activity was not dependent on the concentration, as shown in Figure 5.14. The lower concentrations (LC_{10}) tended to

induce higher activity of CAT compared to the 2*LC_{10} groups. However, this observation was not statistically significant for every strain.

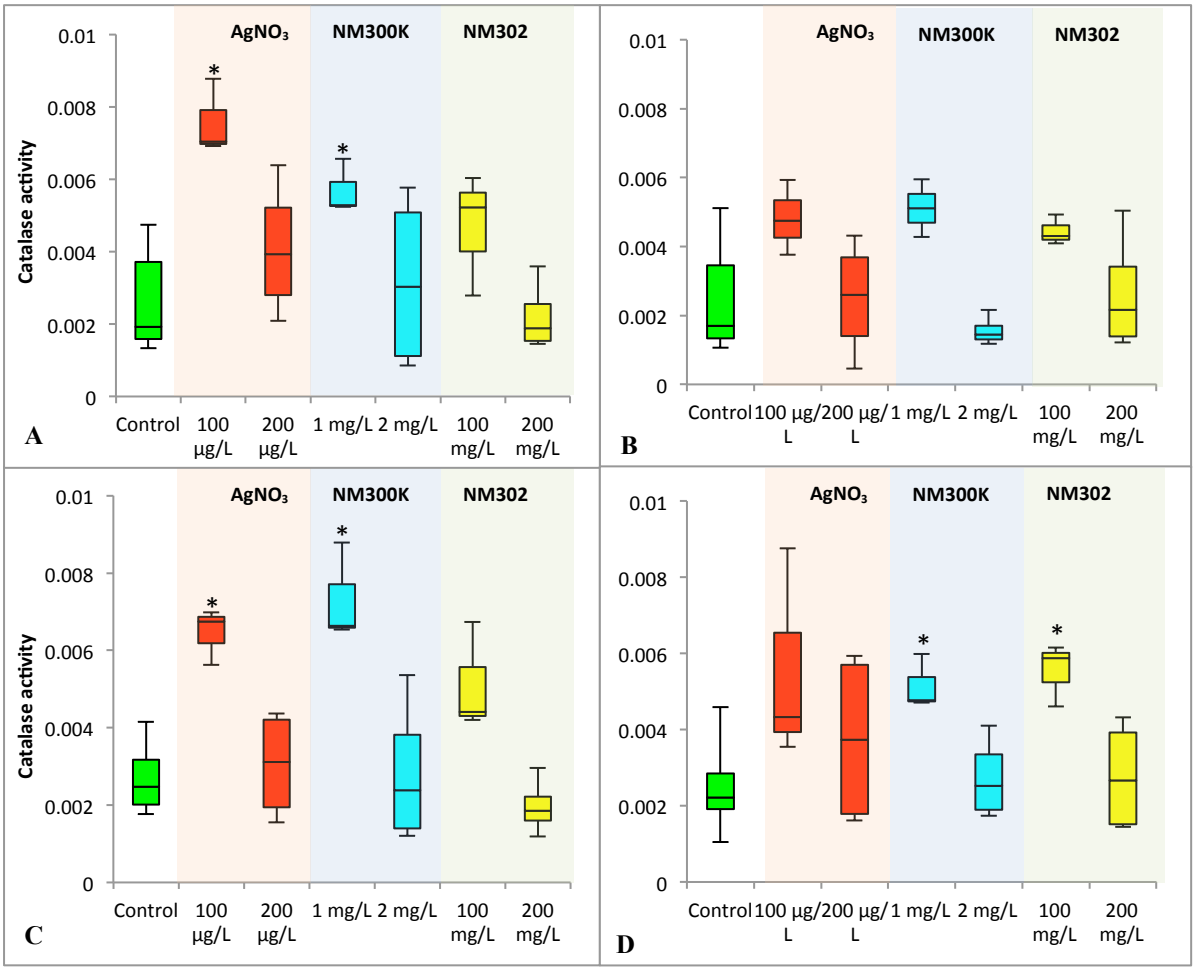

Figure 5.14: Activity of catalase following exposure to each toxicant at 24 hours, **A**: Wild type *C. elegans* (N2), **B**: *ced-3* (-ve), **C**: *sod-3* (-ve), and **D**: *mtl-2* (-ve). The differences in CAT activity were analysed within strains by using one-way ANOVA, any significant differences are represented by *.

To explore the sensitivity of the *C. elegans* mutants compared to the wild type, any significant differences in CAT activity after exposure to the various test substances were analysed. Since the levels of CAT in the non-treated groups varied among the strains, as shown in Figure 5.14, CAT activity was normalised to the mean values of non-treated groups for each of the strains. One-way ANOVA analysis was performed by comparing the normalised CAT activity of each mutant to the wild type, and post hoc Tukey test was used to indicate which mutants had a significant difference in CAT activity. There was no significant CAT activity of knockout strains compared to the wild type, as seen in Figure 5.15.

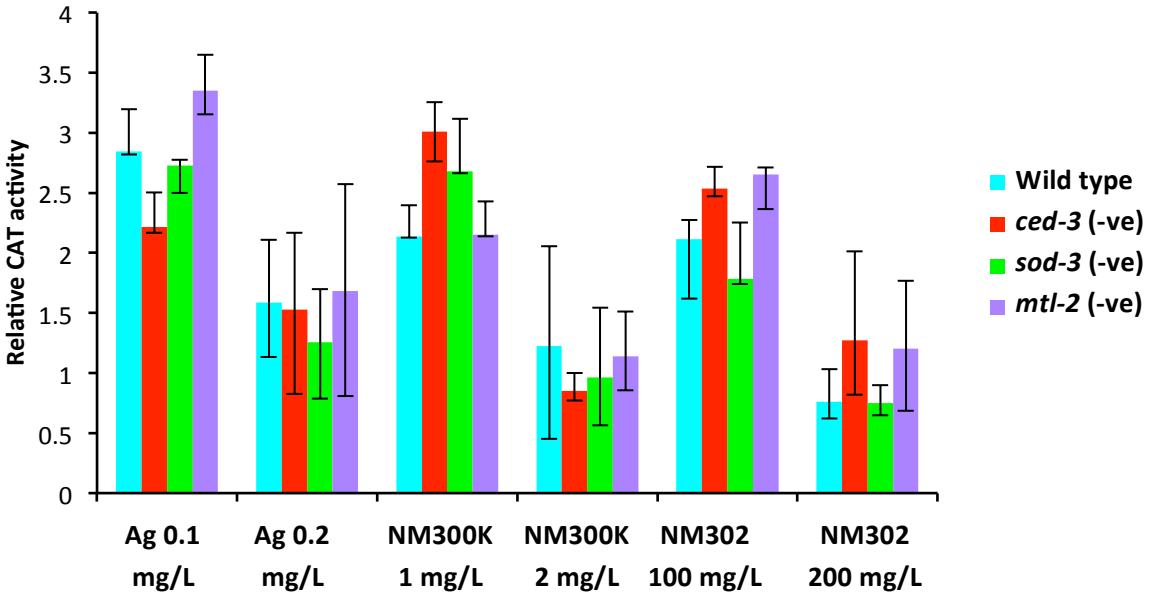

Figure 5.15: Reanalysis of Figure 5.14 by normalising the data with the mean values of the non-treated groups of the respective strain. The relative catalase activity is represented as median ± IQR. Comparison to the wild type was performed by one-way ANOVA, followed by Tukey test. No statistically significant differences were found.

5.5 Discussion

5.5.1 ROS production

The objective of this work was to elucidate the induction of oxidative stress by AgNMs. The oxidative stress is defined by the imbalance in the amount of ROS and the detoxification system in cells, which consequently leads to oxidative damage (Kannan and Jain, 2000). This study was designed to investigate the effects of silver materials on the different strains of nematode in regards to the production of ROS. It was established that both factors were important. All silver toxicants induced higher amounts of ROS when compared to the non-treated group. Moreover, the investigation on the susceptibility of strains carried out by using the normalised level of ROS showed that both *sod-3* (-ve) and *mtl-2* (-ve) had statistically higher ROS levels than the wild type, while there was no difference in ROS levels between the *ced-3* (-ve) and the wild type. Since superoxide dismutase and metallothionein have a role in counteraction and prevention of oxidative stress, the deletion of these genes should result in the higher sensitivity of the mutants in regards to oxidative stress. The finding that *sod-3* (-ve) and *mtl-2* (-ve) had higher ROS levels than the wild type supported the view that silver toxicants induce the production of ROS to the level that the detoxification or prevention by these mutants could not cope with, which might lead to oxidative stress. The study of the effects of concentration of the test toxicants on the induction of toxicity revealed that the pattern of toxicity from all toxicants was concentration-dependent. The concentration of 2*LC_{10} caused a statistically significant increase in toxicitycompared to the controls. Although the fluorescence intensities of nematodes exposed to LC_{10} of silver toxicants was also higher than the control, a significant difference was not established.

It has been stated that ROS may lead to apoptosis. The excess of ROS could lead to the alteration of mitochondrial membrane permeability, interference with the respiratory chain, and activation of the apoptotic machinery (Park *et al*., 2008; Yu *et al*., 2015). The increase in ROS induced by AgNMs occurs in a concentration-dependent fashion according to studies in cell lines and animal models, as reviewed in Table 5.2. Those studies were conducted using a range of time points from 24 to 48 hours, with higher concentrations than used in this study, and different sizes of AgNMs, but they reported similar effects to those observed in this study. Although the same time point of 2 hours has also been used, oxidative stress was not observed in a study using rainbow trout hepatocytes (Farkas, 2010). Another study from this author found that the level of

glutathione, the detoxification molecule, increased in the rainbow trout gill cells after a longer time of exposure to AgNM (48 hours) (Farkas, 2011). This indicates the diverse response between cell types, as well as the time points chosen for the particular cell type. The shorter time of exposure (2-6 hours) was also used in certain publications. Studies assessing oxidative stress following *E. coli* and mouse fibroblasts exposure to AgNMs found an alteration in oxidative stress related genes and in the level of glutathione (GuO, 2010; Lee, 2014). This supports the evidence that oxidative stress response varies between test models and time points. The study on *C. elegans* by Ahn and colleagues also found an increase in ROS generation after 24 hours of exposure to 3.26 mg/L AgNM (<100 nm) (Ahn *et al.,* 2014). This suggests that even in the same test model, different materials may also exhibit a diverse stress response since there was a trend in this study where the DCF fluorescence intensity dropped after two hours of exposure. Regardless of the difference in time and concentration used, findings from this thesis and other publications indicate the ability of AgNMs to induce the production of ROS. However, studying the production of ROS might not be enough to establish the occurrence of oxidative stress. Park *et al.* (2008) stated that NM may exhibit toxicity by altering the level of ROS and by interfering with detoxification processes (Park *et al*., 2008). Therefore, the study of activity of detoxification enzymes would provide supplementary data on the initiation of oxidative stress in *C. elegans*.

5.5.2 Superoxide dismutase assay

The aim of this study was to verify the findings of the DCFH assay that AgNMs would trigger oxidative stress by focusing on a particular detoxification enzyme, superoxide dismutase. The action of this enzyme is to convert superoxide, one of the ROS, into oxygen and hydrogen peroxide, another form of ROS, which could be further removed by catalase. The methodology used in this study was derived from Del Maestro and McDonald (1987). This method was involved in UV detection of the auto-oxidation product of pyrogallol, in which the rate of this reaction was decelerated by SOD.

From this study, it was found that the activity of SOD increased at 24 hours, and the pattern of toxicity was shown be concentration-dependent. Although all silver toxicants exhibited significant levels of SOD compared to the respective non-treated groups, the difference in SOD activity between both types of AgNM was not statistically significant. It was also found that the factor strain had an influence on the

activity of SOD. The *sod-3* (-ve) and *mtl-2* (-ve) had showed higher SOD activity than the wild type, nonetheless, this was not observed following exposures to every toxicant. The different susceptibility of the strains was consistent with the ROS production assay. As described in section 5.5.1 these strains are designed differently in regards to their susceptibility to oxidative stress. As previously stated that the strain *sod-3* (-ve) lacks one isoform of *sod* genes. Although it was found that the level of SOD in *sod-3* (-ve) in the non-treated group was as high as in the other strains, and was even higher than other strains when they were xposed to the toxicants, this could be explained by the redundancy of *sod* genes since there are five *sod* genes in *C. elegans*, as described in section 5.1.2. The *sod-3* gene encodes MnSOD, which is also produced by the *sod-2* gene (Back, Braeckman and Matthijssen, 2012).

Although SOD activity is commonly used as an endpoint for oxidative stress in the literature, the findings reported are not consistent. Some studies have found an increase in SOD activity after the exposure to AgNMs, while others have reported a decrease in SOD activity. The increased SOD activity has been explained by the activation of oxidative stress, which consequently induced the production of detoxification enzymes (Posgai *et al.*, 2011; Wu and Zhou, 2012; Suliman *et al.*, 2013). However, the decreased SOD activity was described by the depletion of these enzymes when encountering oxidative stress (Liu *et al.*, 2010b; Liu *et al.*, 2011; Cozzari *et al.*, 2015). From this explanation, it was suggested that the alteration in SOD activity, either increase or decrease, was the indicator of oxidative stress. However, it is worth noting that the reduction of detoxification enzymes found in some publications (Liu *et al.*, 2010b; Liu *et al.*, 2011; Cozzari *et al.*, 2015) might be an indicator of the different cellular responses, such as inflammation or cell death, which occurs at high levels of oxidative stress, as shown in Figure 1.1. Some studies also reported the reduction in oxidative stress in the presence of antioxidants e.g. N-acetyl cysteine (NAC) (Posgai *et al.*, 2011; Suliman *et al.*, 2013), which indicated AgNMs-induced oxidative stress. The findings in this thesis further supported that AgNMs are able to induce oxidative stress by enhancing the activity of one of the detoxification enzymes. In the next section, the results from the study of another detoxification enzyme, which worked concomitantly to superoxide dismutase, catalase, are discussed.

5.5.3 Catalase

The goal of this study was to assess the ability of AgNMs to produce oxidative stress in *C. elegans* by focusing on the alteration of a specific detoxification enzyme. The results from the CAT study support the findings reported in the previous section. As stated previously, one of the products from the conversion of superoxide is another ROS molecule, H_2O_2. Catalase is also key in the process of ROs detoxification, specifically H_2O_2. The conversion of H_2O_2 produces water and oxygen. The methodology used in this studied followed Claiborne (1985). The principle of this method was to detect the turnover rate of the substrate of this enzyme, H_2O_2 by using UV-Vis spectrophotometry. The higher turnover rate meant a higher amount of catalase. The study was designed in the same way as the SOD study, which was focused on either time points or concentrations.

It was clearly indicated that toxicants had a major effect on CAT activity. Similarly to the SOD assay, all silver toxicants induced a higher level of CAT than that found in the correspondent non-treated groups. However, the difference in CAT activity between the two types of AgNMs was still inconclusive. The difference between SOD and CAT activity tests, was that the CAT level increased after 6 hours of exposure. Moreover, the pattern of toxicity was not concentration-dependent, and the susceptibility of mutants compared to the wild type was not statistically significant. The difference in the findings between these two tests might be explained by the protocol to assess CAT activity. The assay of CAT activity was the UV detection of H_2O_2. In this reaction, the by-product O_2 was generated as bubbles, which might interfere with the readings. Another explanation can be that these enzymes act at different time points, or there might be depletion of catalase during the exposure to the toxicants. Rosety *et al.* (2005) who used the same protocol, also found that CAT activity of gilthead seabream gills started to decline after 24 hours of exposure to malathion, while the activity of other enzymes i.e. SOD and GPx, increased steadily over a 96-hour period. These authors stated that the explanation behind this finding remained unclear (Rosety *et al*, 2005).

The findings of other publications on CAT activity were contradictory just as the findings from the SOD assay. Cozzari and colleagues found a reduction in catalase activity in the ragworm after 11 days of exposure to AgNMs (Cozzari *et al.*, 2015), while Suliman *et al.* (2013) found an increase in catalase activity in human lung epithelial cells after exposure to AgNMs for 24 hours, which could be described as the

activation or the depletion of detoxification enzyme (Suliman *et al.*, 2013). From this study, it was found that the catalase activity was highest at six hours of exposure. Therefore, it might also be suggested that particular models would act on oxidative stress differently. However, the finding in this thesis indicated that AgNMs were able to alter the activity of detoxification enzymes, which is the initial cellular response to oxidative stress.

5.6 Summary of this chapter

The aim of this chapter was to establish the induction of oxidative stress caused by an exposure to AgNMs using three end points, ROS production, SOD activation, and CAT activation. The study was conducted using the concentrations of LC_{10} or $2*LC_{10}$ of all toxicants to prevent the death of nematodes during the experiments (sub-lethal exposures). The findings can be summarised according to the null hypotheses:

1. "NMs would not induce the production of ROS in *C. elegans*".

This hypothesis was rejected because both AgNMs induced ROS generation. This induction was observed when using the higher concentration of $2*LC_{10}$ of both materials. However, there was no difference in ROS production between spherical AgNM and the silver nanorod.

2. "NMs would not alter the activity of enzymes which are antioxidants"

This hypothesis was rejected with regards to the SOD endpoint. The increase in SOD activity was found after exposure to both AgNMs at LC_{10} and $2*LC_{10}$. However, the activity of SOD was not significantly different between the groups exposed to spherical AgNM and silver nanorod. The timepoint study showed that the level of SOD was highest after 24 hours of exposure. As for the CAT activity, this hypothesis was also rejected when considering only one type of AgNM. The spherical AgNM significantly induced an increase in CAT activity after 6 hours of exposure, however the silver nanorod did not change the level of CAT at any time point, which led to the acceptance of the null hypothesis.

3. "There would be no difference in the response regarding oxidative stress endpoints between strains of nematodes exposed to the same toxicant"

This hypothesis was rejected when considering particular endpoints. There was a major difference in ROS production and in SOD activity between mutants and wild type. The

sod-3 (-ve) and *mtl-2* (-ve) strains had higher levels of ROS and SOD than the wild type, while there was no difference in these responses between *ced-3* (-ve) and wild type. On the other hand, this hypothesis was accepted when considering the CAT endpoint. There was no difference in CAT activity between any mutants and the wild type.

4. "There would be no difference in the response between various Ag toxicants tested in the same strain of nematode"

This hypothesis was accepted. All endpoints showed a minor difference between the responses to silver toxicants, which was not statistically significant.

There was a difference in the findings between the two detoxification enzymes. SOD activity increased and reached the highest activity at 24 hours after exposure, whereas CAT activity seemed to peak at 6 hours after exposure. The explanation to this different time of action still needs to be investigated. Moreover, the pattern of toxicity was also contrary between endpoints. While the SOD study suggested a concentration-dependent fashion of toxicity, the CAT activity assay indicated that the lower concentration increased the activity of CAT more than the higher concentration. This finding also requires further study. Although the main aim was achieved in this study, detailed information on the time of action between the two enzymes and the pattern of toxicity should be further addressed.

Chapter 6: Programmed cell death induced by NMs

6.1 Introduction

In this chapter apoptosis was investigated since it can be linked to oxidative stress and because the findings from the previous chapter indicated oxidative stress caused by NMs. It is possible that apoptosis could be an important pathway of toxicity from AgNMs. In this chapter, the machinery of apoptosis, particularly in *C. elegans*, and the evidence of NMs induced apoptosis will be reviewed.

6.1.1 The machinery of apoptosis

Apoptosis comprises four major biochemical components: caspases, death receptors, mitochondria and cytochrome *c*, and pro- and anti-apoptotic proteins (Oleinick, Morris and Belichenko, 2002). Each component is discussed below.

The first component, caspases are a family of cysteine aspartate-specific proteases which are synthesised as pro-enzymes, pro-caspases. They can be classified into three groups according to their function; initiators (Caspase-2, -8, -9, -10), executioners (Caspase-3, -6, -7), and inflammatory caspases (Caspase-1, -4, -5) (Cohen, 1997; Rai *et al.*, 2005). To trigger the apoptotic signalling pathway, pro-caspases need to be activated by other caspases in a cascade (Lawen, 2003). The caspase cascade initiates from the autocatalytic proteolysis of initiator caspases, consequently the downstream executioner pro-caspases are cleaved through signal transmission and the active executioner caspases are functionalised (Salvesen and Dixit, 1999). The activation of executioner caspases leads to the impairment of the actin and filament network inside cells, the arrest of protein synthesis, and the induction of DNase (Enari *et al.*, 1998). The executioner caspase-3 has the ability to suppress many important cellular proteins e.g. ICAD (inhibitor of caspase-activated DNase), and ROCKI (Rho-associated coil-coil forming kinase I). The suppression of ICAD leads to DNA fragmentation, while the inhibition of ROCKI induces membrane blebbing, and consequently cell death (Lawen, 2003).

Another constituent in apoptotic machinery, death receptors are some of the important components involving the extrinsic pathway of apoptosis. They are members of the tumour-necrosis factor (TNF) receptor gene superfamily (Locksley, Killeen and Lenardo, 2001). The receptors in this superfamily are composed of the cysteine-rich

extracellular domains and an intracellular domain with approximately 80 amino acids called the death domain (DD), which is an important domain in apoptotic signal transmission (Ashkenazi and Dixit, 1998). The apoptotic signals are transmitted by the binding of ligands to these receptors. To date, ligands known to bind these receptors and trigger the apoptotic signal are FasL/FasR, TNF-α/TNFR1, Apo3L/DR3, Apo2L/DR4, and Apo2L/DR5 (Chicheportiche *et al.*, 1997; Ashkenazi and Dixit, 1998; Peter and Krammer, 1998; Rubio-Moscardo *et al.*, 2005). The extrinsic pathway of apoptosis is best explained with the FasL/FasR and TNF-α/TNFR1 models, which are involved in the complexation of receptors upon ligand binding, adaptor proteins, and initiator caspases (Procaspase-8 for Fas model, and-10 for TNF model) (Lawen, 2003; Elmore, 2007). In the Fas model, the apoptotic signal initiates from the binding of Fas ligand to Fas receptor, which recruits the adaptor protein, Fas-associated death domain protein (FADD). While in the TNF model, TNF receptor-associated death domain protein (TRADD) is recruited with FADD and receptor interacting protein (RIP) upon the binding of TNF ligand to TNF receptors (Hsu, Xiong and Goeddel, 1995; Grimm *et al.*, 1996; Wajant, 2002), creates a complex called death-inducing signalling complex (DISC) (Kitschkel *et al.*, 1995), which leads to the autocatalysis of initiator caspases and induces the next apoptotic sequence, the execution phase (Elmore, 2007). The inhibition of extrinsic pathway is regulated by a protein called c-FLIP (FLICE-inhibitory protein), which binds to FADD and caspase-8 causing them to become inactive (Kataoka *et al.*, 1998; Scaffidi *et al.*, 1999).

The intrinsic pathways of apoptosis does not involve death receptors and are initiated by mitochondria. The induction of apoptosis via the mitochondrial pathway can lead to either positive or negative regulation. Cellular apoptosis regulated by a negative control is involved in the lack of some growth factors, hormones, and cytokines which suppresses the death program. The positive regulation can be triggered by extra- or intracellular stimuli including radiation, toxins, and free radicals (Elmore, 2007). Cellular signals inducing mitochondria-mediated apoptosis lead to the release of two major groups of inactive pro-apoptotic proteins into the cytosol (Saelens *et al.*, 2004). The first group of proteins including cytochrome *c*, Smac/DIABLO, and HtrA2/Omi has a major function in triggering the caspase-dependent intrinsic pathway (Cai, Yang and Jones, 1998; Du *et al.*, 2000; van Loo *et al.*, 2002; Garrido *et al.*, 2006). Released cytochrome *c* forms a complex with Apaf-1 and procaspase-9 called apoptosome. Procaspase-9 in the apoptosome undergoes catalytic activation to the active form caspase-9 and consequently activates execution caspases (Chinnaiyan, 1999; Hill *et al.*,

2004). The amplification of apoptotic activity of Smac/DIABLO and HtrA2/Omi was suggested to antagonise IAP (Inhibitors of apoptotic proteins) (De Laurenzi and Melino, 2000; Du *et al.*, 2000; Green, 2000; Verhagen *et al.*, 2000). Another group of pro-apoptotic proteins that are released in the mitochondrial- mediated apoptotic events are AIF (Apoptosis inducing factor), endonuclease G, and CAD. These proteins are discharged to the cytosol in the phase that cells are already committed to die (Elmore, 2007). AIF and endonuclease G induce cell death in a caspase-independent manner by translocating into the nucleus and causing DNA fragmentation, also AIF induces chromatin condensation, referred to as a stage I condensation (Susin *et al.*, 2000; Hunot and Flavell, 2001; Joza *et al.*, 2001; Li, Luo and Wang, 2001). CAD has to be cleaved by caspase-3 after translocation into the nucleus, the active CAD induces the DNA fragmentation (Enari *et al.*, 1998) and chromatin condensation referred as stage II condensation (Susin *et al.*, 2000).

The family of Bcl-2 proteins controls the apoptotic events by functioning as anti- or pro-apoptotic. The regulation of apoptosis where these proteins primarily take part in is the mitochondria and is thought to involve cytochrome *c*. The proteins characterised as anti-apoptotic include Bcl-2, Bcl-x, Bcl-XL, Bcl-XS, Bcl-w, BAG, while the pro-apoptotic function is found in Bcl-10, Bax, Bak, Bid, Bad, Bim, Bik, and Blk (Elmore, 2007). These proteins can be classified as sensors, guardians, and effectors. These three groups of Bcl-2 family proteins all contain Bcl-2 homology (BH) regions, but in different numbers. The guardians including Bcl-2 and Bcl-XL act as anti-apoptotic proteins with all four regions, BH1-4. The effectors, Bax and Bak, have three regions, BH1-3. The sensors such as Bad, Bim, and Bid comprise of BH3 domain which is important to bind to anti-apoptotic guardians, so their pro-apoptotic function involved in preparing and releasing of the effectors from the guardians (Conradt, 2013). The schematic of function of Bcl-2 family proteins is illustrated in Figure 6.1.

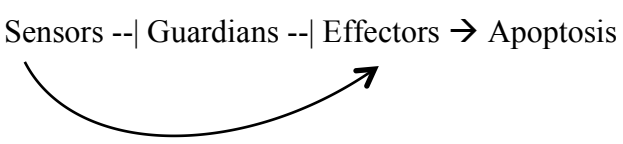

Figure 6.1: The regulation of apoptosis controlled by Bcl-2 family proteins (Conradt, 2013)

Apoptosis can be induced via another pathway, perforin/granzyme in which the cells destined to die are killed by cytotoxic T lymphocytes (CTLs). Cells are recognized to be destroyed by CTLs via the extrinsic pathway and the Fas interaction

(Brunner *et al.*, 2003). In addition, cells can be destroyed by CTLs via the same pathway as tumour and viral infected cells which involves the secretion of perforin, the molecule that creates transmembrane pore in which granules containing serine proteases granzyme A and granzyme B can translocate into the target cells (Trapani and Smyth, 2002). Granzyme B activates pro-caspase-10 and cuts ICAD (Sakahira, Enari and Nagata, 1998), as well as amplifying an apoptotic signal via the mitochondrial pathway by cleaving Bid specifically to the active form, truncated Bid (tBid), and inducing the release of cytochrome *c* (Barry and Bleackley, 2002; Russell and Ley, 2002). In addition, caspase-3 can be directly activated by granzyme B; therefore, the execution phase of apoptosis is straightforwardly triggered (Elmore, 2007). The function of granzyme A involves activating DNA nicking by NM23-H1 (DNase); the gene encoding this DNase is normally inhibited by nucleosome assembly protein SET. Granzyme A can also cut SET and promote DNA degradation. SET complex has another function in maintaining chromatin and DNA structure, as well as DNA repair (Fan *et al.*, 2003). Cleavage of the SET complex leads to the promotion of apoptosis via DNA and chromatin degradation (Elmore, 2007). The induction of the apoptotic pathway via the extrinsic and intrinsic pathways is shown in Figure 6.2.

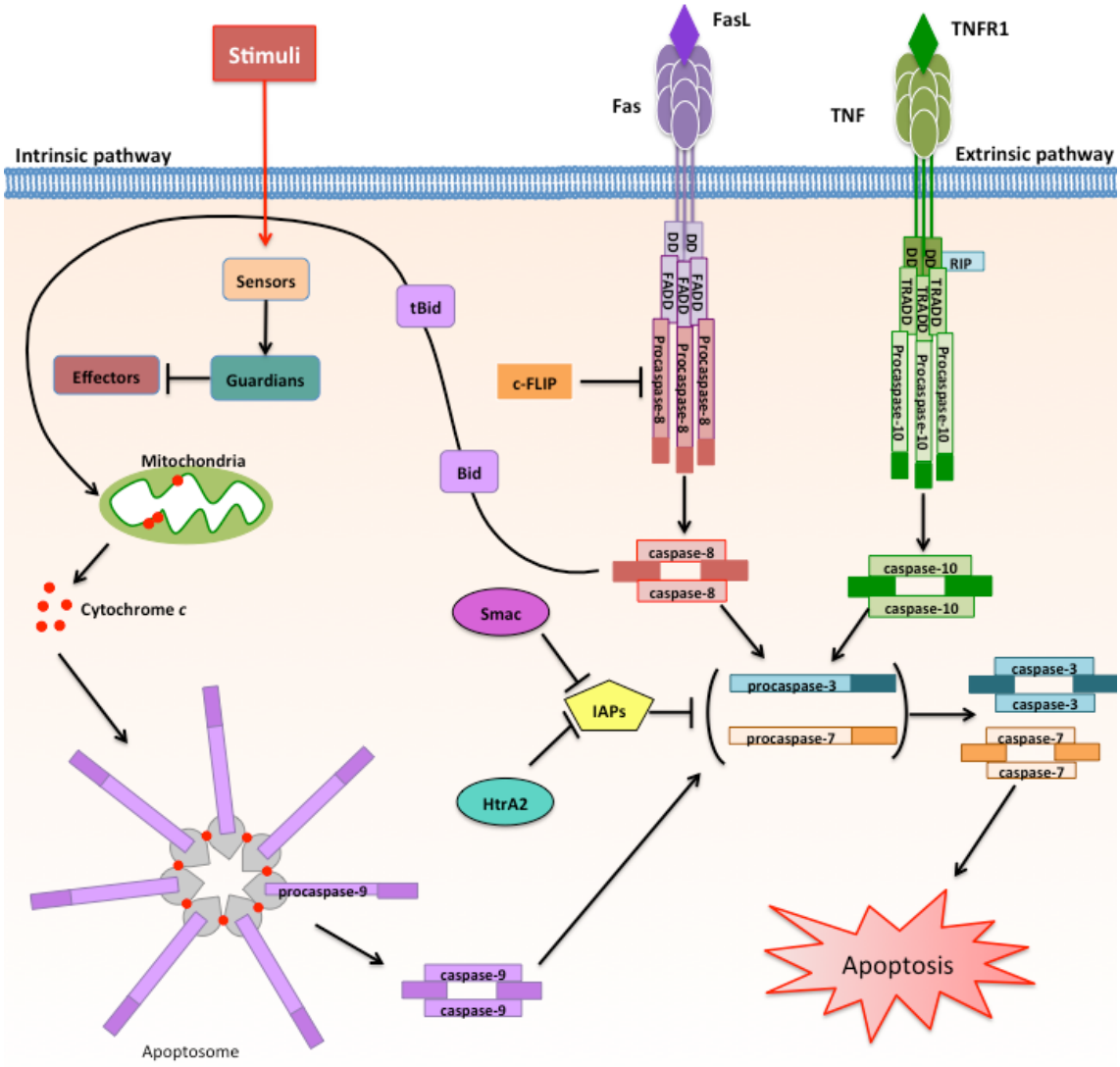

Figure 6.2: The extrinsic and intrinsic pathway to induce the apoptotic signal (Adapted from Elmore, 2007).

Programmed cell death has been investigated in *C. elegans*, and found to be conserved with that of humans (Lawen, 2003). The function and structure of proteins regulating the death machinery in human and *C. elegans* is similar, as can be seen in Table 6.1.

Table 6.1: Conservation of apoptotic proteins in *C. elegans* and mammals (Lawen, 2003)

	C. elegans	Mammals	
		Intrinsic	Extrinsic
Promoter	EGL-1	Bax BH3-only proteins	Fas/FasL TNFR1/TNF-α DR4,5/TRAIL
Inhibitor	CED-9	Bcl-2, Bcl-X_L	FLIP
Adaptor	CED-4	Apaf-1	FADD TRADD
Initiator caspase	CED-3	Caspase-9	Caspase-8
Caspase inhibitor		IAP	IAP
Inhibitor of IAP		Smac/Diablo Omi/HtrA2	Smac/Diablo
Effector caspase	CED-3	Caspase-3, caspase-7	Caspase-3, caspase-7

6.1.2 Apoptosis in C. elegans

The deletion of unwanted cells in *C. elegans* is extremely precise. *C. elegans* hermaphrodites have an exact number of 1090 somatic cells. During embryogenesis and larval development, 131 of these cells are eliminated via programmed cell death. A total of 116 that are destined to be deleted have been determined to be nerve cells and the others are ectoderm (Lawen, 2003). Apoptosis in *C. elegans* can be distinguished into three different phases: specification, killing and execution phases, which are controlled by different genes.

Programmed cell death in *C. elegans* occurs in an autonomous manner in which cells are determined at their birth whether to live or die (Sulston and White, 1980). The most upstream genes that regulate apoptosis in the specification phase of *C. elegans* are *eor-1* and *eor-2* (*eor*, enhancer of Raf) which control the death of hermaphrodite-specific neurons (HSNs). These neurons control the movement of the vulva of hermaphrodites during egg-laying, therefore, are eliminated in males via apoptosis. In contrast, the deletion of neuro-secretory motorneuron (NSM) sister cells are regulated by *ces-2* (*ces*, cell death selection abnormal). These cells are divided from NSM

precursors apart from NSMs, thus they are eliminated so to leave only NSMs to function. The probable direct regulators of transcription of *egl-1* (*egl*, egg-laying defective; gene in the killing phase) are *tra-1* (*tra,* transformer) which controls the death of HSNs, while *hlh-2*, *hlh-3* (*hlh*, helix-loop-helix transcriptional factor), and *ces-1* are direct regulators of *egl-1* to kill NSM sister cells (Conradt and Xue, 2005).

The killing phase in *C. elegans* is controlled by four genes: *egl-1*, *ced-9*, *ced-4*, and *ced-3* (*ced*, cell death abnormal). The gene *egl-1* has been found to be extremely important for apoptosis (Conradt and Xue, 2005). It encodes a small protein with a BH3 (BH3, Bcl-2 homology region 3) domain that has been found in all pro-apoptotic Bcl-2 family proteins (Conradt and Horvitz, 1998; Bouillet and Strasser, 2002). The gene *ced-3* encodes proteases enzymes named CED-3, whose proteolytic-activity is essential for apoptosis in *C. elegans*. This enzyme is required for DNA fragmentation and cell engulfment (Xue, Shaham and Horvitz, 1996). The gene *ced-4* encodes a protein, CED-4 whose activity is similar to human Apaf-1 (Apaf, Apoptotic protease activating factors), which is important to activate the apoptotic signalling cascade (Yuan and Horvitz, 1990; Zou *et al.*, 1997). The pro-apoptotic gene, *ced-4,* might also produce a spliced transcript, *ced-4L* that acts against programmed cell death. The anti-apoptotic gene, *ced-9*, encodes a protein similar to the proteins translated from human *bcl-2*, which prevent apoptosis (Hengartner and Horvitz, 1994).

Finally, the execution phase is the disassembly process which consists of nuclear DNA fragmentation, cytoplasm shrinkage, and presenting of "eat-me" signals on the cell surface (Steller, 1995). Genes that are found to be involved in this phase are *crn-1* to *crn-6* (*crn*, cell death related nucleases), *cyp-13* (*cyp*, cyclophillins), *nuc-1* (*nuc*, nuclease defective), *cps-6* (*cps*, CED-3 protease suppressors), *wah-1* (*wah*, worm AIF homologue), *ced-1*, *ced-7*, *ced-6*, *ced-2*, *ced-5*, *ced-10*, *ced-12*, and *psr-1* (*psr*, phosphatidylserine receptor homologue). To degrade DNA into fragments, genes act in multiple pathways: *cps-6*, *wah-1*, *crn-1*, *crn-4*, *crn-5*, and *cyp-13* act in one pathway, while *crn-2* and *crn-3* regulate another pathway (Wang *et al.*, 2002; Parish and Xue, 2003). The partial redundancy is also found in the corpse engulfment process which *ced-2*, *ced-5*, *ced-10*, and *ced-12* are involved in actin skeleton rearrangement to promote the movement and engulfment of the engulfing cells (Reddien and Horvitz, 2000), while *ced-1*, *ced-6*, and *ced-7* regulate cell corpse recognition (Zhou, Hartwieg and Horvitz, 2001). The schematic pathway of programmed cell death in *C. elegans* is illustrated in Figure 6.3.

The main aim of this chapter was to capture the DNA fragmentation, and corpse engulfment (execution phase, figure 6.3) of the apoptotic cells in *C. elegans* which can be stained by fluorescent dyes. These dyes bind to the apoptotic cells at specific stages of apoptosis. Acridine orange and propidium iodide (conjugated with Annexin V) are the markers for DNA fragmentation, while Annexin V selectively binds to the specific molecules that are presented during the corpse engulfment phase, as will be discussed in section 6.3.3. The protein determination focused on the intrinsic pathway, which includes proteins in Bcl-2 family, nuclear proteins, and the inhibitor of IAP. Although some of these proteins might be absent, or presented as the homologues in *C. elegans*, it was expected that the similar active sites between mammalian and *C. elegans* homologues would provide information on how apoptotic proteins in *C. elegans* alter their expression after exposure to the test substances.

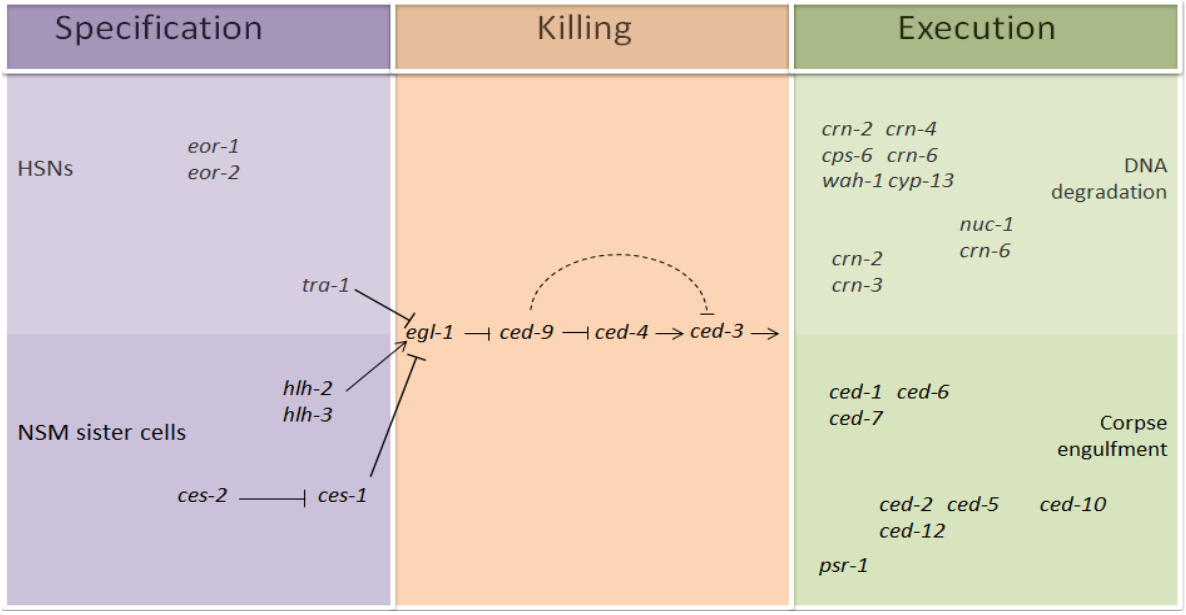

Figure 6.3: Genes involved in apoptotic phases in *C. elegans* (Conradt and Xue, 2005)

6.1.3 Apoptosis induced by NMs

As the connection between oxidative stress and apoptosis, as well as the findings of the induction of oxidative stress leading to apoptosis caused by AgNMs, were described in Chapter 5, the activation of apoptosis triggered by various NMs are reviewed in this chapter. It is evident that exposure to various types of NMs may result in the activation of the apoptotic machinery. Those studies reported in the literature were conducted in many types of cell lines and animal models, as shown in Table 6.2.

Table 6.2: Studies focusing on the alteration of the apoptotic endpoints caused by exposure to nanomaterials in various types of cell lines and animal model.

Cell line/species	NM type	Size (nm)	Time of exposure	Conc.	Change in apoptotic endpoints	Ref.
Human liver carcinoma cells	Silica	15	72 h	200 µg/mL	↑ cell cycle checkpoint gene (*p53*), pro-apoptotic gene (*bax*), *caspase-3* ↓ anti-apoptotic gene (*bcl-2*)	Ahmad et al, 2012
Human epithelial cells and mouse L929 cells	Silica coated MnO	19.5 ± 5.1	24 h	10-200 µg/mL	↑ depolarisation of mitochondrial activity, cells in G2/M and sub G1 phase, apoptotic cells (AnnexinV/PI), expression of p53, Bax, caspase-3 ↓ expression of Bcl-2 L929 cells were more sensitive than HeLa cells	Yu et al, 2015
Human liver carcinoma cells	Nickel	28.39	24 h	25-100 µg/mL	↓ mitochondrial membrane potential, mRNA of *bcl-2* ↑ activity of caspase-3, mRNA of *p53, bax, caspase-3* ↑ cells in sub G1 phase indicated the apoptosis	Ahmad et al, 2013
Human blood monocytes	CeO_2	10-30	40 h	5, 10 µg/mL	↑ mitochondrial damage, activated form of Bax, apoptotic inducing factor (AIF)	Hussain et al, 2012
Human lung carcinoma cells	Ag	100	4, 24 h	50, 100 µg/mL	↑ cells in G2/M and sub G1 phase, expression of p21, p53, pro-apoptotic proteins (Bax, Bid) ↓ anti-apoptotic proteins (Bcl-2, Bcl-w), pro-caspases-8, -3	Lee et al, 2011
Human T-lymphoma cells	Ag	28-35	4-24 h	0.05-0.2 mg/L	↑ p38, cells in G2/M phase, cells stained with AnnexinV/PI and Hoechst33342 ↓ mitochondrial membrane potential	Eom et al, 2010
Human Chang liver cells and Chinese hamster lung fibroblasts	Ag	100	12 h	1-8 µg/mL	↑ mitochondrial Ca^{2+} level, expression of caspase-12	Zhang et al, 2012

Table 6.2 (Cont.): Studies focusing on the alteration of the apoptotic endpoints caused by exposure to nanomaterials in various types of cell lines and animal model.

Cell line/species	NM type	Size (nm)	Time of exposure	Conc.	Change in apoptotic endpoints	Ref.
Human liver carcinoma cells	ZnO	30	12 h	14, 20 µg/mL	↑ apoptotic cells stained with AnnexinV and Hoechst33342, expression of Bax, p53, phosphorylated p38 ↓ mitochondrial membrane potential, expression of Bcl-2, pro-caspase-9	Sharma et al, 2012
Human bronchial epithelial cells	TiO_2	27.39 ± 0.031	24 h	5-100 µg/mL	↑ apoptotic cells stained by YP and AnnexinV, mRNA of caspase-3, expression of p53, Bax, cytochrome *c*, caspase-9 ↓ expression of Bcl-2	Shi et al, 2010
Human liver carcinoma cells	TiO_2	30-70	24, 48 h	20-80 µg/mL	↓ mitochondrial membrane integrity, expression of Bcl-2 ↑ early and late stage apoptosis, expression of p53, cytochrome *c*, Bax, caspase-9, caspase-3, Apaf-1	Shukla et al, 2011
Rat pheochromocytoma cells	TiO_2	Anatase/ Rutile 20	24 h	25-200 µg/mL	↓ mitochondrial membrane potential, expression of Bcl-2 ↑ apoptotic and necrotic cells (AnnexinV), cells in G2/M phase, expression of JNK, c-Jun, p53, p21, Bax, caspase-3 Anatase induced these endpoints > Rutile	Wu et al, 2010
Mouse male somatic cells and spermatogonial stem cells	Ag	10, 20	24 h	10-100 µg/mL	↑ expression of p53, Bax, mRNA levels of *caspase-3, -8, -9* The induction was higher in 10 nm AgNM	Zhang et al, 2015
Dalton's ascites lymphoma in Swiss albino mice	Ag	19-42	10 d	35 µg/kg	↑ caspase-3, -8, -9, -12, p53, cytochrome *c*	Jacob, 2015
Mouse blastocytes	Ag	13	24 h	25, 50 µM	↑ apoptotic cells stained with TUNEL and AnnexinV/PI	Li et al, 2010

Table 6.2 (Cont.): Studies focusing on the alteration of the apoptotic endpoints caused by exposure to nanomaterials in various types of cell lines and animal model.

Cell line/species	NM type	Size (nm)	Time of exposure	Conc.	Change in apoptotic endpoints	Ref.
Wister rats brain	TiO_2	21	4 wk	IV: 5, 25, 50 mg/kg	↑ apoptotic cells stained with AnnexinV, expression of p53 and Bax, activation of caspase-3 ↓ expression of Bcl-2	Meena et al, 2015
Immortalised mouse hippocampal cells	CuO	31	6-24 h	1-80 µg/mL	↑ expression of Bax ↓ expression of Bcl-2	Niska et al, 2015
Swiss albino mice	Ag	43.6 ± 6.4	24, 72 h	IP: 26, 52, 78 mg/kg	↑ Apoptotic cells in liver along with the ↑ liver enzymes	Gurabi et al, 2015
Juvenile *Epinephelus coioides*	Cu	10-30	25 d	20, 100 µgCu/L	↑ apoptotic cells (TUNEL), caspase-3, -9, mobilisation of cytochrome *c* to cytosol	Wang et al, 2015
Drosophila melanogaster, 3rd instar larvae	Ag	10.9 ± 4.58	24, 48 h	50, 100 µg/mL	↑ activity of caspase-3, -9, p53, p38 ↓ mitochondrial activity	Ahamed et al, 2010

6.2 Aim of this chapter

This chapter aimed to investigate whether apoptosis was observed as a consequence of AgNMs exposure to *C. elegans*. As the results presented in Chapter 4 showed that the *C. elegans* strain lacking a pro-apoptotic gene was more tolerant to the Ag toxicants than the other strains in terms of mortality and reproduction, it was likely that apoptosis might be one of the pathways of toxicity following exposure to AgNMs. The null hypotheses tested were:

1. NMs would not induce apoptosis in *C. elegans*
2. There would be no difference in the response regarding the apoptotic endpoints between strains of nematode exposed to the same toxicant
3. There would be no difference in the response between various silver toxicants tested in the same strain of nematode

6.3 Materials and methods

6.3.1 Pilot studies

The method of using acridine orange in the visualisation of apoptotic cells in *C.elegans* was tested with various concentrations of camptothecin (10-200 μM) to find which concentration was suitable to induce apoptosis, and did not kill the nematodes. The detection of apoptotic cells by visualisation was done every hour in the first 4 hours, then at 6, and 24 hours using camptothecin as a positive control.

6.3.2 Acridine orange straining

Acridine orange is a dye which binds to the nucleic acids and can be detected using fluorescence microscopy. DNA fragmentation induced by apoptosis results in the emission of a red colour by acridine orange. To conduct the experiment using acridine orange, a total of 10 nematodes were exposed to a concentration of 100 μM of positive control (camptothecin, sourced from Sigma-Aldrich) or LC_{10} and LC_{50} of all Ag toxicants for 24 hours prior to staining in the petri dishes. The nematodes were then collected and washed to remove the toxicants by centrifugation and re-suspended using SSPW. After that 20 μg/mL acridine orange (purchased from Sigma-Aldrich) was added to stain the nematodes. The staining procedure was done for 2 hours in the dark

to ensure the dye was taken up by the nematodes. Before transferring to the agar pad for visualisation, the nematodes were allowed to recover on a *E. coli* seeded plate for 10 minutes, and then were picked and mounted onto the agar pad containing the paralysing agent, 1 mM levamisole (obtained from the School of Veterinary Studies, University of Edinburgh), in order to anesthetise the nematodes during the visualisation.

The visualisation was performed using a Zeiss Axiophot fluorescence microscope equipped with the live-view camera, Zeiss AxioCam ERc5s. The images were taken using the software, Zen 2012, at excitation wavelength of 450-490 nm and emission wavelength of 520 nm with magnification of 10x and 40x. The apoptotic cells appeared as yellow-orange, while the live cells were visible as a consistently green colour. In addition, the visualisation was performed using confocal microscopy to obtain Z-stack images, which provide the view of apoptotic cells in depth. The model of confocal microscope used was Leica TCS SP 2 with the software, LAS-AF. The images were taken using the same emission/excitation wavelength and at a magnification of 20x.

6.3.3 Annexin V staining

The Annexin V/Propidium iodide (PI) detection kit was purchased from NBS Biologicals. Annexin V/PI was used to detect the early stage of apoptosis, in which the membrane phospholipid phosphatidylserine (PS) is translocated to the outer side. The flipping consequently exposes the PS molecule, which is bound by Annexin V. The conjunction of PI in the kit was used as an indicator for the late stage apoptosis or necrosis. The principle of this conjugated staining is depicted in Figure 6.4. The exposure of *C. elegans* to a positive control and toxicants was similar to the acridine orange assay, as described in section 6.3.2. However, instead of re-suspending the nematodes in SSPW, the Annexin V binding solution was used to re-suspend the nematodes to obtain the final volume of 100 µL, and 5 µL of Annexin V and FITC conjugate and 5 µL of PI were added to stain *C. elegans*. The incubation was done for 15 minutes in the dark. After that nematodes were transferred into the agar pad containing levamisole and were examined using the Zeiss fluorescence microscope at the wavelength of 450-490/520 for FITC and 546/590 for PI in the magnification of 40x.

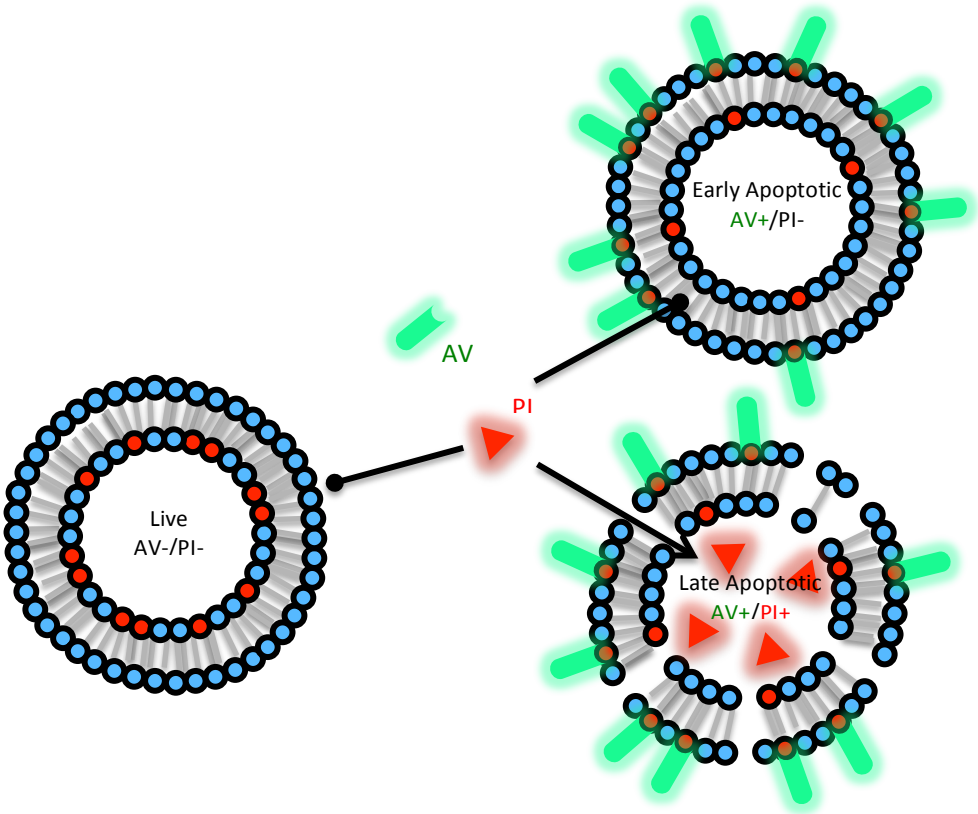

Figure 6.4: The principle of Annexin V and PI staining for the detection of apoptotic cells. Red circles represent phosphatidylserine (PS) on the cell membrane, AV is Annexin V, and PI is propidium iodide. The live cells express PS in the inner cell membrane. This molecule is turned out to the outer cell membrane in apoptotic cells, which AV can bind to. The apoptotic cells in the late stage have the deformity of cell and nuclear membrane, as well as DNA fragmentation. The defect in the membrane allows PI to penetrate and intercalate with the DNA fragments.

6.3.4 Apoptotic protein determination

The determination of apoptotic proteins was conducted using Bio-Plex Pro RBM Apoptosis Assay Panel 1 (sourced from Bio-Rad), which is suitable to analyse mammalian apoptotic proteins; Bak, Bax, Lamin B, and Smac. The exposure of nematodes to the test substances was similar to the previous assays as described in section 6.3.2 (LC_{10} and LC_{50}, 24 h). However, the protein determination required much more tissue, therefore, six plates of nematodes were used for each replicate (approx. 9000 nematodes). After the exposure procedure, nematodes were washed and re-

suspended in the lysate buffer containing protease inhibitor to prevent the degradation of proteins. The nematodes were then homogenised using an electrical homogeniser. The tissue lysate was then frozen using liquid nitrogen and thawed immediately before sonication for 20 seconds to promote the lysis of nematodes. The tissue lysate was then centrifuged at 4500 xg for five minutes at 4 °C and supernatant collected. The amount of protein in each sample was determined using the fluorescamine assay, which will be explained in section 6.3.5. The apoptotic protein determination was based on immunocytochemistry. The proteins of interest are bound to the specific antibody, which is fused with a magnetic bead, consequently the proteins of interest are fixed and were quantified by the detection antibody which conjugated with a fluorescent reporter, as illustrated in Figure 6.5. Samples were prepared according to the protocol, depicted in Figure 6.6, before reading in the Bio-Plex 200 reader (Bio-RAD MAGPIX Multiplex Reader). The data were collected using the Bio-Plex Manager software. Each sample was tested in duplicate as stated in the protocol obtained with the kit.

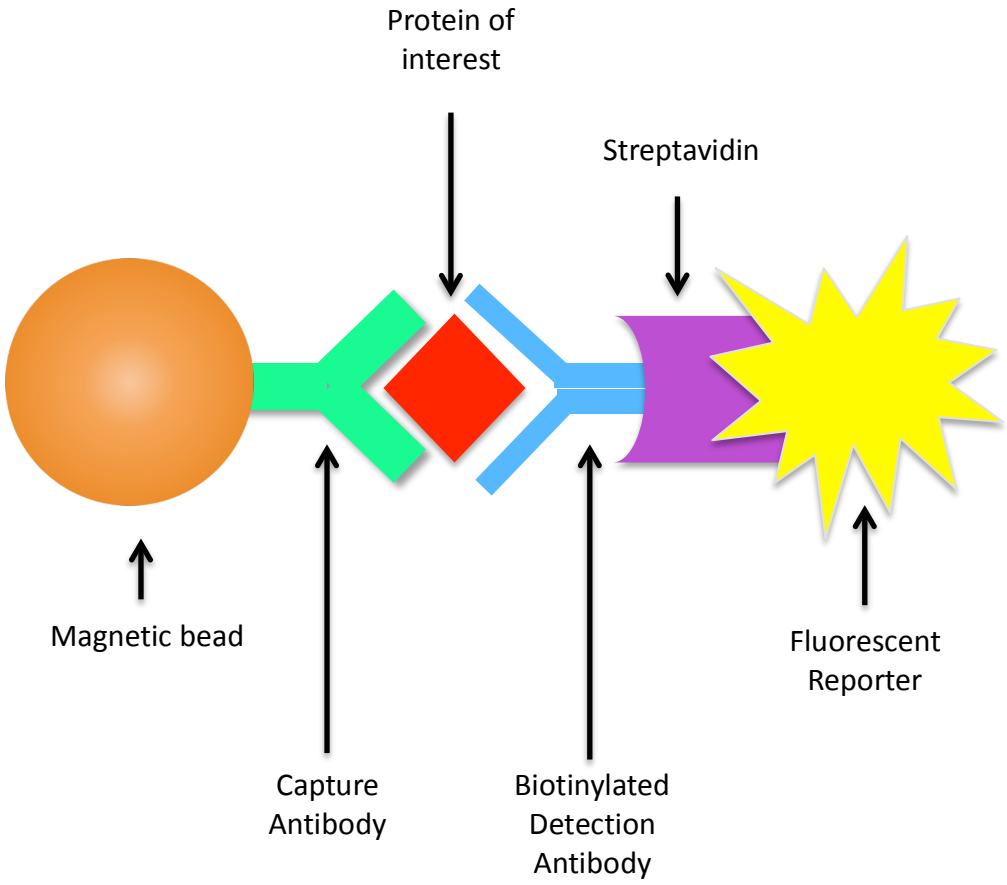

Figure 6.5: The principle of determination of apoptotic proteins using the Bio-Plex Pro RBM Apoptosis Assay Panel 1 (Bioplex Pro™ Manual, Panel 1, Bio-Rad)

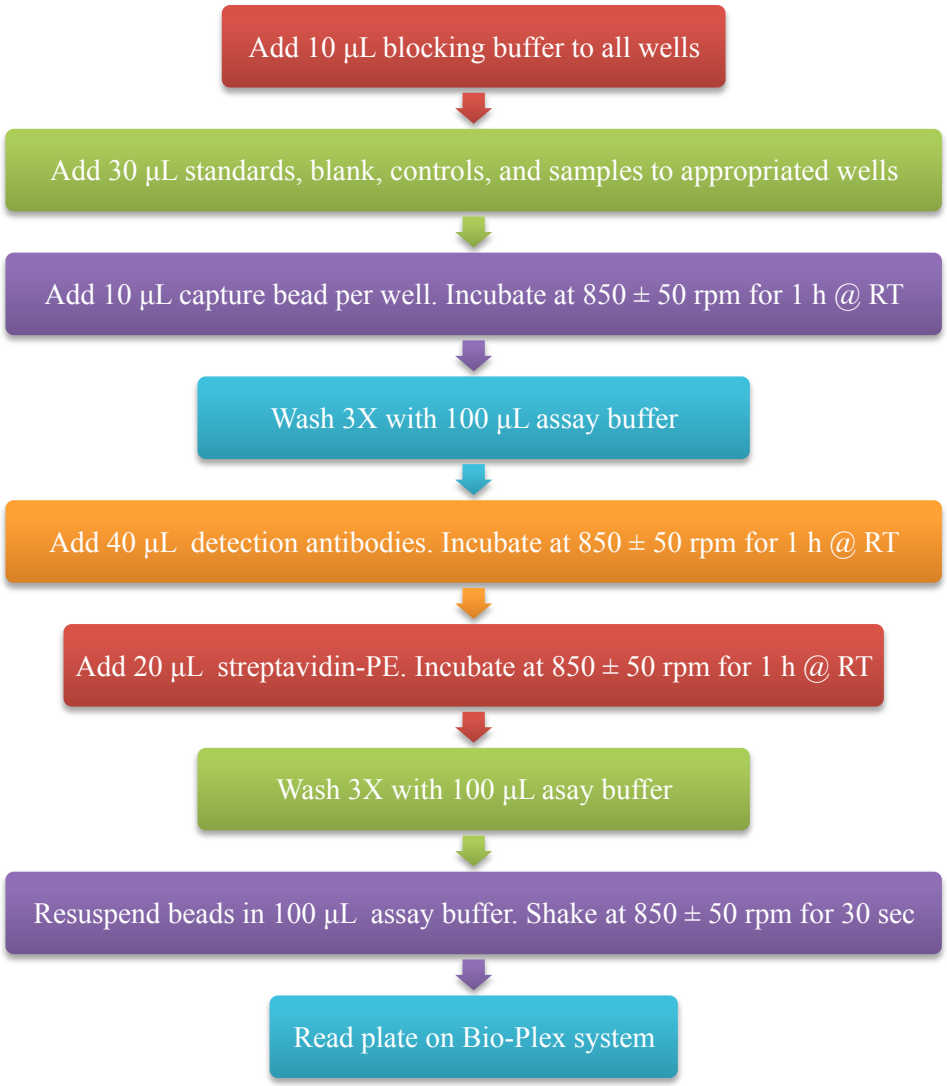

Figure 6.6: The workflow of apoptotic proteins determination

6.3.5 Protein determination

The fluorescamine assay was first described by Udenfriend *et al.* (1972), and was developed into the protocol of Lorenzen *et al.* (1993) (Udenfriend *et al.*, 1972; Lorenzen and Kennedy, 1993). The principle of this method was to quantify the fluorophore obtained by the simultaneous reaction of fluorescamine and primary amine. Fluorescamine itself is not fluorescent, but the fluorophore product is. Therefore, proteins can be quantified using fluorospectroscopy. The protein standard, BSA was diluted serially, as described in section 5.3.4. The protein determination was carried out

by adding 25 μL of standard or samples in the appropriate wells, followed by 25 μL of fluorescamine (1.5 mg in 10 mL acetonitrile). The mixture was shaken on the plate shaker for 2 minutes, and then the fluorescence intensity was read at 360/450 nm. The standard curve was constructed using MS Excel to obtain a linear relationship, and the amount of protein in samples was calculated.

6.3.6 Statistical analysis

Statistical analysis was performed using SPSS software version 22. Data normality distribution and homogeneity of variances of apoptotic proteins were tested before comparison of means were computed using one-way or Welch ANOVA tests, followed by post hoc Tukey or Games-Howell tests, depending on the data distribution. It was noted that the number of replicates might impair the robustness of the statistical tests.

6.4 Results

6.4.1 Pilot studies

The suitable concentration of camptothecin without inducing the death of nematodes was 100 μM. It was not possible to detect any apoptotic cells during the first 4 hours or at 6 hours after exposure, but the apoptotic cells were obvious at 24 hours. Therefore, this time point was chosen for the experiments.

6.4.2 Acridine orange staining

Apoptotic cells in *C. elegans* stained with acridine orange were detected in the positive control group (100 μM camptothecin). As seen in Figure 6.7 (picture A and B), apoptotic cells appeared as red dots in each nematode, while the living cells were visible as uniformly green. It was observed that apoptotic cells were scattered around the nematode (figure 6.7, picture B), and made it challenging to count in two-dimensions. Therefore, confocal microscopy with Z-stack detection was thought to be helpful to visualise the apoptotic cells in depth. However, with this technique it was not possible to distinguish any differences between images taken from the positive control and

control groups, as seen in Figure 6.8. In addition, no apoptotic cells were observed in exposures to any Ag toxicants at the concentration of LC50 in the time point of 24 hours, as seen in Figure 6.9. Therefore, the apoptotic cell count was not conducted using the acridine orange test.

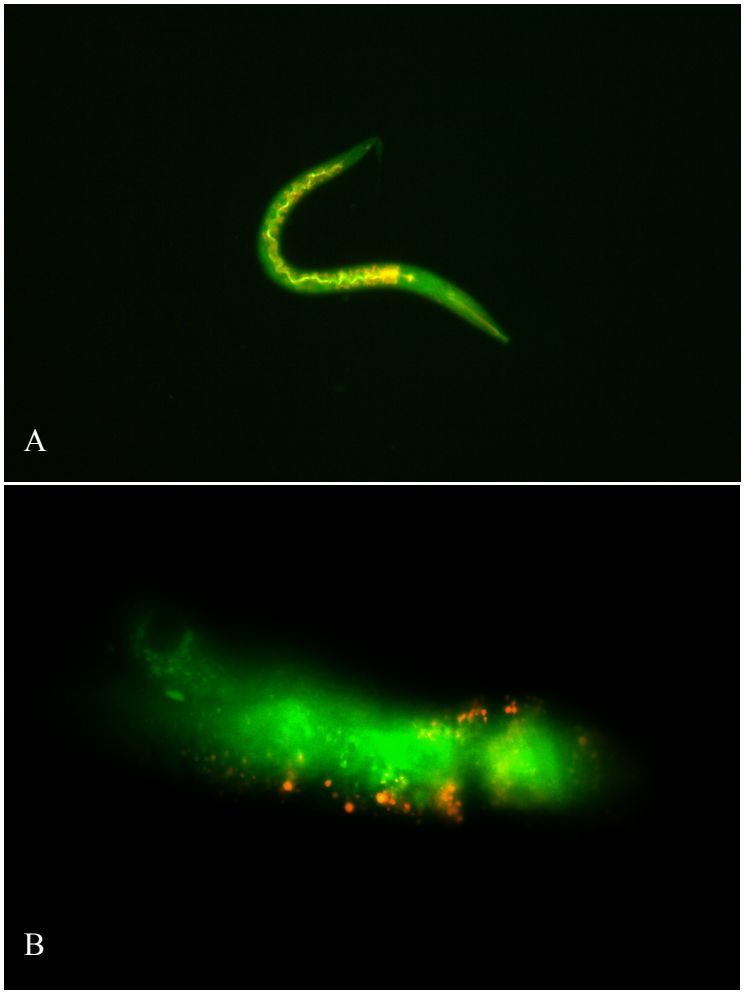

Figure 6.7: Apoptotic cells (red dots) stained with acridine orange detected in wild type *C. elegans* exposed to 100 µM camptothecin. Picture A was obtained using the magnification of 10x, B in the magnification of 40x focusing on the germline.

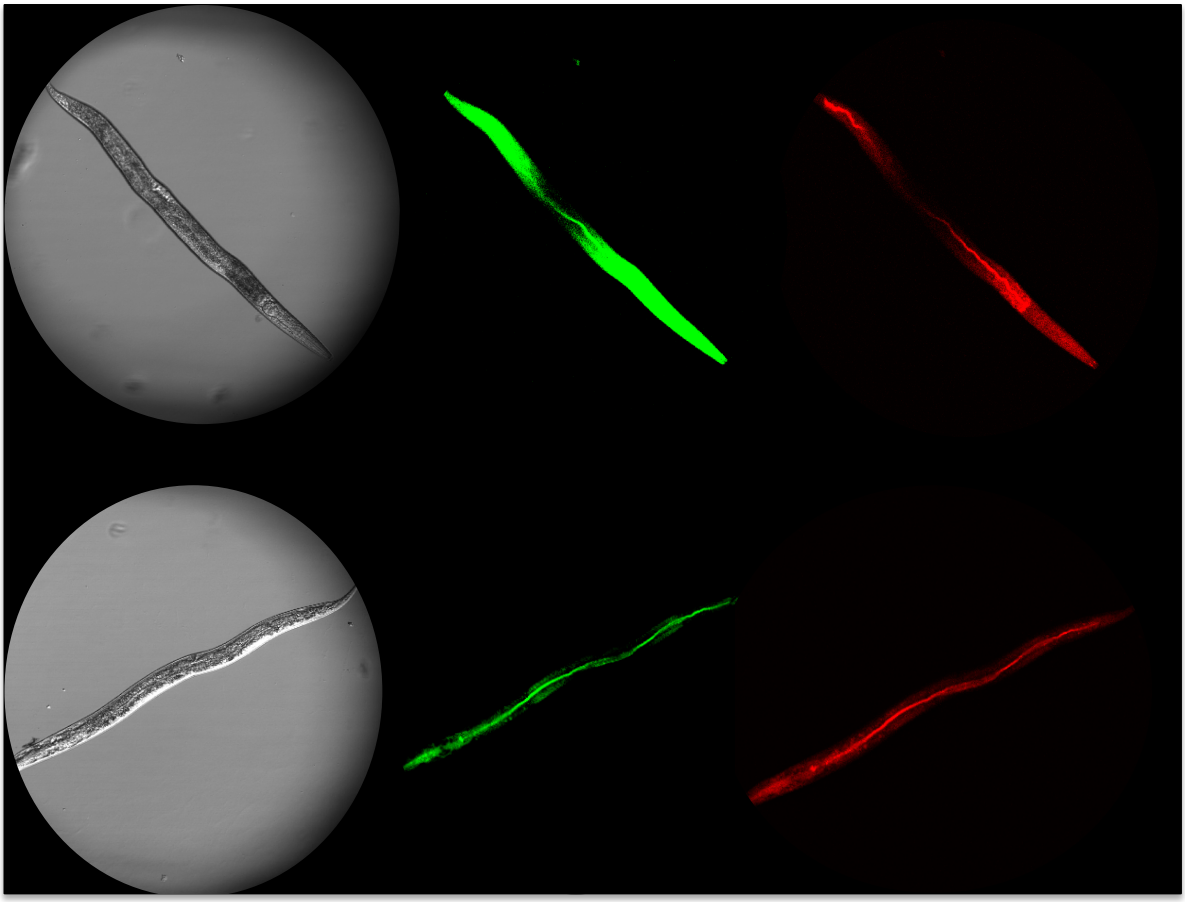

Figure 6.8: Confocal images of wild type *C. elegans* at the magnification of 20x using different detection wavelengths according to the excitation/emission wavelength of acridine orange; the green images were taken using the wavelength of 450 nm, while the red images were taken at the wavelength of 520 nm. The upper panel is the nematode in the control group whereas the lower panel is the nematode exposed to 100 μM camptothecin.

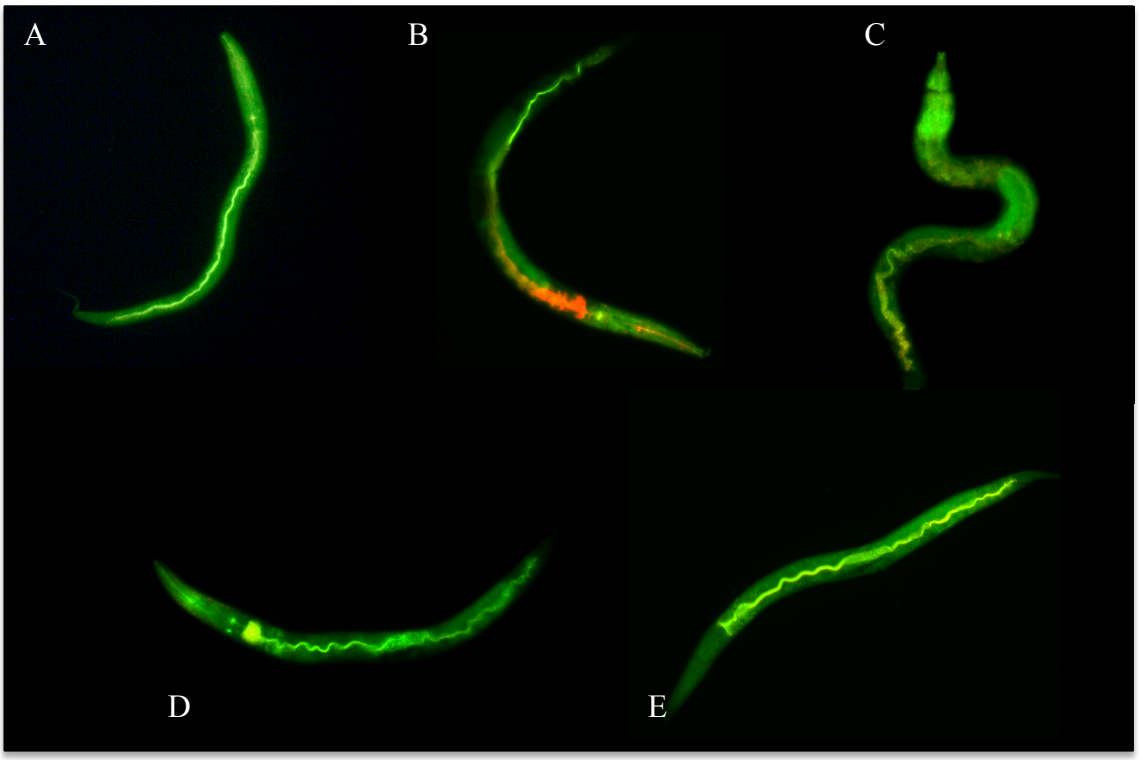

Figure 6.9: The wild type nematodes stained with acridine orange to visualise the apoptotic cells. In A: Control, B: 100 µM camptothecin, C: 180 µg/L $AgNO_3$, D: 3 mg/L NM300K, E: 250 mg/L NM302. The images of other strains are included in Appendix A3.

6.4.3 Annexin V staining

Unlike acridine orange, Annexin V selectively stains apoptotic cells. Moreover, with the conjugation of PI, the early and late stage apoptosis could be distinguished. Therefore, this method is useful to detect apoptotic cells in *C. elegans*. Although the early apoptotic cells were stained by this dye, it was faint, as seen in Figure 6.10. Furthermore, these apoptotic cells were visualised only in the positive control group, not in the Ag exposed treatments (at the concentrations of LC_{10} and LC_{50}, 24 hours of exposure), which was consistent with the results from acridine orange staining. The inability to detect apoptotic cells in the Ag treatment groups led to the decision to end the staining experiments and move on to the determination of apoptotic proteins.

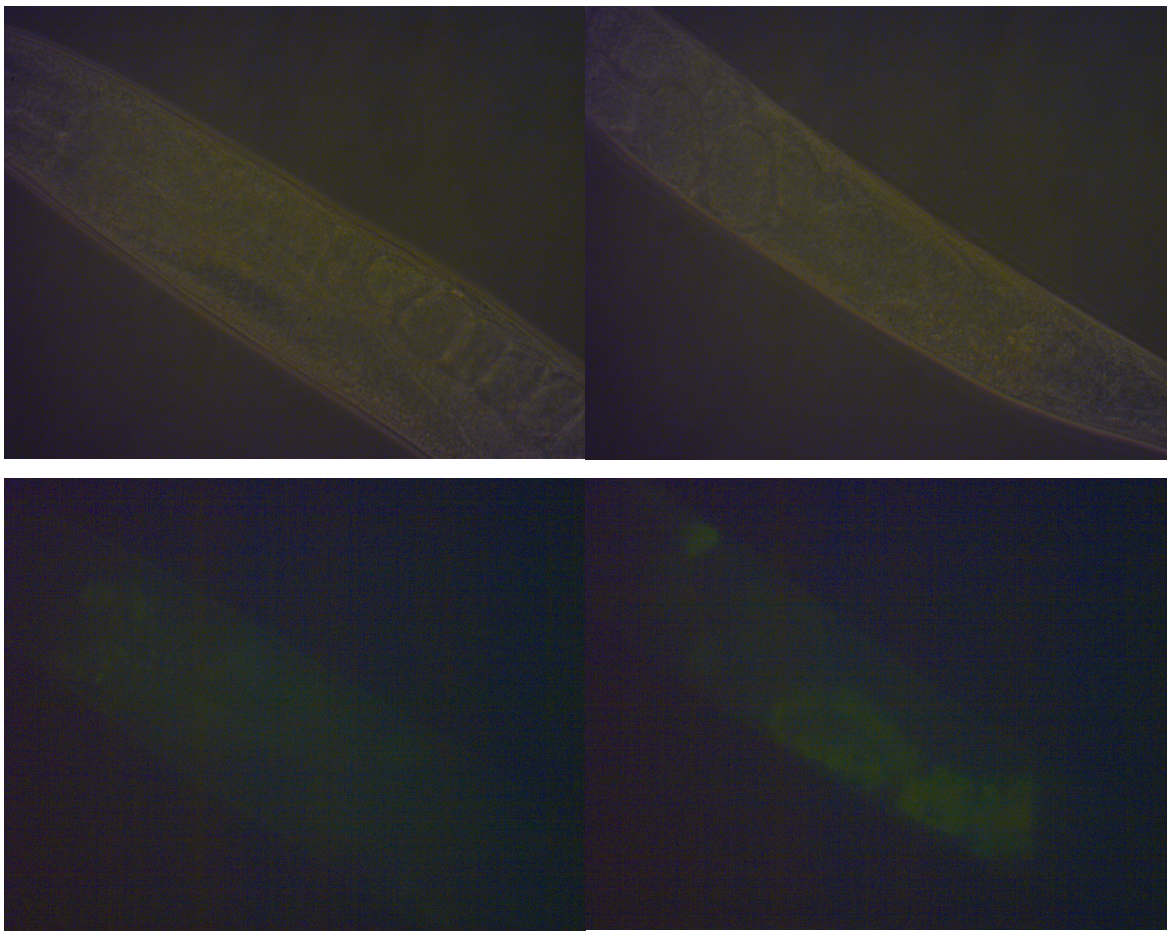

Figure 6.10: Wild type *C. elegans* stained with Annexin V/PI. The upper panel images were taken using normal light microscopy, while the lower panel were taken with the fluorescence filter. The left panel was a nematode from the control group whereas the right panel was a nematode from the positive control group (100 μM camptothecin). The apoptotic cells were lightly stained as a green area as in the camptothecin group.

6.4.4 Apoptotic protein determination

Apoptotic proteins were determined in the nematodes exposed to the positive control (20 and 100 μM) and Ag toxicants at the concentrations of LC_{10} and LC_{50} for 24 hours. The proteins were measured in terms of fluorescence intensity, and the amount of proteins was then calculated as ng/mL using the derived standard curve. The commercial kit used in this test focused on the proteins working in the intrinsic pathway of apoptosis, which are Smac, Bax, Bak, and Lamin B. Although the standard reagents included in the kit were successfully determined, the apoptotic proteins in nematode samples were very low, and were out of the detection range in some samples, as shown in Figure 6.11. It was found that the levels of Smac, Bax, Lamin B, and Bak were significantly higher in the *ced-3* (-ve). The comparison within strain using one-way or

Welch ANOVA followed by post hoc Tukey or Game-Howell, showed that the protein levels of nematodes exposed to some toxicants were significantly lower or higher than the control, as depicted in Figure 6.11. Nevertheless, the results from statistical analysis should be examined carefully since the number of replicates in each sample was limited, and normality of data distribution and homogeneity of variances could not be verified. This limitation arose from the condition of the commercial kit since each kit could analyse 37 samples in duplicate only. Furthermore, it has to be taken into consideration that the structure or domain of proteins in mammalian and *C. elegans* might be different, resulting possibly in dissimilar binding to the detection antibodies, and thus impairing the fluorescence detection. Therefore, the conclusions to be drawn from this experiment should be taken with caution.

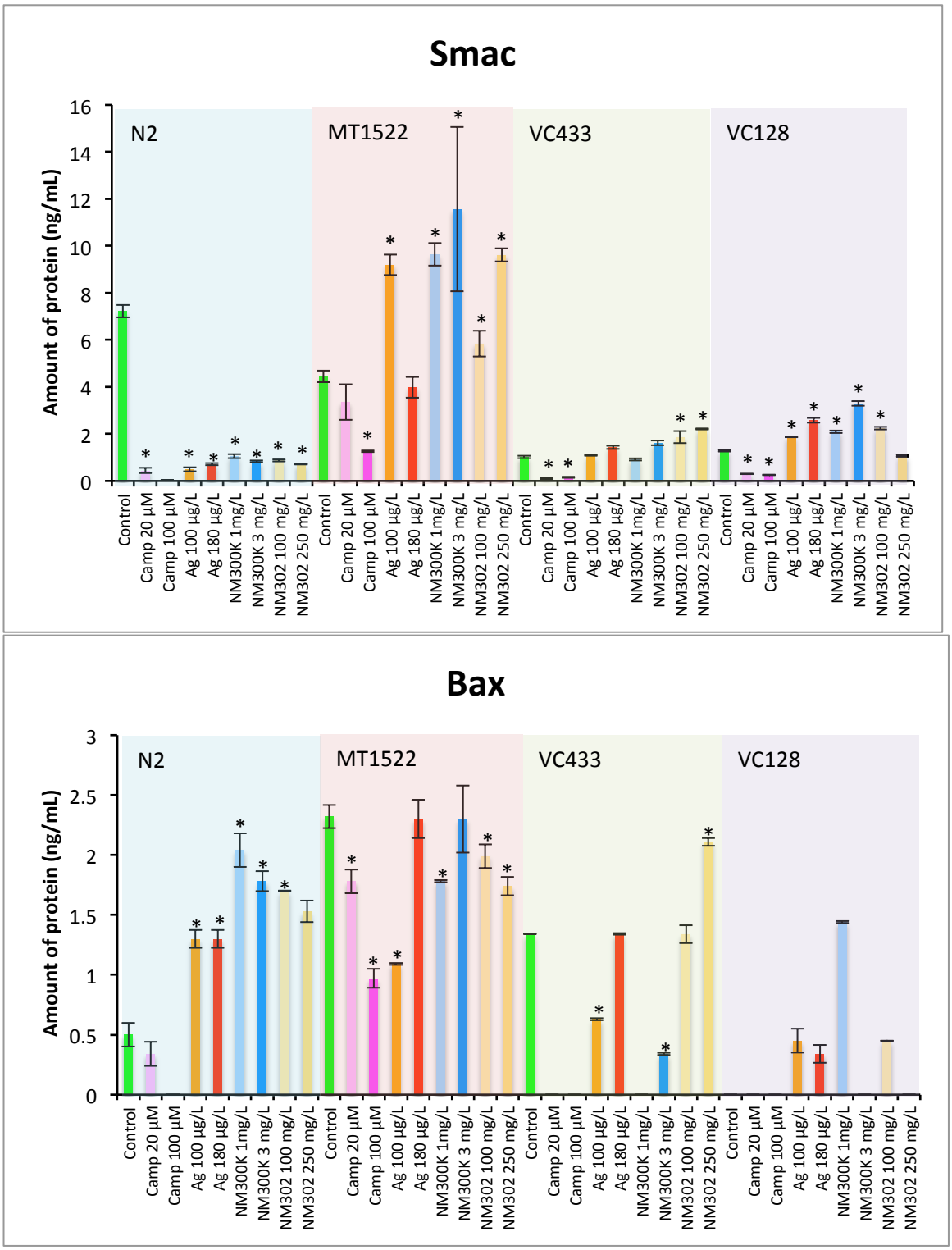

Figure 6.11: Levels of mammalian apoptotic proteins in nematodes exposed to different toxicants at the time point of 24 hours. The comparison within strain was performed and the significance ($p < 0.05$) is shown by the asterisks, however, it has to be considered that ANOVA was operated using a limited number of replicates, and the normality of data distribution and homogeneity of variances were violated.

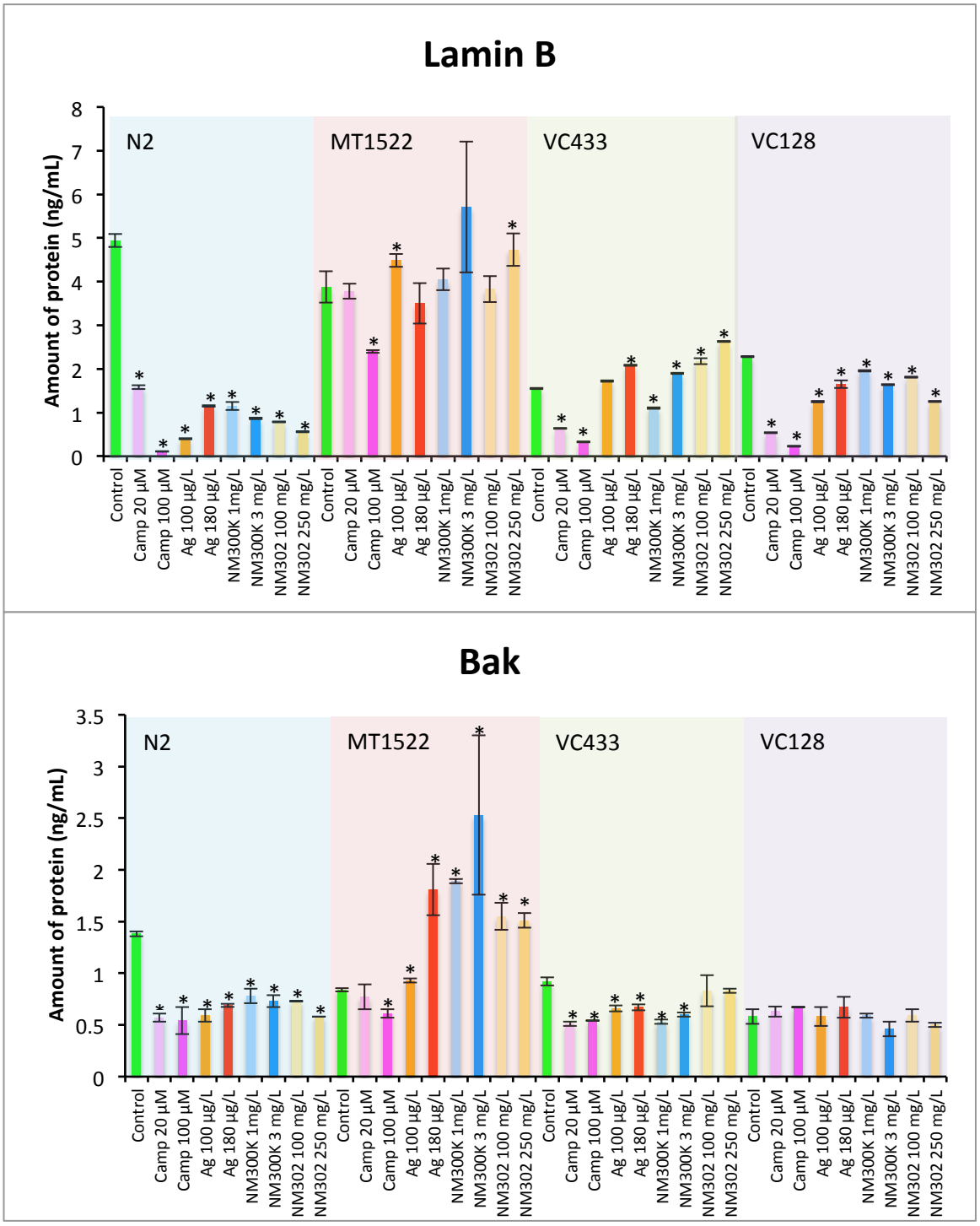

Figure 6.11 (Cont.): Levels of mammalian apoptotic proteins in nematodes exposed to different toxicants at the time point of 24 hours. The comparison within strain was performed and the significance ($p < 0.05$) is shown by the asterisks, however, it has to be considered that ANOVA was operated using a limited number of replicates, and the normality of data distribution and homogeneity of variances were violated.

6.5 Discussion

6.5.1 Acridine orange staining

The aim of this study was to visualise apoptotic cells inside *C. elegans*. Acridine orange is a membrane-permeable dye that binds to nucleic acids. It gives a distinct fluorescence emission depending on the types of nucleic acids it intercalates with. In other words, acridine orange emitted green fluorescence when it binds to double stranded nucleic acid, while red fluorescence is detected when intercalating with single stranded nucleic acid.

The design of this experiment took advantage of *C. elegans*'s transparent body, which is beneficial to visualise the apoptotic cells. Using camptothecin as a positive control with the concentration of 100 μM in the exposure time of 24 hours, the apoptotic cells appeared as red dots in the germline of *C. elegans*. Although the technique worked well with the positive control, apoptotic cells were not detected in the nematodes exposed to any Ag toxicants with a concentration up to LC_{50}. In addition, it was unable to distinguish the apoptotic cells in *C. elegans* using confocal microscopy.

Acridine orange was widely used to identify apoptotic cells and distinguish the cell cycle in many cell lines and animals including *C. elegans*. Moreover, there is an established procedure of using acridine orange to detect the apoptotic cells in germ cell corpses (Gartner and eVilleneuve, 2004). Furthermore, there are some studies detecting apoptotic cells by using acridine orange in *C. elegans* exposed to arsenite, sodium arsenite, and sodium fluoride for 24 hours (Wang *et al.*, 2007; Pei *et al.*, 2008; Qiao *et al.*, 2012). Therefore, it could be proposed that the failure in the detection of apoptotic corpses in this study could be that Ag toxicants might not induce apoptosis in *C. elegans*, or the induction was not as high as the threshold of the activation of programmed cell death in nematodes. However, it was found earlier that the tolerance of the strain lacking the pro-apoptotic gene was considerably higher than the wild type with regards to mortality. Therefore, it was inconceivable to rule out the connection of apoptosis to the toxicity from AgNMs. The explanation to the finding in this experiment could be that the concentration of Ag toxicants used was inappropriate, resulting in undetectable levels of apoptosis. The study of apoptosis induced by AgNMs could be conducted using another staining technique, Annexin V to further explore the results from this experiment.

6.5.2 Annexin V staining

The goal of this experiment was to obtain the images of apoptotic cells in *C. elegans* as the confirmative study of the acridine orange staining. Annexin V is a stain that binds to PS molecule, which is normally distributed in the inner layer of the membrane. However, in a cell undergoing apoptosis, this phospholipid is turned over to the outer layer, hence the apoptotic cells expose many of these phospholipid molecules, which Annexin V can bind to. Therefore, Annexin V is specific to the apoptotic cells. The combination of Annexin V with another dye, PI is considered useful to investigate the stage of apoptosis. The cell membrane is intact in both normal and early-state apoptotic cells, whereas the late-stage apoptotic cells indicates deformity of the cell membrane, which PI can penetrate into, and binds to the nucleic acids inside cells, thus emits different fluorescence from Annexin V. Therefore, cells in the late-state apoptosis are stained by both Annexin V and PI (Elmore, 2007).

The experiment was conducted under the same conditions as for the acridine orange test to explore the previous finding. It was consistent that germ cells in *C. elegans* exposed to 100 μM camptothecin underwent apoptosis. The faint green fluorescence observed showed that the exposure to camptothecin at the time point of 24 hours triggered early stage apoptosis. In addition, apoptosis was not detected in *C. elegans* exposed to any Ag toxicant, which confirmed the previous finding from the acridine orange test. This confirmed the suggestion that apoptosis might not be involved in the exposure to AgNMs, at least in the conditions used in this experiment (LC_{10} and LC_{50}). However, the detection of those apoptotic cells under fluorescence microscopy might not be as sensitive as the study of apoptotic protein expression. Therefore, the determination of pro-apoptotic proteins might clarify the connection of apoptosis to the toxicity from AgNMs better than using the visualisation technique.

It was stated by Lu *et al.* (2009) that the apoptotic cells in *C. elegans* embryo were engulfed very quickly within 80 minutes (Lu et al., 2009). In this thesis, it was difficult to determine the initiation time of apoptosis and detect apoptotic cells in AgNMs-treated samples. Since only one time point was chosen in this thesis, it might not fully indicate whether apoptosis was another pathway of toxicity from AgNM. Apoptosis might already occur before the time point or might not occur at all. Although it was successful to visualise the apoptotic cells induced by camptothecin at this time point, the different substances i.e. AgNMs might induce apoptosis at a different time points. According to Sundquist and colleagues (2006), factors such as cell types,

apoptosis-inducing stimuli, concentration or intensity of stimuli, and exposure time result in different outcomes of apoptosis. The detection of apoptosis might be better observed using time-lapse experiments (Sundquist *et al.,* 2006). Li *et al.* (2013) also established a methodology to visualise the engulfment of apoptotic cells in *C. elegans* by using time-lapse DIC microscopy. The real-time recording protocol was successful in distinguishing the early stage and the engulfed apoptotic cells in the gene reporter mutant (CED-1::GFP) (Li *et al.,* 2013). Therefore, it was suggested that a time-lapse experiment should provide better information in the identification of the relevance of apoptosis in the toxicity of AgNMs.

6.5.3 Apoptotic proteins determination

This study aimed to examine the level of pro-apoptotic proteins in *C. elegans* as a supplement to the visualisation technique. The measurement of pro-apoptotic protein levels is likely to be useful in the assessment of apoptosis at the biochemical level. The commercial kit used in this experiment is designed to detect mammalian apoptotic proteins in the mitochondrial pathway, i.e. Bax, Bak, Smac, and Lamin B. It was found that all these proteins were detected in very small amounts in *C. elegans*. Although these proteins seemed to be expressed comparatively highly in the strain lacking the pro-apoptotic gene, MT1522, the findings were inconclusive because the trend of protein levels was not consistent with respect to the different samples. As well as some proteins also relatively expressed in the control groups, the variability in the particular samples was large. Therefore the statistical analysis could not be performed in ideal conditions.

It has to be considered that using a commercial kit developed for mammalian apoptotic proteins might not be the best option to determine apoptotic proteins in *C. elegans*. Bax and Bak are both pro-apoptotic proteins in the Bcl-2 family. These proteins were multi-domain, which possessed BH1, BH2, and BH3 domains (Gewies, 2003). The function of both Bax and Bak is to induce apoptosis hence they are called effectors. The effector in the apoptotic machinery is conserved in *C. elegans* as EGL-1, or the promoter of apoptosis, as described in Table 6.1. However, there is some difference between pro-apoptotic proteins in mammalian and *C. elegans*. Firstly, the structure of these proteins was distinctive. EGL-1 contains only BH3 domain, which is not identical to multi-domain proteins, Bax and Bak (Rosenberg, 2011). From the

difference in the structure and domain of these effector proteins, it could be considered that the affinity of proteins to the detection antibody in the kit might be reduced. Secondly, mammalian apoptotic machinery consists of more functioning proteins than in invertebrates, as described in Table 6.1. In mammalian cells, Smac acts as an antagonist of IAP (inhibitor of apoptotic protein) whereas this type of protein function in *C. elegans* is absent. Finally, the same type of protein might work differently in mammalian and *C. elegans*. In mammalian, lamins are the nuclear protein meshwork, which form channels in the nuclear envelope. There are four types of lamina, A, B_1, B_2, and C. The role of both types of lamin B were to preserve the nuclear structure. The organisation of lamin B has been proved to be involved in cell survival (Burke, 2001). It has also been found that apoptosis is activated by the inability to congregate lamin B (Steen and Collas, 2001). Furthermore, it has been proposed that the cleavage of this lamin happens in the beginning of nuclear disruption in cells undergoing apoptosis (Burke, 2001). Therefore, lamin B is used as an indicator for the early stage of apoptosis. On the other hand, there was only one type of lamin in *C. elegans*, named Ce-lamin. Although the function of Ce-lamin is involved in nuclear structure, the degradation of Ce-lamin was observed after DNA fragmentation. Furthermore, the Ce-lamin is not a substrate for CED-3. From these findings, the suggestion has been proposed that Ce-lamin degradation was not necessary for apoptosis in *C. elegans* (Tzur *et al.*, 2002).

Although the difference in pro-apoptotic proteins in mammalians and *C. elegans* might be a major drawback for the use of the commercial kit, it was still the better option regarding time and laboratory practical aspects. Regardless of the drawbacks, including the previous results from the visualisation technique, it might be presumed that apoptosis might not be a key pathway of toxicity from AgNMs, at least at the concentrations used in this study, and exposure time.

6.6 Summary of this chapter

This chapter aimed to establish the connection of apoptosis to the toxicity from AgNMs in *C. elegans* by using visualisation approaches and the determination of apoptotic protein levels. The visualisation technique provided the *in vivo* imaging of apoptotic cells inside *C. elegans*, while the protein level measurement supported the expression of apoptotic proteins in *C. elegans*. A summary of the results in relation to the proposed null hypotheses is provided below. It is important to emphasise that NH could not be tested in full given the low replication allowed in these experiments for the reasons explained in the previous sections.

1. "NMs would not induce apoptosis in *C. elegans*"

This null hypothesis was neither accepted nor rejected since the experiments were conducted at only one time point. However, it can be concluded that there were no detectable apoptotic cells in *C. elegans* after exposure to both AgNMs in the concentrations of LC_{10} and LC_{50} at the specific time point of 24 hours, whereas the apoptotic corpses were visible in the nematodes exposed to camptothecin (positive control).

2. "There would be no difference in the response regarding the apoptotic endpoints between strains of nematode exposed to the same toxicant"

This null hypothesis was neither accepted nor rejected. Considering the visualisation endpoint, all strains had the same response to camptothecin and AgNMs. Apoptosis was induced when they were exposed to camptothecin, while it was not possible to detect any apoptotic cell corpses in the Ag-treated groups. However, considering the apoptotic protein determination, the *ced-3* (-ve) had significantly higher amounts of all apoptotic proteins than other strains. Nonetheless, this result was obtained with only limited replicates (n=2), and the variation in protein levels was wide. Moreover, the measurement of apoptotic proteins using the commercial kit for mammalian cells did not provide supportive information about the activity of those proteins in *C. elegans* as there was a difference between mammalian and nematode apoptotic proteins. Therefore, this conclusion should be taken with caution.

3. "There would be no difference in the response between various silver toxicants tested in the same strain of nematode"

This null hypothesis was accepted at the LC_{10} and LC_{50} concentrations of Ag toxicants tested at 24 hours. This was also concluded with regards to the determination of apoptotic proteins. There was no difference in the impact of any Ag substances on the levels of apoptotic proteins in any strains. However, as mentioned above, the conditions used in this study were limited to two concentrations of Ag toxicants and one time point. It should be considered that the occurrence of apoptosis might take place in different conditions. Therefore, the overall conclusion should be taken with caution.

Although it is proposed that apoptosis was not induced during exposure to AgNMs in the experimental conditions adopted, it was indicated in the previous chapter reporting on lethality that apoptosis might be one of the pathways of toxicity from AgNMs. Considering that the elimination of apoptotic cells in *C. elegans* occurs very quickly, the initiation time of the apoptotic process is difficult to determine. The concentration of apoptotic-stimulating agents had a major impact on the occurrence of apoptosis, therefore future work focusing on a wider range of concentrations and time-lapse experiments should be conducted to conclude the relevance of apoptosis to the adverse effects from NMs.

Chapter 7: Omics studies following exposures to AgNM

7.1 Introduction

Understanding the pathways of toxicity from NMs is essential for the use and management of products containing NMs but also to the design of safer NMs in the future. The research described in this chapter aimed to explore further the biological pathways of toxicity induced by AgNMs in *C. elegans*. Comparing the susceptibility of *C. elegans* lacking in particular genes provided a degree of information on toxicological pathways, therefore an omics study was another approach that allowed an assessment of the regulation of genes or proteins, which can provide additional information. Transcriptomic and proteomic studies are often able to quantify the expression of genes and proteins following exposures to NMs.

7.1.1 The definition of genomics, transcriptomics, and proteomics

To understand the omics approach, it is important to understand the definition of genome, transcriptome and proteome. Genome is the entire supply of genetic information to build an organism and control its living function (Xiong, 2006). The genome consists of DNA (deoxyribonucleic acid) or RNA (ribonucleic acid) in both coding regions, portion of gene's DNA or RNA that codes for proteins, as well as non-coding regions. The function of the genome requires a set of particular proteins to transcribe it into copies of active coding RNA, so called transcriptome, which is later translated into proteome (Brown, 2002). Proteome is therefore the complete set of translated proteins, which is the product of the transcriptome (Xiong, 2006).

Genomics is generally the study of genomes, which is performed by the analysis of a great quantity of genes, with complex outcome data analysed by the assistance of computers. The scope of a genomic study relates to both structural and functional genomics. The structural genomic study involves genome mapping, genome sequencing and annotation, while the functional genomics focuses on the functions and interactions of genes in a genome. While the genomic study aims on the whole to provide information on the genome i.e. mapping, sequencing and annotation, transcriptomics is a study that focuses on the actively transcribed RNA, which provides information on gene expression under specific circumstances, in this case, following exposure to AgNM (Xiong, 2006). A proteomic study involves the analyses of the

proteome ranging from the quantification of proteins to the determination of proteins. Similar to genomics, the application of proteomics is divided into comparative and functional proteomics. Comparative or quantitative proteomics relates to the identification of target protein and the discovery of biomarker whereas the functional proteomics focuses in the functions of proteins (Xiong, 2006).

Proteomics has benefits over transcriptomic studies in terms of the study of gene function because the study of the transcriptome alone is not sufficient to understand the whole biological system. In other words, one particular gene can be transcribed and finally translated into many proteins with different functions in the cell due to the process such as alternative splicing, etc. (Xiong, 2006). Moreover, the quantity of proteins is not proportional to the quantity of mRNA. The abundance of proteins in the cell is usually regulated by other processes, such as translation and degradation. In addition, the post-translational modification e.g. glycosylation and phosphorylation of a particular protein generates the variation of proteins that share the same amino acid sequence and allows the proteins to be monitored by only functional proteomics. Therefore transcriptomics is only a first step to study other omics approaches (Lengauer, 2007).

7.1.2 Omics approaches in the nanotoxicological studies

In the field of nanotoxicology, omics approaches are useful tools to obtain a broad understanding of the impact of NMs on cellular processes. The potential negative effects and pathways of adverse outcome, including the correlation to organismal health impact, can be examined by a single experiment of gene expression profiling. This makes the transcriptomic study a fast and arguably cost-effective approach (Bourdon *et al.*, 2013). This financial aspect is not agreed with by all authors, with some indicating the high costs involved in such approaches. Omics approaches have been used to determine the pathways of adverse effects from NMs by focusing on transcriptional biomarkers, which can provide information on the potential toxicity from NMs (Maojo *et al.*, 2012).

According to Pubmed, there have been more than 3,000 articles on gene expression profiling and NM toxicity since 2010. Some of these studies focus on gene profiles of small organisms, e.g. yeast, zebrafish, crustaceans. This has offered the ability to compare key gene functions between species and the possibility to extrapolate

this information to other species that share genetic material. The major molecular pathways, which are found to be affected by NMs are the responses by immune and inflammatory systems, apoptosis, oxidative stress, metabolic processes, cell cycle, ion transport, signal transduction, cell proliferation, and cell differentiation (Tino *et al.*, 2014). Although proteomics is another powerful tool to determine protein biomarkers indicating pathways of effects from NMs, proteomics is less standardised than transcriptomics with limited annotated protein function (Cauerhff *et al.*, 2014).

7.1.3 The C. elegans genome

The genome of *C. elegans* was completely sequenced in 1998. It was found that the 100-Mb genome contains more than 19,000 genes, with over 40% predicted proteins conserved in other species (The *C. elegans* genome sequencing consortium, 1998). It was discovered that the mitochondrial genome of *C. elegans* consists of 100,291,840 base pairs (bp) (Hillier *et al.*, 2005). The gene annotation list from Wormbase predicts the protein count to be 22,420 (22,269 unique peptide sequence) from 19,735 genes (with 2685 alternative splice form) (Chen *et al.*, 2005). It was found that *C. elegans* has noncoding RNA (ncRNAs) like other eukaryotes. These ncRNAs are not coded into proteins, however, they function in other ways. For example, ribosomal RNAs (rRNAs) are important for protein synthesis as they are the component of the ribosome; transfer RNAs (tRNAs) are also essential for protein synthesis by translating mRNA into amino acids; small nuclear RNAs (snRNAs) play a role in the elimination of intron and tran-splicing, microRNAs (miRNAs) work by silencing the RNA and regulating the gene expression; and small nucleolar RNAs (snoRNAs) control the other RNAs modifications (Hillier *et al.*, 2005). Stricklin and colleagues (2005) have identified approximately 1,300 noncoding genes in *C. elegans* and found 590 tRNAs, 275 rRNAs, 140 snRNAs, 120 miRNAs, and 30 snoRNAs (Stricklin, Griffiths-Jones and Eddy, 2005). From these well-annotated genes, the study of proteins and the interactions between them can be studied.

7.1.4 The C. elegans proteome

Since *C. elegans* are relatively small, it is difficult to use any techniques that require a large amount of tissue such as proteomics. However, improvements provided by the biochemical separation method and MS, as well as bioinformatics, make the study of *C. elegans* proteomes possible. Merrihew and colleagues (2008) used a shotgun approach in combination with molecular fractionation, in tandem with MS/MS, to create the proteome database of *C. elegans* and found the total of 6779 proteins (67,047 peptides), 348 of which were annotated in Wormbase (WS150) but deficient in cDNA or experimental support (Merrihew *et al.*, 2008). Although these quantitative proteomics have not been fully carried out, the annotated protein database is still informative and can be used as a source to study the function of proteins that are abnormally expressed following exposure to NMs, which is useful in the prediction of the pathways of toxicity from NMs.

7.2 Aim of this chapter

The aim of this chapter is to gather detailed information on how transcriptomes and proteomes of wild type *C. elegans* are altered when exposed to one of the toxic NM, JRCNM03002a. As previous chapters showed, the toxicity regarding the viability, reproduction, and biochemical endpoints (oxidative stress, apoptosis), added by knowledge on molecular endpoints such as genes and proteins, provides understanding of the pathways of toxicity. The null hypotheses proposed before starting the omics studies were:

1. There was no alteration of gene and protein regulation during the time of study;

2. Genes and proteins involved in oxidative stress and apoptosis would retain their expression in the same manner as in the control group when *C. elegans* are exposed to NM.

7.3 Materials and methods

7.3.1 Transcriptomics

In collaboration with the EU MARINA project, the JRCNM03002a was chosen to assess the alteration of transcriptomes in *C. elegans* following AgNM exposure. The experiments were conducted as follows: organisms were exposed at Heriot-Watt University, where RNA samples were extracted from the exposed *C. elegans*; these samples were then sent to Max Delbrück Centre for Molecular Medicine, Berlin (MDC-Berlin). This institute was a partner within the MARINA project and this collaboration allowed these samples' analysis.

7.3.2 Proteomics

In collaboration with the EU MARINA project, the JRCNM03002a was selected as described above. The experiments were conducted as follows: organisms were exposed at Heriot-Watt University, samples prepared (see below), and posted to the University of Salzburg for proteomic analysis. This institute was a partner within the Marina project and this collaboration allowed these samples' analysis.

7.3.3 Sample preparation

Samples were prepared in two sets, one was for the transcriptomic study, and the other was for the proteomic study. Each set of samples consisted of four groups of *C. elegans* according to time of exposure and treatment. Each group consisted of approximately 90 mg of nematodes (~135,000 nematodes). The exposure was done in petri dishes containing 15 mL of test suspension/45,000 nematodes (SSPW including *E. coli* as a food source) in three replicates. Due to the requirement of high amounts of nematodes, the time of exposure was limited to 0 and 24 hours and the test substance was confined to JRCNM03002a at a concentration of 1 mg/L (LC_{10}), only. Each group of *C. elegans* was exposed in SSPW with NM (treatment: T) and without NM (control: C), and was collected at the time points of 0 or 24 hours. The group of nematodes were primarily coded as C0, C24, T0, and T24. Nematodes were washed using the sucrose floatation technique in order to remove all NMs and bacterial food source. This technique was done within 30 minutes of terminating the experiment. Therefore, the

group with the time point of 0 hour (C0, T0) was actually exposed to NM for 30 minutes before the clean-up procedure finished, therefore this group was called T_{30} instead of T0.

7.3.4 Cleaning up C. elegans samples by sucrose floatation

As adapted from Wormbook.org, *C. elegans* samples were washed to remove *E. coli* and NM using the sucrose floatation technique described below.

In 15 mL centrifuge tubes, collected *C. elegans* samples were spun down for 2 minutes at 3200 x g and the supernatant was discarded, then 4 mL 0.1 M NaCl was used to resuspend the worm pellets. After leaving the tubes on ice for 15 minutes, 4 mL of 60% sucrose was added. The suspension in the tubes was inverted to mix well the content before centrifuging at 9000 x g 4 minutes. The layers of worms at the top of the tubes were transferred to the new tubes containing 4 mL of 0.1 M NaCl to wash off excess sucrose. Worms were pelleted again by centrifugation at 9000 xg for 4 minutes. The supernatant was discarded and replaced with RNAlater™ (Sigma-Aldrich®) to preserve the samples. For the transcriptomic work, total RNA was extracted from samples as described in the section below.

7.3.5 RNA extraction

RNAlater was removed by centrifugation at 9000 xg for 10 minutes and the supernatant was discarded. The extraction of RNA was performed by using MagMax™-96 Total RNA isolation kit (Ambion®). The quality of RNA samples was analysed by Nanodrop and gel electrophoresis. The RNA samples with a value of A260/A280 ~2.0 and A260/A230 of 2.0-2.2, and the quantity of total RNA of more than 500 ng (Nanodrop) with no RNA integrity observed (gel electrophoresis) were acceptable samples, and were stored at -80 °C before shipping to Berlin.

7.3.6 Transcriptomic analysis

This work was conducted by MDC-Berlin. According to their protocol, the quality of RNA samples was tested (QC) by using Nanodrop and a Bioanalyser. The quality threshold of more than 500 ng and RNA integrity number (RIN) of 8 were used, to represent good quality samples suitable for RNA sequencing. Illumina stranded total RNA libraries were prepared with the iNMut concentrations of 500 ng using the TruSeq Stranded Total RNA LT Sample Prep Kit. Then, the sequencing was performed using an Illumina HiSeq 2000 for 2x101nucleotide (nt) at shallow coverage. The data were returned to Heriot-Watt University in the format of gzipped .fastq, which contained the raw RNA sequences (RNAseq).

7.3.7 Transcriptomics data Interpretation

This work was performed by SysBioC Ltd in the University of Edinburgh. According to SysBioC, the quality of raw RNAseq was assessed by using FASTQC. A composite Ensembl *C. elegans* transcript set was used as a reference for alignments. The alignments were conducted in the end-to-end mode and at the very sensitive settings, to the reference using *Bowtie2*. Raw tag counts per sample were normalised to the sample with the lowest number of tags, and counts converted to log2. Pairwise comparisons of sample groups were performed on the tag counts using linear modelling (Bioconductor *limma* package). A series of four group-wise comparisons was undertaken to identify fold changes. Each fold change has associated significance statistics using empirical Bayesian approaches at the significance level of adjusted p value < 0.01. Although the more relaxed threshold of $p < 0.05$ could be considered for statistical robustness, adopting this approach makes the data and conclusions made more robust. Significant segments in each comparison were assessed for their annotated information using KEGG pathways and GO terms using a hypergeometric test with a p value of less than 0.05 and less than 0.001, respectively. Although there is a degree of overlap between functional annotations from different sources, each set has information not available in the others, therefore it is generally beneficial to consider more than one. Overlapping Venn diagram was generated for relevant comparisons, and the functional characteristics of the members of each segment of the Venn diagram were explored.

7.3.8 Protein extraction and digestion

This part of the work was carried out by a partner at the University of Salzburg. According to their protocol, proteins were extracted by adding methanol to disrupt *C. elegans* on ice. The protein pellet was collected by centrifugation. Trifluoroethanol (TFE) was added to denature, reduce and alkylate proteins. After that, they were re-precipitated by adding acetone. Proteins were dissolved in 0.1 M triethylammonium bicarbonate buffer (TEAB), and analysed the concentration using Bradford assay, then digested by trypsin overnight. Peptides were labelled with tandem mass tag (TMT) for a quantitative analysis.

7.3.9 Protein analysis and data evaluation

This part of the work was carried out by the MARINA partner at the University of Salzburg. According to their protocol, peptides were separated by capillary ion-pair reversed phase HPLC in a 150 x 0.2 mm i.d. monolithic column with 5 hour 0-40% acetonitrile gradient at 1 μL/min followed by ion trap-Orbitrap mass spectrometry (MS). Three data-dependent collision-induced dissociation MS/MS scans were performed, followed by three higher-energy collisional dissociation scans in the Orbitrap on the same precursors for quantification. Each sample was measured three times. The determination of significantly changed proteins was performed by using an analysis workflow combining OpenMS with the R package *isobar*.

7.4 Results

7.4.1 Transcriptomics

Although the quality of RNA sample was acceptable when analysed at Heriot-Watt University, it turned out that these samples were degraded during the shipment to Berlin. Therefore, RNA samples were sequenced and interpreted with missing replicates in the treatment group. The 20 most identified loci in the RNAseq were either ribosomal RNA (rRNA), mitochondrial DNA (MtDNA), or non-coding in origin. The numbers of significant array features with more than two-fold change in each comparison are presented in Table 7.1. The number of array features exhibiting various fold change thresholds in each comparison were also calculated regardless of statistics.

Figure 7.1 shows a heat-map of the fold change for all loci exhibiting an up- or down-16-fold change in one or more of the comparisons. Array features are shown on the X-axis and the comparisons on the Y-axis. In the comparison heat-map, a red colour indicates up-regulation, and blue down-regulation. Clustering of genes and comparisons are indicated by the cladograms on the images. Although there was a majority of up-regulated loci in the comparison of treatments at different time-points, it has to be taken into account that the limitation in the number of replicates in the treatment group would impair a statistical judgement. The heat-maps with other degrees of fold change are included in the Appendix A4.

Table 7.1: Number of differentially expressed genes when comparing between groups based on treatment and time points. The number of genes was chosen at the level of 2-fold difference.

Comparison undertaken	Significant, >2-fold change
Controls: 24 h relative to 30 min	1496
Treatments: 24 h relative to 30 min	0
30 min: Treatment relative to control	5462
24 h: Treatment relative to control	2301

Note: significant level of adjusted $p < 0.01$

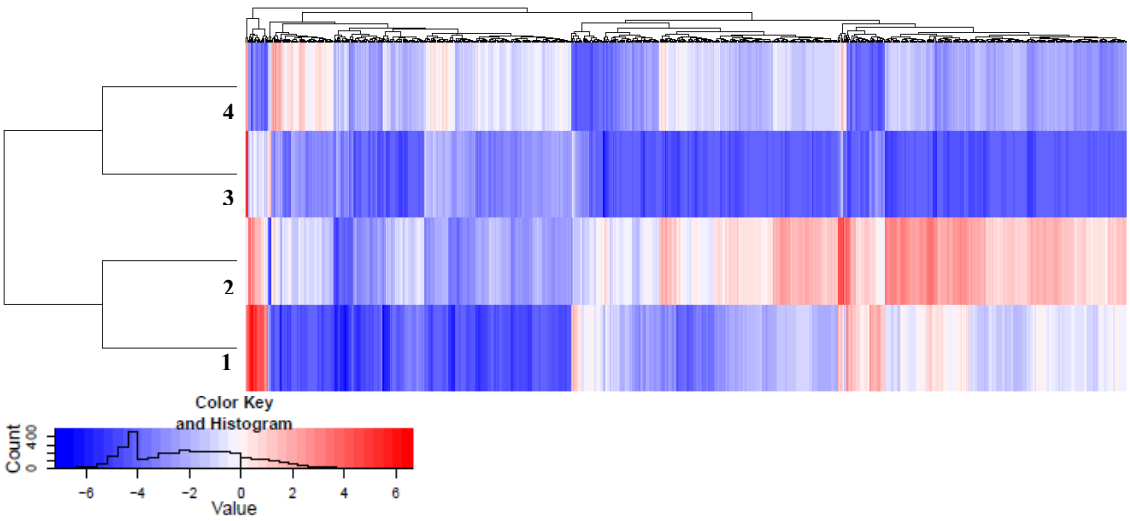

Figure 7.1: Heat-map of 928 loci exhibiting up- or down- 16-fold changes regardless of statistics. The number on the Y-axis represents the comparison group; 1: C24vsC_{30}, 2: T24vsT_{30}, 3: T_{30}vsC_{30}, 4: T24vsC24, where C = control, T= treatment, $_{30}$ = 30 min, 24 = 24 hours.

Kyoto encyclopaedia of genes and genomes (KEGG) pathway and Gene ontology (GO) term enrichment were assessed for up- and down-regulated genes separately. Since there were no array features expressed significantly in the comparison of treatments at 24 h relative to 30 min ($T24vsT_{30}$), it was not possible to assess the KEGG pathway or GO terms enrichment in this comparison. As shown in Figure 7.2, the KEGG pathway enrichment revealed the down-regulation of genes in the pathway of biosynthesis of unsaturated fatty acids and polyketide sugar unit within the comparison of controls at 24 h relative to 30 min ($C24vsC_{30}$), while the genes in the pathway of oxidative phosphorylation and lysosome were specifically down-regulated in the comparison of 30 minutes of exposure in the treatment group relative to control group ($T_{30}vsC_{30}$). In addition, the genes in the pathway of ribosome were exclusively down-regulated when comparing the treatment to the control regardless the time points. It was found that genes in the pathway of ribosome were down-regulated at the higher statistical degree in the time-point of 24 hours. Furthermore, the GO term enrichment analysis showed the down-regulated pathways of structural constituent of cuticle and structural molecule activity in the comparison of $C24vsC_{30}$, the down-regulation of genes in the pathways of transporter activity and transmembrane activity in the comparison of $T_{30}vsC_{30}$, and the down-regulation of genes in the pathways of structural constituent of ribosome, ribosome and translation in the comparison T24vsC24, as depicted in Figure 7.3.

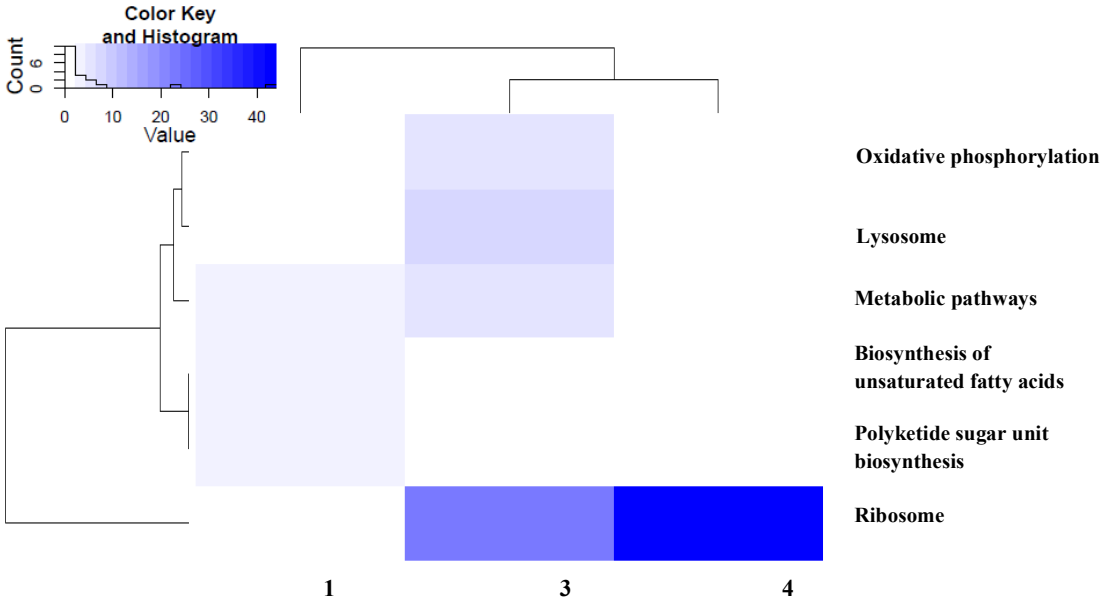

Figure 7.2: Down-regulated pathway assessed by KEGG pathway enrichment with comparisons along the X-axis, and KEGG pathways along the Y-axis. The blue colour representing down-regulated pathways, was assigned on a 20 point scale based on the minus log10 (enrichment *p* value), with white being the least statistically robust using a significance threshold of $p < 0.001$. The number on the X-axis represents the comparison group; 1: $C24vsC_{30}$, 3: $T_{30}vsC_{30}$, 4: T24vsC24, where C = control, T= treatment, $_{30}$ = 30 min, 24 = 24 hours.

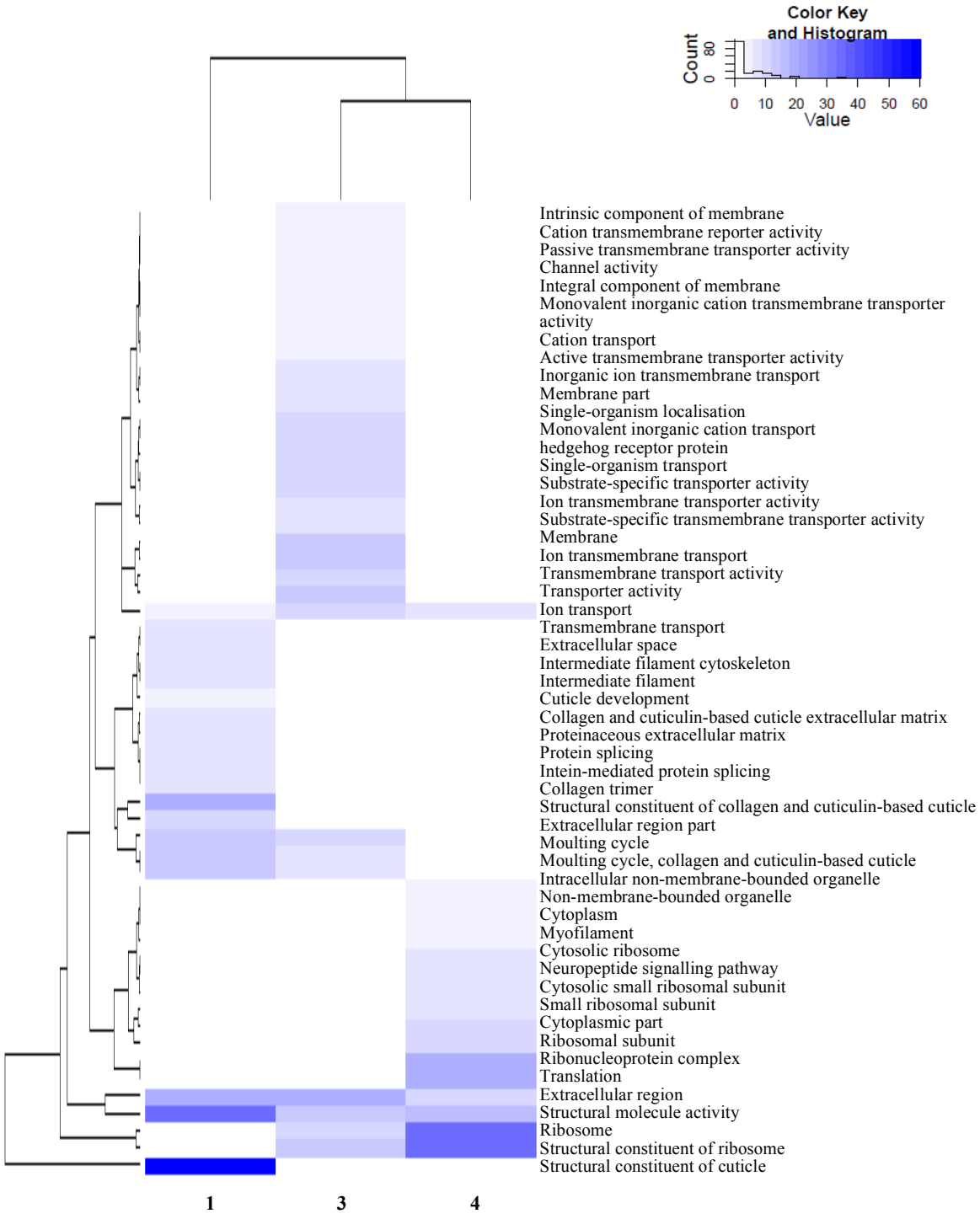

Figure 7.3: Down-regulated pathway assessed by the GO term enrichment with comparisons along the X-axis, and GO term along the Y-axis. The blue colour representing down-regulated pathways, was assigned on a 20 point scale based on the minus log10 (enrichment *p* value), with white being least statistically robust. For the purposes of display, only GO terms with an enrichment *p* value less than 1E-05, were included. The number on the X-axis representing the comparison group; 1: $C24vsC_{30}$, 3: $T_{30}vsC_{30}$, 4: T24vsC24, where C = control, T= treatment, $_{30}$ = 30 min, 24 = 24 hours.

The array features that changed in their regulation significantly are depicted in a Venn diagram, as seen in Figure 7.4. Profiles for the constituent members of each of the seven regions are shown in the heat-map, as seen in Figure 7.5, where the 69 significant loci found in all comparisons are illustrated. The members particularly found in Group 2 and Group 3 will be illustrated and discussed later. The remainder heat-maps of other region are included in the Appendix A4.

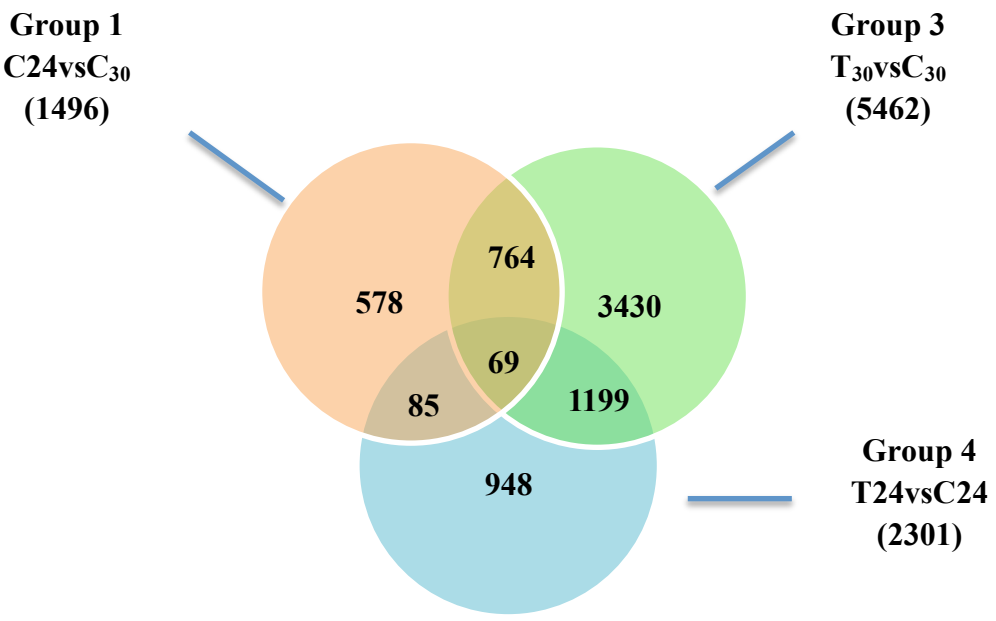

Figure 7.4: Distribution of array features which expressed significantly in each comparison according to time points or treatment (numbers in the brackets are total features in each comparison)

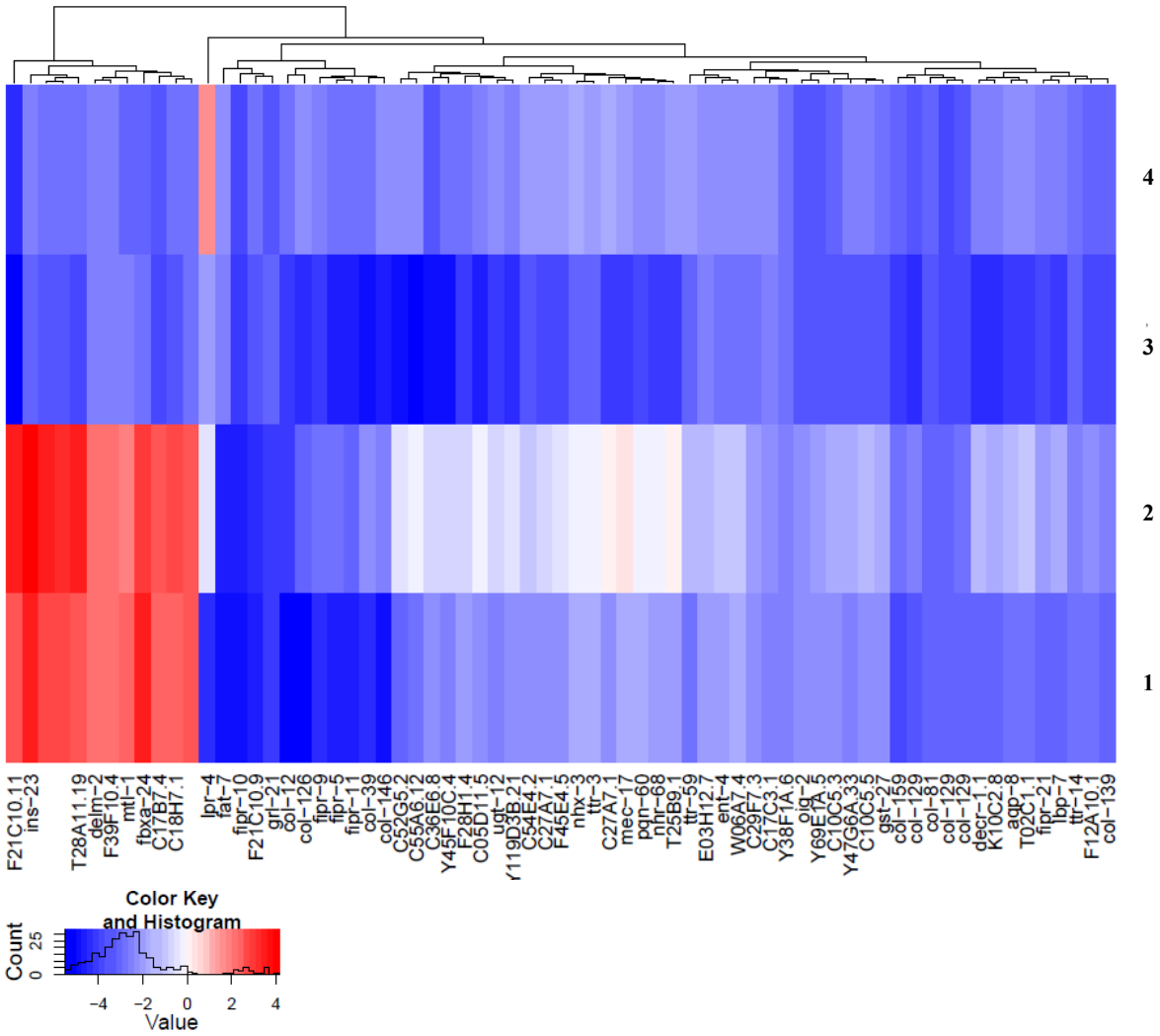

Figure 7.5: Heat-map of the significant loci found in all comparison. Array features are shown on the X-axis, with the comparisons on the Y-axis. A red colour indicates up regulation and blue down regulation. The number represents the comparison group; 1: $C24vsC_{30}$, 2: $T24vsT_{30}$, 3: $T_{30}vsC_{30}$, 4: T24vsC24, where C = control, T= treatment, $_{30}$ = 30 min, 24 = 24 hours.

To focus on the gene expression between control and treatment group, it was found that 5,462 and 2,301 array features expressed significantly at the adjusted $p < 0.01$ level at the time-points of 30 minutes and 24 hours, respectively. In a total of 5,462 features, 3,430 features were particularly significantly expressed at the time-point of 30 minutes, whereas 948 of 2,301 features were exclusively found at the time-point of 24 hours. The number of array features commonly found in both time points was 1,199.

The up- and down-regulated array features were assessed for KEGG pathways and across all three ontologies of GO term enrichment. In the time-point of 30 minutes, there was no statistically KEGG pathway enriched in the up-regulated features, however, there were 15 KEGG pathways enriched in the down-regulated array features. On the other hand, there were statistically seven KEGG pathways enriched at the time-point of 24 hours, one of which involved significant up-regulated genes whereas six of which were involved in down-regulated genes. The top ten most enriched pathways containing either up- or down-regulated features in the treatment groups for both time-points are depicted in Tables 7.2, 7.3 and 7.4. Although there was the complete list of these KEGG pathways reported, it was better to focus on the pathways with high *p* value and percentage of genes significant. The summary of these common pathways found between comparisons is shown in Figure 7.2. The GO terms enrichment analysis found 83 GO terms significantly enriched in only down-regulated loci of the 30 minutes comparison group ($T_{30}vsC_{30}$), while in the 24 hours comparison group (T24vsC24), 52 GO terms were statistically enriched with all involved in significant down-regulated genes. The top ten GO term enrichment analysis of treatment groups at both time-points are shown in Tables 7.5 and 7.6. The summary of common GO terms found between comparisons is shown if Figure 7.3.

Table 7.2: The top 10 most enriched KEGG pathways of down-regulated array features in the comparison of treatment to the control group at the time-point of 30 minutes

Pathway Description	*p* Value	Number of significant genes	% pathway genes significant
Ribosome	3.15E-24	58	72
Lysosome	6.29E-08	35	49
Oxidative phosphorylation	5.32E-06	40	43
Metabolic pathways	1.36E-05	175	28
MAPK signaling pathway	2.75E-03	20	33
Arginine and proline metabolism	4.07E-03	17	46
Glutathione metabolism	1.46E-02	15	40
Other glycan degradation	1.73E-02	7	50
Phagosome	1.79E-02	16	33
Sphingolipid metabolism	1.86E-02	9	41

Table 7.3: KEGG pathway enrichment of up-regulated array features in the comparison of treatment to the control group at the time point of 24 hours

Pathway description	*p* value	Number of significant genes	% pathway genes significant
Biosynthesis of unsaturated fatty acids	6.01E-03	1	8

Table 7.4: KEGG pathway enrichment of down-regulated array features in the comparison of treatment to the control group at the time-point of 24 hours

Pathway description	*p* value	Number of significant genes	% pathway genes significant
Ribosome	1.34E-44	61	76
Tyrosine metabolism	3.25E-03	7	32
Oxidative phosphorylation	1.59E-02	18	20
Lysosome	1.86E-02	13	19
Phenylalanine, tyrosine and tryptophan biosynthesis	2.27E-02	3	43
Pantothenate and coA biosynthesis	4.72E-02	3	34

Table 7.5: The top 10 most enriched GO terms in down-regulated significant features found in the comparison of treatment to the control group at the time-point of 30 minutes

Ontology	GO term	*p* Value
CC	Extracellular region	2.95E-21
MF	Transporter activity	1.23E-15
MF	Transmembrane transporter activity	3.82E-15
BP	Transmembrane transport	4.23E-14
MF	Structural constituent of ribosome	5.89E-13
MF	Structural molecule activity	7.08E-13
BP	Ion transport	9.03E-13
CC	Extracellular region part	2.71E-11
CC	Ribosome	3.31E-11
MF	Substrate-specific transmembrane transporter activity	4.67E-11

Note: MF = Molecular function, CC = Cellular component, BP = Biological process

Table 7.6: The top 10 most enriched GO terms in down-regulated significant features found in the comparison of treatment to the control group at the time-point of 24 hours

Ontology	GO term	*p* value
MF	Structural constituent of ribosome	1.06E-36
CC	Ribosome	1.45E-35
BP	Translation	1.41E-19
CC	Ribonucleoprotein-complex	1.66E-19
MF	Structural molecule activity	4.61E-17
CC	Ribosomal subunit	5.08E-12
CC	Extracellular region	5.37E-12
CC	Cytoplasmic part	7.78E-10
CC	Small ribosomal subunit	8.40E-09
CC	Cytosolic small ribosomal subunit	1.23E-07

Note: MF = Molecular function, CC = Cellular component, BP = Biological process

7.4.2 Proteomics

It was revealed that there were 149 proteins altered in their regulation, 12 of which were particularly found changed in the comparison of treatment relative to control group after 24 hours of exposure (T24vsC24). Moreover, there were 40 proteins altered in the comparison of treatment to relative control group at time point of 30 minutes as shown in Figure 7.6. As categorised by their functions, it was found that 57.72% of total proteins had annotated functions, as illustrated in Figure 7.7. The majority of known proteins found in the treatment group involved in catalysis (9.40%), with 68.42% of catalytic proteins were oxidoreductases.

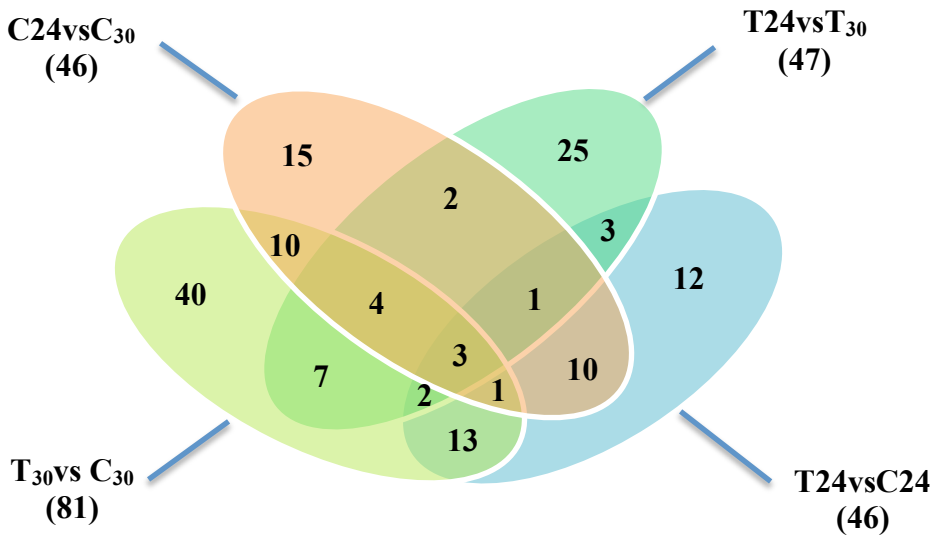

Figure 7.6: Distribution of proteins which have significantly changed in regulation. Comparison by time-points and treatment (C=Control, T= Treatment, 24 h, or 30 min of exposure, numbers in the brackets are total proteins in each comparison.

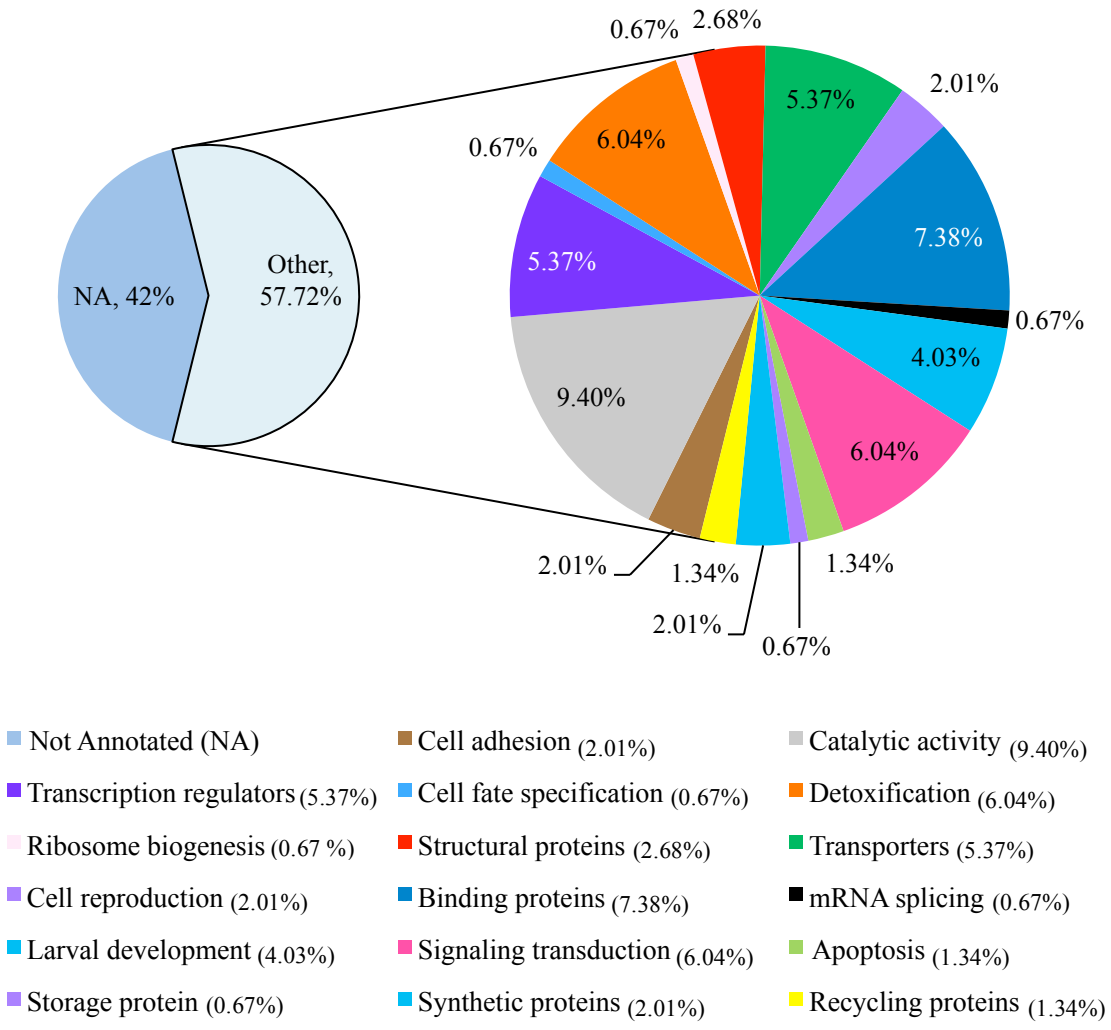

Figure 7.7: Distribution of 149 identified proteins categorized by their functions.

To focus on the particular proteins found in the comparison of treatment relative to the control group, it was found that dynamin-related protein (DRP-1) and glucuronosyltransferase (UGT-55) were down-regulated at the highest degree at the time-point of 30 minutes and 24 hours, respectively, whereas RDE-4 which has RNA-binding activity and transmembrane signalling receptor, K11E4.6 were the proteins with the highest up-regulation for each time-point as seen in Figures 7.8 and 7.9. The lists of proteins that altered in their regulation with their functions are depicted in Tables 7.7 and 7.8, respectively.

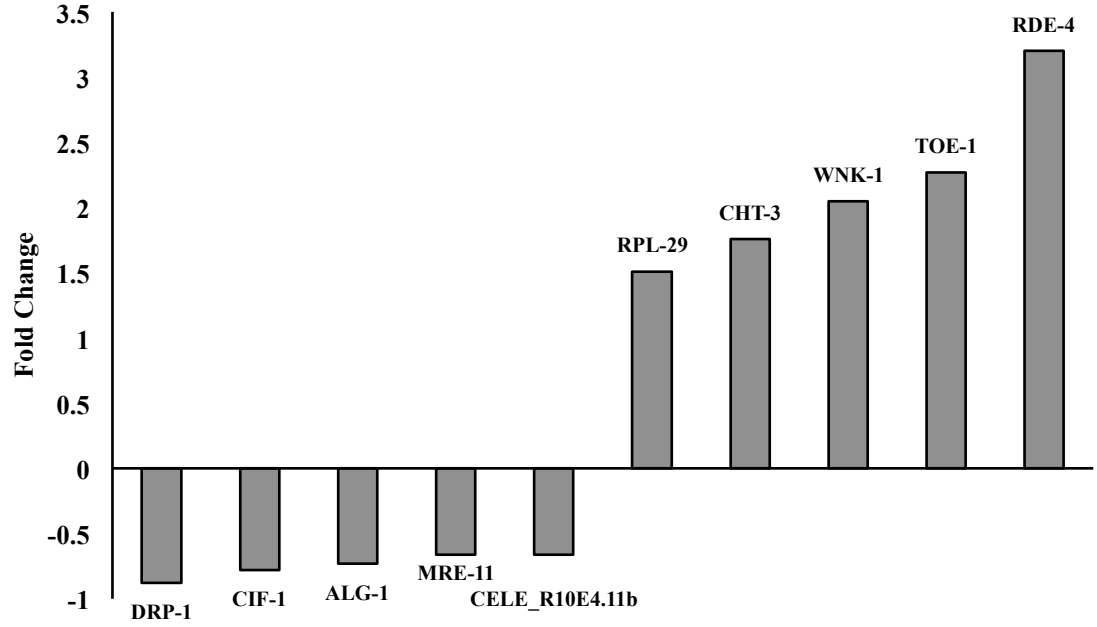

Figure 7.8: The top five of up- or down-regulated proteins with known function found in a comparison between control and treatment at 30 minutes ($T_{30}vsC_{30}$).

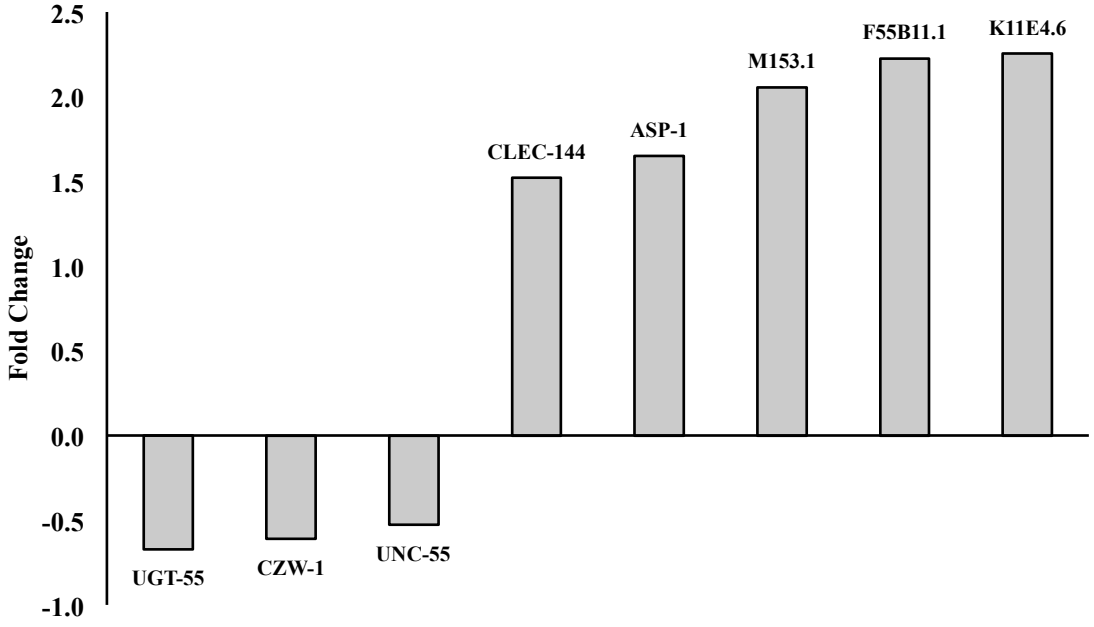

Figure 7.9: Degree of change in expression of annotated proteins found in a comparison between control and treatment at 24 hours (T24vsC24).

Table 7.7: The complete list of annotated proteins and their fold change in the comparison group of treatment relative to control at the time-point of 30 minutes. The negative values of fold change represent the down-regulation, the positive values the up-regulation

Gene	Protein name	Function	Fold change
rde-4	RNA interference promoting factor	RNA binding	3.20
toe-1	HEAT repeat-containing protein 1 homolog	Involved in ribosome biosynthesis	2.27
wnk-1	C46C2.1k	ATP binding; kinase activity; ion channel transport (REACTOME)	2.05
cht-3	Chitinase-like protein C25A8.4	Chitinase activity, polysaccharide metabolic process	1.76
rpl-29	B0513.3a	Structural constituent of ribosome	1.51
mlp-1	T04C9.4b	Zinc ion binding	1.34
kin-10	Casein kinase II subunit beta	Ribosome biogenesis, Wnt signaling pathway (KEGG)	1.17
F17E5.2	Calcium-binding mitochondrial carrier F17E5.2	Transmembrane transport	1.13
CELE_Y38C1AB.1	Y38C1AB.1	Transferase activity	1.06
lge-1	Glycosyltransferase-like protein LARGE	Transferase activity	-0.34
nhr-110	Y46H3D.5b	DNA binding	-0.44
dhhc-14	Palmitoyltransferase	Protein-cysteine S-palmitoyltransferase activity; metabolic process	-0.48
clec-82	Y54G2A.8a	Innate immune response; C-type lectin	-0.52
mrrf-1	Ribosome-recycling factor, mitochondrial	Responsible for the release of ribosomes from messenger RNA at the termination of protein biosynthesis	-0.55
dli-1	C39E9.14b	Microtubule motor activity; phagosome (KEGG)	-0.55
nhr-135	VC5.5	DNA binding	-0.58
mxl-2	F40G9.11	Transcription regulation; determine the progression of ageing	-0.58
mre-11	Double-strand break repair protein mre-11	Involved in DNA double-strand break repair (DSBR); cellular response to stress (REACTOME)	-0.66
CELE_R10E4.11b	R10E4.11b	Metal binding	-0.66
alg-1	Protein argonaute	Probably involved in the RNA silencing pathway	-0.73

Table 7.7 (Cont.): The complete list of annotated proteins and their fold change in the comparison group of treatment relative to control at the time-point of 30 minutes. The negative values of fold change represent the down-regulation, the positive values the up-regulation

Gene	Protein name	Function	Fold change
cif-1	COP9/Signalosome and eIF3 complex-shared subunit 1	Component of the eukaryotic translation initiation factor 3 (eIF-3) complex, which is involved in protein synthesis	-0.78
drp-1	Dynamin-related protein	GTPase activity; mediate mitochondrial fragmentation in cell death; Apoptosis (REACTOME)	-0.88

Table 7.8: The complete list of annotated proteins found altered in their regulation in the comparison group of treatment relative to control at the time-point of 24 hours. The negative values of fold change represent the down-regulation, the positive values the up-regulation

Gene	Protein name	Function	Fold change
K11E4.6	K11E4.6	Transmembrane signaling receptor activity: Sensory perception of chemical stimulus	2.26
F55B11.1	F55B11.1	Electron carrier activity; metabolic pathway	2.23
M153.1	M153.1	Proline biosynthetic process	2.06
asp-1	Aspartic protease-1	Protein catabolic process	1.65
clec-144	CLEC-144	Carbohydrate binding	1.52
unc-55	UNC-55 isoform a	Transcription regulation	-0.53
czw-1	CZW-1	Mitotic nuclear division; apoptotic process (GO)	-0.61
ugt-55	Putative UDP-glucuronosyltransferase ugt-55	Catalytic activity; glucuronosyltransferase; metabolism of xenobiotics by CYP450 (KEGG)	-0.62

As listed in Tables 7.7 and 7.8, some identified proteins had functions in apoptosis, ribosome, phagosome, and metabolism of xenobiotics by cytochrome P450, the latter being correlated with oxidative stress. Therefore the findings from proteomics were in accordance with the results from the transcriptomics which proposed the pathway of toxicity from JRCNM03002a to be involved in the disturbance of ribosome function, hence protein synthesis, phagosome, oxidative stress, and apoptosis.

7.5 Discussion

7.5.1 Transcriptomics

The objective of the transcriptomic study was to collect information on how *C. elegans* transcriptome altered following exposure to Ag toxicants at various time-points. Initially, it was planned to study the transcriptomic response of nematodes exposed to $AgNO_3$, JRCNM03002a and NM302 at the time points of 0, 2, 6 and 24 hours, compared to the non-treated control group. However, the yield of total RNA extracted from nematodes was scant, and this study required large sample amounts, hence it had to be focused only on JRCNM03002a at time-points of 0 and 24 hours, since this chemical was the one of most interest. The nematodes had to be washed off from the medium and NM, therefore it was not practical to collect them at the exact time-point of 0 hour, consequently, these groups of nematodes were actually collected and frozen 30 minutes after exposure. It is possible that the level of certain particular genes might change rapidly within 30 minutes. A study of Ag^+ toxicity to the single-cell green algae, *Chlamydomonas reinhardtii*, found a significant oxidative stress gene response after the short period of 15 minutes (Pillai *et al.*, 2014). Therefore, it had to be taken into account that within 30 minutes, the level of some genes might be altered.

The results have shown that most up-regulated genes were not significant, therefore it was not possible to analyse the pathway enrichment from those up-regulated genes. However, the nonsignificant results might be accounted from the rigid threshold of *p*-value adopted, which is mandatory when there is a limited number of replicates. Future work to obtain the required number of replicates might support current findings.

To sum up, it was revealed by KEGG pathway analysis that genes working in the pathways of biosynthesis and structural constituent of cuticle were significantly down-regulated in the comparison between controls ($C24vsC_{30}$). In contrast the

comparison of the treatment group relative to the control group at both time points (T_{30}vsC_{30} and T24vsC24) exhibited the down-regulation of genes involved in ribosome, oxidative phosphorylation and lysosome. In T24vsC24, the genes involved in ribosome were especially down-regulated at a higher statistical degree than T_{30}vsC_{30}. This finding was in accordance to Poynton and colleagues (2012), who found that the genes involved in ribosome function were down-regulated in *Daphnia magna* exposed to coated AgNM for 24 hours (Poynton *et al.*, 2012). Furthermore, Ma and colleagues (2011) found a similar effect in human dermal fibroblast cells exposed to AgNM (Ma, Lu and Huang, 2011). The role of a ribosomal function in the regulation of processes such as cell growth and death is inevitable considering these cellular processes involves the alteration of particular genes. Ribosomes are important for the translation of these genes. The increase in ribosomal function was proven to relate to the proliferative activity, which is an attribute of cell growth (Naora, 1999). The arrest of ribosomal function might indicate the shutdown of protein synthesis, which usually leads to cell death (Chen and Ioannou, 1999).

In the comparison of T_{30}vsC_{30}, genes working in the MAPK signalling pathway, GSH metabolism, phagosome, transporter activity, and transmembrane activity were significantly down-regulated. As stated by Garrington and Johnson (1999), MAPK is the signalling cascade to control the growth, differentiation, survival, and apoptosis of cells. MAPK pathway responds to not only intracellular stimuli, it also reacts to the environmental stresses (Garrington and Johnson, 1999). The three components of MAPK include extracellular signal regulated kinase (ERK), c-Jun N-terminal kinase (JNK), and p38 pathways. It was thought that the ERK cascade was crucial to maintain the cell state, and JNK and p38 play a role in stress response and apoptosis (Wada and Penninger, 2004). According to Lim et al (2012), both gene and protein expressions of PMK-1, the p38 mitogen-activated protein kinase, elevated in *C. elegans* exposed to AgNMs along with the increased in glutathione-S-transferase (GST) activity, which suggested oxidative stress as the major pathway of toxicity from AgNMs via the p38 MAPK cascade (Lim *et al.*, 2012). Roh and colleagues (2012) also demonstrated a correlation between MAPK signalling to oxidative stress induced by AgNMs in *C. elegans* by exhibiting an increase in expression of certain genes involved in the different components of MAPK pathway. They also showed that those gene levels peaked at 24 hours of exposure (Roh, Eom and Choi, 2012). From this study, it was found that genes involved in MAPK signalling such as *cst-1*, F11F1.1, *jnk-1*, and *ras-2* were down-regulated significantly, which suggests that oxidative stress might underlie the toxicity

from JRCNM03002a. The down-regulation of genes in the GSH metabolism pathway also supported that there was oxidative stress involved in the AgNM toxicity since the enzymes in the GSH metabolism are important for the detoxification process (Leiers *et al.*, 2003). However, the down-regulation of these genes might indicate that they were already utilised for the transcription. Otherwise the toxicity of JRCNM03002a might induce a severe stress response and consequently lead to the transcriptional shut-down as also found in single-walled carbon nanotube (SWCNT) toxicity in *C. elegans,* which was observed by Eom *et al.* (2015). In this thesis, it was found that 33% of genes in the MAPK signaling pathway and 40% of genes in glutathione metabolism were down-regulated significantly. The comparison was made between AgNM-treated and non-treated group after 30 minutes of exposure. The transcriptomic study was able to support the relevance of oxidative stress to the toxicity of AgNM by indicating the percentage of differentially expressed genes in the pathway of interest. The higher the percentage, the more likely the pathway is involved in the toxicity. Although less than 50% of genes related to MAPK signaling and glutathione metabolism were down-regulated in the response to AgNM, it was noteworthy to consider that these pathways were affected by AgNM.

Moreover, the down-regulation of genes involved in lysosome and phagosome might also support that phagocytosis would link to the uptake of JRCNM03002a and hence the toxicity. This was also observed in multi-walled carbon nanotubes toxicity by Eom *et al.* (2015). After all, it had to be taken into consideration that the missing replicates due to the degradation of total RNA during the shipment might impair the statistical analysis, therefore the conclusion should be taken in the degree of caution. The future work to achieve the accurate understanding, for example, the analysis of the repetitive replicates should be conducted to establish the conclusion of transcriptomics.

7.5.2 Proteomics

The aim of the proteomic study was to collect the information on how *C. elegans* protein levels changed following the exposure to JRCNM03002a, as well as to compare with the results from the transcriptomic study. The proteomics work was designed to study the regulation of proteins at various time-points. However, it was challenging to obtain a sufficient amount of nematodes for each sample, thus the time points had to be reduced to 0 and 24 hours to compare with the results from transcriptomics. As described in section 7.5.1, it was impractical to collect *C. elegans* at the exact time point of 0 hour, and therefore, all the results had to be reported as the time point of 30 minutes.

To summarise, 149 proteins were found to alter their expression. The top five functions of these proteins as ranked by their majority were: catalysis (9.40%), binding proteins (7.38%), detoxification proteins (6.04%), signalling transductors (6.04%), transcription regulators (5.37%), and transporters (5.37%). To focus on the proteins found in the treatment group, there were 40 proteins specifically altered in the comparison of treatment relative to control group at time point of 30 minutes ($T_{30}vsC_{30}$), and 12 in the time-point of 24 hours (T24vsC24). Most proteins found changed at the time point of 30 minutes were signalling transductors. Interestingly, four of the proteins found in this comparison were involved in the apoptosis, phagosome, and DNA strand break repair, which was the response to cellular stress. However, these proteins were altered in their regulation with a small fold change (less than 2 fold change).

In the comparison of 24 hours group (T24vsC24), two proteins involved in the apoptotic and detoxification process were also found down-regulated in this comparison with a small fold change. It was intriguing that the proteins involved in the potential pathway of toxicity were down-regulated. The explanation to this was that the proteins might have been used to counteract with the toxicological effect or JRCNM03002a might trigger the severe stress response which resulted in the molecular shut-down (Eom *et al.*, 2015). Although the small number of proteins found changed in their regulation has limited the possibility of conducting protein pathway analysis in this study. It was promising that these pathways might be involved in the toxicity induced by AgNM as Kim and colleagues suggested in the study of AgNM in rats (Kim *et al.*, 2010). In addition, the study of AgNM toxicity in human colon carcinoma cells found that proteins involved in antioxidant activity and cell death were up-regulated. The

protein-protein interaction map indicated that the small ubiquitin-related modifier 2 (SUMO2, cluster I) was among those up-regulated proteins. These modifiers were thought to be triggered by DNA damage, ROS, and apoptosis. However, the authors pointed out that the actual mechanism of these modifiers was still unclear and under debate (Verano-Braga *et al.*, 2014). From the findings of the transcriptomic study, it was indicated that there the majority of genes in the ribosomal pathway were down-regulated in the AgNM-treated group compared with the non-treated group. The decrease in ribosomal activity could lead to the reduction in protein synthesis, which might describe the small number of proteins detected in the proteomic study. Moreover, ribosomes have a function to translate a large number of essential proteins to maintain the cellular state i.e. growth and death (Naora, 1999). The decrease in ribosomal activity indicates a loss in cellular activity, which is normally found in dying cells (Chen and Ioannou, 1999).

Although those proteins working in the detoxification processes were altered their regulation, the degree of the alteration was small (less than 2 fold change), therefore it should be taken into the consideration that those proteins which changed their regulation with a higher degree should be more relevant to the toxicity from AgNMs. Considering a threshold more than 2 fold change, proteins working in RNA binding, ribosome biosynthesis, and ion channel transport were up-regulated significantly in the comparison of T_{30}vsC_{30}, while proteins involved in transmembrane signalling receptor, biosynthetic process, and metabolic pathway were up-regulated significantly in the comparison of T24vsC24. However, the limitation in this study was that the number of identified proteins in the treatment groups was small and it was challenging to analyse these results in relation to the pathway enrichment. Furthermore, some *C. elegans* proteins were not annotated and their functions were hypothetical. Therefore, a solid conclusion from the proteomic study could not be drawn alone. The findings from both the transcriptomic and proteomic studs are discussed below.

7.5.3 The link between transcriptomics and proteomics

As stated in section 7.1, the omics approaches are helpful to gain overall information on the NMs toxicity pathways. However, using one of the omics approaches might only give an access to a small part of the information. Therefore, it was important to study the different omics approaches and integrate the findings to acquire a comprehensive understanding of NMs toxicity.

As found in the transcriptomic study, the potential pathways that NMs might act on are ribosome, oxidative phosphorylation and lysosome. This indicates that the function of cells in ribosome, hence protein synthesis, was the main effect from AgNM exposure and the internalisation of AgNM might take place via phagocytosis. In addition, time of exposure was also important on how *C. elegans* responded to AgNM. At the early time point (30 minutes), genes in the MAPK signalling pathway, GSH metabolism, phagosome, transporter activity, and transmembrane activity were significantly affected by NM, while genes in the pathway of ribosome and translation were altered in the higher statistical degree at the longer time point (24 hours). MAPK signalling, especially the JNK pathway was involved in the stress response leading to cell death. It can be implied that oxidative stress and/or apoptosis were the major pathway in the early exposure, while the function of ribosome remained the target for AgNM toxicity in the longer time point.

Results from the transcriptomic study could also explain the findings from the proteomic study, in which the products of those genes in the affected pathways were altered in their regulation, which included proteins in RNA binding, ribosome biosynthesis, ion channel transport, transmembrane signalling receptor, biosynthetic process, and metabolic pathway, as well as the detoxification proteins, proteins involved in apoptosis and phagosome were differentially expressed in the exposure to JRCNM03002a.

Nevertheless, it had to be considered that the results from the transcriptomic study were derived with a limited number of replicates. Furthermore, both transcriptomic and proteomic studies should be conducted with various time points. In addition, it would be helpful to study the transcriptomic and proteomic effects of Ag^{+} to compare the different pathways across the different Ag forms. Future analysis with a larger number of replicates would be beneficial. Furthermore, the pathway analysis for proteomics data would be more informative to draw a solid conclusion if there was a

tool capable to analyse the small number of identified proteins. Finally, more frequent time points would also be interesting to understand the time-lapse of nematode reaction to AgNM exposures.

7.6 Summary of this chapter

This chapter aimed to study molecular processes occurring after exposure to one of the tested AgNM, JRCNM03002a. By investigating the alteration in genes and protein levels, and analysing their function, the pathway of AgNM toxicity was further explored. It was found in the previous chapter that oxidative stress and apoptosis might be induced by exposure to AgNMs, and hence underlying the toxicity in *C. elegans.* To summarise, the omics approaches were advantageous to establish the pathway of toxicity from AgNM. By identifying and analysing the functions of genes and proteins that changed in their regulation, the pathway of toxicity from JRCNM03002a could be predicted. From the transcriptomics study, it was shown that the main pathway of toxicity from JRCNM03002a was involved in ribosome and protein synthesis. The uptake of AgNM into cells was predicted to be by phagocytosis. In addition, the toxicity and response from JRCNM03002a in *C. elegans* was time-dependent. Oxidative stress leading to cell death was suggested to be additionally involved in the early time of exposure (30 min); these responses seemed to disappear in the longer time period (24 h) remaining only the response in ribosome and translation. Furthermore, the findings from proteomics also supported the results from transcriptomics. However, the limitation from this study, including the lack of appropriate replicates, and the incapability to analyse the pathway enrichment for identified proteins, prevented a solid conclusion to be drawn in this chapter. Future work should ensure that a larger number of replicates with more time points, are available to explore the results obtained.

The results from these studies are summarised below in relation to the tested Null Hypotheses.

1. "There was no alteration of genes and protein regulation during the time of study"

This null hypothesis was rejected. There was a change in expression of both genes and proteins between 30 minutes and 24 hours. This observation was found in both treated- and non-treated groups.

2. “Genes and proteins working on oxidative stress and apoptosis would retain their expression in the same manner as in the control group when *C. elegans* exposed to NM”

This null hypothesis was rejected. It was found from the transcriptomic study that some genes in the pathways of MAPK signalling and glutathione metabolism were down-regulated comparing between AgNM-treated and non-treated groups. These pathways relate to the response from oxidative stress. Moreover, the AgNM treatment also induced the down-regulation of genes in the ribosomal pathway, which indicated reduction in the ribosomal activity. The decrease in ribosomal function could lead to the shutdown of protein synthesis, which was found in the dying cells. It was also found in the proteomic study that some proteins involved oxidative stress and apoptosis altered their regulation. Although a small number of these proteins were found, it was worth noting that the pathway of oxidative stress and apoptosis might be affected by the exposure to AgNM.

Chapter 8: General discussion

8.1 Summary of the findings in this thesis

The work described in this thesis was able to evaluate the toxicity of a group of NMs, focusing particularly on Ag of different forms. Copper materials were also investigated initially but due to the low toxicity observed and the fact that the plan was to investigate in detail the pathways of toxicity observed, these studies were discontinued. Results obtained indicated that different types of Ag induced dissimilar degrees of toxicity. The smaller spherical AgNM, JRCNM03002s was more toxic than the larger rod shape, NM302. However, the AgNMs were not as toxic as their ionic form, $AgNO_3$.

The diverse responses of the various nematode strains indicated a difference in susceptibility to the Ag toxicants between those strains. Since particular genes involved in oxidative stress or apoptosis were deleted in those mutant strains, it could be deduced that these pathways were involved in the response to the Ag toxicants. Experiments focusing on these pathways were performed, and it was established that oxidative stress was relevant to the toxicity from Ag substances. However, specific assays to determine a connection between apoptosis and the observed toxicity was ambiguous.

It was discovered during the omic studies that time of study was important to the pathway of toxicity. At the short time of exposure (30 minutes), genes in the pathway of MAPK signalling, GSH metabolism, and phagosome altered their expression significantly. At the longer time of exposure (24 hours), the most significant gene expression was found in the pathway of ribosome and translation. Moreover, the proteomic study revealed that there was an alteration of proteins in the detoxification process and apoptosis in both short and long time of exposure. The findings of this thesis are summarised and presented in Table 8.1.

Table 8.1: Summary of the findings in this thesis

Chapter	Endpoint	Exposure time	Toxicant	Strain	Toxic conc. (mg/L)	Toxicity observed	Protocol suitable for testing
4	Lethality	24 h	$AgNO_3$	N2 MT1522 VC433 VC128	0.15-0.19 0.24-0.27 0.15-0.18 0.21-0.27	✔	✔
			NM300K	N2 MT1522 VC433 VC128	2.93-3.33 3.66-3.94 2.87-3.16 2.78-3.08	✔	
			NM302	N2 MT1522 VC433 VC128	183.51-222.81 248.89-303.06 182.36-219.13 242.30-295.49	✔	
			$CuCl_2$	N2 MT1522 VC433 VC128	173.70-182.31 205.51-218.93 155.83-165.43 184.93-202.86	✔	
			CuO bulk	All	>750	✖	
			CuO nano	All	>750	✖	
	Reproduction	72 h	$AgNO_3$	N2 MT1522 VC433 VC128	0.10-0.14 0.11-0.15 0.05-0.06 0.04-0.14	✔	✔
			NM300K	N2 MT1522 VC433 VC128	1.83-2.25 2.53-2.69 1.09-1.71 1.31-1.86	✔	
			NM302	N2 MT1522 VC433 VC128	72.00-80.45 31.22-83.89 33.61-51.36 16.15-43.78	✔	

Table 8.1 (Cont.): Summary of the findings in this thesis

Chapter	Endpoint	Exposure time	Toxicant	Strain	Toxic conc. (mg/L)	Toxicity observed	Protocol suitable for testing
5	ROS generation	2 h	$AgNO_3$	N2	-	✖	✔
				MT1522	0.2	✔	
				VC433	0.2	✔	
				VC128	0.2	✔	
			NM300K	N2	2	✔	
				MT1522	-	✖	
				VC433	2	✔	
				VC128	-	✖	
			NM302	N2	-	✖	
				MT1522	200	✔	
				VC433	200	✔	
				VC128	200	✔	
	SOD activity	24 h	$AgNO_3$	N2	0.2	✔	✔
				MT1522	0.2	✔	
				VC433	0.1, 0.2	✔	
				VC128	0.1, 0.2	✔	
			NM300K	N2	2	✔	
				MT1522	2	✔	
				VC433	2	✔	
				VC128	2	✔	
			NM302	N2	-	✖	
				MT1522	-	✖	
				VC433	200	✔	
				VC128	100, 200	✔	
	CAT activity	24 h	$AgNO_3$	N2	0.1	✔	✔
				MT1522	-	✖	
				VC433	0.1	✔	
				VC128	-	✖	
			NM300K	N2	1	✔	
				MT1522	-	✖	
				VC433	1	✔	
				VC128	1	✔	

Table 8.1 (Cont.): Summary of the findings in this thesis

Chapter	Endpoint	Exposure time	Toxicant	Strain	Toxic conc. (mg/L)	Toxicity observed	Protocol suitable for testing
5	CAT activity	24 h	NM302	N2 MT1522 VC433 VC128	- - - 100	✖ ✖ ✖ ✔	✔
6	AO staining	24 h	All	All	-	✖	✖
	Annexin V/PI	24 h	All	All	-	✖	✖
	Apoptotic proteins determination	24 h	$AgNO_3$	All	-	✖	✖
			NM300K	All	-	✖	
			NM302	All	-	✖	
7	Omics	30 min/24h	NM300K	N2	1	✔	✔

Note: The single ✔ according to each toxicant represents that the toxicity was observed in all strains, while when it appears with ✖, it means the toxicity was established in some strains. The strain that exhibited the toxicity is represented with ✔ and the concentration that induced toxicity is provided. The symbols, ✔ and ✖ also indicate the suitability of protocol for the testing. The appropriateness of the protocol was judged by the ability to detect the toxicity of Ag toxicants.

Toxicity of AgNMs was observed in *C. elegans* in regards to mortality and reproduction in the exposure time of 24 and 72 hours, respectively. The toxicological exposure was carried out using the medium SSPW, which was shown to be appropriate to investigate the toxicity of Ag substances in *C. elegans* since this medium had low ionic strength and chloride content, as well as the fact that the reproduction of *C. elegans* was not suppressed in this medium (Tyne *et al.*, 2013).

The mortality test was carried out to explore the range of concentrations for future toxicological tests. The range of concentrations inducing death of nematodes was found to be 1-8 mg/L and 50-500 mg/L for JRCNM03002a and NM302, respectively.

A more sensitive endpoint, the reproduction test, was chosen to investigate the adverse effects in the longer times of exposure, as well as to find out the connection between the reduction in the number of offspring and the occurrence of apoptosis in germ cells of *C. elegans*. The range of concentrations of 1-5 mg/L and 25-400 mg/L was found to reduce the number of progeny in *C. elegans* exposed to JRCNM03002a and NM302, respectively. However, the toxicity from $AgNO_3$ was the greatest among all Ag substances with the range of concentration of 0.05-0.5 mg/L for mortality test, and 0.05-0.3 mg/L for the reproduction test. From this finding, it was possible that the toxicity from AgNMs might derive from the size, shape, and the amount of dissolved Ag^+.

Considering AgNMs, smaller spherical JRCNM03002a triggered negative effects in nematodes at the lower concentration than bigger rod-shaped NM302. It is likely that bioavailability of JRCNM03002a higher that of NM302. TEM images showed that both JRCNM03002a and NM302 tend to bind together as aggregates/agglomerates in the test medium. Aggregates of JRCNM03002a were not bigger than two microns approximately, while the length of only one NM302 particle/aggregate could be up to four microns. With this dimension of particles and the width of *C. elegans* mouth (approximately three microns), it could be suggested that JRCNM03002a could fit into the nematode's mouth better than NM302. Ellegaard-Jensen and colleagues stated that the bioavailability of AgNM to *C. elegans* was not to be considered by having comparatively little size, but their size should be proper to be ingested by the nematode as they found bigger PVP-coated AgNM to be more toxic than smaller ones (Ellegaard-Jensen, Jensen and Johansen, 2012).

The amount of dissolved Ag^+ could also account for the toxicity of AgNMs. Results from ICP-MS indicated that JRCNM03002a released a higher amount of Ag^+ with the solubility of approximately 50% compared with NM302, which yielded only 0.1% of Ag^+ after 24 hours of AgNMs addition to the medium. The size of NMs was found to be the major factor in the dissolution. As Peretyazhko and colleagues found the dissolution rate constant of AgNMs decreased toward the size of AgNMs (Peretyazhko, Zhang and Colvin, 2014), as well as high surface area of small AgNM might increase the reaction to water molecule and thus enhance the solubility. From these explanations, the the differences in toxicity between the two types of AgNMs can be explained.

The potential pathways of toxicity were determined by comparing the susceptibility of different strains of nematodes lacking particular genes. From the toxicity tests, it was found that the mutant lacking pro-apoptotic gene, *ced-3* was more tolerant than wild type regarding the death endpoint. From this finding, apoptosis was expected to be the potential pathway of toxicity from AgNMs. Although, in the same endpoint, another mutant lacking one of the metallothionein genes, which acts in the detoxification process, was also more enduring than the wild type, however, when considering the reduction of progeny, this strain was more sensitive than the wild type. Furthermore, the mutant lacking one of the superoxide dismutase genes was more susceptible to the AgNMs than the wild type. Since both metallothionein and superoxide dismutase were both involved in the oxidative stress pathway, it was suggested that oxidative stress could be an important pathway of toxicity from AgNMs.

The relevance of oxidative stress to the toxicity observed in *C. elegans* was established by focusing on the production of ROS and the alteration in the detoxification enzyme activities using the concentration of LC_{10} and $2*LC_{10}$ of all Ag toxicants. The generation of ROS after 2 hours of exposure was shown to increase in a concentration-dependent manner compared with the control group of each strain. A significance in the increase was mostly identified in the mutant which lacked both detoxification genes in the group of $2*LC_{10}$. Furthermore, the comparison of ROS generation between the mutants and wild type also indicated that these detoxification-gene-deleted strains were statistically more susceptible to AgNMs than wild type.

The same findings were also observed when analysing the activity of SOD, which removes the superoxide anion. The toxicity from Ag toxicants was concentration-dependent, and the significance was mostly established in the $2*LC_{10}$ groups of mutants lacking detoxification genes, indicating that these mutants were significantly more sensitive than the wild type. The time point study demonstrated that the activity of SOD was found to increase over time, and reached the highest level at 24 hours.

On the other hand, the determination of CAT activity indicated that the activity of the enzyme peaked at 6 hours of exposure, and the lower concentration of LC_{10} induced higher activity of catalase when compared to the higher concentration of $2*LC_{10}$. Therefore, the groups of nematodes exposed to LC_{10} of every Ag substance were found to have significantly increased CAT activity. Despite the difference in toxicity patterns from SOD, a statistical difference in CAT activity was observed,

mostly in the strains which lacked the detoxification genes. However, no statistical differences were found between the mutants strains and the wild type.

The inconsistencies in these findings between SOD and CAT might be explained by the difference in time of action of these enzymes, or the depletion of CAT during the experiment, or the interference from the CAT determination procedure. As the measurement was done by UV detection of the H_2O_2, which was degraded by CAT, the reading might be disturbed by the bubbles generated in the reaction. Although this determination technique was established and used in many studies (Claiborne, 1985), the alternative choice of using the commercial kit could be more suitable to ascertain the alteration in CAT activity.

Although oxidative stress was indicated to be relevant to the toxicity from AgNMs, and the connection of oxidative stress and apoptosis was demonstrated in the cellular signaling pathway (Martindale and Holbrook, 2002), as well as the death of nematodes, the lack of pro-apoptotic genes was lower than the wild type. It was not possible to demonstrate apoptosis in this project using the visualisation technique and the apoptotic protein determination, at least in this test condition (24 hours of exposure, LC_{10} or LC_{50}). However, the stains used in this project were shown to be effective to detect apoptotic cells in the positive control, camptothecin.

The failure to visualise the apoptotic corpses could mean that apoptosis was not linked to the toxicity from AgNMs, or the condition might not be suitable. Although many studies which chose an experiment time of 24 hours and succeeded in showing apoptotic cells in *C. elegans*, those studies were focused on different test substances such as arsenite, sodium arsenite, sodium fluoride, and fullerol NM (Wang *et al.*, 2007; Pei *et al.*, 2008; Cha, Lee and Choi, 2012; Qiao *et al.*, 2012). The studies concerning apoptosis induced by Ag substances were limited in this test model, yet were most established in cell lines using time points of up to 24 hours (Eom and Choi, 2010; Zhang *et al.*, 2012; Lee *et al.*, 2014; Zhang *et al.*, 2015). In addition, most studies in organisms, e.g. fruit flies, mice, and rats, determined apoptosis by using the time of exposure from 24 hours up to 10 days (Ahamed *et al.*, 2010a; Posgai *et al.*, 2011; Tiwari, Jin and Behari, 2011). Therefore, the time of exposure selected in this project might not be suitable to detect apoptosis, and the longer time period should be used to conduct the experiment in future, as well as the concentration and this should be adapted to be applicable for the time period.

The failure of the visualisation technique has led to a different approach to establish the occurrence of apoptosis. The decision to use the commercial kit to determine the invertebrate apoptotic proteins was due to the fact that these proteins are highly conserved in the organisms. However, the application of the apoptotic protein determination kit also revealed inconsistent results as the amount of apoptotic proteins detected was sparse, and large variation was observed in particular samples. Although the function of some of these proteins was conserved in *C. elegans*, the structure of them was not entirely similar. The fact that the commercial kit utilises an ELISA principle for the detection, the affinity of proteins to the detection antibody might have an impact on the results.

As mammalian and invertebrate proteins share partial structure (Gewies, 2003; Rosenberg, 2011), this might impair the binding of proteins to the antibody. Moreover, some functions of protein are absent in *C. elegans*, but exist in the higher organisms. The detection of these proteins could not explain the findings since the results may derive from the binding of other proteins that highly resembl the structure of those particular proteins. In addition, similar protein in the different organisms might not entirely perform an identical function (Burke, 2001; Tzur *et al.*, 2002). For these reasons, it was challenging to draw a full conclusion from this experiment. Since there was no apoptotic commercial kit specifically for *C. elegans* on the market, future work to evaluate apoptotic genes or proteins in this organism should evaluate futher the potential for apoptosis to be induced from AgNMs.

The omics approaches were applied to study the alteration of genes and proteins in wild type exposed to 1 mg/L JRCNM03002a after 30 minutes and 24 hours exposure. Although the transcriptomic study had an impairment in the number of replicates which resulted in a rigid threshold of the statistical application, it was found that, at both time points, the down-regulated genes functioned in the pathways of ribosome, oxidative phosphorylation, and lysosome. Interestingly, at the time point of 30 minutes, the genes in the MAPK signaling pathway, GSH metabolism, phagosome, transporter activity, and transmembrane activity were significantly down-regulated.

As the MAPK signaling pathway controls the state of the cell (alive or dead) (Garrington and Johnson, 1999), as well as GSH, it is related to the detoxification process of foreign substances (Leiers *et al.*, 2003). The oxidative stress pathway from JRCNM03002a was proposed to play a role in the toxicity of this AgNM. Since MAPK signaling connects to the initiation of apoptosis (Garrington and Johnson, 1999), it was

suspected that apoptosis could be triggered by JRCNM03002a. Moreover, the pathway in the lysosome and phagosome indicated that phagocytosis could also be involved in the toxicity of AgNM. As Eom and colleagues have shown phagocytosis plays an important role in carbon nanotube uptake, which consequently leads to toxicity (Eom *et al.*, 2015).

Although it was not possible to carry out the pathway analysis of the results from proteomics, the identification of protein function revealed that most proteins found to change in the time point of 30 minutes were signaling transducers. More importantly, there were four proteins altering their expression which involved apoptosis, phagosome, and DNA strand break repair at this time point, while there were two proteins acting in the apoptosis and the detoxification process at the time point of 24 hours. From this result, the findings from the transcriptomic study were supported. Although the alteration of these proteins were down-regulated, the explanation to this could be that these proteins were utilised to balance the NMs toxicity, or the toxicity from JRCNM03002a could induce the severe stress response, which leads to the molecular shutdown as described by Eom *et al.* (2015).

8.2 Brief summary of current AgNMs toxicity literature and similarities of the findings of this thesis

Despite the number of articles on toxicological studies of AgNMs, it was still challenging to derive an explicit understanding iofn the toxicity derived from the AgNMs since the available nanotoxicological data are varied and depends on experimental design. Furthermore, most studies focused on the adverse effects from AgNMs in particular biological models, particularly cells, which did not answer the question on how AgNMs affect the whole organism, or the environment. In addition, the knowledge of the pathways of toxicity induced by AgNMs is still not fully established. This thesis aimed to contribute novel information to the current literature.

Most studies suggest that the toxicity of AgNMs is strongly dependent on the NM physicochemical properties such as size, shape, surface charge, and solubility (Schrand *et al.*, 2010; Castranova, 2011). The potential to release Ag ions is a consequence from the high surface area of NMs, and thus the released Ag^{+} is thought to be one of the factors involved in the toxicity from AgNMs (Navarro *et al.*, 2008; Kawata, Osama and Okabe, 2009). However, this understanding is in contrast with

Kim *et al.* (2009) who pointed out that the toxicity from AgNMs was relevant to oxidative stress and was independent on the release of Ag^+ (Kim *et al.*, 2009).

Although there is a conflict between the findings from the nanotoxicological studies, it was found universally that dissolved Ag^+ is at least an important contributor of toxicity from AgNMs. The specific NM effect on the toxicity was also found in some studies. Beer *et al.* (2012) indicated that toxicity from particular fractions of AgNM suspensions was significantly different in human lung carcinoma cells. The toxicity from the supernatant fraction, which should mostly consist of dissolved Ag^+, was significantly lower than that found in the nanoparticulate fraction. From this finding, the authors suggested the impact of other factors on the toxicity rather than Ag^+ (Beer *et al.*, 2012). Studer *et al.* (2010) also found this phenomenon in CuO NMs and explained that the plasma membrane of cells, which acted as the natural barrier, allowed the CuO NMs to translocate inside cells, and led to the toxicity of released copper ions, so called Trojan horse effect (Studer *et al.*, 2010).

Although Beer and colleagues did not provide valid support on the Trojan horse effect by AgNMs, they found that oxidative stress from AgNMs was likely to be relevant to the dissolved Ag^+ as the generation of ROS was significantly higher in the supernatant fraction (Beer *et al.*, 2012). In addition, a study emphasised the effect of released Ag^+ from AgNM indicating the importance of the dissolution of Ag ion to cytotoxicity in human epithelial and human lung carcinoma cells. De Matteis *et al.* (2015) found that the amount of released Ag^+ in the medium was less than in the cellular lysosome; furthermore the dissolved Ag ions in the medium were bound to some proteins or chelated with the counterions in the medium. This suggested that toxicity from AgNM was mainly dependent on the Ag^+ inside cells as AgNM could be taken up into cells by endocytosis, and ended up in the lysosome, where the release of Ag^+ had taken place. The importance of the dissolution of AgNM was shown by the addition of Ag ion chelating agent, which prevented the death of these cells (De Matteis *et al.*, 2015).

The research in transcriptomics of fathead minnow and human liver carcinoma cells after exposure to $AgNO_3$ and PVP-coated AgNM revealed that the combination of both dissolved Ag ion and AgNM was likely to cause toxicity. Garcia-Reyero *et al.* (2014) reported shared and different pathways of toxicity from $AgNO_3$ and PVP-coated AgNM. The main pathways of toxicity induced by Ag^+ was involved in the interference of Na^+ and Cl^- transport across the gills, the generation of ROS, and the induction of

cellular stress via MAPK signaling, while the exposure to AgNM caused the alteration in genes in the transcription factor pathways and nuclear receptors. From this finding, the hypothesis of the specific nanoparticulate effect in toxicity has been supported (Garcia-Reyero *et al.*, 2014).

As depicted in many articles, one of the mechanisms of toxicity from AgNMs was shown to relate to oxidative stress. Many studies established the relevance of oxidative stress to the exposure of AgNMs by using various endpoints. The increase in the generation of ROS, which is strongly linked to oxidative stress, has been shown in both cell lines and animal models treated with AgNMs (Braydich-Stolle *et al.*, 2010; Eom and Choi, 2010; Foldbjerg, Dang and Autrup, 2011; Nishanth *et al.*, 2011; Piao *et al.*, 2011; Sanpui, Chattopadhyay and Ghosh, 2011; Tiwari, Jin and Behari, 2011; Lim *et al.*, 2012; Wu and Zhou, 2012; Ahn *et al.*, 2014b; Shi *et al.*, 2014). Furthermore, the amount of detoxification molecules and enzymes such as GSH, SOD and CAT were also found to alter after the exposure to AgNMs, which also indicated that oxidative stress was induced by AgNMs (Farkas *et al.*, 2011; Liu *et al.*, 2011; Piao *et al.*, 2011; Posgai *et al.*, 2011; Wu and Zhou, 2012; Suliman *et al.*, 2013; Cozzari *et al.*, 2015). From these findings, it was deduced that oxidative stress was involved in the toxicity of AgNMs. It was established that the consequence of excess ROS could lead to oxidative damage to proteins, lipids, and DNA (Kannan and Jain, 2000), as well as triggering cell death by both the necrotic and apoptotic pathways (Martindale and Holbrook, 2002).

Since oxidative stress could induce apoptosis, it is possible that there is a relationship between AgNMs and apoptosis. Many studies in various cell lines have indicated the induction of apoptosis following exposure to different types of NMs, including Ag. It was found that there was an alteration of apoptotic gene expression, the activities of apoptotic proteins, or the number of apoptotic cells in the exposure to AgNMs (Ahamed *et al.*, 2010a; Eom and Choi, 2010; Zhang *et al.*, 2012; Lee *et al.*, 2014; Gurabi *et al.*, 2015; Jacob and Shanmugam, 2015), which suggested the involvement of AgNMs in the induction of apoptosis.

Results from this thesis have provided further information on how AgNMs affect a particular species, *C. elegans*. Although the toxicity from AgNMs has been widely studied, the mechanisms of toxicity are still unclear. Most of these studies to date have focused on particular cell types, and the conditions used in most cases is not environmentally relevant. Therefore the studies reported in this thesis, on the whole

organism using the relevant environmental conditions are informative and provide inroads in the understanding on the effects of AgNMs in the environment.

This thesis has shown that AgNMs can induce toxicity in *C. elegans* in terms of viability and reproduction. However, the degree of toxicity was different between each type of AgNMs. Spherical-shaped JRCNM03002a, which had a diameter of 20 nm, was more toxic than rod-shaped NM302 (50 nm in diameter). Dissolution of these AgNMs revealed that JRCNM03002a led to releases of higher amounts of Ag^{+}, which might be the explanation for the different degree of toxicity. Knock-out strains of nematodes, which lack particular genes of interest, responded to the AgNMs differently, which suggest that the adverse effects from AgNMs were related to the pathways of oxidative stress or apoptosis.

Oxidative stress was verified, in this thesis, to be involved in the toxicity from AgNMs as the amount of ROS and detoxification enzymes were elevated in the nematodes exposed to AgNMs. However, apoptosis was not shown to be relevant to the toxicity in the nematodes, at least in the experimental conditions used in this thesis.

The study of transcriptomics of nematodes exposed to JRCNM03002a revealed that pathways of ribosome, oxidative phosphorylation, and lysosome were related to the toxicity of AgNM. Shorter exposure time (30 minutes) to this NM led to the alteration of genes in the MAPK signalling pathway, GSH metabolism, phagosome, transporter activity, and transmembrane activity, while at the longer exposure time (24 hours), only genes in the ribosome pathway were down-regulated. However the down-regulation was found to be at higher significance level than that found at the shorter time point. The proteomic study also demonstrated a change in expression of proteins in the response to cellular stress, i.e. apoptosis, phagosome, and DNA strand break repair in the short exposure time (30 minutes), as well as the proteins involved in apoptosis and detoxification processes in the 24 hours of exposure.

8.3 Future works based on the finding from this thesis

Although this thesis has addressed the toxicity from AgNMs in *C. elegans* and some of the toxicity pathways, it also led to further questions. First of all, the toxicological tests conducted in this thesis consisted of mortality and the inhibition of reproduction using the exposure times of 24 and 72 hours, respectively. It would be interesting to find out the toxicological effects on other endpoints such as growth, movement, the uptake of AgNMs, as well as the impact on other generations produced

from the nematodes exposed to the AgNMs. Moreover, it would be more informative to study the behaviour of nematodes by performing chronic studies as these tests would result in a better understanding of toxicity from AgNMs in regards to their ecological relevance.

The characterisation of AgNMs in this thesis focused on the properties of AgNMs in terms of hydrodynamic diameter, zeta potential, size and shape, and the solubility of AgNMs. However, the determination of hydrodynamic diameter and zeta potential using DLS was not suitable for the rod shaped NM302. Therefore, it would be advisable to find a technique that can be applied to non-spherical NMs. Moreover, it would be interesting to understand other properties such as the reactive surface area to provide information on which AgNM was more reactive.

Although oxidative stress was shown to be involved in the toxicity from AgNMs in this thesis, only three endpoints were explored. It would be interesting to perform oxidative stress assays focusing on other endpoints, e.g. the level of GSH, the generation of biomarkers for oxidative stress such as MDA and LPO. In addition, it would be interesting to examine these endpoints at longer time periods to understand oxidative damage following chronic exposures.

Apoptosis was not shown to be relevant to the toxicity from AgNMs in the test conditions used in this thesis. The inability to detect apoptosis might have derived from the concentrations used, times of exposure, as well as the techniques used to determine apoptosis. Therefore, future studies should consider a wider range of concentrations and time points. Moreover, suitable apoptotic protein determination, which specifically detects proteins from *C. elegans*, should be used.

The studies of gene and protein regulation using omics approaches were beneficial to understand the pathway of toxicity from JRCNM03002a. However, additional replicates should be considered in order to enhance the robustness of the statistics. In addition, the transcriptomics and proteomics of *C. elegans* exposed to $AgNO_3$ and NM302 should also be investigated to compare the potential pathways of toxicity across the different Ag materials, particularly in order to understand the effect of released Ag^+ to the toxicity from particular AgNMs. Furthermore, it would be interesting to study the change in genes and proteins at other time points as some genes or proteins might be regulated faster or slower than others.

8.4 Final remarks

Although AgNMs are some of the most widely used NMs and research on the toxicity of AgNMs has been universally targeted, there are a number of issues that have not yet been fully addressed in the current literature regarding the their environmental toxicity and pathways of toxicity. Therefore, this thesis aimed to improve the knowledge on the toxicity of AgNMs in environmentally relevant conditions, as well as to investigate the pathways of toxicity from the chosen AgNMs. Although the toxicity induced by AgNMs was demonstrated in this thesis, and oxidative stress was shown to be linked to the toxicity observed, the pathway of apoptosis was not shown to be involved in the adverse effects from AgNMs, at least at the chosen concentrations and time points. The potential pathways of toxicity, especially apoptosis, should be further investigated to improve the knowledge of AgNMs toxicity in order to design safer NMs.

References

Ahamed, M., Posgai, R., Gorey, T. J., Nielsen, M., Hussain, S. M. and Rowe, J. J. (2010a) 'Silver nanoparticles induced heat shock protein 70, oxidative stress and apoptosis in *Drosophila melanogaster*', *Toxicology and Applied Pharmacology*, 242, pp. 263-269.

Ahamed, M., Siddiqui, M. A., Akhtar, M. J., Ahmad, I., Pant, A. B. and Alhadlaq, H. A. (2010b) 'Genotoxic potential of copper oxide nanoparticles in human lung epithelial cells', *Biochemical and Biophysical Research Communications*, 396(2), pp. 578-583.

Ahn, J., Eom, H., Yang, X., Meyer, J. N. and Choi, J. (2014a) 'Comparative toxicity of silver nanoparticles on oxidative stress and DNA damage in the nematode, Caenorhabditis elegans', *Chemosphere*, 108, pp. 343-352.

Ahn, J. M., Eom, H. J., Yang, X., Meyer, J. N. and Choi, J. (2014b) 'Comparative toxicity of silver nanoparticles on oxidative stress and DNA damage in the nematode, Caenorhabditis elegans', *Chemosphere*, 108, pp. 343-352.

Altun, Z. F. and Hall, D. H. (2009) 'Handbook of C. elegans anatomy', in *WormAtlas*.

Arora, S., Jain, J., Rajwade, J. and Paknikar, K. (2008) 'Cellular Responses Induced by Silver Nanoparticles: *in vitro* Studies', *Toxicology Letters*, 179, pp. 93-100.

Arora, S., Jain, J., Rajwade, J. and Paknikar, K. (2009) 'Interactions of Silver Nanoparticles with Primary Mouse Fibroblasts and Liver Cells', *Toxicology and Applied Pharmacology*, 236, pp. 310-318.

Asharani, P., Mun, G. L. K., Hande, M. P. and Valiyaveettil, S. (2009) 'Cytotoxicity and Genotoxicity of Silver Nanoparticles in Human Cells', *ACS Nano*, 3, pp. 279-290.

Asharani, P., Wu, Y., Gong, Z. and Valiyaveettil, S. (2008) 'Toxicity of Silver Nanoparticles in Zebrafish Models', *Nanotechnology*, 19, pp. 1-8.

Ashkenazi, A. and Dixit, V. M. (1998) 'Death Receptors: Signaling and Modulation', *Science*, 281(1305-1308).

Ayyadevara, S., Engle, M. R., Singh, S. P., Dandapat, A., Lichti, C. F., Benes, H., Shmookler-Reis, R. J., Liebau, E. and Zimniak, P. (2005) 'Lifespan and stress resistance of Caenorhabditis elegans are increased by expression of glutathione transferases capable of metabolizing the lipid peroxidation product 4-hydroxynonenal', *Aging Cell*, 4, pp. 257-271.

Babier, B. M. (1978) 'Oxygen-dependent microbial killing by phagocytes', *The New England Journal of Medicine*, 298, pp. 659-668.

Back, P., Braeckman, B. P. and Matthijssen, F. (2012) 'ROS in aging Caenorhabditis elegans: Damage or signaling', *Oxidative Medicine and Cellular Longevity*.

Barry, M. and Bleackley, R. C. (2002) 'Cytotoxic T Lymphocytes: All Roads Lead to Death', *Nature Reviews Immunology*, 2, pp. 401-409.

Beer, C., Foldbjerg, R., Hayashi, Y., Sutherland, D. S. and Autrup, H. (2012) 'Toxicity of silver nanoparticles-Nanoparticle or silver ion?', *Toxicology Letters*, 208, pp. 286-292.

Bolak, Y. and Danumah, C. (2014) 'Analysis of cellulose nanocrystal rod lengths by dynmic light scattering and electron microscopy', *Journal of Nanoparticle Research*, 16(2174), pp. 1-4.

Bondarenko, O., Juganson, K., Ivask, A., Kasemets, K., Mortimer, M. and Kahru, A. (2013) 'Toxicity of Ag, CuO, and ZnO Nanoparticles to Selected Environmentally Relevant Test Organisms and Mammalian Cells *in vitro*: a Critical Review', *Archives of Toxicology*, 87, pp. 1181-1200.

Bootz, A., Vogel, V., Schubert, D. and Kreuter, J. (2004) 'Comparison of scanning electron microscopy, dynamic light scattering and analytical ultracentrifugation for the sizing of poly(butyl cyanoacrylate) nanoparticles', *European Journal of Pharmaceutics and Biopharmaceutics*, 57, pp. 369-375.

Borkow, G. and Gabbay, J. (2004) 'Putting Copper into Action: Copper-Impregnated Products with Potent Biocidal Activities', *The FASEB Journal*, 18(14), pp. 1728-1730.

Borkow, G., Gabbay, J., Dardik, R., Eidelman, A. I., Lavie, Y., Grunfeld, Y., Ikher, S., Huszar, M., Zatcoff, R. C. and Marikovsky, M. (2010a) 'Molecular Mechanisms of Enhanced Wound Healing by Copperoxide Impregnated Dressings', *Wound Repair and Regeneration*, 18(2), pp. 266-275.

Borkow, G., Zatcoff, R. C. and Gabbay, J. (2009) 'Reducing the Risk of Skin Pathologies in Diabetics by Using Copper Impregnated Socks', *Medical Hypotheses*, 73(6), pp. 883-886.

Borkow, G., Zhou, S. S., Page, T. and Gabbay, J. (2010b) 'A Novel Anti-influenza Copper Oxide Containing Respiratory Face Mask', *PLoS ONE*, 5(6), p. e11295.

Bossy-Wetzel, E., Bakiri, L. and Yaniv, M. (1997) 'Induction of apoptosis by the transcription factor c-Jun', *The EMBO Journal*, 16, pp. 1695-1709.

Bouillet, T. A. and Strasser, A. (2002) 'BH3-only Proteins-Evolutionarily Conserved Proapoptotic Bcl-2 Family Members Essential for Initiating Programmed Cell Death', *Journal of Cell Science*, 115, pp. 1567-1574.

Bourdon, J. A., Williams, A., Kuo, B., Moffat, I., White, P. A., Halappanavar, S., Vogel, U., Wallin, H. and Yauk, C. L. (2013) 'Gene expression profiling to identify potentially relevant disease outcomes and support human health risk assessment for carbon black nanoparticle exposure', *Toxicology*, 303, pp. 83-93.

Braydich-Stolle, L., Hussain, S. M., Schlager, J. and Holfmann, M. C. (2005) '*In vitro* Cytotoxicity of Nanoparticles in Mammalian Germline Stem Cells', *Toxicological Sciences*, 88, pp. 412-419.

Braydich-Stolle, L. K., Lucas, B., Schrand, A., Murdock, R. C., Lee, T., Schlager, J. J., Hussain, S. M. and Hofmann, M. C. (2010) 'Silver nanoparticles disrupt GDNF/Fyn kinase signalling in spermatogonial stem cells', *Toxicological Sciences*, 116, pp. 577-589.

Brown, R. J. C. and Gilham, R. J. J. (2010) *AMC Technical Brief: Nanoparticle characterisation*.

Brown, T. A. (2002) 'Genome, transcriptomes, and proteomes', in *Genomes*. 2 edn. UK: Garland Science, pp. 3-25. 1.

Brunner, T., Wasem, C., Torgler, R., Cima, I., Jakob, S. and Corazza, N. (2003) 'Fas (CD95/Apo-1) Ligand Recognition in T Cell Homeostasis, Cell-mediated Cytotoxicity and Immune Pathology', *Seminars in Immunology*, 15, pp. 167-176.

Budd, C. D. (2008) *Toxicology studies in Carnorhabditis elegans*. MSc thesis. University of Nottingham.

Burke, B. (2001) 'Lamins and apoptosis: a two-way street', *Cell Biology*, 153(3), pp. F5-F7.

Bystrzejewska-Piotrowska, G., Golimowski, J. and Urban, P. L. (2009) 'Nanoparticles: Their Potential Toxicity , Waste and Environmental Management', *Waste Management*, 29(9), pp. 2587-2595.

Cai, J., Yang, J. and Jones, D. P. (1998) 'Mitochondrial control of apoptosis: the role of cytochrome c', *Biochimica et Biophysica Acta*, 1366, pp. 139-149.

Calafato, S., Swain, S., Hughes, S., Kille, P. and Stürzenbaum, S. R. (2008) 'Knock down of Caenorhabditis elegans cutc-1 exacerbates the sensitivity toward high levels of copper', *Toxicological Sciences*, 106(2), pp. 384-391.

Carlson, C., Hussain, S. M., Schrand, A., Braydich-Stolle, L., Hess, K. L., Jones, R. L. and Schlager, J. (2008) 'Unique Cellular Interaction of Silver Nanoparticles: Size-dependent Generation of Reactive Oxygen Species', *Journal of Physical Chemistry B*, 112, pp. 13608-13619.

Carnes, L. C. and Klabunde, K. J. (2003) 'The Catalytic Methanol Synthesis over Nanoparticles Metal Oxide Catalysts', *Journal of Molecular Catalysis A: Chemical*, 194(1-2), pp. 227-236.

Castranova, V. (2011) 'Overview of current toxicological knowledge of engineered nanoparticles', *Journal of Occupational and Environmental Medicine*, 53(6), pp. S14-S17.

Cauerhff, A., Martinez, Y. N., Islan, G. A. and Castro, G. R. (2014) 'Nanostability', in Durán, N., Guterres, S. S. and Alves, O. L. (eds.) *Nanotoxicology: materials, methodologies, and assessments*. USA: Springer Science and Business, pp. 57-96.

CEC (1996) *CEC (Commission of the European Communities) Technical Guidance Document in Support of Commission Directive 93/67/EEC on Risk Assessment for New Notified Substances. PartII, Environmental Risk Assessment*. Luxembourg.

Cerkez, I., Kocer, H. B., Worley, S. D., Broughton, R. M. and Huang, T. S. (2012) 'Multifunctional Cotton Fabric: Antimicrobial and Durable Press', *Journal of Applied Polymer Sciences*, 124(5), pp. 4230-4238.

Cha, Y. J., Lee, J. and Choi, S. S. (2012) 'Apoptosis-Mediated in vivo Toxicity of Hydroxylated Fullerene Nanoparticles in Soil Nematode *Caenorhabditis elegans*', *Chemosphere*, 87, pp. 49-54.

Chang, Y.-N., Zhang, M., Xia, L., Zhang, J. and Xing, G. (2012) 'The toxic effects and mechanisms of CuO and ZnO nanoparticles', *Materials*, 5, pp. 2850-2871.

Chen, N., Harris, T. W., Antoshechkin, I., Bastiani, C., Bieri, T., Blasier, D., Bradnam, K., Canaran, P., Chan, J., Chen, C. K., Chen, W. J., Cunnigham, F., CDavis, P., Kenny, E., Kishore, R., Lawson, D., Lee, R., Muller, H. M., Nakamura, C., Pai, S., Ozersky, P., Petcherski, A., Rogers, A., Sabo, A., Schwartz, E. M., Van Auken, K., Wang, Q., Durbin, R., Spieth, J., Sternberg, P. W. and Stein, L. D. (2005) 'Wormbase: a comprehensive data resource for Caenorhabditis biology and genomics', *Nucleic acids Research*, 33, pp. D383-D389.

Chen, X. and Schluesener, H. (2008) 'Nanosilver: A Nanoproduct in Medical Application', *Toxicology Letters*, 176, pp. 1-12.

Chernousova, S. and Epple, M. (2013) 'Silver as Antibacterial Agent: Ion, Nanoparticles, Metal', *Angewandte Chemie*.

Chicheportiche, Y., Bourdon, P. R., Xu, H., Hsu, Y. M., Scott, H., Hession, C., Garcia, I. and Browning, J. L. (1997) 'TWEAK, A New Secreted Ligand in the Tumor Necrosis Factor Family that Weakly Induces Apoptosis', *the Journal of Biological Chemistry*, 272, pp. 32401-32410.

Chinnaiyan, A. M. (1999) 'The apoptosome: heart and soul of the cell death machine', *Neoplasia*, 1, pp. 5-15.

Choi, O. and Hu, Z. (2008) 'Size Dependent and Reactive Oxygen Species Related Nanosilver Toxicity to Nitrifying Bacteria', *Environmental Sciences and Technology*, 42, pp. 4583-4588.

Claiborne, A. (1985) 'Catalase activity', in Greenwald, R. A. (ed.) *Handbook of methods for oxygen radical research*. Florida, USA: Boca Raton, pp. 283-284.

Cohen, G. M. (1997) 'Caspases: the Executioners of Apoptosis', *Biochemical Journal*, 326, pp. 1-16.

Connolly, M., Fernandez-Cruz, M., Quesada-Garcia, A., Alte, L., Segner, H. and Navas, J. M. (2015) 'Comparative cytotoxicity study of silver nanoparticles (AgNPs) in a variety of rainbow trout cell lines (RTL-W1, RTH-149, RTG-2) and primary hepatocytes', *International Journal of Environmental Research and Public Health*, 12, pp. 5386-5405.

Conradt, B. (2013) 'Programmed Cell Death', [Video Lecture], 9 February 2013.

Conradt, B. and Horvitz, H. R. (1998) 'The *C. elegans* Protein EGL-1 is Required for Programmed Cell Death and Interacts with the Bcl-2-like Protein CED-9', *Cell*, 93, pp. 519-529.

Conradt, B. and Xue, D. (2005) 'Programmed Cell Death', in Community, T. *C. E.* R. (ed.) *Wormbook*.

consortium, T. C. e. g. s. (1998) 'Genome sequence of the nematode C. elegans: a platform for investigating biology', *Science*, 282, pp. 2012-2018.

Corsi, A. K., Wightman, B. and Chalfie, M. (2015) 'A transparent window into biology: A primer on Caenorhabditis elegans', in Community, T. *C. E.* R. (ed.) *Wormbook*.

Cozzari, M., Elia, A. C., Pacini, N., Smith, B. D., Boyle, D., Rainbow, P. S. and Khan, F. R. (2015) 'Bioaccumulation and oxidative stress responses measured in the estuarine

ragworm (Nereis diversicolor) exposed to dissolved nano- and bulk-sized silver', *Environmental Pollution*, 198, pp. 32-40.

Crane, M. and Handy, R. D. (2007) *An assessment of regulatory testing strategies and methods for characterizing the ecotoxicological hazards of nanomaterials*. London, UK. [Online]. Available at: http://randd.defra.gov.uk/Document.aspx?DocumentID=2270.

Datta, S. R., Brunet, A. and Greenberg, M. E. (1991) 'Cellular survival: a play in three Akts', *Genes and Development*, 13, pp. 2905-2927.

De Laurenzi, V. and Melino, G. (2000) 'Apoptosis. The Little Devil of Death', *Nature*, 406(135-136).

De Matteis, V., Malvindi, M. A., Galeone, A., Brunetti, V., De Luca, E., Kote, S., Kshirsagar, P., Sabella, S., Bardi, G. and Pompa, P. P. (2015) 'Negligible particle-specific toxicity mechanism of silver nanoparticles: the role of Ag+ ion release in the cytosol', *Nanomedicine: Nanotechnology, Biology, and Medicine*, 11, pp. 731-739.

Del Maestro, R. and McDonald, W. (1987) 'Distribution of superoxide dismutase, glutathione peroxidase and catalase in developing rat brain', *Mechanisms of Ageing and Development*, 41(1-2), pp. 29-38.

Dhawan, R., Dusenbery, D. B. and Williams, P. L. (1999) 'Comparison of Lethality, Reproduction, and Behavior as Toxicological Endpoints in the Nematode *Caenorhabditis elegans*', *Journal of Toxicology and Environmental Health*, 58(Part A), pp. 451-462.

Dibrov, P., Dzioba, J., Gosink, K. and Hase, C. (2002) 'Chemiosmotic mechanism of antimicrobial activity of Ag^{+} in *Vibrio cholerae*', *Antimicrobial Agents and Chemotherapy*, 46, pp. 2668-2670.

Donaldson, K., Stone, V., Clouter, A., Renwick, L. and MacNee, W. (2001) 'Ultrafine particles', *Occupational and Environmental Medicine*, 58(3), pp. 211-216.

Donaldson, K. and Tran, C. L. (2002) 'Inflammation caused by particles and fibers', *Inhalation Toxicology*, 14(1), pp. 5-27.

Donkin, S. G. and Williams, P. L. (1995) 'Influence of developmental stage, salts and food presence on various end points using *Caenorhabditis elegans* for aquatic toxicity testing', *Environmental Toxicology and Chemistry*, 14(12), pp. 2139-2147.

Doonan, R., McElwee, J. J., Matthijssen, F., Walker, G. A., Houthoofd, K., Back, P., Matscheski, A., Vanfleteren, J. R. and Gems, D. (2008) 'Against the oxidative damage

theory of aging: superoxide dismutases protect against oxidative stress but have little or no effect on life span in Caenorhabditis elegans', *Genes and Development*, 22, pp. 3236-3241.

Du, C., Fang, M., Li, Y., Li, L. and Wang, X. (2000) 'Smac, a Mitochondrial Protein that Promotes Cytochrome C-dependent Caspase Activation by Eliminating IAP Inhibition', *Cell*, 102, pp. 33-42.

Dubas, S. T. and Pimpan, V. (2008) 'Humic acid assisted synthesis of silver naniparticles and its application to herbicide detection', *Materials Letters*, 62, pp. 2661-2663.

Ebrahimnia-Bajestan, E., Niazmand, H., Duangthongsuk, W. and Wongwises, S. (2011) 'Numerical Investigation of Effective Parameters in Convective Heat Transfer of Nanofluids Flowing under a Laminar Flow Regime', *International of Heat and Mass Transfer*, 54(19-20), pp. 4376-4388.

Elechiguerra, J., Burt, J., Morones, J., Camacho-Bragado, A., Gao, X., Lara, H. and Yacaman, M. (2005) 'Interaction of silver nanoparticles with HIV-1', *Journal of Nanobiotechnology*, 3, p. 6.

Ellegaard-Jensen, L., Jensen, K. A. and Johansen, A. (2012) 'Nano-Silver Induces Dose-Response Effects on the Nematode *Caenorhabditis elegans*', *Ecotoxicology and Environmental Safety*, 80, pp. 216-223.

Elmore, S. (2007) 'Apoptosis: A Review of Programmed Cell Death', *Toxicologic Pathology*, 34, pp. 495-516.

Enari, M., Sakahira, H., Yokoyama, H., Okawa, K., Iwamatsu, A. and Nagata, S. (1998) 'A Caspase-activated DNase that Degrades DNA during Apoptosis, and Its Inhibitor ICAD', *Nature*, 391(6662), pp. 43-50.

Eom, H.-J., Roca, C. P., Roh, J.-Y., Chatterjee, N., Jeong, J.-S., Shim, I., Kim, H.-M., Kim, P.-J., Choi, K., Giralt, F. and Choi, J. (2015) 'A systems toxicology approach on the mechanism of uptake and toxicity of MWCNT in *Caenorhabditis elegans*', *Chemico-biological Interactions*, 239, pp. 153-163.

Eom, H. and Choi, J. (2010) 'p38 MAPK activation, DNA damage, cell cycle arrest and apoptosis as mechanisms of toxicity of silver nanoparticles in Jurkat T cells', *Environmental Sciences and Technology*, 44(21), pp. 8337-8342.

EPA (2007) *Nanotechnology white paper*. Washington, DC. [Online]. Available at: http://es.epa.gov/ncer/nano/publications/whitepaper12022005.pdf.

Fabrega, J., Luoma, S. N., Tyler, C. R., Galloway, T. S. and Lead, J. R. (2011) 'Silver nanoparticles: Behaviour and effects in the aquatic environment', *Environment International*, 37, pp. 517-531.

Fahmy, B. and Cormier, S. A. (2009) 'Copper oxide nanoparticles induce oxidative stress and cytotoxicity in airway epithelial cells', *Toxicology in Vitro*, 23, pp. 1365-1371.

Fan, Z., Beresford, P. J., Oh, D. Y., Zhang, D. and Lieberman, J. (2003) 'Tumor Suppressor NM23-H1 is a Granzyme A-activated DNase during CTL-mediated Apoptosis, and the Nucleosome Assembly Protein SET is Its Inhibitor', *Cell*, 112, pp. 659-672.

Farkas, J., Christian, P., Gallego-Urrea, J. A., Roos, N., Hassellöv, M., Tollefsen, K. E. and Thomas, K. V. (2011) 'Uptake and effects of manufactured silver nanoparticles in rainbow trout (Oncorhynchus mykiss) gill cells', *Aquatic Toxicology*, 101, pp. 117-125.

Fent, K. (2010) 'Ecotoxicology of Engineered Nanoparticles', in Frimmel, F. H. and Nießner, R. (eds.) *Nanoparticles in the Water Cycle*. Berlin Heidelberg: Springer-Verlag, pp. 183-205. 11.

Finkel, T. and Holbrook, N. J. (2000) 'Oxidants, oxidative stress and the biology of ageing', *Nature*, 408, pp. 239-247.

Foldbjerg, R., Dang, D. A. and Autrup, H. (2011) 'Cytotoxicity and genotoxicity of silver nanoparticles in the human lung cancer cells, A549', *Archives of Toxicology*, 85, pp. 743-750.

Fujii, M., Ishii, N., Joguchi, A., Yasuda, K. and Ayusawa, D. (1998) 'A novel superoxide dismutase gene encoding membrane-bound and extracellular isoforms by alternative splicing in Caenorhabditis elegans', *DNA Research*, 5, pp. 25-30.

Gabbay, J., Mishal, J., Magen, E., Zatcoff, R. C., Shemar-Avni, Y. and Borkow, G. (2006) 'Copper Oxide Impregnated Textiles with Potent Biocidal Activities', *Journal of Industrial Textiles*, 35, pp. 323-335.

Gao, J., Powers, K., Wang, Y., Zhou, H., Roberts, S. M., Moudgil, B. M., Koopman, B. and Barber, D. S. (2012) 'Influence of Suwannee River humic acid on particle properties and toxicity of silver nanoparticles', *Chemosphere*, 89, pp. 96-101.

Garay, M., Gaarde, W., Monia, B. P., Nero, P. and Cioffi, C. L. (2000) 'Inhibition of hypoxia/reoxygenation-induced apoptosis by an antisense oligonucleotide targeted to JNK1 in human kidney cells', *Biochemical Pharmacology*, 59, pp. 1033-1043.

Garcia-Reyero, N., Kennedy, A. J., Escalon, B. L., Habib, T., Laird, J. G., Rawat, A., Wiseman, S., Hecker, M., Denslow, N., Steevens, J. A. and Perkins, E. J. (2014) 'Differential effects and potential adverse outcomes of ionic silver and silver nanoparticles in vivo and in vitro', *Environmental Sciences and Technology*, 48, pp. 4546-4555.

Garrido, C., Galluzzi, L., Brunet, M., Puig, P. E., Didelot, C. and Kroemer, G. (2006) 'Mechanisms of cytochrome c release from mitochondria', *Cell Death and Differentiation*, 13, pp. 1423-1433.

Garrington, T. P. and Johnson, G. L. (1999) 'Organization and regulation of mitogen-activated protein kinase signaling pathways', *Cell Biology*, 11, pp. 211-218.

Gartner, A., A.J., M. and AVilleneuve, A. M. (2004) 'Methods for analysing checkpoint responses in Caenorhabditis elegans', in Schönthal, A. H. (ed.) *Methods in molecular biology*. New Jersey, USA: Humana Press Inc., pp. 257-274. 12.

Gewies, A. (2003) 'Introduction to apoptosis', *ApoReview*, pp. 1-26. (Accessed: 20 Dec 2015).

Ghabbour, E. A., Davies, G., Kretzschmar, R. and Chirstl, I. (2001) 'Proton and metal cation binding to humic substances in relation to chemical composition and molecule size', in Ghabbour, E. A. and Davies, G. (eds.) *Humic substances: Structure, models and functions*. London, UK: RSC publishing, pp. 153-164.

Giglio, M. P., Hunter, T., Bannister, J. V., Bannister, W. H. and Hunter, G. J. (1994) 'The manganese superoxide dismutase gene of Caenorhabditis elegans', *Biochemistry and Molecular Biology International*, 33, pp. 37-40.

Gomes, T., Pereira, C. G., Cardoso, C., Pinheiro, J. P., Cancio, I. and Bebianno, M. J. (2012) 'Accumulation and toxicity of copper oxide nanoparticles in the digestive gland of *Mytilus galloprovincialis*', *Aquatic Toxicology*, 15, pp. 118-119.

Gopalakrishna, R. and Jaken, S. (2000) 'Protein kinase C signaling and oxidative stress', *Free Radical Biology and Medicine*, 28, pp. 1349-1361.

Green, D. R. (2000) 'Apoptotic Pathways: Paper Wraps Stone Blunts Scissors', *Cell*, 102, pp. 1-4.

Grimm, L. M., Goldberg, A. L., Poirer, G. G., Schwartz, L. M. and Osborne, B. A. (1996) 'Proteosomes Play an Essential Role in Thymocyte Apoptosis', *EMBO Journal*, 15, pp. 3835-3844.

Guo, Z., Ng, W., Yee, G. L. and Hahn, H. T. (2009) 'Differential Scanning Calorimetry Investigation on Vinyl Ester Resin Curing Process for Polymer Nanocomposite Fabrication', *Journal of Nanoscience and Nanotechnology*, 9(5), pp. 3278-3285.

Gurabi, M. A. A., Ali, D., Alkahtani, S. and Alarifi, S. (2015) 'In vivo DNA damaging and apoptotic potential of silver nanoparticles in Swiss albino mice', *OncoTargets and Therapy*, 8, pp. 295-302.

Hancock, J. T., Desikan, R. and Neill, S. J. (2001) 'Role of reactive oxygen species in cell signalling pathways', *Biochemical Society Transactions*, 29, pp. 345-350.

Handy, R. D., von der Kammer, F., Lead, J. R., Hassellöv, M., Owen, R. and Crane, M. (2008) 'The Ecotoxicology and Chemistry of Manufactured Nanoparticles', *Ecotoxicology*, 17(4), pp. 287-314.

Hassellöv, M., Readman, J. W., Ranville, J. F. and Tiede, K. (2008) 'Nanoparticle analysis and characterisation methodologies in environmental risk assessment of engineered nanoparticles', *Ecotoxicology*, 17, pp. 344-361.

Hengartner, M. O. and Horvitz, H. R. (1994) '*C. elegans* Cell Survival Gene *ced-9* Encodes a Functional Homolog of the Mammalian Proto-oncogene *bcl-2*', *Cell*, 76, pp. 665-676.

Hill, M. M., Adrain, C., Duriez, P. J., Creagh, E. M. and Martin, S. J. (2004) 'Analysis of the composition, assembly kinetics and activity of native Apaf-1 apoptosome', *EMBO Journal*, 23, pp. 2134-2145.

Hillier, L. W., Coulson, A., Murray, J. I., Bao, Z., Sulston, J. E. and Waterston, R. H. (2005) 'Genomics in C. elegans: so many genes, such a little worm', *Genome Research*, 15, pp. 1651-1660.

Holt, K. and Bard, A. (2005) 'Interaction of silver(I) ions with the respiratory chain of *Escherichia coli*: and electrochemical and scanning electrochemical microscopy study of the anitimicrobial mechanism of micromolar Ag', *44*, (13214-13223).

Honda, Y. and Honda, S. (2002) 'Oxidative Stress and Life Span Determination in the Nematode *Caenorhabditis elegans*', *Annals New York Academy of Sciences*, 959, pp. 466-474.

Hsin, Y., Chena, C., Huang, S., Shih, T., Lai, P. and Chueh, P. (2008) 'The Apoptotic Effect of Nanosilver is Mediated by a ROS- and JNK-dependent Mechanism Involving the Mitochondrial Pathway in NIH3T3 Cells', *Toxicology Letters*, 179, pp. 130-139.

Hsu, H., Xiong, J. and Goeddel, D. V. (1995) 'The TNF Receptor 1-associated Protein TRADD Signals Cell Death and NF-kappa B Activation', *Cell*, 81, pp. 495-504.

Hu, P. J. (2007) 'Dauer', in Community, T. *C. E.* R. (ed.) *Wormbook*.

Hunot, S. and Flavell, R. A. (2001) 'Apoptosis. Death of a Monopoly?', *Science*, 292, pp. 865-866.

Hunter, T., Bannister, W. H. and Hunter, G. J. (1997) 'Cloning, expression, and characterization of two manganese superoxide dismutases from Caenorhabditis elegans', *The Journal of Biological Chemistry*, 272, pp. 28652-28659.

Hussain, S. M., Hess, K. L., Gearhart, J. M., Geiss, K. T. and Schlager, J. (2005) '*In vitro* Toxicity of Nanoparticles in BRL-3A Rat Liver Cells', *Toxicology in Vitro*, 19, pp. 975-983.

Hussain, S. M., Javorina, A., Schrand, A., Duhart, H., Ali, S. and Schlager, J. (2006) 'The Interaction of Manganese Nanoparticles with PC-12 Cells Induces Dopamine Depletion', *The Journal of Toxicological Sciences*, 92, pp. 456-463.

Hwang, E., Lee, J., Chae, Y., Kim, Y., Kim, B., Sang, B. and Gu, M. (2008) 'Analysis of the Toxic Mode of Action of Silver Nanoparticles Using Stress-Specific Bioluminescent Bacteria', *Small*, 4, pp. 746-750.

Hydutsky, B. W., Mack, E. J., Beckerman, B. B., Skluzacek, J. M. and Mallouk, T. E. (2007) 'Optimization of Nano- and Microiron Transport through Sand Columns Using Polyelectrolyte Mixtures', *Environmental Sciences and Technology*, 41, pp. 6418-6424.

Igney, F. H. and Krammer, P. H. (2002) 'Death and Anti-death: Tumour Resistance to Apoptosis', *Nature Reviews Cancer*, 2, pp. 277-288.

Jacob, J. A. and Shanmugam, A. (2015) 'Silver nanoparticles provoke apoptosis of Dalton's ascites lymphoma in vivo by mitochondria dependent and independent pathways', *Colloids and Surfaces B: Biointerfaces*, 136, pp. 1011-1016.

Jendelová, P., Herynek, V., Urdzíková, L., Glogarová, K., Kroupová, J., Andersson, B., Bryja, V., Burian, M., Hájek, M. and Syková, E. (2004) 'Magnetic Resonance Tracking of Transplanted Bone Marrow and Embryonic Stem Cells Labeled by Iron Oxide Nanoparticles in Rat Brain and Spinal Cord', *Journal of Neuroscience Research*, 76, pp. 232-243.

Jensen, L. T. and Culotta, V. C. (2005) 'Activation of CuZn superoxide dismutases from Caenorhabditis elegans does not require the copper chaperone CCS', *The Journal of Biological Chemistry*, 280, pp. 41373-41379.

Jolly, C. and Morimoto, R. I. (2000) 'Role of the heat shock response and molecular chaperones in oncogenesis and cell death', *Journal of National Cancer Institute*, 92, pp. 1564-1572.

Jones, D. P. and Candido, E. P. M. (1999) 'Feeding is inhibited by sublethal concentrations of toxicants and by heat stress in the nematode Caenorhabditis elegans: Relationship to the cellular stress response', *Journal of Experimental Zoology*, 284, pp. 147-157.

Joza, N., Susin, S. A., Daugas, E., Stanford, W. L., Cho, S. K., Li, C. Y., Sasaki, T., Elia, A. J., Cheng, H. Y., Ravagnan, L., Ferri, K. F., Zamzami, N., Wakeham, A., Hakem, R., Yoshida, H., Kong, Y. Y., Mak, T. W., Zúñiga-Pflücker, J. C., Kroemer, G. and Penninger, J. M. (2001) 'Essential Role of the Mitochondrial Apoptosis-inducing Factor in Programmed Cell Death', *Nature*, 410(6828), pp. 549-554.

Ju-Nam, Y. and Lead, J. R. (2008) 'Manufactured Nanoparticles: An Overview of Their Chemistry, Interactions and Potential Environmental Implications', *Science of the Total Environment*, 400, pp. 396-414.

Kaletta, T. and Hengartner, M. O. (2006) 'Finding Function in Novel Targets: *C.elegans* as a Model Organism', *Nature Reviews Drug Discovery*, 5, pp. 387-398.

Kannan, K. and Jain, S. K. (2000) 'Oxidative stress and apoptosis', *Pathophysiology*, 7(27), pp. 153-163.

Karlsson, H. L., Cronholm, P., Gustafsson, J. and Möller, L. (2008) 'Copper oxide nanoparticles are highly toxic: A comparison between metal oxide nanoparticles and carbon nanotubes', *Chemical Research in Toxicology*, 21, pp. 1726-1732.

Kasemets, K., Suppi, S., Künnis, K. and Kahru, A. (2013) 'Toxicity of CuO Nanoparticles to Yeast *Saccharomyces cerevisiae* BY4741 Wild-type and Its Nine Isogenic Single-gene Deletion Mutants', *Chemical Research in Toxicology*, 26(3), pp. 356-367.

Kataoka, T., Schroter, M., Hahne, M., Schneider, P., Irmler, M., Thome, M., Froelich, C. J. and Tschopp, J. (1998) 'FLIP Prevents Apoptosis Induced by Death Receptora but not by Perforin/Granzyme B, Chemotherapeutic Drugs, and Gamma Irradiation', *The Journal of Immunology*, 161, pp. 3936-3942.

Kawata, K., Osama, M. and Okabe, S. (2009) 'In vitro toxicity of silver nnaoparticles at noncytotoxic doses to HepG2 human hepatoma cells', *Environmental Sciences and Technology*, 43, pp. 6046-6051.

Kedar, N. P. (2003) 'Can We Prevent Parkinson's and Alzheimer's Disease?', *Journal of Postgraduate Medicine*, 49, pp. 236-245.

Khanna, N., Cressman, C. P. r., Tatara, C. P. and P.L, W. (1997) 'Tolerance of the nematode Caenorhabditis elegans to pH, salinity, and hardness in aquatic media', *Archives of Environmental Contamination and Toxicology*, 32(1), pp. 110-114.

Khare, P., Sonane, M., Nagar, Y., Moin, N., Ali, S., Gupta, K. C. and Satish, A. (2015) 'Size dependent toxicity of zinc oxide nanoparticles in soil nematode *Caenorhabditis elegans*', *Nanotoxicology*, 9(4), pp. 423-432.

Khouri, S., Shams, M. and Tam, K. C. (2014) 'Determination and prediction of physical properties of cellulose nanocrystals from dynamic light scattering measurements', *Journal of Nanoparticle Research*, 16(2499), pp. 1-7.

Kim, E., Chu, Y. C., Han, J. Y., Lee, D. H., Kim, Y. J., Kim, H.-C., Lee, S. G., Lee, S. J., Jeong, S. W. and Kim, J. M. (2010) 'Proteomic analysis of silver nanoparticle toxicity in rats', *Toxicology and Environmental Health Sciences*, 2, pp. 251-262.

Kim, J. (2007) 'Antibacterial Activity of Ag+ Ion-Containing Silver Nanoparticles Prepared Using the Alcohol Reduction Method', *Journal of Industrial and Engineering Chemistry*, 13, pp. 718-722.

Kim, K., Sung, W., Moon, S., Choi, J., Kim, J. and Lee, D. (2008a) 'Antifungal Effect of Silver Nanoparticles on Dermatophytes', *Journal of Microbiology and Biotechnology*, 18, pp. 1482-1484.

Kim, S., Choi, J. E., Choi, J., Chung, K. H., Park, K., Yi, J. and Ryu, D. Y. (2009) 'Oxidative stress-dependent toxicity of silver nanoparticles in human hepatoma cells', *Toxicology in Vitro*, 23, pp. 1076-1084.

Kim, S. and Ryu, D. Y. (2013) 'Silver nanoparticle-induced oxidative stress, genotoxicity and apoptosis in cultured cells and animal tissues', *Journal of Applied Toxicology*, 33, pp. 78-89.

Kim, S. W., Nam, S. and An, Y. (2012) 'Interaction of Silver Nanoparticles with Biological Surfaces of *Caenorhabditis elegans*', *Ecotoxicology and Environmental Safety*, 77, pp. 64-70.

Kim, Y., Kim, J., Cho, H., Rha, D., Kim, J., Park, J., Choi, B., Lim, R., Chang, H., Chung, Y., Kwon, I., Jeong, J., Han, B. and Yu, I. (2008b) 'Twenty-eight-day Oral Toxicity, Genotoxicity, and Gender-related Tissue Distribution of Silver Nanoparticles in Sprague-Dawley Rats', *Inhalation Toxicology*, 20, pp. 575-583.

Kitschkel, F. C., Hellbardt, S., Behrmann, I., Germer, M., Pawlita, M., Krammer, P. H. and Peter, M. E. (1995) 'Cytotoxicity-dependent APO-1 (Fas/CD95)-associated Proteins from a Death-inducing Signaling Complex (DISC) with the Receptor', *EMBO Journal*, 14, pp. 5579-5588.

Klein, C. L., Comero, S., Stahlmecke, B., Romazanov, J., Kuhlbusch, T. A. J., Van Doren, E., P., D. T., Mast, J., Wick, P., Krug, H., Locoro, G., Hund-Rinke, K., Kördel, W., Friedrichs, S., Maier, G., Werner, J., Linsinger, T. and Gawlik, B. M. (2011) *NM-series of representative manufactured nanomaterials : NM-300 silver characterisation, stability, homogeneity*. Italy.

Knaapen, A. M., Borm, P. J. A., Albrecht, C. and Schins, R. P. F. (2004) 'Inhaled particles and lung cancer, part A: mechanisms', *International Journal of Cancer*, 109(6), pp. 799-809.

Koniakhin, S. V., Eliseev, I. E., Terterov, I. N., Shvidchenko, A. V., Eidelman, E. D. and Dubbina, M. V. (2015) 'Molecular dynamics-based refinement of nanodiamond size measurements obtained with dynamic light scattering', *Microfluid Nanofluid*, 15, pp. 1189-1194.

Kurata, S. (2000) 'Selective activation of p38 MAPK cascade and mitotic arrest caused by low level oxidative stress', *The Journal of Biological Chemistry*, 275, pp. 23413-13416.

Kvitek, L., Panacek, A., Soukupova, J., Kolar, M., Vecerova, R., Prucek, R., Holecova, M. and Zboril, R. (2008) 'Effect of surfactants and polymers on stability and antibacterial activity of silver nanoparticles (NPs)', *Journal of physical Chemistry C*, 112, pp. 5825-5834.

Landis, G. N. and Tower, J. (2005) 'Superoxide dismutase evolution and life span regulation', *Mechanisms of Ageing and Development*, 126, pp. 365-379.

Larsen, P. L. (1993) 'Aging and resistance to oxidative damage in Caenorhabditis elegans', *Proceedings of the National Academy of Sciences*, 90, pp. 8905-8909.

Lawen, A. (2003) 'Apoptosis-an Introduction', *BioEssays*, 25(9), pp. 888-896.

Le Pape, H., Solano-Serena, F., Contini, P., Devillers, C., Maftah, A. and Leprat, P. (2004) 'Involvement of reactive oxygen species in the bactericidal activity of activated carbon fibre supporting silver bactericidal activity of ACF(Ag) mediated by ROS', *Journal of Inorganic Biochemistry*, 98, pp. 1054-1060.

Lead, J. R. (2010) 'Manufactured Nanoparticles in the Environment', *Environmental Chemistry*, 7(1).

Leadley, D. (2010) *Transmission Electron Microscopy (TEM)*. Available at: http://www2.warwick.ac.uk/fac/sci/physics/current/postgraduate/regs/mpags/ex5/techniques/structural/tem/ (Accessed: 11 June 2015).

Ledin, A., Karlsson, S., Duker, A. and Allard, B. (1994) 'Measurements in situ of concentration and size distribution of colloidal matter in deep groundwaters by photon-correlation spectroscopy', *Water Research*, 28, pp. 1539-1545.

Lee, Y. H., Cheng, F. Y., Chiu, H. W., Tsai, J. H., Fang, C. Y., Chen, C. W. and Wang, Y. J. (2014) 'Cytotoxicity, oxidative stress, apoptosis and the autophagic effects of silver nanoparticles in mouse embryonic fibroblasts', *Biomaterials*, 35, pp. 4706-4715.

Leiers, B., Kampkötter, A., Grevelding, C. G., Link, C. D., Johnson, T. E. and Henkle-Dührsen, K. (2003) 'A stress-responsive glutathione-s-transferase confers resistance to oxidative stress in Caenorhabditis elegans', *Free Radical Biology and Medicine*, 34, pp. 1405-1415.

Lengauer, T. (2007) 'Introduction in bioinformatics from genomes to therapies', in *The building block: molecular sequences and structures*. Germany: Wiley-VCH, p. pp. 10. 1.

Leroy, P., Tournassat, C. and Bizi, M. (2011) 'Influence of surface conductivity on the apparent zeta potential of TiO2 nanoparticles', *Journal of Colloid and Interface Science*, 356(2), pp. 442-453.

Lesniak, W., Bielinska, A. U., Sun, K., Janczak, K. W., Shi, X., Baker, J. R. J. and Balogh, L. P. (2005) 'Silver/Dendrimer Nanocomposites as Biomarkers: Fabrication, Characterization, *in vitro* Toxicity, and Intracellular Detection', *Nano Letters*, 5, pp. 2123-2130.

Lettre, G. and Hengartner, M. O. (2006) 'Developmental Apoptosis in *C. elegans*: A Complex CEDnario', *Developmental Cell Biology*, 7, pp. 97-108.

Leung, M. C. K., Williams, P. L., Benedetto, A., Au, C., Helmcke, K. J., Aschner, M. and Meyer, J. N. (2008) '*Caenorhabditis elegans*: An Emerging Model in Biomedical and Environmental Toxicology', *Toxicological Sciences*, 106(1), pp. 5-28.

Levard, C., Hotze, E. M., Lowry, G. V. and Brown Jr., G. E. (2012) 'Environmental transformations of silver nanoparticles: Impact on stability and toxicity', *Environmental Sciences and Technology*, 46, pp. 6900-6914.

Lewis, J. A. and Fleming, J. T. (1995) 'Basic culture methods', in Epstein, H. F. and Shakes, D. C. (eds.) *Caenorhabditis elegans, modern biological analysis of an organism*. California: Academic press, pp. 4-27.

Li, L. Y., Luo, X. and Wang, X. (2001) 'Endonuclease G is an apoptotic DNase when released from mitochondria', *Nature*, 412, pp. 95-99.

Li, X. and Lenhart, J. J. (2012) 'Aggregation and dissolution of silver nanoparticles in natural surface water', *Environmental Sciences and Technology*, 46, pp. 5378-5386.

Li, Y., Liang, J., Tao, Z. and Chen, J. (2007) 'CuO Particles and Plates: Synthesis and Gas-Sensor Application', *Materials Research Bulletin*, 43, pp. 2380-2385.

Lim, D., Roh, J. Y., Eom, H. J., Choi, J. Y., Hyun, J. and Choi, J. (2012) 'Oxidative stress-related PMK-1 P38 MAPK activation as a mechanism for toxicity of silver nanoparticles to reproduction in the nematode Caenorhabditis elegans', *Environmental Toxicology and Chemistry*, 31, pp. 585-592.

Liu, J. and Hurt, R. H. (2010) 'Ion release kinetics and particle persistence in aqueous nano-silver colloids', *Environmental Sciences and Technology*, 44, pp. 2169-2175.

Liu, J., Sonshine, D. A., Shervani, S. and Hurt, R. H. (2010a) 'Controlled release of biologically active silver from nanosilver surfaces', *ACS Nano*, 4(11), pp. 6903-6913.

Liu, P., Guan, R., Ye, X., Jiang, J., Liu, M., Huang, G. and Chen, X. (2011) 'Toxicity of nano- and micro- sized silver particles in human hepatocyte cell line L02', *Journal of Physics: Conference Series*, 304, p. 012036.

Liu, W., Wu, Y., Wang, C., Li, H. C., Wang, T., Liao, C. Y., Cui, L., Zhou, Q. F., Yan, B. and Jiang, G. B. (2010b) 'Impact of silver nanoparticles on human cells: effect of particle size', *Nanotoxicology*, 4, pp. 319-330.

Locksley, R. M., Killeen, N. and Lenardo, M. J. (2001) 'The TNF and TNF Receptor Superfamilies: Integrating Mammalian Biology', *Cell*, 104, pp. 487-501.

Lok, C., Ho, C., Chen, R., He, Q., Yu, W., Sun, H., Tam, P., Chiu, J. and Che, C. (2006) 'Proteomic analysis of the mode of antibacterial action of silver nanoparticles', *Journal of Proteome Research*, 5, pp. 916-924.

López-Serrano, A., Olivas, R. M., Landaluze, J. S. and Cámara, C. (2014) 'Nanoparticles: a global vision. Characterization, separation, and quantification methods. Potential environmental and health impact', *Analytical Methods*, 6, pp. 38-56.

Lorenzen, A. and Kennedy, S. W. (1993) 'A fluorescence-based protein assay for use with a microplate reader', *Analytical and Bioanalytical Chemistry*, 214(1), pp. 346-348.

Lu, L., Sun, R., Chen, R., Hui, C., Ho, C., Luk, J., Lau, G. and Che, C. (2008) 'Silver nanoparticles inhibit hepatitis B virus replication', *Amtiviral Therapy*, 13, pp. 253-262.

Luo, Y., Umegaki, H., Wang, X., Abe, R. and Roth, G. S. (1998) 'Dopamine induces apoptosis through an oxidation-invovled SAPK/JNK activation pathway', *The Journal of Biological Chemistry*, 273, pp. 3756-3764.

Ma, H., Bertsch, P. M., Glenn, T. C., Kabengi, N. J. and Williams, P. L. (2009) 'Toxicity of Manufactured Zinc Oxide Nanoparticles in the Nematode *Caenorhabditis elegans*', *Environmental Toxicology and Chemistry*, 28(6), pp. 1324-1330.

Ma, J., Lu, X. and Huang, Y. (2011) 'Genomic analysis of cytotoxicity response to nanosilver in human dermal fibroblasts', *Journal of Biomedical Nanotechnology*, 7, pp. 263-275.

Malvern (2010) *Malvern Technical Note*. USA.

Manke, A., Wang, L. and Rojanasakul, Y. (2013) 'Mechanisms of nanoparticle-induced oxidative stress and toxicity', *BioMed Research International*, 942916.

Maojo, V., Fritts, M., Martin-Sanchez, F., Mitchell, J. A., Anguita, A., Baker, N., Barreiro, J. M., Benitez, S. E., De la Calle, G., Facelli, J. C., Ghazal, P., Geissbuhler, A., Gonzalez-Nilo, F., Graf, N., Grangeat, P., Hermosilla, I., Hussein, R., Kern, J., Koch, S., Legre, Y., Lopez-Alonso, V., Lopez-Campos, G., Milanesi, V., Munteanu, C., Otero, P., Pazos, A., Perez-Rey, D., Potamias, G., Sanz, F. and Kulikowski, C. (2012) 'Nanoinformatics: developing new computing applications for nanomedicine', *Computing in Science and Engineering*, 94(6), pp. 521-539.

Marambio-Jones, C. and Hoek, E. M. V. (2010) 'A Review of the Antibacterial Effects of Silver Nanomaterials and Potential Implications for Human Health and the Environment', *Journal of Nanoparticle Research*, 12, pp. 1531-1551.

Martindale, J. L. and Holbrook, N. J. (2002) 'Cellular response to oxidative stress: Signaling for suicide and survival', *Journal of Cellular Physiology*, 192, pp. 1-15.

Martinvalet, D., Zhu, P. and Lieberman, J. (2005) 'Granzyme A Induces Caspase-independent Mitochondrial Damage, a Required First Step for Apoptosis', *Immunity*, 22, pp. 355-370.

Maurer, L. L., Yang, X., Schindler, A. J., Taggart, R. K., Jiang, C., Hsu-Kim, H., Sherwood, D. R. and Meyer, J. N. (2015) 'Intracellular trafficking pathways in silver nanoparticle uptake and toxicity in *Caenorhabditis elegans*', *Nanotoxicology*, pp. 1-5.

Maynard, A. D., Aitken, R. J., Butz, T., Colvin, V., Donaldson, K., Oberdörster, G., Philbert, M. A., Ryan, J., Seaton, A., Stone, V., Tinkle, S. S., Tran, L. and Walker, N. J. W., D.B. (2006) 'Safe handling of nanotechnology', *Nature*, 444, pp. 267-269.

Merrihew, G. E., Davis, C., Ewing, B., Williams, G., Käll, L., Frewen, B. E., Noble, W. S., Green, P., Thomas, J. H. and MacCoss, M. J. (2008) 'Use of shotgun proteomics for the identification, confirmation, and correction of C. elegans gene annotation', *Genome Research*, 18(10), pp. 1660-1669.

Meyer, J. N., Lord, C. A., Yang, X. Y., Turner, E. A., Badireddy, A. R., Marinakos, S. M., Chilkoti, A., Wiesner, M. R. and Auffan, M. (2010) 'Intracellular Uptake and Associated Toxicity of Silver Nanoparticles in *Caenorhabditis elegans*', *Aquatic Toxicolology*, 100, pp. 140-150.

Midander, K., Cronholm, P., Karlsson, H. L., Elihn, K., Möller, L., Leygraf, C. and Wallinder, I. O. (2009) 'Surface characteristics, copper release, and toxicity of nano- and micrometer-sized copper and copper(II) oxide particles: a cross-disciplinary study', *Small*, 5(3), pp. 389-399.

Middendorf, P. L. and Dusenbery, D. B. (1993) 'Fluoroacetic acid is a potent and specific inhibitor of reproduction in the nematode Caenorhabditis elegans', *Journal of Nematology*, 25, pp. 573-577.

Misra, S. K., Nuseibeh, S., Dybowska, A., Berhanu, D., Tetley, T. D. and Valsami-Jones, E. (2014) 'Comparative study using spheres, rods and spindle-shaped nanoplatelets on dispersion stability, dissolution and toxicity of CuO nanomaterials', *Nanotoxicology*, 8(4), p. 422.

Mortimer, M., Kasemets, K. and Kahru, A. (2010) 'Toxicity of ZnO and CuO nanoparticles to ciliated protozoa *Tetrahymena thermophila*', *Toxicology*, 269, pp. 182-189.

Mutwakil, M. H. A. Z., Steele, T. J. G., Lowe, K. C. and de Pomerai, D. I. (1997) 'Surfactant stimulation of growth in the nematode Caenorhabditis elegans', *Enzyme and Microbial Technology*, 20, pp. 462-470.

Naiim, M., Boualem, A., Ferre, C., Jabloun, M., Jalocha, A. and Ravier, P. (2015) 'Multiangle dynamic light scattering for the improvement of multimodal particle size distribution measurements', *Soft Matter*, 11, pp. 28-32.

Nair, L. S. and Laurencin, C. T. (2007) 'Silver Nanoparticles: Synthesis and Therapeutic Applications', *Journal of Biomedical Nanotechnology*, 3, pp. 301-316.

NanoComposix.com (n.d.) *Schematic of the electrical double later at the surface of solution-phase nanoparticles*. Available at:

http://nanocomposix.com/pages/characterization-techniques#zeta-potential (Accessed: 5 Feb 2015).

Navarro, E., Piccapietra, F., Wagner, B., Marconi, F., Kaegi, R., Odzak, N., Sigg, L. and Behra, R. (2008) 'Toxicity of silver nanoparticles to Chlamydonas reinhardtii', *Environmental Sciences and Technology*, 42, pp. 8959-8964.

Neher, D. A. (2001) 'Role of Nematodes in Soil Health and Their Use as Indicators', *Journal of Nematology*, 33(4), pp. 161-168.

Nel, A., Xia, T. and Li, N. (2006) 'Toxic Potential of Materials at the Nanolevel', *Science*, 311, pp. 622-627.

Nishanth, R. P., Jyotsna, R. G., Schlager, J. J., Hussain, S. M. and Reddanna, P. (2011) 'Inflammatory responses of RAW 264.7 macrophages upon exposure to nanoparticles: Role of ROS-NFKB signaling pathway', *Nanotoxicology*, 5, pp. 502-516.

Nowack, B. and Bucheli, T. (2007) 'Occurrence, Behavior, and Effects of Nanoparticles in the Environment', *Environmental Pollution*, 150, pp. 5-22.

Nowack, B., Krug, H. F. and Height, M. (2011) '120 Years of Nanosilver History: Implications for Policy Makers', *Environmental Sciences and Technology*, 45(4), pp. 1177-1183.

Oberdörster, E. (2004) 'Manufactured Nanomaterials (Fullerenes, C60) Induce Oxidative Stress in the Brain of Juvenile Largemouth Bass', *Environmental Health Perspectives*, 112(10), pp. 1058-1062.

Oberdörster, G., Maynard, A., Donaldson, K., Castranova, V., Fitzpatrick, J., Ausman, K., Carter, J., Karn, B., Kreyling, W., Lai, D., Olin, S., Monteiro-Riviere, N., Warheit, D., Yang, H. and Group, I. R. F. R. S. I. N. T. S. W. (2005) 'Principles for characterizing the potential human health effects from exposure to nanomaterials: elements of a screening strategy', *Particle and Fibre Toxicology*, 2, p. 8.

Oleinick, N. L., Morris, R. L. and Belichenko, I. (2002) 'The Role of Apoptosis in Response to Photodynamic Therapy: What, Where, Why, and How', *Photochemical and Photobiological Sciences*, 1, pp. 1-21.

Ott, M., Gogvadze, V., Orrenius, S. and Zhivotovsky, B. (2007) 'Mitochondria, oxidative stress and cell death', *Apoptosis*, 12, pp. 913-922.

Parish, J. Z. and Xue, D. (2003) 'Functional Genomic Analysis of Apoptotic DNA Degradation in *C. elegans*', *Molecular Cell*, 11, pp. 987-996.

Pei, B., Wang, S., Guo, X., Wang, J., Yang, G., Hang, H. and Wu, L. (2008) 'Arsenite-induced germline apoptosis through a MAPK-dependent p53-independent pathway in Caenorhabditis elegans', *Chemical Research in Toxicology*, 21, pp. 1530-1535.

Peretyazhko, T. S., Zhang, Q. and Colvin, V. L. (2014) 'Size-controlled dissolution of silver nanoparticles at neutral and acidic pH conditions: kinetics and size changes', *Environmental Sciences and Technology*, 48, pp. 11954-11961.

Perreault, F., Melegari, S. P., Costa, C. H., Rossetto, A.-F., Popovic, R. and Gerson-Matias, W. (2012) 'Genotoxic effects of copper oxide nanoparticles in Neuro 2A cell cultures', *The Science of the Total Environment*, 441, pp. 117-124.

Peter, M. E. and Krammer, P. H. (1998) 'Mechanisms of CD95 (APO-1/Fas) Mediated Apoptosis', *Current Opinion in Immunology*, 10, pp. 545-551.

Piao, M. J., Kang, L. A., I.K., L., Kim, H. S., Kim, S., Choi, J. Y., Choi, J. and Hyun, J. W. (2011) 'Silver nanoparticles induce oxidative damage in human liver cells through inhibition of reduced glutathione and induction of mitochondria-involved apoptosis', *Toxicology Letters*, 201, pp. 92-100.

Piccinno, F., Gottschalk, F., Seeger, S. and Nowack, B. (2012) 'Industrial Production Quantities and Uses of Ten Engineered Nanomaterials for Europe and the World', *Journal of Nanoparticle Research*, 14, pp. 1109-1120.

Pillai, S., Behra, R., Nestler, H., Suter, M., Sigg, L. and Schirmer, K. (2014) 'Linking toxicity and adaptive responses across the transcriptome, proteome, and phenotype of Chlamydonas reinhardtii exposed to silver', *Proceedings of the National Academy of Sciences of the United States of America*, 111, pp. 3490-3495.

Piret, J. P., Jacques, D., Audinot, J. N., Meija, J., Boilan, E., Noël, F., Fransolet, M., Demazy, C., Lucas, S., Saout, C. and Toussaint, O. (2012) 'Copper(II) oxide nanoparticles penetrate into HepG2 cells, exert cytotoxicity via oxidative stress and induce pro-inflammatory response', *Nanoscale*, 22, pp. 7168-7184.

Pirkkala, L., Nykanen, P. and Sistonen, L. (2001) 'Roles of the heat shock transcription factors in regulation of the heat shock response and beyond', *The FASEB Journal*, 15, pp. 1118-1131.

Pluskota, A., Horzowski, E. and von Mikecz, A. (2009) 'In *Caenorhabditis elegans* Nanoparticles-Bio-Interactions Become Transparent: Silica-Nanoparticles Induce Reproductive Senescence', *PLoS One*, 4, p. e6622.

Posgai, R., Cipolla-McCulloch, C. B., Murphy, K. R., Hussain, S. M., Rowe, J. J. and Nielsen, M. G. (2011) 'Differential toxicity of silver and titanium dioxide nanoparticles

on Drosophila melanogaster development, reproductive effort, and viability: Size, coatings and antioxidants matter', *Chemosphere*, 85, pp. 34-42.

Potapova, O., Basu, S., Mercola, D. and Holbrook, N. J. (2001) 'Protective role for c-Jun in the cellular response to DNA damage', *The Journal of Biological Chemistry*, 276, pp. 28546-28553.

Poynton, H. C., Lazorchak, J. M., Impellitteri, C. A., Blalock, B. J., Rogers, K., Allen, H. J., Loguinov, A., Heckman, J. L. and Govindasmawy, S. (2012) 'Toxicogenomic responses of nanotoxicity in Daphnia magna exposed to silver nitrate and coated silver nanoparticles', *Environmental Sciences and Technology*, 46, pp. 6288-6296.

Pradhan, A., Seena, S., Pascoal, C. and Cássio, F. (2012) 'Copper oxide nanoparticles can induce toxicity to the freshwater shredder *Allogamus ligonifer*', *Chemosphere*, 89(9), pp. 1142-1150.

Qiao, L., Hua, Z. S., Hua, Y. Y., Ping, W. L., Wen, G. S. and Fei, L. P. (2012) 'Toxicity of sodium fluoride to Caenorhabditis elegans', *Biomedical and Environmental Sciences*, 25(2), pp. 216-223.

Raffi, M., Hussain, F., Bhatti, T., Akhter, J., Hameed, A. and Hasan, M. (2008) 'Antibacterial Characterization of Silver Nanoparticles against *E. coli* ATCC-15224', *Journal of Materials Science and Technology*, 24, pp. 192-196.

Rai, N. K., Tripathi, K., Sharma, D. and Shukla, V. K. (2005) 'Apoptosis: a Basic Physiologic Process in Wound Healing', *The International Journal of Lower Extrmity Wounds*, 4, pp. 138-144.

Reddien, P. W. and Horvitz, H. R. (2000) 'CED-2/CrkII and CED-10/Rac Control Phagocytosis and Cell Migration in *Caenorhabditis elegans*', *Nature Cell Biology*, 2, pp. 131-136.

Rocheleau, S., Arbour, M., Elias, M., Sunahara, G. I. and Masson, L. (2015) 'Toxicogenomic effects of nano- and bulk-TiO2 particles in the soil nematode *Caenorhabditis elegans*', *Nanotoxicology*, 9(4), pp. 502-512.

Roh, J., Sim, S. J., Yi, J., Park, K., Chung, K. H., Ryu, D. and Choi, J. (2009) 'Ecotoxicity of Silver Nanoparticles on the Soil Nematode *Caenorhabditis elegans* Using Functional Ecotoxicogenomics', *Environmental Sciences and Technology*, 43, pp. 3933-3940.

Roh, J. Y., Eom, H.-J. and Choi, J. (2012) 'Involvement of *Caenorhabditis elegans* MAPK signaling pathways in oxidative stress response induced by silver nanoparticles exposure', *Toxicology Research*, 28, pp. 19-24.

Rosenberg, S. H. (2011) 'Mammalian apoptosis in a parasitic worm', *Proceedings of the National Academy of Sciences*, 108(17), pp. 6695-6696.

Rubio-Moscardo, F., Blesa, D., Mestre, C., Siebert, R., Balasas, T., Benito, A., Rosenwald, A., Climent, J., Martinez, J. I., Schilhabel, M., Karran, E. L., Gesk, S., Esteller, M., deLeeuw, R., Staudt, L. M., Fernandez-Luna, J. L., Pinkel, D., Dyer, M. J. and Martinez-Climent, J. A. (2005) 'Characterization of 8p21.3 Chromosomal Deletions in B-cell Lymphoma: TRAIL-R1 and TRAIL-R2 as Candidate Dosage-dependent Tumor Suppressor Genes', *Blood*, 106, pp. 3214-3222.

Russell, J. H. and Ley, T. J. (2002) 'Lymphocyte-mediated Cytotoxicity', *Annual Review of Immunology*, 20, pp. 323-370.

Ruttkey-Nedecky, B., Nejdl, L., Gumulee, J., Zitka, O., Masarik, M., Eckschlager, T., Stiborova, M., Adam, V. and Kizek, R. (2013) 'The role of metallothionein in oxidative stress', *International Journal of Molecular Sciences*, 14, pp. 6044-6066.

Saelens, X., Festjens, N., Vande Walle, L., Vvan Gurp, M., van Loo, G. and Vandenabeele, P. (2004) 'Toxic proteins released from mitochondria in cell death', *Oncogene*, 23, pp. 2861-2874.

Sakahira, H., Enari, M. and Nagata, S. (1998) 'Cleavage of CAD Inhibitor in CAD Activation and DNA Degradation during Apoptosis', *Nature*, 391(96-99).

Sal'nikov, D. S., Pogorelova, A. S., Makarov, S. V. and Vashurina, I. Y. (2009) 'Silver ion reduction with peat fulvic acid', *Russian Journal of Applied Chemistry*, 82(4), pp. 545-548.

Salehisadeh, H. and Shojaosadati, S. A. (2001) 'Extracellular biopolymeric flocculants: recent trends and biotechnological importance', *Biotechnology Advances*, 19, pp. 371-385.

Salvesen, G. S. and Dixit, V. M. (1999) 'Caspase Activation: the Induced-proximity Model', *Proceedings of the National Academy of Sciences*, 96, pp. 10964-10967.

Sanpui, P., Chattopadhyay, A. and Ghosh, S. S. (2011) 'Induction of apoptosis in cancer cells at low silver nanoparticle concentrations using chitosan nanocarrier', *ACS Applied Materials and Interfaces*, 3, pp. 218-228.

Sau, T. K., Rogach, A. L., Jäckel, F., Klar, T. A. and Feldmann, J. (2010) 'Properties and Applications of Colloidal Nonspherical Noble Metal Nanoparticles', *Advanced Materials*, 22(16), pp. 1805-1825.

Scaffidi, C., Schmitz, I., Krammer, P. H. and Peter, M. E. (1999) 'The Role of c-FLIP in Modulation of CD95-induced Apoptosis', *The Journal of Biological Chemistry*, 274, pp. 1541-1548.

SCENIHR (2005) *Opinion on the appropriateness of existing methodologies to assess the potential risks associated with engineered and adventitious products of nanotechnology*. [Online]. Available at: http://ec.europa.eu/health/ph_risk/committees/04_scenihr/docs/scenihr_o_003b.pdf.

SCENIHR (2011) *Commission recommendation on the definition of nanomaterial*.

Scheffer, A., Engelhard, C., Sperling, M. and Buscher, W. (2008) 'ICP-MS as a new tool for the determination of gold nanoparticles in bioanalytical applications', *Analytical and Bioanalytical Chemistry*, 390, pp. 249-252.

Schrand, A., Braydich-Stolle, L. K., Schlager, J., Dai, L. and Hussain, S. M. (2008) 'Can Silver Nanoparticles Be Useful as Potential Biological Labels?', *Nanotechnology*, 19, pp. 1-13.

Schrand, A. M., Rahman, M. F., Hussain, S. M., Schlager, J. J., Smith, D. A. and Syed, A. F. (2010) 'Metal-based nanoparticles and their toxicity assessment', *Wiley Interdisciplinary Reviews Systems Biology and Medicine*, 2, pp. 544-568.

Schreurs, W. and Rosenberg, H. (1982) 'Effect of silver ions on transport and retention of phosphate by *Escherichia coli*', *Journal of Bacteriology*, 152, pp. 7-13.

Schvedova, A. A., Pietroiusti, A., Fadeel, B. and Kagan, V. E. (2012) 'Mechanisms of carbon nanotube-induced toxicity: focus on oxidative stress', *Toxicology and Applied Pharmacology*, 261(2), pp. 121-133.

Shi, J., Sun, X., Lin, Y., Zou, X., Li, Z., Liao, Y. and Du, M. (2014) 'Endothelial cell injury and dysfunction induced by silver nanoparticles through oxidative stress cvia IKK/NF-KB pathways', *Biomaterials*, 35, pp. 6657-6666.

Shub, D. A. (1994) 'Bacterial Viruses. Bacterial Altruism?', *Current Biology*, 4, pp. 555-556.

Siddiqui, M. A., Alhadlaq, H. A., Ahmed, J., Al-Khedhairy, A. A., Musarrat, J. and Ahamed, M. (2013) 'Copper oxide nanoparticles induced mitochondria mediated apoptosis in human hepatocarcinoma cells', *PLoS ONE*, 8(8), p. e69534.

Smetana, A., Klabunde, K. J., Marchin, G. and Sorensen, C. (2008) 'Biocidal Activity of Nanocrystalline Silver Powders and Particles', *Langmuir*, 24, pp. 7457-7464.

Sohlenius, B. (1980) 'Abundance, Biomass and Contribution to Energy Flow by Soil Nematodes in Terrestrial Ecosystems', *Oikos*, 34, pp. 186-194.

Sondi, I. and Salopek-Sondi, B. (2004) 'Silver Nanoparticles as Antimicrobial Agent: A Case Study on *E. coli* as a Model for Gram-Negative Bacteria', *Journal of Colloid and Interface Science*, 275, pp. 177-182.

Starnes, D. L., Lichtenberg, S. S., Unrine, J. M., Starnes, C. P., Oostveen, E. K., Lowry, G. V., Bertsch, P. M. and Tsyusko, O. V. (2016) 'Distinct transcriptomic responses of *Caenorhabditis elegans* to pristine and sulfidized silver nanoparticles', *Environmental Pollution*, 213, pp. 314-321.

Steen, R. L. and Collas, P. (2001) 'Mistargeting of B-type lamins at the end of mitosis: implications on cell survival and regulation of lamins A/C expression', *Cell Biology*, 153, pp. 621-626.

Stein, K. K. and Golden, A. (2015) 'The *C. elegans* eggshell', in Community, T. *C. E.* R. (ed.)*Wormbook*. pp. 2-31.

Steller, H. (1995) 'Mechanisms and Genes of Cellular Suicide', *Science*, 267, pp. 1445-1449.

Stohs, S. J. and Bagchi, D. (1995) 'Oxidative mechanisms in the toxicity of metal-ions', *Free Radical Biology and Medicine*, 18, pp. 321-336.

Stricklin, S. L., Griffiths-Jones, S. and Eddy, S. R. (2005) 'C. elegans noncoding RNA genes', in Hodgkin, J. and Anderson, P. (eds.)*Wormbook*.

Studer, A. M., Limbach, L. K., Van Duc, L., Krumeich, F., Athanassiou, E. K., VGerber, L. C., Moch, H. and Stark, W. J. (2010) 'Nanoparticle cytotoxicity depends on intracellular solubility: comparison of stabilised copper metal and degradable copper oxide nanoparticles', *Toxicology Letters*, 197, pp. 169-174.

Suliman, Y., Ali, D., Alarifi, S., Harrath, A. H., Mansour, L. and Alwasel, S. H. (2013) 'Evaluation of cytotoxic, oxidative stress, proinflammatory and genotoxic effect of silver nanoparticles in human lung epithelial cells', *Environmental Toxicology*. doi: 10.1002/tox.21880.

Sulston, J. E. and White, J. G. (1980) 'Regulation and Cell Autonomy During Postembryonic Development of *Caenorhabditis elegans*', *Developmental Biology*, 78, pp. 577-597.

Sun, J., Wang, S., Zhao, D., Hun, F. H., Weng, L. and Liu, H. (2011) 'Cytotoxicity, permeability, and inflammation of metal oxide nanoparticles in human cardiac

microvascular endothelial cells: cytotoxicity, permeability, and inflammation of metal oxide nanoparticles', *Cell Biology and Toxicology*, 27(5), pp. 333-342.

Sun, T., Yan, Y., Zhao, Y., Guo, F. and Jiang, C. (2012) 'Copper oxide nanoparrticles induce autophagic cell death in A549 cells', *PLoS ONE*, 7(8), p. e43442.

Sung, J., Ji, J., Yoon, J., Kim, D., Song, M., Jeong, J., Han, B., Han, J., Chung, Y., Kim, J., Kim, T., Chang, H., Lee, E., Lee, J. and Yu, I. (2008) 'Lung Function Changes in Sprague-Dawley Rats after Prolonged Inhalation Exposure to Silver Nanoparticles', *Inhalation Toxicology*, 20, pp. 567-574.

Susin, S. A., Daugas, E., Ravagnan, L., Samejima, K., Zamzami, N., Loeffler, M., Costantini, P., Ferri, K. F., Irinopoulou, T., Prevost, M. C., Brothers, G., Mak, T. W., Penninger, J. M., Earnshaw, W. C. and Kroemer, G. (2000) 'Two distinct pathways leading to nuclear apoptosis', *The Journal of Experimental Medicine*, 192, pp. 571-580.

Suzuki, Y. J., Forman, H. J. and Sevanian, A. (1997) 'Oxidants as stimulators of signal transduction', *Free Radical Biology and Medicine*, 22, pp. 269-285.

Sze, A., Erickson, D., Ren, L. and Li, D. (2003) 'Zeta-potential measurement using the Smoluchowski equation and the slope of the current–time relationship in electroosmotic flow', *Journal of Colloid and Interface Science*, 261(2), pp. 402-410.

Taub, J., Lau, J. F., Ma, C., Hahn, J. H., Hoque, R., Rothblatt, J. and Chalfie, M. (1999) 'A cytosolic catalase is needed to extend adult lifespan in C. elegans *daf*-C and *clk-1* mutants', *Nature*, 399, pp. 162-166.

Thomas, R. (2013) 'An overview of ICP-MS', in *Practical guide to ICP-MS: A tutorial for beginners*. 3rd edn. Florida, USA: CRC press, p. pp. 1.

Tikekar, R. V. (2015) 'Characterisation of nanoscale delivery systems', in Sabliov, C., Chen, H. and Yada, R. (eds.) *Nanotechnology and functional foods: Effective delivery of bioactive ingredients*. USA: John Wiley and Sons, pp. 112-190.

Tino, A., Ambrosone, A., Marchesano, V. and Tortiglione, C. (2014) 'Molecular bases of nanotoxicology', in Ruiz-Molina, D., Novio, F. and Roscini, C. (eds.) *Bio- and bioinspired nanomaterials*. Germany: Wiley-VCH, pp. 229-253. 9.

Tiwari, D. K., Jin, T. and Behari, J. (2011) 'Dose-dependent in-vivo toxicity assessment of silver nanoparticle in Wistar rats', *Toxicology Mechanisms and Methods*, 21, pp. 13-24.

Trapani, J. A. and Smyth, M. J. (2002) 'Functional Significance of the Perforin/Granzyme Cell Death Pathway', *Nature Reviews Immunology*, 2, pp. 735-747.

Tyne, W., Lofts, S., Spurgeon, D. J., Jurkschat, K. and Svendsen, C. (2013) 'A new medium for *Caenorhabditis elegans* toxicology and nanotoxicology studies designed to better reflect natural soil solution conditions', *Environmental Toxicology and Chemistry*, 32(8), pp. 1711-1717.

Tzur, Y. B., Hersh, B. M., Horvitz, H. R. and Gruenbaum, Y. (2002) 'Fate of the nuclear lamina during Caenorhabditis elegans apoptosis ', *Journal of Structural Biology*, 137, pp. 146-153.

Udenfriend, S., Stein, S., Böhlen, P., Dairman, W., Leimgruber, W. and Weigele, M. (1972) 'Fluorescamine: a reagent for assay of amino acids, peptides, proteins, and primary amines in the picomole', *Science*, 178(4063), pp. 871-872.

van Loo, G., van Gurp, M., Depuydt, B., Srinivasula, S. M., Rodriguez, I., Alnemri, E. S., Gevaert, K., Vandekerckhove, J., Declercq, W. and Vandenabeele, P. (2002) 'The serine protease Omi/HtrA2 is released from mitochondria during apoptosis. Omi interacts with caspase-inhibitor XIAP and induces enhanced caspase activity', *Cell Death and Differentiation*, 9, pp. 20-26.

Vaux, D. L. and Strasser, A. (1996) 'The Molecular Biology of Apoptosis', *Proceedings of the National Academy of Sciences*, 93, pp. 2239-2244.

Verano-Braga, T., Miethling-Graff, R., Wojdyla, K., Rogowska-Wrzesinska, A., Brewer, J. R., Erdmann, H. and Kjeldse, F. (2014) 'Insights into the cellular response triggered by silver nanoparticles using quantitative proteomics', *ACS Nano*, 8, pp. 2161-2175.

Verhagen, A. M., Ekert, P. G., Pakusch, M., Silke, J., Connolly, L. M., Reid, G. E., Moritz, R. L., Simpson, R. J. and Vaux, D. L. (2000) 'Identification of DIABLO, a Mammalian Protein that Promotes Apoptosis by Binding to and Antagonizing IAP Proteins', *Cell*, 102, pp. 43-53.

Vertelov, G., Krutyakov, Y., Effremenkova, O., Olenin, A. and Lisichkin, G. (2008) 'A versatile synthesis of highly bactericidal Myramistin stabilized silver nanoparticles', *Nanotechnology*, 19.

Wada, T. and Penninger, J. M. (2004) 'Mitogen-activated protein kinases in apoptosis regulation', *Oncogene*, 23, pp. 2838-2849.

Wajant, H. (2002) 'The Fas Signaling Pathway: More Than a Paradigm', *Science*, 296, pp. 1635-1636.

Wang, H., Wick, R. L. and Xing, B. (2009) 'Toxicity of Nanoparticles and Bulk ZnO, Al_2O_3 and TiO_2 to the Nematode *Caenorhabditis elegans*', *Environmental Pollution*, 157, pp. 1171-1177.

Wang, S., Zhao, Y., Wu, L., Tang, M., Su, C., Hei, T. K. and Yu, Z. (2007) 'Induction of germline cell cycle arrest and apoptosis by sodium arsenite in Caenorhabditis elegans', *Chemical Research in Toxicology*, 20, pp. 181-186.

Wang, X., Yang, C., Chai, J., Shi, Y. and Xue, D. (2002) 'Mechanisms of AIF-mediated Apoptotic DNA Degradation in *Caenorhabditis elegans*', *Science*, 298, pp. 1587-1592.

Wang, Y., Aker, W. G., Hwang, H. M., Yedjou, C. G., Yu, H. and Tchounwou, P. B. (2011) 'A study of the mechanism of *in vitro* cytotoxicity of metal oxide nanoparticles using catfish primary hepatocytes and human HepG2 cells', *The Science of the Total Environment*, 409(22), pp. 4753-4762.

Wang, Z., Li, N., Zhao, J., White, J. C., Qu, P. and Xing, B. (2012) 'CuO nanoparticle interaction with human epithelial cells: Cellular uptake, location, export, and genotoxicity', *Chemical Research in Toxicology*, 25, pp. 1512-1521.

Wilkinson, K. J. and Lead, J. R. (2007) *Environmental colloids and particles: Behaviour, separation and characterisation*. Chichester, UK: John Wiley and Sons.

Williams, P. L. and Dusenbery, D. B. (1990) 'Aquatic toxicity testing using the nematode Caenorhabditis elegans', *Environmental Toxicology and Chemistry*, 9, pp. 1285-1290.

Wu, Y. and Zhou, Q. (2012) 'Dose- and time-related changes in aerobic metabolism, chorionic disruption, and oxidative stress in embryonic medaka (Oryzias latipes): Underlying mechanisms for silver nanoparticle developmental toxicity', *Aquatic Toxicology*, 124-125, pp. 238-246.

Xia, T., Kovochich, M., Brant, J., Hotze, M., Sempf, J., Oberley, T., Sioutas, C., Yeh, J. I., Wiesner, M. R. and Nel, A. E. (2006) 'Comparison of the abilities of ambient and manufactured nanoparticles to induce cellular toxicity according to an oxidative stress paradigm', *Nano Letters*, 6(8), pp. 1794-1807.

Xiong, J. (2006) 'Genomics and proteomics', in *Essential bioinformatics*. USA: Cambridge University Press, pp. 243-296. 6.

Xu, J., Li, Z., Xu, P., Xiao, L. and Yang, Z. (2012) 'Nanosized copper oxide induces apoptosis through oxidative stress in podocytes', *Archives of Toxicology*.

Xu, R. (2008) 'Progress in nanoparticles characterization: sizing and zeta potential measurement', *Particuology*, 6(2), pp. 112-115.

Xue, D., Shaham, S. and Horvitz, H. R. (1996) 'The *Caenorhabditis elegans* Cell-death Protein CED-3 is a Cysteine Protease with a Substrate Specificities Similar to Those of the Human CPP32 Protease', *Genes and Development*, 10, pp. 1073-1083.

Yang, W., Shen, C., Ji, Q., An, H., Wang, J., Liu, Q. and Zhang, Z. (2009) 'Food storage material silver nanoparticles interfere with DNA replication fidelity and bind with DNA', *Nanotechnology*, 20.

Yang, X., Gondikas, A. P., Marinakos, S. M., Auffan, M., Liu, J., Hsu-Kim, H. and Meyer, J. N. (2012) 'Mechanism of Silver Nanoparticles Toxicity is Dependent on Dissolved Silver and Surface Coating in *Caenorhabditis elegans*', *Environmental Science and Technology*, 46, pp. 1119-1127.

Yeo, M. and Kang, M. (2008) 'Effects of Nanometer Sized Silver Materials on Biological Toxicity during Zebrafish Embryogenesis', *Bulletin of the Korean Chemical Society*, 29, pp. 1179-1184.

Yeo, M. and Yoon, J. (2009) 'Comparison of the Effects of Nano-silver Antibacterial Coatings and Silver Ions on Zebrafish Embryogenesis ', *Molecular and Cellular Toxicology*, 5, pp. 23-31.

Yuan, J. and Horvitz, H. R. (1990) 'The *Caenorhabditis elegans* Cell Death Gene *ced-4* Encodes a Novel Protein and is Expressed during the Period of Extensive Programmed Cell Death', *Development*, 116, pp. 309-320.

Zarkower, D. (2006) 'Somatic sex determination', in Community, T. *C. E.* R. (ed.) *Wormbook*.

Zeitoun-Ghandour, S., Leszczyszyn, O. I., Blindauer, C. A., Geier, F. M., Bundy, J. G. and Stürzenbaum, S. R. (2011) '*C. elegans* Metallothioneins: Response to and Defence against ROS Toxicity', *Molecular Biosystems*, 7, pp. 2397-2406.

Zhang, R., Piao, M. J., Kim, K. C., Kim, A. D., Choi, J.-Y., Choi, J. and Hyun, J. W. (2012) 'Endoplasmic reticulum stress signaling is involved in silver nanoparticles-induced apoptosis', *The international Journal of Biochemistry and Cell Biology*, 44, pp. 224-232.

Zhang, W., Sun, B., Zhang, L., Zhao, B. and Nie, G. (2011) 'Biosafety of $Gd@C_{82}(OH)_{22}$ Nanoparticles on *Caenorhabditis elegans*', *Nanoscale*, 3, pp. 2636-2641.

Zhang, X.-F., Choi, Y.-J., Han, J. W., Kim, E., Park, J. H., Gurunathan, S. and Kim, J.-H. (2015) 'Differential nanoreprotoxicity of silver nanoparticles in male somatic cells and spermatogonial stem cells', *International Journal of Nanomedicine*, 10, pp. 1335-1357.

Zhang, Y., Chen, Y., Westerhoff, P. and Crittenden, J. (2009) 'Impact of natural organic matter and divalent cations on the stability of aqueous nanoparticles', *Water Research*, 43, pp. 4249-4257.

Zhao, J., Wang, Z., Liu, X., Xie, X., Zhang, K. and Xing, B. (2011) 'Distribution of CuO nanoparticles in juvenile carp (*Cyprinus carpio*) and their potential toxicity', *Journal of Hazardous Materials*, 197, pp. 304-310.

Zhou, Z., Hartwieg, E. and Horvitz, H. R. (2001) 'CED-1 is a Transmembrane Receptor that Mediates Cell Corpse Engulfment in *C. elegans*', *Cell*, 104, pp. 43-56.

Zhuang, S., Demirs, J. T. and Kochevar, I. E. (2000) 'p38 mitogen-activated protein kinase mediates bid cleavage, mitochondrial dysfunction, and caspase-3 activation during apoptosis induced by singlet oxygen but not hydrogen peroxide', *The Journal of Biological Chemistry*, 275, pp. 25939-25948.

Zook, J. M., Halter, M. D., Cleveland, D. and Long, S. E. (2012) 'Disentangling the Effects of Polymer Coatings on Silver Nanoparticle Agglomeration, Dissolution, and Toxicity to Determine Mechanisms of Nanotoxicity', *Journal of Nanoparticle Research*, 14, p. 1165.

Zou, H., Henzel, W. J., Liu, X., Lutschg, A. and Wang, X. (1997) 'Apaf-1, a Human Protein Homolougous to C. elegans CED-4, Participates in Cytochrome C-Dependent Activation of Caspase-3', *Cell*, 90, pp. 405-413.